Institut für Festkörperphysik
Fakultät Mathematik und Naturwissenschaften
Technische Universität Dresden

Magnetic Properties of Gadolinium Compounds

Habilitationsschrift
zur Erlangung des akademischen Grades
Dr. rer. nat. habil.

vorgelegt von

Martin Rotter

Dresden, 2003

Folgende Publikationen werden mit einer Zusammenfassung als Habilitationsschrift eingereicht:

[**R1**] A. Lindbaum and M. Rotter, "Spontaneous Magnetoelastic Effects in Gadolinium Compounds", in: *Magnetic Materials* Vol. 14, ed. K. H. J. Buschow, Elsevier Sci. Pub. Amsterdam,The Netherlands (2002) 307

[**R2**] M. Rotter, M. Loewenhaupt, M. Doerr, A. Lindbaum and H. Michor, "Noncollinear Amplitude Modulated Magnetic Order in Gd Compounds", *Phys Rev.* **B 64** (2001) 014402

[**R3**] M. Rotter, M. Loewenhaupt, M. Doerr, A. Lindbaum, H. Sassik, K. Ziebeck and B. Beuneu, "The Dipole Interaction and Magnetic Anisotropy in Gadolinium Compounds", *Phys. Rev. B* (2003), accepted

[**R4**] M. Rotter, M. Loewenhaupt, S. Kramp, T. Reif, N. M. Pyka, W. Schmidt and R. v. d. Kamp, "Anisotropic Magnetic Exchange in orthorhombic RCu_2 Compounds (R=rare earth)", *Europ. Phys. J.* **B 14** (2000) 29

[**R5**] M. Rotter, A. Lindbaum, E. Gratz, H. Müller, G. Hilscher, H. Sassik, H. E. Fischer, M. T. Fernandes-Diaz, R. Arons and E. Seidl, "The Magnetic Structure of $GdCu_2$", *J. Mag. Magn. Mat.* **214** (2000) 281

[**R6**] M. Rotter, M. Doerr, M. Loewenhaupt, A. Lindbaum, H. Müller, J. Enser and E. Gratz, "Magnetic Exchange driven Magnetoelastic Properties in $GdCu_2$", *J. Magn. Mag. Mat.* **236** (2001) 267

[**R7**] M. Rotter, A. Schneidewind, M. Loewenhaupt, M. Doerr, A. Stunault, A. Hiess, A. Lindbaum, E. Gratz, G. Hilscher and H. Sassik, "Magnetic Scattering on $GdCu_2$", *Physica* **B 284-288** (2000) 1329

[**R8**] M. Rotter, A. Schneidewind, M. Doerr, M. Loewenhaupt, M. el Massalami, H. Michor and G. Hilscher, "Interpreting Magnetic X-ray Scattering of Gd-compounds using the McPhase Simulation Program", *Physica B* (2003), accepted

[**R9**] M. Rotter, M. Doerr, M. Loewenhaupt, A. Lindbaum, K. Ziebeck and B. Beuneu, "Diffraction Experiments on $GdCu_2$In using Hot Neutrons", *Physica B* (2003), accepted

[**R10**] E. Gratz, A. Lindbaum and M. Rotter, "The Influence of the Crystal Field on the Anisotropic Thermal Expansion in $TmCu_2$", *J. Phys. Cond. Mat.* **5** (1993) 7955

[**R11**] M. Rotter, H. Müller, E. Gratz, M. Doerr and M. Loewenhaupt, "A new Miniature Capacitance Dilatometer for Thermal Expansion and Magnetostriction", *Rev. Sci. Instrum.* **69** (1998) 2742

[**R12**] M. Rotter, M. Doerr and M. Loewenhaupt, "Modeling Magentostriction in RCu_2 Compounds using *McPhase*", *J. of Appl. Physics* **91** (2002) 8885

[**R13**] P. Svoboda, M. Doerr, M. Loewenhaupt, M. Rotter, T. Reif, F. Bourdarot and P. Burlet, "Structural Change in $DyCu_2$ Single Crystal Induced by Magnetic Field", *Europhys. Lett.* **48** (1999) 410

[**R14**] M. Rotter, M. Doerr, M. Loewenhaupt, U. Witte, P. Svoboda, J. Vejpravová, H. Sassik, C. Ritter, D. Eckert, A. Handstein and D. Hinz, "Anomalous Magnetic Exchange Interactions in $SmCu_2$", *Phys. Rev.* **B 64** (2001) 134405

[**R15**] E. Gratz, M. Rotter, A. Lindbaum, H. Müller, E. Bauer and H. Kirchmayr, "The Influence of the Crystal Field on the Anisotropic Thermal Expansion in $ErCu_2$ and $NdCu_2$", *J.Phys. Cond. Mat.* **5** (1993) 567

Eine vollständige Liste *aller* Publikationen befindet sich im Anhang.

Die Zusammenfassung besteht aus folgenden Kapiteln:

1 Introduction

Since the fifties of the last century the magnetic properties of rare earths have been investigated. Due to the localized character of their magnetic 4f electrons rare earth elements and compounds served as test materials for many models of magnetism. A large number of experimental techniques and theoretical approaches has been developed in order to understand the complex magnetic properties of the rare earth elements. These efforts led to the so called "standard model of rare earth magnetism" [1].

One of the major results with respect to application is, that the large magnetic moments and the anisotropy of rare earths may be used to produce very advanced permanent magnetic materials. The most important source of anisotropy in rare earth compounds is believed to be the electric field generated by the crystalline environment of the rare earth atom. It is called crystal field (CF) and leads to a deformation of the spherical $4f$ charge density. This distortion is small at high temperatures and increases when lowering the kinetic energy of the $4f$ electrons by reducing the temperature. Because the movement of the electrons at low temperature is influenced by the non spherical CF potential, the magnetic moment generated by this movement when applying a magnetic field will depend on the direction of the magnetic field, i.e. the magnetic properties will be anisotropic. It is important to remember, that due to the localization of the 4f charge density the CF is sufficiently screened by the outer electrons to enable an orbital movement of the electrons, which is connected with an orbital magnetic moment[1]. A simple example of a 4f ion surrounded by two positive charges is shown in fig. 1. A quantitative investigation of the CF effect shows, that the anisotropy, which is generated, depends on the number of $4f$ electrons involved and may be characterized by a parameter α named after Stevens [2]. The CF concept has been put forward already in the sixties [3]. Since then a large number of methods have been proposed and applied to predict [4, 5, 6, 7, 8] and measure [9, 10, 11] the strength of the CF [12], which is frequently characterized by CF-parameters as described in [3, 13, 14].

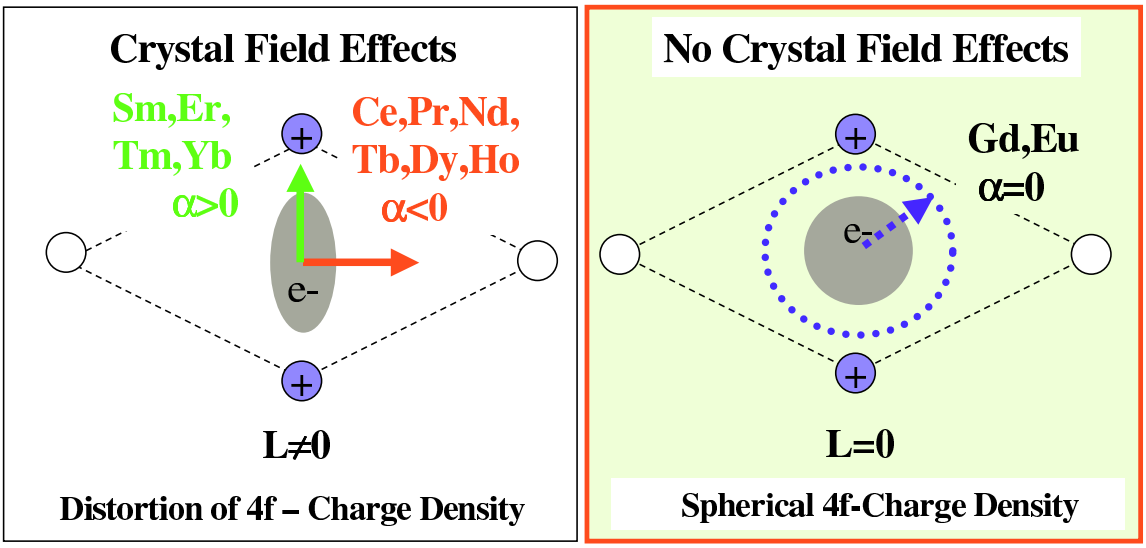

Figure 1: Distortion of the $4f$ charge density for different rare earth ions as induced by the crystal field generated by two charges (+). The distortion is associated with a magnetic anisotropy leading to an easy direction of magnetization characterized by the Steven's coefficient α and shown by the arrows (left). In the special case of a pure spin moment (L=0) there is no distortion of the charge and correspondingly no crystal field anisotropy (right).

Magnetic phenomena do not only depend on the orbital magnetic moment of the electrons, but also on the spin. The spin and the orbital magnetic moments are correlated by a relativistic effect, the spin-orbit coupling, which is very large for atoms with a large number of electrons such as the rare earth elements (here it is much larger than the CF). The spin orbit coupling stabilizes a ground state multiplet, which depends on the number of $4f$ electrons according to Hund's rules. The spin orbit ground state of a free

[1] compare the case of the transition metals, where the CF is much stronger and the orbital moment vanishes (is "quenched").

rare earth ion is characterized by the orbital momentum L, the spin momentum S and the total angular momentum J. It is $2J+1$ degenerate and this degeneracy may be lifted partly by the CF.

Among the members of the rare earth series the element Gadolinium (Gd) is outstanding, because the Gd^{3+} ion has the largest spin moment (S=7/2) among all elements. Furthermore the orbital momentum vanishes (L=0)[2]. The magnetic properties of Gadolinium metal are well studied (see e.g. [15] and [16] and references therein). It has the highest magnetic ordering temperature among all rare earth elements (T_C = 294 K) and remains ferromagnetic down to liquid helium temperature. The paramagnetic to ferromagnetic transition at T_C is of second order type and recently the universality class has been determined [17]. Neutron diffraction experiments [18] showed that from T_C down to the spin reorientation temperature $T_{SR} \approx 232$ K the moments are aligned along the hexagonal axis (i.e. c-direction). It is a common view that it is the classical magnetic dipole interaction, which is responsible for this orientation of the magnetic moment. Below T_{SR} the moment direction departs from the c-direction and the angle between the hexagonal axis and the moment direction changes with temperature.

It is worthwhile to mention that the magnetic properties of Gadolinium metal remain a puzzle. It was reported recently [19], that Gadolinium is probably not really a ferromagnet between T_{SR} and T_C, but that the magnetic structure is some long-period modulated structure, similar to the incommensurate structure found in erbium. This conclusion has been drawn from susceptibility measurements around T_{SR} and T_C, but experiments for observing the long-period modulation are still missing. More recent susceptibility and low field magnetization measurements [20] confirm again the widely accepted view that Gadolinium is a collinear ferromagnet between T_{SR} and T_C.

Whereas Gd metal is well studied, comparatively little interest has been taken in the magnetic properties of Gd compounds. One reason is, that due to the vanishing orbital moment of Gd the magnetic anisotropy is very small and therefore the materials are not interesting for application as permanent magnets. Another reason is, that one of the most powerful experimental methods for the investigation of magnetic properties - the neutron scattering technique - is hampered by the extremely large absorption cross section of ^{157}Gd (16% natural abundance) for neutrons.

In the following it will be shown, how my study of Gd compounds made essential contributions to our knowledge about magnetic interactions, which in turn led to modifications of some well established concepts. To give an example, the current explanations for the giant magnetostriction effect [21] have to be modified.

[2]note that in contrast to the transition metals the orbital moment in Gd is not quenched but vanishes due to the first and second Hund's rule.

2 Magnetostriction in Gadolinium Compounds

In contrast to the case of transition metals the orbital momentum is not quenched in Gd but vanishes due to the first and second Hund's rule, which stabilize the $|L = 0, S = 7/2, J = 7/2, m_J\rangle$ ground state multiplet of the $4f$ electrons ($m_J = -J, -J+1, \ldots, +J$). Only for the case of 7 electrons in the $4f$-shell (Gd^{3+},Eu^{2+}) the orbital momentum and the Stevens factors vanish. As a consequence the charge density of the magnetic electrons is rigid in first order and does not deform in electric fields such as the crystal field. The magnetic properties are isotropic as shown in fig. 1 (right).

This rigid $4f$ charge density is particularly interesting with respect to the study of magnetoelastic interactions. The common opinion is, that in rare earth compounds the deformation of the $4f$ charge density induced by the crystal electric field is responsible for the magnetoelastic interactions leading to large magnetostriction effects [22, 23]. Fig. 2 (left) indicates this mechanism. At low temperatures the $4f$-electrons occupy only low-lying energy levels and the $4f$ charge distribution assumes a non spherical shape corresponding to the crystal field potential. This change in the $4f$ charge distribution generates an electric force onto the sources of the crystal field which in turn leads to a change in the crystal lattice.

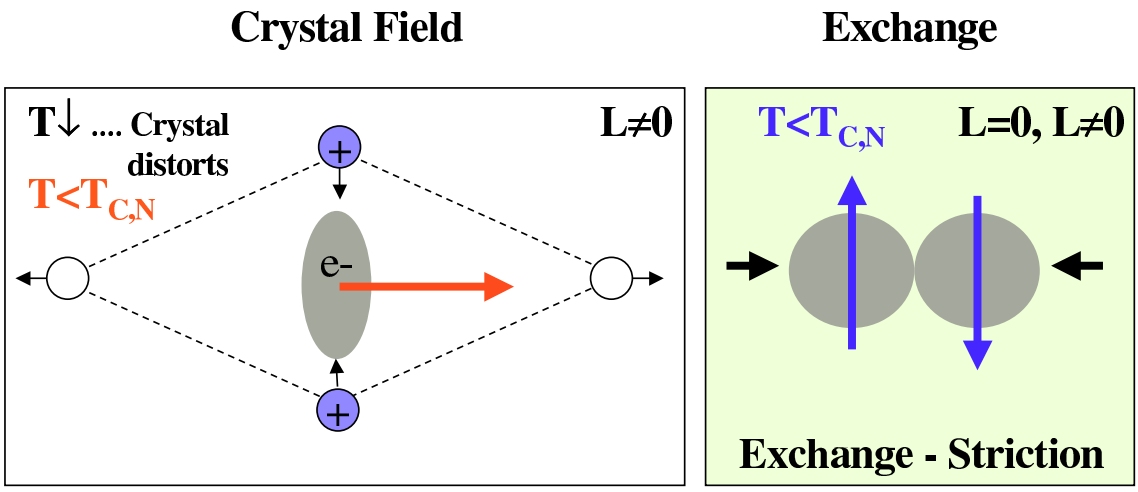

Figure 2: The distortion of the $4f$ charge density acts back on the crystal leading to magnetostrictive strains (indicated by small arrows) when the temperature is lowered (left). Large effects are associated with magnetic phase transitions. However, even in the paramagnetic regime there is a magnetic contribution to the thermal expansion [R10]. In the special case of a pure spin moment (L=0) crystal field effects are negligible and other mechanisms are responsible for magnetoelastic effects. The exchange interaction may be strain dependent leading to the exchange striction (right).

In [R1] we have shown from experimental data on a large set of Gd compounds, that it cannot be this crystal field effect alone, which generates large magnetostrictive effects in rare earth compounds. Using the X-ray diffraction technique at variable temperature we measured the thermal expansion on a large number of Gd compounds. These measurements were complemented by magnetostriction data on single crystals using the capacitance method [R6] (after improving it by the development of a high field - miniature dilatometer [24, R11]). We found that the order of magnitude of the magnetostriction is very variable in Gd compounds and in some cases may exceed 1% (see fig. 3 for an overview). Such large values of the magnetostriction are commonly called "giant magnetostriction"(GMS) and have not been expected for Gd compounds, because, as mentioned before, only crystal field effects are made responsible for GMS [21].

In [R1] we interpreted the data on Gd compounds on the basis of the exchange striction model [25, 26]. In this model the strain dependence of the exchange interaction is regarded as the driving force of magnetostrictive effects as indicated in fig. 2 (right) for an antiferromagnet. The magnetic order has to be attributed to the exchange interaction, which depends on the overlap of the wave functions of the magnetic electrons. When the material is cooled below the Néel temperature, the system may lower it's free energy by increasing this overlap. The resulting strain is called exchange striction. In Gd

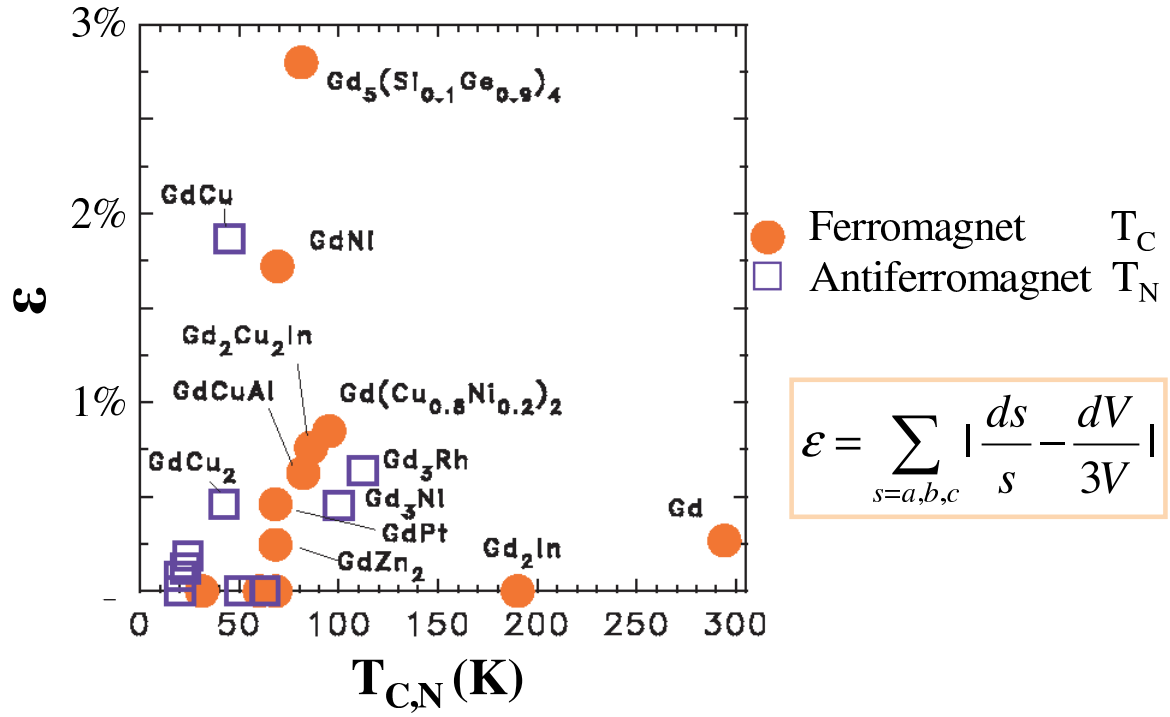

Figure 3: Anisotropic magnetostriction ϵ of Gd compounds versus the magnetic ordering temperature.

The measurements on Gd compounds show that the exchange striction mechanism has to be regarded as important as the crystal field effect and may lead even to a giant magnetostriction effect of more than 1%. At present however, no predictions can be made for its magnitude in a specific compound and it requires very advanced techniques to distinguish it from the CF mechanism [R12]. Fig. 3 shows, that there is no correlation with the ordering temperature, which is a measure of the exchange interaction strength. This means that the strain dependence of the exchange interaction is not necessarily large if the exchange interaction itself is large. On the other hand also small exchange interactions may show a large strain dependence[3] leading to a large magnetostriction. In the case of metals this property may be understood by considering the oscillatory behavior of the RKKY interaction with distance (see fig. 4). A small change in distance of the neighbors may lead to a large variation of the interaction also if the interaction itself is small.

It is interesting to compare the effect of a magnetic field for the CF and the exchange mechanism. When a magnetic field is applied to an antiferromagnet and drives the moments into the ferromagnetic state, the thermally induced magnetostriction is reversed for both, the crystal field mechanism and the exchange striction as shown in fig. 5.

Another important finding reported in [R1] is, that in Gd compounds large magnetostrictive effects are not associated with a lattice distortion. This means that the magnetostriction can be anisotropic, however, leaving the symmetry of the crystal unchanged. A distortion of the lattice which involves a change of the symmetry is not possible if the driving force is the isotropic exchange interaction and the order is ferromagnetic. However, in antiferromagnets such distortions are not forbidden by symmetry. The experiments show, that these distortions are very small (strain $\epsilon \leq 10^{-4}$) in comparison to the large effects on the lattice parameters (which conserve the symmetry). Such a behavior has to be put into contrast to the large changes in symmetry associated with the crystal field mechanism (Jahn-Teller-effect) [28, 29].

[3]This bavior is unexpected and in contrast to the familiar Grüneisen approach, which is based on the assumption that the strain derivative of an energy (or interaction constant) is large, if the energy itself is large. For example the lattice expansion due to phonons can be interpreted successfully by assuming, that large interactions also have large anharmonic contributions [27] such that $\omega^{-1}\frac{\partial\omega}{\partial\epsilon}$ is constant (ω denotes the eigenfrequency of a phonon mode).

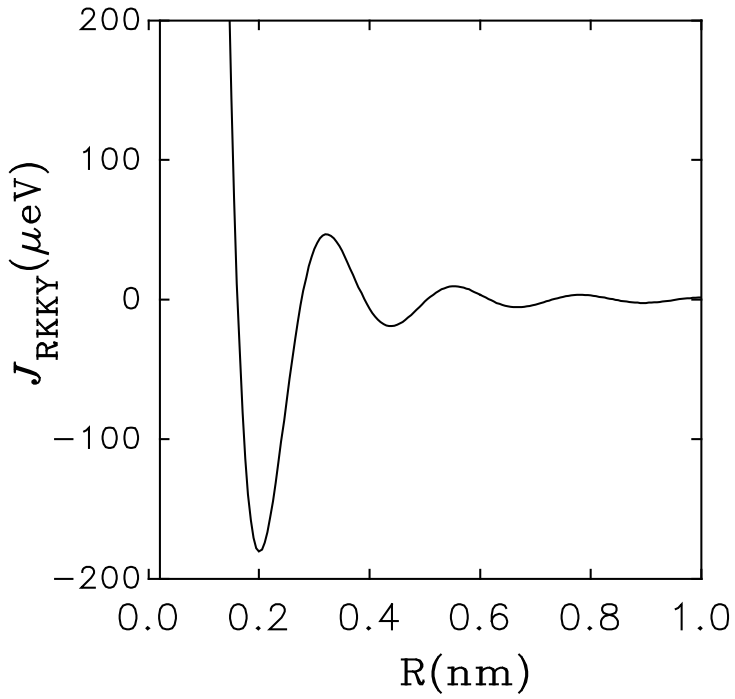

Figure 4: Variation of the RKKY interaction with interatomic distance (compare e.g. [1]).

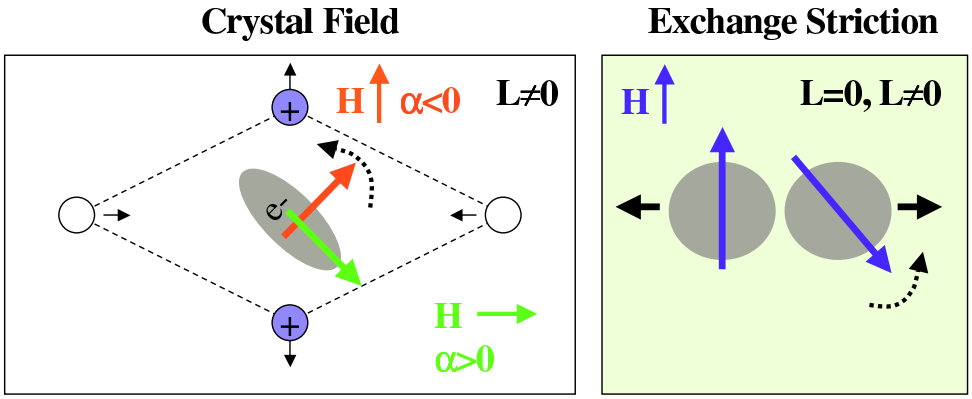

Figure 5: Effect of a magnetic field for the crystal field mechanism (left) and the exchange striction (right). The small black arrows indicate the magnetostrictive strain induced by the magnetic field.

3 Magnetic Interactions in Gadolinium Compounds

In section 2 it was shown that magnetoelastic interactions based on the exchange energy (i.e. the "exchange striction") may be large. In order to find out more about this mechanism all details about magnetic interactions which are present in Gd compounds are required. A first step is to determine the spin configurations of the complex magnetic structures in these compounds. I have applied two methods to find out the magnetic structure - a model analysis of the specific heat [R2] and magnetic diffraction experiments using hot neutrons and synchrotron radiation [R3].

Although a bulk method, the specific heat can give some important information about the type of magnetic order present in a Gd based magnet: the discontinuity at the magnetic ordering temperature can be measured and directly associated with a type of magnetic structure (i. e. collinear amplitude modulated, equal moment or non-collinear amplitude modulated, for details see [R2]).

In order to determine the magnetic structure in more detail, diffraction experiments are needed. For hot neutrons with a wavelength below 0.06 nm the absorption cross section of Gd is small enough to enable scattering experiments. In [R3] the results of powder diffraction experiments on a large number of Gd compounds with exactly one Gd atom per unit cell is discussed. For complex magnetic structures I had to develop and apply advanced numerical methods to calculate the low temperature magnetic structure.

Based on a study of 19 Gd compounds [R9] I came to the following conclusion: In most cases the classical dipole interaction is responsible for the magnetic anisotropy. Note that the isotropic interactions (such as RKKY exchange interactions etc.) are at least one order of magnitude larger than the dipolar interaction and lead to ordering temperatures of more than 100 K. The neutron diffraction experiments indicate, that in Gd systems these other interactions are isotropic to a very high degree of accuracy and that the small dipolar interaction only determines the magnetic anisotropy. This is true for ferromagnets as well as for antiferromagnets. It is remarkable, that although the magnetic anisotropy of Gd compounds is much smaller than that of other rare earth compounds, it can be predicted with high accuracy from first principles.

4 $GdCu_2$ - a Member of the RCu_2 Series

As an example the magnetic properties of $GdCu_2$ are mentioned, because this is probably one of the best characterized Gd - antiferromagnets. All 1:2 compounds of lanthanides with Cu (with the exception of $LaCu_2$) exhibit the orthorhombic $CeCu_2$-type structure (see fig. 6 [30], space group *Imma*, Ce on 4*e* sites with point symmetry *mm*, Cu on 8*h*). $LaCu_2$ displays the related hexagonal AlB_2 structure with space group P_6/mmm [31]. The orthorhombic $CeCu_2$ structure can be viewed as a distorted AlB_2-type structure. In some RCu_2 compounds a martensitic transition in high magnetic fields has been observed and associated with a conversion of the $CeCu_2$ to the AlB_2 type of structure [R13].

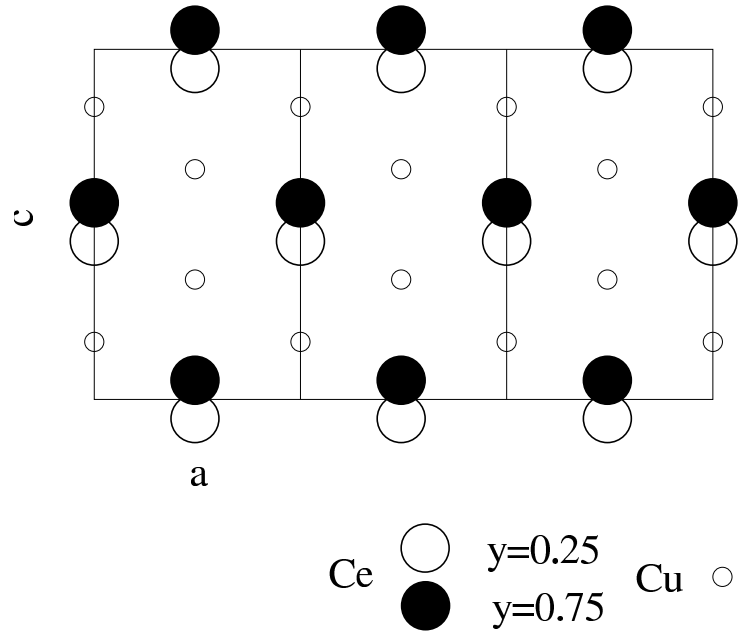

Figure 6: Orthorhombic $CeCu_2$ structure projected into the quasi-hexagonal *ac* plane.

Bulk magnetic properties of $GdCu_2$ are known already since more than a decade ago [32, 33]. I took the initiative to extend the analysis to magnetoelastic properties and to use neutron and magnetic X-ray scattering to determine the magnetic structure [R5,R6]. The interest in this special system stems from a very close investigation of the RCu_2 series [R4], which led to the discovery of large exchange anisotropies, which cannot be due to the classical dipole interaction. I could show in [R14], that the sign of this exchange anisotropy is reversed in $SmCu_2$.

For the $GdCu_2$ system the isotropic exchange interaction plus a very small anisotropy due to the classical dipolar interaction can account for the observed magnetic structure [R5,R7], the magnetization [R8] and the magnetoelastic properties [R6] as described in the following.

4.1 Magnetostriction

In the RCu_2 series the contribution of the exchange striction mechanism to the magnetostriction mentioned in section 2 may be easily identified using the simple picture developed in fig. 2. Keeping in mind that the orthorhombic $CeCu_2$ structure may be viewed as a distorted hexagonal AlB_2 type of structure, the effect of the crystal field mechanism must always lead to an increase of the distortion when lowering the temperature (shown in fig. 7).

Note that in the hexagonal AlB_2 structure the hexagonal plane corresponds to the *ac* plane of the orthorhombic $CeCu_2$ structure. In RCu_2 compounds the distortion of the lattice can be viewed by plotting the temperature dependence of the c/a ratio, which for the hexagonal case assumes the ideal value of 1.732. In compounds with low ordering temperatures the orthorhombic distortion *increases* indeed when lowering the temperature due to a magnetoelastic effect as can be seen by comparing the c/a-ratio to the nonmagnetic reference compound YCu_2 (fig. 8).

I have analyzed quantitatively the crystal field and exchange striction mechanism in $NdCu_2$ [R12], $ErCu_2$ [R15] and $TmCu_2$ [R10] by extending a model by Divis et al. [23] to anisotropic effects. If the

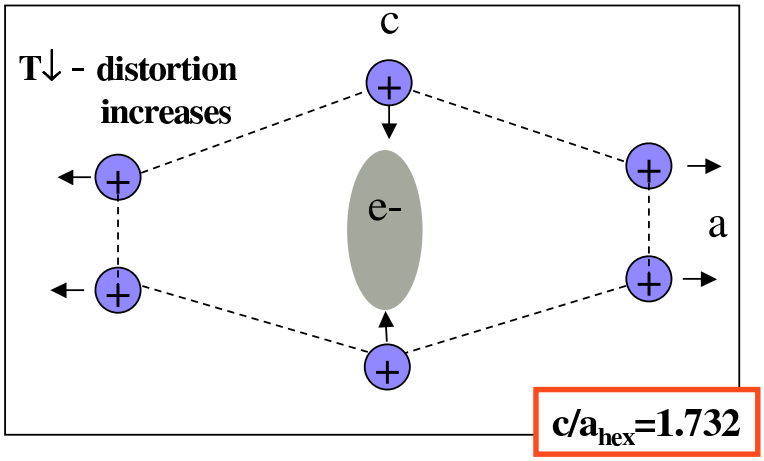

Figure 7: The effect of the crystal field mechanism of magnetostriction onto the orthorhombic $CeCu_2$ lattice. The charge density of the rare earth (shown in the middle) is distorted by the orthorhombic CF of neighboring Cu ions. This distortion increases when lowering the temperature and generates a force onto the Cu atoms as indicated by the arrows.

magnetoelastic effects lead to a *decrease* of the orthorhombic distortion when lowering the temperature, clearly another mechanism than the crystal field has to account for it. Such a decrease of the distortion is found in the case of $GdCu_2$ and $TbCu_2$ for temperatures below the Néel temperature T_N as shown in a plot of the c/a ratio (fig. 9). This comparison shows, that the exchange striction may be large not only for Gd compounds (L=0), but also for rare earth compounds with a large orbital momentum (L=3 for Tb^{3+}).

4.2 Magnetic Anisotropy

Now I come back to the discussion of the magnetic structure and anisotropy of $GdCu_2$. I analyzed the magnetic contribution to the specific heat using an analytical model calculation [R2]. The magnetic entropy as calculated from the specific heat reaches its theoretical value of $R \ln 8$ at 47 K, just above $T_N \approx 42$ K [34]. The shape of the curve agrees very well with the prediction of the calculation [R2] based on an equal moment magnetic structure. Scattering experiments verified this conclusion [R5,R7] and indicated a noncollinear cycloidal magnetic structure with a propagation vector of (2/3 1 0).

However, traces of other interactions may be clearly identified in this system by comparing experimental data to results of quantitative calculations [R8]: the transition field to the ferromagnetic phase is larger than predicted, at temperatures below 10 K there is a change of the magnetic structure in zero magnetic field. However, the transition is only seen in the susceptibility in c direction and in the magnetic moment component in c-direction as measured by magnetic X-ray scattering [R8]. No indication of such a phase transition can be found in specific heat, in the thermal expansion and in magnetic measurements with fields in a or b direction. The behavior of $GdCu_2$ has been compared to another noncollinear antiferromagnet, $GdNi_2B_2C$ in [R8]. In $GdNi_2B_2C$ a spin reorientation within the magnetically ordered state is well established and corresponds to the results of a numerical model calculation.

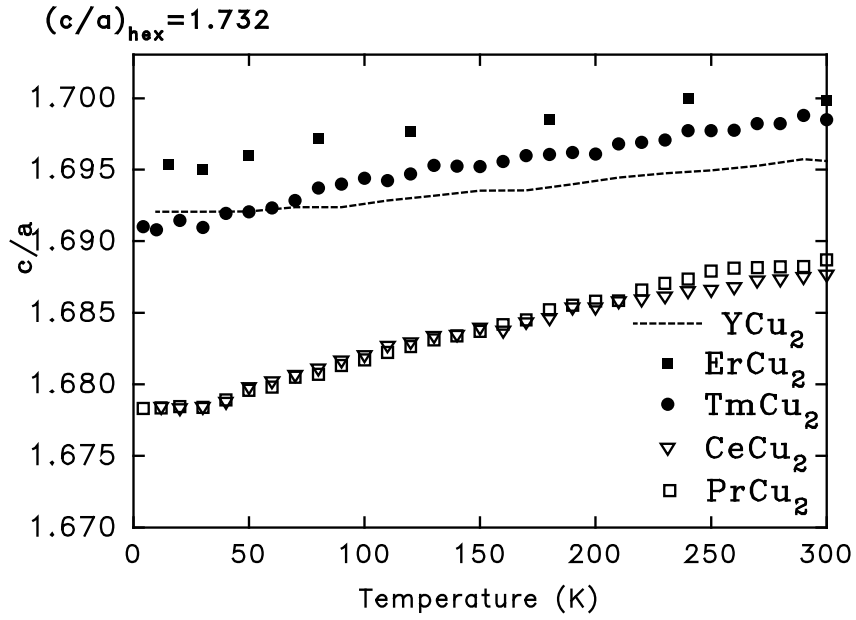

Figure 8: Temperature dependence of the c/a ratio in magnetic RCu_2 compounds in comparison with the nonmagnetic isostructural reference compound YCu_2. The results have been obtained by temperature dependent powder X-ray diffraction [24]. The effect of the crystal field mechanism of magnetostriction in RCu_2 (R=Ce, Pr, Er, Tm) leads to a larger deviation from the ideal hexagonal c/a ratio when lowering the temperature than in YCu_2.

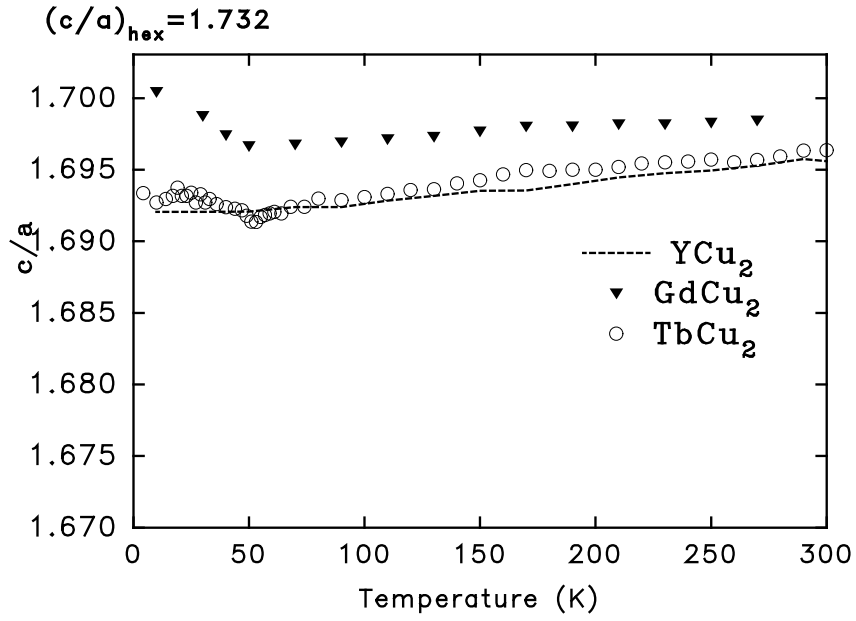

Figure 9: Temperature dependence of the c/a ratio for $GdCu_2$ and $TbCu_2$ in comparison with the nonmagnetic isostructural reference compound YCu_2. The results have been obtained by temperature dependent powder X-ray diffraction [24]. The increase of the c/a ratio below the ordering temperature can only be interpreted by the exchange striction mechanism and not by a crystal field effect.

5 Personal contribution to the collaborative scientific work

- **[R1] Spontaneous Magnetoelastic Effects in Gadolinium Compounds** A. Lindbaum and M. Rotter

  Using the X-ray diffraction technique at variable temperatures (which I significantly improved in accuracy [35]) A. Lindbaum measured the thermal expansion on a large number of Gd compounds. These measurements I complemented by magnetostriction data on single crystals using the capacitance method [R6] (after improving it by the development of a high field - miniature dilatometer [24, R11]). I interpreted the data on Gd compounds on the basis of the exchange striction model and showed, that it cannot be this crystal field effect alone, which generates large magnetostrictive effects in rare earth compounds.

- **[R2] Noncollinear Amplitude Modulated Magnetic Order in Gd Compounds** M. Rotter, M. Loewenhaupt, M. Doerr, A. Lindbaum and H. Michor

  Using th specific heat data provided by the other authors I analyzed the magnetic contribution to the specific heat by a model calculation [R2].

- **[R3] The Dipole Interaction and Magnetic Anisotropy in Gadolinium Compounds** M. Rotter, M. Loewenhaupt, M. Doerr, A. Lindbaum, H. Sassik, K. Ziebeck and B. Beuneu

  I took part in the neutron diffraction experiments and interpreted the experimental data by the dipolar model.

- **[R4] Anisotropic Magnetic Exchange in orthorhombic RCu_2 Compounds (R=rare earth)** M. Rotter, M. Loewenhaupt, S. Kramp, T. Reif, N. M. Pyka, W. Schmidt and R. v. d. Kamp

  The neutron spectroscopy I did in close collaboration with the other authors. It led me to propose a model for the magnetic interactions in the RCu_2 series [R4] based on large exchange anisotropies, which cannot be due to the classical dipole interaction. In [R14] I could show, that the sign of this exchange anisotropy is reversed in $SmCu_2$.

- **[R5] The Magnetic Structure of** $GdCu_2$ M. Rotter, A. Lindbaum, E. Gratz, H. Müller, G. Hilscher, H. Sassik, H. E. Fischer, M. T. Fernandes-Diaz, R. Arons and E. Seidl

  The neutron experiments were performed by the other authors. I worked on the interpretation of the data, suggested the model for the magnetic structure and did the analysis within a mean field theory. Using this model I interpreted also the magnetization measurements done by the other authors.

- **[R6] Magnetic Exchange driven Magnetoelastic Properties in** $GdCu_2$ M. Rotter, M. Doerr, M. Loewenhaupt, A. Lindbaum, H. Müller, J. Enser and E. Gratz

  My part in this work was to assist in the performance of the dilatometer measurements (we used the miniature dilatometer which I developed [R11]). Furthermore I took the initiative to extend the analysis to magnetoelastic properties and to measure all 3x3 components of the magnetostrictive strains. I did the model analysis of the magnetoelastic interactions. I have estimated quantitatively the crystal field and exchange striction mechanism also in $NdCu_2$ [R12], $ErCu_2$ [R15] and $TmCu_2$ [R10] by extending a model by Divis et al. [23] to anisotropic effects.

- **[R7] Magnetic Scattering on** $GdCu_2$ M. Rotter, A. Schneidewind, M. Loewenhaupt, M. Doerr, A. Stunault, A. Hiess, A. Lindbaum, E. Gratz, G. Hilscher and H. Sassik

I assisted in the sample preparation and took the initiative to use magnetic X-ray scattering to determine the magnetic structure of $GdCu_2$. The time consuming experiment and analysis of the data was performed in close collaboration with the other authors.

- **[R8] Interpreting Magnetic X-ray Scattering of Gd-compounds using the McPhase Simulation Program** M. Rotter, A. Schneidewind, M. Doerr, M. Loewenhaupt, M. el Massalami, C. Detlefs

  My part in this work was to do the model calculation and perform a magnetic scattering experiment on $GdCu_2$. The experimental data on $GdNi_2B_2C$ was contributed by the other authors.

- **[R9] Diffraction Experiments on $GdCu_2In$ using Hot Neutrons** M. Rotter, M. Doerr, M. Loewenhaupt, A. Lindbaum, K. Ziebeck and B. Beuneu

  Together with M. Doerr, M. Loewenhaupt and B. Beuneu I performed the neutron diffraction experiment on samples provided by the other authors. My main part in the data analysis was to perform a numerical modeling of the low temperature magnetic properties of $GdCu_2In$, which served to interpret the experimental diffraction pattern.

- **[R10] The Influence of the Crystal Field on the Anisotropic Thermal Expansion in $TmCu_2$** E. Gratz, A. Lindbaum and M. Rotter

  I contributed to the measurement and the analysis of the data with the crystal field model.

- **[R11] A new Miniature Capacitance Dilatometer for Thermal Expansion and Magnetostriction** M. Rotter, H. Müller, E. Gratz, M. Doerr and M. Loewenhaupt

  I was responsible for the review of available literature, the design of the dilatometer, and the correct set up of the measurement hard- and software including the testing of the calibration procedure. This work was based on the large expierence, which I collected during my PhD thesis in the design of capacitance dilatometers. In close collaboration with H. Müller and E. Gratz the experimental set up was tested in Vienna and subsequently together with M. Doerr and M. Loewenhaupt in a different cryogenic environment in Dresden.

  In the meantime the dilatometer meets increasing interest in the scientific community and industry. The use in a PPMS (Quantum Design) - measurement system has been demonstrated, Oxford Instruments published an article about it in their newsletter and the dilatometer is being used in ultrahigh magnetic fields at GHMFL (CNRS, GRenoble).

- **[R12] Modeling Magentostriction in RCu_2 Compounds using** *McPhase* M. Rotter, M. Doerr and M. Loewenhaupt

  It was a challenge for me to extend the *McPhase* program package to the calculation of magnetostriction with the option to take into account two different mechanisms - the crystal field and the exchange striction. Together with the other authors the measurements of magnetostriction on the $NdCu_2$ single crystal have been performed.

- **[R13] Structural Change in $DyCu_2$ Single Crystal induced by Magnetic Field** P. Svoboda, M. Doerr, M. Loewenhaupt, M. Rotter, T. Reif, F. Bourdarot and P. Burlet

  The main part of the neutron diffraction experiment and data analysis was done by P. Svoboda and M. Doerr. I assisted in the interpretation of the data and by outlining the paper.

- **[R14] Anomalous Magnetic Exchange Interactions in $SmCu_2$** M. Rotter, M. Doerr, M. Loewenhaupt, U. Witte, P. Svoboda, J. Vejpravová, H. Sassik, C. Ritter, D. Eckert, A. Handstein and D. Hinz

This work was an experimental challenge both experimentally and theoretically. The costly preparation of the sample for neutron diffraction was performed by H. Sassik. C. Ritter and myself performed the neutron diffraction experiment. The other authors were engaged in the preparation of and experiments on single crystals. My interpretation of all data was based on the model of anisotropic exchange in RCu_2 compounds [R4].

- **[R15] The Influence of the Crystal Field on the Anisotropic Thermal Expansion in $ErCu_2$ and $NdCu_2$** E. Gratz, M. Rotter, A. Lindbaum, H. Müller, E. Bauer and H. Kirchmayr

  In this paper I extended the model by Divis [23] for the volume expansion of RCu_2 compounds to anisotropic magnetostrictive effects caused by the crystal field. The experimental challenge to measure these small effects by temperature dependent X-ray diffraction required a close collaboration with all other authors.

References

[1] J. Jensen and A. R. Mackintosh, *Rare Earth Magnetism*, Clarendon Press Oxford (1991)

[2] K. W. H. Stevens, *Proc. Phys. Soc.* **A 65** (1952) 209

[3] M. T. Hutchings, "Point Charge Calculations of Energy Levels of magnetic Ions in Crystalline Electric Fiels", in: *Handbook of Magnetic Materials* Vol. 16, ed. F. Seitz and D. Thurnbull, Academic Press, New York and London (1964) 227

[4] D. J. Newman and N. Betty, "The superposition model of crystal fields", *Rep. Prog. Phys.* **52** (1989) 699

[5] M. Divis, H. Nakotte, F. R. de Boer, P. F. de Chatel and V. Sechovsky, "Determination of the crystal-field parameters for CePtSn", *J. Phys. Cond. Mat.* **6** (1994) 6895

[6] M. Divis, J. Kuriplach and P. Novak, "Ab initio calculations of crystal field in MAl_2 (M=La, Y, Sc) Laves Phases", *J. Magn. Magn. Mat.* **140-144** (1995) 1117

[7] M. Divis and J. Kuriplach, "Crystal field in rare earth intermetallics with CsCl structure", *Physica B* **205** (1995) 353

[8] M. Colarieti-Tosti, O. Eriksson, L. Nordström, J. Wills and M. S. S. Brooks, "Crystal-field levels and magnetic susceptibility in PuO_2", *Phys. Rev.* **B** (2002) 195102

[9] A. Furrer, T. Strässle and D. R. Temprano, "New excitement with crystal field excitations", *J. Alloys and Comp.* **323-324** (2001) 649

[10] M. D. Kuzmin, "A method of determining the crystal field parameters in rare earth paramagnets by means of torque magnetometry", *J. Magn. Magn. Mat.* **154** (1996) 333

[11] H. Martinho, J. A. Sanjurjo, C. Rettori, P. C. Canfield and P. G. Pagliuso, "Raman scattering study of crystal-field excitations in $ErNi_2B_2C$", *J. Magn. Magn. Mat* **226-230** (2001) 978

[12] P. Fulde and M. Loewenhaupt, "Magnetic Excitations in crystal field split 4f systems", *Adv. in Physics* **34** (1986) 589

[13] K. Takegahara, "Matrix elements of crystal electric fields in rare earth compounds", *J. Phys. Soc. Jap.* **69** (2000) 1572

[14] U. Walter, "Crystal Field splitting in icosahedral symmetry", *Phys. Rev.* **B 36** (1987) 2504

[15] K A McEwen, in: *Handbook on the Physics and Chemistry of Rare Earths* Vol. 1, ed. Jr. K. A. Gschneidner and Le Roy Eyring, North-Holland, Amsterdam (1978) 411

[16] S. Y. Dankov, A. M. Tishin, V. K. Pecharsky and K. A. Gschneidner, "Magnetic phase transitions and the magnetothermal properties of gadolinium", *Phys. Rev.* **B 57** (1998) 3478

[17] E. Frey, F. Schwabl, S. Henneberger, O. Hartmann, R. Wäppling, A. Kratzer and G. M. Kalvius, "Determination of the Universality Class of Gadolinium", *Phys. Rev. Lett.* **79** (1997) 5142

[18] J.W. Cable and E.O. Wollan, *Phys. Rev.* **165** (1968) 733

[19] J. M. Coey, V. Skumryev and K. Gallagher, "Is gadolinium really ferromagnetic ¿', *Nature* **401** (1999) 35

[20] S. N. Kaul and S. Srinath, "Gadolinium: A helical antiferromagnet or a collinear ferromagnet", *Phys. Rev.* **B 62** (2000) 1114

[21] I. D: Mayergoyz, *Handbook of giant magnetostrictive materials*, Academic Press (2000)

[22] P. Morin and D. Schmitt, "Quadrupolar interaction and magnetoelastic effects in rare earth intermetallic compounds", in: *Ferromagnetic Materials* Vol. 5, ed. K. H. J. Buschow and E. P. Wohlfarth, Elsevier Sci. Pub. Amsterdam,The Netherlands (1990) 1

[23] M. Divis, P. Lukac and P. Svoboda, "Magnetoelastic interactions in the orthorhombic $RECu_2$ compounds (RE = Tb, Dy, Ho, Er, Tm)", *J. Phys. Cond. Mat.* **2** (1990) 7569

[24] M. Rotter, "Bestimmung des Kristallfeldeinflusses auf die anisotrope thermische Ausdehnung in Selten-Erd-Verbindungen mit Hilfe temperaturabhängiger Röntgendiffraktometrie", PhD thesis Technische Universität Wien (1994)

[25] E. Callen and H. B. Callen, "Static Magnetoelastic Coupling in Cubic Crystals", *Phys. Rev.* **129** (1963) 578

[26] E. Callen and H. B. Callen, "Magnetostriction, Forced Magnetostriction and Anomalous Thermal Expansion in Ferromagnets", *Phys. Rev.* **139** (1965) A455

[27] T. H. K. Barron, J. G. Collins and G. K. White, *Adv. Phys.* **29** (1980) 609

[28] R. Settai, S. Araki, P. Ahmet, M. Abliz, K. Sugiyama, Y. Onuki, T. Goto, H. Mitamura, T. Goto and S. Takayanagi, "Anisotropic Cooperative Jahn-Teller Effect and Metamagnetism in $PrCu_2$", *J. Phys. Soc. Jpn.* **67** (1998) 636

[29] K. Andres, P. S. Wang, Y. H. Wong, B. Lüthi and H. R. Ott, "Jahn-Teller transition in $PrCu_2$", *AIP Conf. Proc.* **34** (1976) 222

[30] D. Debray, "Crystals of the $CeCu_2$- Type Structure", *Journal of the Less-Common Metals* **30** (1973) 237

[31] A. R. Storm and K. E. Benson, "Lanthanide-copper intermetallic compounds having the $CeCu_2$ and AlB_2 structures", *Acta Cryst.* **16** (1963) 701

[32] M. K. Borombaev, R. Z. Levitin, A. S. Markosyan, V. A. Reimer, A. V. Sinitsyn and Z. Smetana, "Magnetic properties of a $GsCu_2$ single crystal", *Z. Sov. Phys. JETP* **66** (1987) 866

[33] M.K. Borombaev and A.S. Markosyan, *Fiz. Met. Metalloved.* **63** (1987) 714

[34] A. Koyanagi, Y. Yoshida, Y. Kimura, R. Settai, K. Sugiyama and Y. Onuki, "Magnetic and Electrical Properties of $GdCu_2$", *J. Phys. Soc. Jpn.* **67** (1998) 2510

[35] Martin Rotter, *Bestimmung des Kristallfeldeinflusses auf die anisotrope thermische Ausdehnung in Selten- Erd- Verbindungen mit Hilfe temperaturabhängiger Röntgendiffraktometrie*, Diploma thesis Technische Universität Wien (1990)

Acknowledgment

It is a great pleasure to express my gratitude to Prof. Michael Loewenhaupt for offering me the possibility to perform this habilitation thesis under his continuous friendly guidance. I would like to thank colleagues who generously agreed to read sections of the draft version of the text; their comments helped to improve the text substantially. I am particularly indebted to Dr. Mathias Doerr for his inspiring comments.

Erklärung

Ich erkläre hiermit, dass die vorliegende Habilitationsschrift von mir selbst und ohne andere als die darin angegebenen Hilfsmittel angefertigt sowie inhaltlich übernommene Stellen als solche gekennzeichnet wurden. Mein Anteil an den beiliegenden gemeinschaftlichen wissenschaftlichen Arbeiten ist im Kapitel 5 erläutert. Ein früheres Habilitationsgesuch an einer anderen Hochschule ist nicht erfolgt.

Declaration

I herewith declare that this habilitation thesis has been completed by me and without other aid than that specified in the thesis. Passages which contain results from other work are accordingly marked. My personal contribution to the collaborative scientific work is documented in section 5. I did not apply earlier for a habilitation at another university or similar institution.

Dresden,

Martin Rotter

List of Publications

[1] M. Rotter, *Bestimmung des Kristallfeldeinflusses auf die anisotrope thermische Ausdehnung in Selten-Erd- Verbindungen mit Hilfe temperaturabhängiger Röntgendiffraktometrie*, Diploma thesis Technische Universität Wien (1990)

[2] H. Figiel, J. Zukrowski, E. Gratz, M. Rotter, A. Lindbaum and A. S. Markosyan, "Measurements of thermal expansion in YMn_2H", *Solid State Communications* **83** 4(1992) 277–278

[3] E. Gratz, M. Rotter, A. Lindbaum, H. Müller, E. Bauer and H. Kirchmayr, "The influence of the crystal field on the anisotropic thermal expansion in $ErCu_2$ and $NdCu_2$", *J.Phys.: Cond. Mat.* **5** (1993) 567–572

[4] E. Bauer, R. Hauser, E. Gratz, G. Schaudy, M. Rotter and A. Lindbaum, "$CePd_2Ga_3$: A new ferromagnetic Kondo lattice", *Zeitschrift für Physik* **B** 92(1993) 411–416

[5] E. Gratz, A. Lindbaum and M. Rotter, "The influence of the crystal field on the anisotropic thermal expansion in $TmCu_2$", *J.Phys.: Cond. Mat.* **5** (1993) 7955–7958

[6] E. Gratz, M. Rotter, A. Lindbaum, H. Müller, E. Bauer and H. Kirchmayr, "Crystal-field influence on the anisotropic thermal expansion in $ErCu_2$ and $NdCu_2$", in: *Material Science Forum* Vol. 133-136, Enschede Holland (1993) 461–466

[7] E. Gratz, A. Lindbaum, M. Rotter, E. Bauer and H. Kirchmayr, "Structural investigations of the intermediate valence systems $Yb(Cu_xAl_{1-x})_5$", in: *Material Science Forum Vol.133-136*, Enschede Holland (1993) 519–522

[8] A. Lindbaum, E. Gratz and M. Rotter, "Anisotropic thermal expansion in $RECu_2$-compounds", in: *Material Science Forum Vol.166-169*, Vienna (1994) 467–472

[9] E. Bauer, M. Rotter, L. Keller, P. Fischer, M. Ellerby and K. A. McEwen, "Magnetic structure and field – dependent properties of $CeCu_5$", *J.Phys.: Cond. Mat.* **6** (1994) 5533–5543

[10] M. Rotter, "Thermische Ausdehnung in intermetallischen Selten- Erd- Verbindungen", PhD thesis Technische Universität Wien (October 1994)

[11] M. Ellerby, K. A. McEwen, M. de Podesta, M. Rotter and E. Gratz, "Detailed magnetization study of $NdCu_2$ at low temperatures", *J.Phys.: Cond. Mat.* **7** (1995) 1897–1907

[12] M. Loewenhaupt, T. Reif, R. Arons, E. Gratz, M. Rotter and B. Lebech, "The magnetic structures of $NdCu_2$ determined by single crystal neutron diffraction", *Z. Phys.* **B** 96(1995) 491–496

[13] S. W. Zochowski, M. Rotter, E. Gratz and K. A. McEwen, "Dilatometric study of $NdCu_2$ in magnetic fields", *Journal of Mag. and Magn. Mat.* **140-144** (1995) 1129–1130

[14] T. Reif, M. Loewenhaupt, P. Svoboda, W. Schweika, E. Gratz, M. Rotter and G. McIntyre, "Diffuse magnetic neutron scattering in $NdCu_2$", *Physica* **B 234-236** (1997) 640–641

[15] M. Loewenhaupt, T. Reif, P. Svoboda, S. Wagner, M. Waffenschmidt, H. v Löhneysen, E. Gratz, M. Rotter, B. Lebech and T. Hauß, "The magnetic phases of $NdCu_2$", *Z.Phys.* **B** 101(1996) 499–510

[16] R. Hauser, E. Bauer, E. Gratz, M. Rotter, G. Hilscher, H. Michor and A. S. Markosyan, "Evidence for separate magnetic ordering in the rare earth- and the d sublattice of $Er_{0.6}Y_{0.4}Co_2$", *Physica* **B 238-239** (1997) 577–578

[17] P. Svoboda, T. Reif, M. Loewenhaupt, M. Rotter, E. Gratz and G. McIntyre, "Observation of higher-order harmonics in AF2 phase of $NdCu_2$", *Physica* **B 234-236** (1997) 642–643

[18] R. Hauser, E. Bauer, E. Gratz, M. Rotter, H. Müller, G. Hilscher, H. Michor and A. S. Markosyan, "Decoupling of the magnetic sublattices in the $Er_{1-x}Y_xCo_2$ compounds driven by Y substitution", *Physica* **B 238-239** (1997) 83–87

[19] M. Loewenhaupt, M. Doerr, L. Jahn, T. Reif, C. Sierks, M. Rotter and H. Müller, "Magnetic phase diagram and temperature dependent Ising - axis conversion of $DyCu_2$ single crystals", *Physica* **B 246-247** (1998) 472–475

[20] M. Rotter, H. Müller, E. Gratz, M. Doerr and M. Loewenhaupt, "A new miniature capacitance dilatometer for thermal expansion and magnetostriction", *Rev. Sci. Instrum.* **69** (1998) 2742–2746

[21] M. Doerr, M. Loewenhaupt, W. Hahn, E. Brueck, I. Hagmusa, J. Klaase and M. Rotter, "Specific heat of $DyCu_2$ single crystals in high magnetic fields", *Physica* **B 262** (1999) 340–347

[22] E. Gratz, E. Goremychkin, M. Latroche, G. Hilscher, M. Rotter, H. Mueller, A. Lindbaum, H. michor, V. Paul-Boncour and T. Fernandez-Diaz, "New magnetic phenomena in $TbNi_2$", *J. Phys.: Cond. Mat.* **11** (1999) 7893–7905

[23] S. Kramp, N. M. Pyka, M. Loewenhaupt and M. Rotter, "Temperature and field dependence of the spin wave gap in $NdCu_2$", *Journal of Applied Physics* **85** (1999) 5645–5647

[24] P. Svoboda, M. Doerr, M. Loewenhaupt, M. Rotter, T. Reif, F. Bourdarot and P. Burlet, "Structural change in $DyCu_2$ single crystal induced by magnetic field", *Europhys. Lett.* **48** (1999) 410–414

[25] M. Rotter, M. Loewenhaupt, S. Kramp, T. Reif, N. M. Pyka, W. Schmidt and R. Kamp, "Anisotropic magnetic exchange in orthorhombic RCu_2 compounds (R=rare earth)", *Europ. Phys. J.* **B 14** (2000) 29–42

[26] M. Rotter, M. Loewenhaupt and M. Doerr, "A Miniature Capacitance Dilatometer for Thermal Expansion and Magnetostriction", *Research Matters (Oxford Instruments)* **12** (2000) 2–3

[27] R. Hauser, E. Bauer, E. Gratz, H. Müller, M. Rotter, H. Michor, G. Hilscher, A. S. Markosyan, K. Kamishima and T. Goto, "Decoupling of the magnetic ordering of the rare-earth and the Co sublattice in $Er_{1-x}Y_xCo_2$ compounds driven by substitution or pressure", *Phys. Rev.* **B 61** 2(2000) 1198–1210

[28] A. Lindbaum, S. Heathman, G. Kresse, M. Rotter, E. Gratz, A. Schneidewind, G. Behr, K. Litfin, T. L. Bihan and P. Svoboda, "Structural stability of $LaCu_2$ and YCu_2 studied by high pressure x-ray diffraction and ab-initio total energy calculations", *J. Phys. Cond. Mat.* **12** (2000) 3219–3228

[29] M. Rotter, M. Loewenhaupt and S. Kramp, "Anisotropic long range interactions in $NdCu_2$", *Physica* **B 276-278** (2000) 598–599

[30] T. Reif, M. Doerr, M. Loewenhaupt, M. Rotter, P. Svoboda and S. Welzel, "Magnetic structure of $DyCu_2$ in the virgin and in the converted state", *Physica* **B 276-278** (2000) 600–601

[31] M. Loewenhaupt, M. Rotter and S. Kramp, "Magnetic Anisotropies of Rare-Earth Compounds", *Physica* **B 276-278** (2000) 602–603

[32] M. Rotter, A. Schneidewind, M. Loewenhaupt, M. Doerr, A. Stunault, A. Hiess, A. Lindbaum, E. Gratz, G. Hilscher and H. Sassik, "Magnetic Scattering on $GdCu_2$", *Physica* **B 284-288** (2000) 1329–1330

[33] M. Doerr, M. Rotter, M. Loewenhaupt, T. Reif and P. Svoboda, "Giant Magneto-Striction in $TbCu_2$ and $DyCu_2$ Crystals", *Physica* **B 284-288** (2000) 1331–1332

[34] S. Kramp, M. Loewenhaupt and M. Rotter, "The spin wave dispersion of $NdCu_2$ in strong magnetic fields", *Physica* **B** 276-278(2000) 628–629

[35] M. Rotter, A. Lindbaum, E. Gratz, H. Müller, G. Hilscher, H. Sassik, H. E. Fischer, M. T. Fernandes-Diaz, R. Arons and E. Seidl, "The magnetic structure of $GdCu_2$", *J. Mag. Magn. Mat.* **214** (2000) 281–290

[36] S. Kramp, M. Doerr, M. Rotter, M. Loewenhaupt and R. van de Kamp, "Magnetostructural transition in $NdCu_2$", *Europ. Phys. J.* **B 18** (2000) 559–563

[37] M. Loewenhaupt, M. Doerr, M. Rotter, T. Reif, A. Schneidewind and A. Hoser, "Magnetic field induced Ising axis conversion in $Tb_{0.5}Dy_{0.5}Cu_2$ single crystals", *Brazilian J. of Phys.* **30** (2000) 754–757

[38] M. Rotter, C. Sierks, M. Loewenhaupt, J. Freudenberger and H. Schober, "Crystal Field Effects in Borocarbides Studied by Inelastic Neutron Scattering", in: *Rare Earth Transition Metal Borocarbides (Nitrides): Superconducting, Magnetic and Normal State Properties*, ed. K. H. Müller and V. Narozhnyi, Nato Advanced Research Workshop Kluwer Academic (2001) 137–153

[39] M. Doerr, M. Loewenhaupt, M. Rotter, R. Kratz, H. Krug, D. Eckert, H. Siegel and P. Verges, "Anomalous Magnetic Behaviour of $NdCu_2$ in High Magnetic Fields", *Physica B* **294-295** (2001) 164–167

[40] M. Rotter, M. Loewenhaupt, M. Doerr, A. Lindbaum and H. Michor, "Noncollinear Amplitude Modulated Magnetic Order in Gd Compounds", *Phys Rev.* **B** (2001) 014402–014409

[41] M. Rotter, A. Berg, H. Langenberger, S. Grampp, H. Imhoff and E. Moser, "Autocorrelation Analysis of Bone Structure", *J. of Magnetic Resonance Imaging* **14** (2001) 87–93

[42] S. Kramp, M. Rotter, M. Loewenhaupt, N. M. Pyka, W. Schmidt and R. van de Kamp, "Spin Waves in the Ferrimagnetic Phase of $NdCu_2$", *J. Mag. Magn. Mat.* **226-230** (2001) 470–472

[43] M. Rotter, M. Doerr, M. Loewenhaupt, P. Svoboda, J. Vejpravová, H. Sassik, C. Ritter, D. Eckert, A. Handstein and D. Hinz, "Anomalous Magnetic Exchange Interactions in $SmCu_2$", *Phys. Rev.* **B** (2001) 134405–134411

[44] M. Rotter, M. Doerr, M. Loewenhaupt, A. Lindbaum, H. Müller, J. Enser and E. Gratz, "Magnetic Exchange driven Magnetoelastic Properties in $GdCu_2$", *J. Magn. Mag. Mat.* **236** (2001) 267–271

[45] M. Doerr, M. Rotter, P. Svoboda, F. Bourdarot and M. Loewenhaupt, "Magnetic field induced change of lattice symmetry in rare earth intermetallics", in: *Proceedings of the ILL millennium symposium & european user meeting, Grenoble, 6 -7 april 2001*, ed. A. J. Dianoux, (2001) 178–180

[46] J. Verjpravova, P. Svoboda, D. Rafaja, I. Cisarova, M. Rotter, M. Doerr and M. Loewenhaupt, "Crystal growth and magnetic properties of $SmCu_2$", *Czechoslovak J. of Physics* **52** suppl. A(2002) A233–236

[47] P. Svoboda, J. Verjpravova, M. Hofmann, R. Schneider, M. Rotter, M. Doerr and M. Loewenhaupt, "Antiferromagnetic ordering in $TmCu_2$", *Czechoslovak J. of Physics* **52** 2(2002) 267–270

[48] O. Chernyavsky, K. Prokes, V. Sechovsky, M. Doerr, M. Rotter and M. Loewenhaupt, "Thermal expansion and magnetostriction study on UNiAl single crystals", *Czechoslovak J. of Physics* **52** 2(2002) A237–240

[49] M. Doerr, M. Rotter, E. E. Massalami, S. Sinning, H. Takeya and M. Loewenhaupt, "Magnetoelastic effects in $ErNi_2B_2C$ single crystal: probing the H-T phase diagram", *J. Phys.: Cond Mat.* **14** (2002) 5609–5618

[50] M. Rotter, M. Doerr and M. Loewenhaupt, "Modeling Magentostriction in RCu_2 Compounds using *McPhase*", *J. of Appl. Physics* **91** 10(2002) 8885–8887

[51] A. Lindbaum and M. Rotter, "Spontaneous Magnetoelastic Effects in Gadolinium Compounds", in: *Ferromagnetic Materials* Vol. 14, ed. K. H. J. Buschow and E. P. Wohlfarth, Elsevier Sci. Pub. Amsterdam,The Netherlands (2002) 307–362

[52] M. Rotter, S. Kramp, M. Loewenhaupt, E. Gratz, W. Schmidt, N. M. Pyka, B. Hennion and R. v.d. Kamp, "Magnetic Excitations in the antiferromagnetic phase of $NdCu_2$", *Applied Phys.* **A 74** (2002) s751–753

[53] P. Svoboda, J. Vejpravova, M. Rotter, M. Doerr, M. Loewenhaupt, M. Hofmann and R. Schneider, "Complex magnetic phase diagram of $TmCu_2$", *Applied Phys.* **A 74** (2002) s748–750

[54] R. Schedler, M. Rotter, M. Loewenhaupt and N. M. Pyka, "Monte Carlo Simulation of the cold triple axis spectrometer (PANDA)", *Applied Phys.* **A 74** (2002) s1468–1470

[55] R. Schedler, M. Rotter, U. Witte, M. Loewenhaupt and W. Schmidt, "Field dependence of spin waves in the Kondo lattice $CeCu_2$", *Acta Physica Polonica B* **34** (2003) 1313–1317

[56] M. Doerr, M. Rotter, M. Ellerby, A. Markosyan, S. S. Saxena, Y. Hosokoshi, K. Inoue and M. Loewenhaupt, "Pressure dependent magnetization of $DyCu_2$ single crystals", *Physica B* (2002), accepted

[57] V. Sechovsky, F. Honda, P. Svoboda, K. Prokes, O. Chernyavsky, M. Doerr, M. Rotter and M. Loewenhaupt, "Antiferromagnetism and magnetoelasticity of UNiAl", *Physica* **B** (2003), accepted

[58] J. Vejpravova, P. S. an M. Rotter, M. Doerr and M. Loewenhaupt, "Thermodynamic properties of $SmCu_2$", *Physica* **B** (2003), accepted

[59] K. Hense, U. Witte, M. Rotter, R. Schedler, E. Gratz, H. Nowotny and M. Loewenhaupt, "Comparison of the CF induced phonon shifts in $CeCu_2$ and $NdCu_2$", *J. Magn. Mag. Mat.* (2003), accepted

[60] M. Rotter, "Using McPhase to calculate Magnetic Phase Diagrams of Rare Earth Compounds", *J. Magn. Mag. Mat.* (2003), accepted

[61] M. Rotter, A. Schneidewind, M. Doerr, M. Loewenhaupt, A. M. el Massalami and C. Detlefs, "Interpreting magnetic X-ray scattering of Gd-compounds using the McPhase simulation program", *Physica B* (2003), accepted

[62] A. Schneidewind, A. Kreyssig, C. Detlefs, A. Hiess, M. Rotter and M. loewenhaupt, "Magnetic X-ray Diffraction of $Tb_{0.5}Dy_{0.5}Cu_2$", *Physica B* (2003), accepted

[63] M. Rotter, M. Doerr, M. Loewenhaupt, W. Kockelmann, R. I. Bewley, R. S. Eccleston, A. Schneidewind and G. Behr, "Pressure dependence of the magnetic structures and excitations in the giant magnetostriction compound $TbCu_2$", *J. Magn. Mag. Mat.* (2003), accepted

[64] M. Rotter, M. loewenhaupt, M. Doerr, A. Lindbaum, H. Sassik, K. Ziebeck and B. Beuneu, "The Dipole Interaction and Magnetic Anisotropy in Gadolinium Compounds", *Phys. Rev.* (2003), accepted

[65] M. Rotter, M. Loewenhaupt, A. Lindbaum, K. Ziebeck and B. Beuneu, "Diffraction experiments on $GdCu_2In$ using hot neutrons", *Physica B* (2003), submitted

[66] R. Schedler, U. Witte, M. Rotter, M. Doerr, M. Loewenhaupt and J. Kulda, "$CeCu_2$ - crystal field transition matrix elements determined by polarized neutron spectroscopy", *Physica B* (2003), submitted

[67] "High Magnetic Field Study of Itinerant Antiferromagnetism in Mn_3Si, CuMnSb and PdMnTe", (2003), toulouse RHMF 2003, submitted

Seminars

1. Birkbeck College, London, Dezember 1992 *Quadrupolar Interactions in UPd_3*
2. TU-Wien, November 1992 *Quadrupolwechselwirkungen in UPd_3*
3. TU-Dresden, Mai 1995 *Kapazitive Messung der thermischen Ausdehnung*
4. TU-Dresden, Jänner 1997 *Magnetische Wechselwirkungen in $NdCu_2$*
5. TU-Wien, März 1997 *Magnetische Wechselwirkungen in $NdCu_2$*
6. TU-Dresden, Juli 1997 *Magnetoelastische Eigenschaften von Selten- Erd- Verbindungen*
7. TU-Wien, Jänner 1998 *Magnetoelastische Eigenschaften von Selten- Erd- Verbindungen*
8. MPI-Stuttgart, Jänner 1998 *Magnetoelastische Eigenschaften von Selten- Erd- Verbindungen*
9. TU-Dresden, Juni 1999 *Magnetism in Gd compounds - $GdCu_2$*
10. TU-Dresden, April 2000 *Magnetische und Magnetoelastische Eigenschaften von RCu_2 Verbindungen*
11. TU-Wien, April 2000 *Magnetic and Magnetoelastic Properties of RCu_2 Compounds*
12. Universität Wien, Mai 2000 *Autocorrelation Analysis of Bone Structure*
13. Tables Rondes, CEA Saclay, Dezember 2000 *Spin-Spin Exchange in Gd Compounds*
14. TU-Dresden, März 2001, *Mcphase- a Simulation Tool for Magnetic Properties of Solids*
15. TU-Wien, März 2002, *Mcphase- a Simulation Tool for Magnetic Properties of Solids*
16. TU-Dresden, Physikalisches Kolloquium, Jänner 2003, *Selten-Erd-Verbindungen ohne Kristallfeldanisotropie - Magnetismus in Gd Verbindunen*
17. Universität Wien, Wissenschaftskolleg Mai 2003, *Rare Earth Compounds without Crystal Field Anisotropy - Magnetism of Gadolinium Compounds*

Conference contributions (invited)

1. M. Rotter *Magnetic and Magnetoelastic interactions in RCu_2 compounds* 5^th Prague Colloquium on f-Electron Systems (2000)

2. M. Rotter *Neutron Spectroscopy of Magnetic Excitations* 53. Jahrestagung der ÖPG (Fachtag der FKP/NESY), Salzburg (2003)

Conference contributions

1. T.Reif, M. Loewenhaupt, M. Rotter, P. Svoboda, B. Lebech, T. Hauss *Die magnetische Struktur von $NdCu_2$*, DPG Frühjahrstagung, Regensburg, März 1996

2. R. Hauser, E. Bauer, E. Gratz, M. Rotter, H. Müller, G. Hilscher, H. Michor, A. S. Markosyan, *Evidence for seperate ordering in the Rare earth and the d - sublattice of $Er_{0.6}Y_{0.4}Co_2$*, Int. Conf. on the Physics of Transition metals, 24.-27.9.96, Osaka, Japan

3. R. Hauser, E. Bauer, M. Rotter, H. Müller, G. Hilscher, H. Michor, A. S. Markosyan, *Decoupling of the magnetic sublattices in the $Er_{1-x}Y_xCo_2$ compounds driven by substitution*, Int. Workshop Kumamoto on Novel Physical Properties of Rare Earth intermetallics, 18.-20.9.1996, Kumamoto, Japan

4. T. Reif, M. Loewenhaupt, P. Svoboda, W. Schweika, E. Gratz, M. Rotter, G. McIntyre *Diffuse magnetic neutron scattering in $NdCu_2$*, ECNS Interlaken, 1996

5. S.Kramp, N.Pyka, M. Loewenhaupt, M. Rotter *Bestimmung der F3-Phase in einem $NdCu_2$ Einkristall*, DPG Frühjahrstagung, Münster, März 1997

6. M.Loewenhaupt, M. Doerr, L. Jahn, T. Reif, C.Sierks, M.Rotter *Magnetic phase diagram and Ising-axis conversion of $DyCu_2$*, ICM, Sydney,Juli 1997

7. M.Rotter, E. Gratz, H. Müller, A. Kottar *Magnetische Instabilitäten in RNi_2 Verbindungen (R=Seltene Erde)*, DPG Frühjahrstagung, Münster, März 1997

8. M. Loewenhaupt, M. Doerr, L. Jahn, T. Reif, C. Sierks, M. Rotter *Magnetic Phase diagram and Ising axis conversion of $DyCu_2$* ICM, Sydney, Juli 1997

9. M. Doerr, M.Loewenhaupt, L. Jahn, A. Schneidewind, M.Rotter *Phasendiagramm und Konversion der magnetischen Ising Achse in $DyCu_2$ Einkristallen*, DPG Frühjahrstagung, März 1998, Regensburg

10. S. Kramp, N.M. Pyka, M. Loewenhaupt, M. Rotter, W. Schmidt, R. van de Kamp *Anisotropic Magnetic Coupling in* $NdCu_2$ 43rd Annual Conference on Magnetism and Magnetic Materials, November 1998, Miami, Florida

11. S. Kramp, M. Rotter, N. Pyka, M. Loewenhaupt, W. Schmidt, R. van de Kamp *Anisotrope magnetische Kopplung in $NdCu_2$ – eine Untersuchung mit inelastischer Neutronenstreuung* Deutsche Neutronenstreutagung, Potsdam, 25.-27.5.99

12. M. Loewenhaupt, M. Rotter, S. Kramp *Magnetische Anisotropien in Selten – Erd – Verbindungen* Deutsche Neutronenstreutagung, Potsdam, 25.-27.5.99

13. M. Rotter, A. Lindbaum, E. Gratz, G. Hilscher, H. Sassik, H. Müller, *Magnetic and Magnetoelastic properties of $GdCu_2$* 22^nd International conference on low temperature physics, Helsinki, Finland, 4.-11.8.99

14. M. Rotter, M. Loewenhaupt, A. Schneidewind, A. Lindbaum, E. Gratz, H. Sassik, M. T. Fernandez *The magnetic structure of $GdCu_2$* 22^nd International conference on low temperature physics, Helsinki, Finland, 4.-11.8.99

15. M. Doerr, M. Rotter, M. Loewenhaupt, T. Reif, P. Svoboda *Giant magnetostriction in $TbCu_2$ and $DyCu_2$ Crystals* 22^nd International conference on low temperature physics, Helsinki, Finland, 4.-11.8.99

16. M. Loewenhaupt, M. Rotter, S. Kramp *Magnetic anisotropies of rare earth compounds* 2^nd European conference on neutron scattering, Budapest, Hungary, 1.-4.9.99

17. M. Rotter, M. Loewenhaupt, S. Kramp *Anisotropic long range interactions in $NdCu_2$* 2^nd European conference on neutron scattering, Budapest, Hungary, 1.-4.9.99

18. R. Hauser, E. Bauer, L. Naber, M. Rotter, H. Michor, G. Hilscher, M. G. Berisso, P. Pedrazzini, J. Sereni, N. Tsujii, K. Yoshimura, S. Schmidt, F. Reinert *From an Intermediate Valence State towards non- Fermi Liquid Properties in Yb-based Compounds* 5^th Prague Colloquium on f-Electron Systems (2000)

19. M. Rotter, A. Lindbaum, E. Gratz, H. Müller, G. Hilscher, H. Michor H. Sassik, M. Loewenhaupt, A. Schneidewind, A. Stunault, H. E. Fischer, M. T. Fernandez, A. Hiess *Magnetische Ordnung in $GdCu_2$* DPG Frühjahrstagung Regensburg (2000)

20. U. Witte, M. Rotter, K. Prokes, M. Loewenhaupt *Das Sättigungsverhalten des Ce- Momentes im Kondo Gitter $CeCu_2$* DPG Frühjahrstagung Regensburg (2000)

21. A. Dreyhaupt, M. Doerr, A. Kreyssig, K. Krug, M. Rotter, E. Ressouche, K. Winzer, M. Loewenhaupt *Magnetisches Phasendiagramm von $DyNi_2B_2C$* DPG Frühjahrstagung Regensburg (2000)

22. A. Berg, M. Rotter, H. Langenberger, S. Grampp, E. Moser *High Resolution MR Imaging and Texture Analysis to differentiate osteoporotic Bone Structure* International Society for Magnetic Resonance in Medicine 8^th meeting,Denver,USA (2000)

23. O. Chernyavski, K. Prokes, V. Sechovski, P. Svoboda,M. Doerr, M. Rotter, M. Loewenhaupt,A. Goukassov *Field Induced Irreversibilities in an Itinerant 5f Electron Antiferromagnet*, Nato Advanced Study Institute: Modern Trends in Magnetostriction - Study and Application, Kyiv, Ukraine (2000)

24. M. Doerr, M. Loewenhaupt, M. Rotter, R. Kratz, H. Krug, D. Eckert, H. Siegel, P. Verges *Anomalous Magnetic Behaviour of $NdCu_2$ in High Magnetic Fields*, RHMF2000 , Porto, Portugal

25. S. Kramp, M. Rotter, M. Loewenhaupt, N. M. Pyka, W. Schmidt, R. van de Kamp *Spin Waves in the Ferrimagnetic Phase of $NdCu_2$*, ICM 2000, Brazil

26. M. Loewenhaupt, M. Doerr, M. Rotter, T. Reif, A. Schneidewind, A. Hoser *Magnetic field induced Ising axis conversion in $Tb_{0.5}Dy_{0.5}Cu_2$ single crystals* Ising Centannial Colloquium (2000),Belo Horizonte, Brazil

27. A. Berg, M. Rotter, H. Langenberger, E. Moser *Hochortsauflösende MR-Bildgebung an einem Hochfeld-Ganzkoerpersystem: Methoden und Anwendungen*, COST B11 meeting - Heidelberg 19-21 October 2000

28. M. Rotter *Spin-Spin Exchange in Gd Compounds*, Round Table Session, 6.-7.12.2000, Saclay, France

29. V. Sechovsky, K. Prokes, P. Svoboda, O. Syhchenko, O. Chernyavski, H. Sato, T. Fujita, T. Suzuki, M. Doerr, M. Rotter, M. Loewenhaupt, A. Goukassov *Magnetic field induced irreversibility in UNiAl* The 8^{th} Joint MMM-Intermag Conference (2001), San Antonio, Texas

30. M. Rotter "Mcphase- a Simulation Tool for Magnetic Properties of Solids", Korrelationstage 2001 (14.-17.2.01), Max-Planck-Intitut für Physik Komplexer Systeme, Dresden

31. M. Rotter, N. M. Pyka, M. Loewenhaupt, R. Schedler *McStas Simulation for PANDA*, Deutsche Neutronenstreutagung, 19.-21.2.2001, Juelich, Germany

32. M. Rotter, M. Doerr, P. Svoboda, C. Ritter, M. Loewenhaupt *Anomalous Magnetic Exchange Interactions in Sm Compounds ?*, Deutsche Neutronenstreutagung, 19.-21.2.2001, Juelich, Germany

33. A. Sippel, M. Loewenhaupt, O. Isnard, R. Bewley, L. Jahn, M. Rotter *Inelastic neutron scattering experiments on $^{154}Sm_2Fe_{17}N_x$ and $Gd_2Fe_{17}D_x$ - a method to trace magnetic interactions in permanent magnets* Deutsche Neutronenstreutagung, 19.-21.2.2001, Juelich, Germany

34. M. Doerr, M. Rotter, P. Svoboda, M. Loewenhaupt *Magnetic field induced change of lattice symmetry in rare earth intermetallics* ILL-Millenium Symposion, Grenoble, April 2001

35. H. Langenberger, M. Rotter, A. Berg, S. Grampp, H. Imhof, E. Moser *Autokorrelationsanalyse in hochaufgelösten MR-Bildern, eine Methode zur Strukturbewertung von osteoporotischem Knochen* , 82. Röntgenkongress, Gemeinsame Jahrestagung der DRG und ÖRG Wiesbaden, 23.-26.5.2001

36. P.Svoboda, J.Vejpravova, M.Hofmann, R.Schneider, M.Rotter, M.Doerr, M.Loewenhaupt, *Antiferromagnetic ordering in $TmCu_2$* 11th Czech and Slovak Conference on Magnetism, Kosice, 20.-23.8.2001

37. J.Vejpravova, P.Svoboda, D. Rafaja, I. Cisarova, M.Rotter, M.Doerr, M.Loewenhaupt, *Crystal growth and magnetic properties of $SmCu_2$* 11th Czech and Slovak Conference on Magnetism, Kosice, 20.-23.8.2001

38. M. Rotter, S. Kramp, M. Loewenhaupt, E. Gratz, W. Schmidt, N.M. Pyka, B. Hennion *Magnetic Excitations in the antiferromagnetic phase of $NdCu_2$* , International Conference on Neutron Scattering, München, 9.-13.9.2001

39. P.Svoboda, J.Vejpravova, M.Rotter, M.Doerr, M.Loewenhaupt, M.Hofmann, R.Schneider *Complex magnetic phase diagram of $TmCu_2$* International Conference on Neutron Scattering, München, 9.-13.9.2001

40. R. Schedler, M. Rotter, M. Loewenhaupt, N.M. Pyka *Monte Carlo Simulation of the cold triple axis spectrometer at the FRM-II* International Conference on Neutron Scattering, München, 9.-13.9.2001

41. A. Berg, M. Rotter, H. Langenberger, E. Moser *MR- basierte Methoden zur strukturellen Charakterisierung osteoporotischer Knochen* 51. Jahrestagung der Österreichischen Physikalischen Gesellschaft, TU Wien, 17.-21.9.2001

42. M. Rotter, M. Doerr, M. Loewenhaupt *Modeling Magentostriction in RCu_2 Compounds using McPhase*, Conference on Magnetism and Magnetic Materials, Seattle, Washington, Nov 2001

43. M.Rotter, A. Schneidewind, M. Doerr, M. Loewenhaupt, M. Frontzeck, E. Faulhaber,A. Hiess, D. Mannix, C. Detlefs *Magnetic Structure of $GdCu_2$* ESRF - User Meeting, Grenoble, 13.2.2002

44. U. Witte, M. Rotter, R. Schedler, M. Loewenhaupt, W. Schmidt *Field dependence of spin waves in the Kondo lattice $CeCu_2$* SCES-02, Krakow, July 10-13, 2002

45. J.Vejpravova, P.Svoboda, M.Rotter, M.Doerr, M.Loewenhaupt, R. Schneider *Magnetic Structures of $TmCu_2$* ESS European Conference, Bonn, May 16-17 2002

46. M. Rotter, M. Doerr, M. Loewenhaupt , R. I. Bewley, R. S. Eccleston, W. Kockelmann, A. Schneidewind, G. Behr *Pressure dependence of magnetism and dynamic response in $TbCu_2$* ESS European Conference, Bonn, May 16-17 2002

47. N. M. Pyka, M. Rotter, M. Loewenhaupt, R. Schedler, R. Sprungk, E. Kaiser, D. Etzdorf, V. Christoph *The polarised cold neutron trhee-axis spectrometer PANDA at the FRM-II* ESS European Conference, Bonn, May 16-17 2002

48. M. Rotter, M. Doerr, M. Loewenhaupt, A. Lindbaum, H. Sassik, H. Mueller, E. Gratz, H. Michor, A. el. Massalami *Magnetoelastic Properties of Gd Compounds* 6^{th} Prague Colloquium on f-electron systems, Charles University, Prague, July 5-9 2002

49. R. Schedler, M. Rotter, M. Doerr, M. Loewenhaupt, U. Witte *Field dependence of spin waves and magnetic phase diagram of the Kondo Lattice $CeCu_2$* International Conference on Strongly Correlated Electron Systems (SCES02), Krakow, Poland, July 10-13 2002

50. V. Sechovsky, F. Honda, P. Svoboda, M. Doerr, M. Rotter, M. Loewenhaupt *Antiferromagnetism and magnetoelasticity of UNiAl* International Conference on low temperature physics (LT23), Hiroshima, Japan, 20.-27.8.2002

51. J. Vepravova, P. Svoboda, M. Rotter, M. Doerr, M. Loewenhaupt *Thermodynamic properties of $SmCu_2$* International Conference on low temperature physics (LT23), Hiroshima, Japan, 20.-27.8.2002

52. M. Doerr, M. Rotter, M. Ellerby, A. Markosyan, S. Sazena, M. Loewenhaupt *Pressure Dependent Magnetization of $DyCu_2$ Single Crystals* International Conference on low temperature physics (LT23), Hiroshima, Japan, 20.-27.8.2002

53. M. Rotter M. Doerr, A. Lindbaum, B. Beuneu, K. Ziebeck, M. Loewenhaupt *Magnetic Structure of $GdCu_2In$* DPG Frühjahrstagung Dresden (2003)

54. R. Schedler, M. Rotter, U. Witte, P. Svoboda, J. Kulda, M. Loewenhaupt *Magnetic Properties of $CeCu_2$ at low temperatures* DPG Frühjahrstagung Dresden (2003)

55. M. Doerr, P. Wisniewski, M. Rotter, M. Loewenhaupt *MAgnetostriction of the ferromagnetic uranium compounds U_3P_4 and U_3As_4* DPG Frühjahrstagung Dresden (2003)

56. M. Doerr, C. Pfleiderer, J. Boeuf, M. Rotter, N. Kozlova, D. Eckert, K. H. Müller, M. Loewenhaupt *High-Magnetic Field Study of the Itinerant-Electron Antiferromagnets Mn_3Si, CuMnSb and PdMnTe* International Conference on Research in High Magnetic Fields (RHMF), Toulouse, July 2003

57. M. Rotter *Using McPhase to Calculate Magnetic Phase Diagrams of Rare Earth Compounds* International Conference on Magnetism (ICM), July 2003

58. K. Hense, U. Witte, M. Rotter, R. Schedler, E. Gratz, H. Nowotny, M. Loewenhaupt *Comparison of the CF induced phonon shifts in $CeCu_2$ and $NdCu_2$* International Conference on Magnetism (ICM), July 2003

59. M. Rotter, A. Schneidewind, M. Doerr, M. Loewenhaupt, M. el Massalami, H. Michor, G. Hilscher, C. Detlefs *Interpreting Magnetic X-ray Scattering of Gd-Compounds using the McPhase Simulation Program* Polarized Neutrons and Synchrotron X-ray for Magnetism (PNSXM), Venice, Italy, 4.-6.8.2003

60. A. Schneidewind, A. Kreyssig, C. Detlefs, A. Hiess, M. Rotter, M. Loewenhaupt *Magnetic X-ray Diffraction of $Tb_{0.5}Dy_{0.5}Cu_2$* Polarized Neutrons and Synchrotron X-ray for Magnetism (PNSXM), Venice, Italy, 4.-6.8.2003

61. M. Rotter, M. Doerr, M. Loewenhaupt, A. Lindbaum, H. Sassik, K. Ziebeck, B. Beuneu *Diffraction experiments on Gd - compounds using hot neutrons*, European Conference on Neutron Scattering (ECNS), Montpellier, France (2003)

62. R. Schedler, U. Witte, M. Rotter, M. Doerr, M. Loewenhaupt, J. Kulda *$CeCu_2$-Crystal Field Transition Matrix Elements Determined by Polarized Neutron Spectroscopy* European Conference on Neutron Scattering (ECNS), Montpellier, France (2003)

Experimental Reports

1. E. Gratz, M. Rotter, M. Loewenhaupt, S. Kramp, *Spin waves in $NdCu_2$* ILL Experimental Report IN12 4-03-891 (1996)

2. E. Gratz, M. Loewenhaupt, T. Reif, M. Rotter, P. Svoboda *Commensurate-incommensurate magnetic transition and diffuse magnetic scattering in $NdCu_2$* ILL Experimental Report D10 5-41-35(1996)

3. S. Kramp, N. Pyka, M. Rotter, *Spin waves in $NdCu_2$ in applied magnetic field* BENSC Experimental Report (1997)

4. S. Kramp, N. Pyka, M. Rotter, M. Loewenhaupt, *Temperature dependence of the spin wave gap in $NdCu_2$* ILL Experimental Report IN12, CRG/KFA 30 (1997)

5. M. Rotter, S. Kramp, N. Pyka, M. Loewenhaupt *Anisotropic spin waves in $NdCu_2$* ILL Experimental Report IN12 4-03-963 (1997)

6. E. Gratz, A. Lindbaum, M. Rotter *Magnetic structure investigation of $GdCu_2$* ILL Experimental Report D9 5-41-85 (1997)

7. S. Kramp, M. Loewenhaupt, N. Pyka, M. Rotter *The spin wave gap - important feature in the excitation spectrum of $NdCu_2$* ILL Experimental Report IN12 CRG-301 (1998)

8. S. Kramp, M. Loewenhaupt, N. Pyka, M. Rotter *Spin waves in the ferrimagnetic phase F1 of $NdCu_2$* ILL Experimental Report IN12 4-03-1037 (1998)

9. S. Kramp, M. Rotter *High field phase transitions and spin dynamics in $NdCu_2$* BENSC Experimental Report (1999)

10. P. Svoboda, M. Doerr, M. Loewenhaupt, M. Rotter *Crystal Structure of the Normal and Converted Phase of $DyCu_2$*, ILL Experimental Report D15 5-15-457 (1999)

11. M. Rotter, M. Loewenhaupt, U. Witte *The magnetic structure of $CeCu_2$* BENSC experimental report PHY-01-803 (1999)

12. A. Schneidewind, T. Gleisberg, M. Loewenhaupt, A. Hiess, S. Kramp, Th. Reif, M. Rotter, E. Gratz *Magnetic Structure and magneto-elastic coupling in RCu_2-systems (R=Gd, Tb, Dy)* ESRF Experimental Report HE-485, BM28 (2000)

13. U. Witte, M. Rotter, M. Loewenhaupt *The crystallographic structure of $CeCu_2$* BENSC experimental report PHY-01-836 (2000)

14. M. Rotter, M. Loewenhaupt, H. Sassik *Magnetic Structure of $SmCu_2$*, ILL Experimental Report D1B 5-31-1173 (2000)

15. U. Witte, M. Rotter, M. Loewenhaupt *Crystal field - phonon coupling in $CeCu_2$* 1T1, LLB experimental report 30.10-7.11.2000

16. S. Kramp, M. Rotter *The Conversion Process in $NdCu_2$ in High Magnetic Field* BENSC experimental report PHY-02-258 (2000)

17. M. Rotter, M. Doerr, M. Loewenhaupt *Pressure dependence of the Crystal Field in Giant Magnetostriction Compounds* ISIS experimental report, HET, RB 12082 (2000)

18. R. Hauser, M. Rotter *Itinerant metamagnetism in $Er_{1-x}Y_xCo_2$* ISIS experimental report, ROTAX, RB 12123 (2000)

19. M. Rotter, A. Lindbaum, M. Ellerby *Magnetic and quadrupolar order in $Pr_{1-x}Nd_xCu_2$* ISIS experimental report, ROTAX, RB 11556 (2000)

20. M. Rotter, M. Doerr, M. Loewenhaupt, A. Lindbaum, E. Gratz, H. Sassik *Spin-Spin exchange in Gd Compounds* LLB experimental report,Saclay, 7C2 - 6120, 21.6-26.6.2001

21. M. Rotter, U. Witte, A. Solodovnikov, M. Loewenhaupt *Anisotropic magnetic exchange in $CeCu_2$* ILL experimental report, IN12, CRG- 578 (2001)

22. A. Schneidewind, M. Rotter, A. Hiess, M. Frontzeck, M. Loewenhaupt *Investigation of the magnetic structure of $GdCu_2$*, BM28 ESRF experimental report HE-1062 (2001)

23. M. Rotter, M. Doerr *The Pressure Dependence of the Magnetic Structure of $TbCu_2$* ISIS Experimental report RB 13570 (2001)

24. U. Witte, R. Schedler, M. Rotter *Crystal field - phonon coupling in $CeCu_2$* ILL Experimental Report 4-03-1258 (2002)

Themenvorschläge für die Probevorlesung

1. **Physik der Musikinstrumente**
2. **Autokorrelationsanalyse von MRI Bildern**
3. **Monte Carlo Simulation von Neutronenstreuexperimenten**

Vorschläge für Gutachter:

- **Prof. K. Becker, TU - Dresden**
- **Prof. E. Gratz, TU – Wien**
- **Prof. J. Jensen, Universität Kopenhagen**
- **Prof. M. Loewenhaupt, TU – Dresden**
- **Prof. K. McEwen, Universität London**
- **Prof. V. Sechovsky, Karlsuniversität – Prag**
- **Prof. F. Steglich, MPI - Dresden**

Erklärung:

Ein an die Fakultät für Naturwissenschaften zu übersendendes Führungszeugnis nach § 30 Abs. 5 Bundeszentralregistergesetz wurde bei der zuständigen Meldenbehörde beantragt.

Dresden,

Dipl. Ing. Dr. Martin ROTTER

Hochschulstr. 13/302
D-01069 Dresden
Tel.: +49 177 913 8989, +43 676 671 3936
Fax.: +43 2243 37987
E-Mail: rotter@physik.tu-dresden.de
web: www.mcphase.de , www.physik.tu-dresden.de/iapd

Persönliche Daten

geboren am 21.9.1968 in Klosterneuburg, NÖ
Vater: Dr. Klaus Rotter, Physiker, emeritierter Vorstandsdirektor der Felten & Guillaume AG
Mutter: Mag. Rosemarie Rotter, geb. Dietrich, Gymnasiallehrerin (Mathematik, Physik) in Pension
Österreichische Staatsbürgerschaft
seit 1998 verheiratet mit Dr.iur.Edith Zeller, Verwendung im höheren Dienst, Unabhängiger Verwaltungssenat Wien
Wehrersatzdienst geleistet vom 1/2/1998 bis 31/1/1999 im Allgemeinen Krankenhaus Wien

Sprachen:
- *Deutsch (Muttersprache)*
- *Englisch (fließend)*
- *Russisch (Matura)*
- *Italienisch (Konversationsniveau)*

Schulausbildung

1974 – 1986: Volksschule in Schrems, NÖ,
Neusprachliches Gymnasium Gmünd, NÖ, Matura mit Auszeichnung.

1986 - 1991: Studium der Technischen Physik and der Technischen Universität Wien,
Diplomarbeit auf dem Gebiet der Tieftemperatur-Röntgenbeugung,
Sponsion mit Auszeichnung.

1992 - 1994: Auslandsstipendium am Birkbeck College (Universität London),
Dissertation “Thermische Ausdehnung von Selten-Erd-Verbindungen” an der Technischen Universität Wien, Promotion mit Auszeichnung.

1986 - 1990: Studium der Instrumentalpädagogik Klarinette und Klavier an der Hochschule für Musik und darstellende Kunst Wien,
Lehrbefähigungsprüfung.

W e i t e r b i l d u n g

Felten & Guillaume AG, Schrems 1984
Lehrwerkstätte
1 Monat Ferialpraktikum

Wylex, Manchester UK 1985
Elektrotechnisches Labor
1 Monat Ferialpraktikum

Felten & Guillaume AG, Schrems 1988
Entwicklungslabor
1 Monat Ferialpraktikum, Schaltgeräte

Siemens AG, Wien 1990
Software - Entwicklung
2 – monatiges Ferialpraktikum

Hochschule für Musik und darstellende Kunst Wien 1990-92
Postgraduiertes Studium Instrumentalpädagogik Klarinette und Klavier

Technische Universität Wien 1994-95
Studium des Technischen Umweltschutzes

Universität Wien 1995-98
Studium der Medizinphysik
parallel zum Wehrersatzdienst (1998) wissenschaftliche Arbeiten auf dem Gebiet der Magnetresonanz - Bildgebung

B e r u f s e r f a h r u n g

Technische Universität Wien *1993 - 1994*
Institut für Experimentalphysik, wissenschaftlicher Mitarbeiter
Forschungsprojekt: "Kapazitive Messung der thermischen Ausdehnung und Magnetostriktion von intermetallischen Verbindungen", Doktorarbeit

Technische Universität Dresden *1995 - 1996*
Institut für Angewandte Physik und Didaktik, Gastwissenschaftler
Aufbau eines Dilatometers (Feld/Temperaturbereich 0-17T/0.3-300K), Mitarbeit bei der Neugestaltung der Forschungslabors und der Formierung des Sonderforschungsbereichs 463 der Deutschen Forschungsgemeinschaft („Seltenerd-Übergangsmetall-Verbindungen: Struktur - Magnetismus - Transport")

Technische Universität Wien *1996 - 1998*
Institut für Experimentalphysik, wissenschaftlicher Mitarbeiter (Post-Doc)
Forschungsprojekt: „Feldinduzierte Magnetostriktionsmessung mittels Kapazitäts-Dilatometrie", Entwicklung eines Miniatur - Dilatometers

Technische Universität Dresden *seit März 1999*
Institut für Angewandte Physik und Didaktik, wissenschaftlicher Mitarbeiter (Post-Doc)
Drittmittelprojekt zur Errichtung von PANDA, dem kalten Dreiachsenspektrometer mit polarisierten Neutronen an der Forschungs-Neutronenquelle FRM-II (München): Koordination von Konstruktion und Aufbau des Sekundärspektrometers.
Entwicklung von McPhase, einem Molekularfeld - Monte - Carlo Programm zur Berechnung magnetischer Phasendiagramme, mikro- und makroskopischer magnetischer Eigenschaften einschließlich magnetischer Anregungen.
Aufbau eines Meßplatzes zur Herstellung und Charakterisierung dünner Schichten mit Hilfe des magnetooptischen Kerr - Effekts.
Habilitation, das formelle Verfahren läuft seit Jänner 2003.

Universität Wien *seit August 2002*
Institut für Physikalische Chemie, wissenschaftlicher Mitarbeiter (Post-Doc)
Aufbau einer Arbeitsgruppe zur Neutronenstreuung an thermoelektrischen Materialien

Veröffentlichungen

66 Artikel in referierten Zeitschriften
17 Vorträge
62 Konferenzbeiträge (davon 1 eingeladen)

Stipendien und Preise

2 Leistungsstipendien (TU Wien)
1 Auslandsstipendium (London 1992) des BMWF

Lehrtätigkeit

TU Wien: Metallphysik - Praktikum, Physikalisches Praktikum

TU Dresden: Physikalisches Praktikum, Physikalische Seminare, Vorlesungsvertretung (Neutronenstreuung, Festkörpermagnetismus), Vorlesung „Neutronenstreuung" (SS 2003)

Universität Wien: Vorlesung „Einführung in die Neutronenstreuung" (SS 2003)

Spontaneous magnetoelastic effects in Gadolinium compounds, file: gdrev_f.tex

A. Lindbaum [a,1] and M. Rotter [b,2]

[a] *Institut für Festkörperphysik, Technische Universität Wien, Wiedner Hauptstrasse 8-10/138, A-1040 Wien, Austria*

[b] *Institut für Angewandte Physik, Technische Universität Dresden, D-01062 Dresden, Germany*

Abstract

The spontaneous magnetoelastic effects in Gd compounds are reviewed showing that the strain dependence of the magnetic exchange interactions leads to significant effects. These effects are equal in magnitude to well established single ion contributions in other rare earth compounds with non vanishing orbital momentum (coming from the strain dependence of the crystal field). In some cases the exchange contribution can produce giant magnetostriction (GMS) or induce structural phase transitions. In order to extract the influence of the Gd-Gd exchange interactions, we consider only Gd compounds with partner elements showing no or only weak induced magnetic moments. The current status of the theory is presented and compared to measurements performed by temperature dependent x-ray diffraction and results of dilatometric measurements.

Key words: Pacs Magnetostriction 75.80

Contents

[1] E-mail: andreas.lindbaum@ifp.tuwien.ac.at

[2] E-mail: rotter@physik.tu-dresden.de

1 Introduction

In the past decade research on Gd compounds has been of interest for several reasons. They are ideal model systems for the study of exchange interactions which are not disturbed by the crystal field (Fontcuberta et al., 1997; Hernando et al., 1996). Recently Köbler et al. (1998, 1999b) showed that it is necessary to consider higher order exchange interactions to account for the behaviour of several ferromagnetic and antiferromagnetic systems with vanishing orbital momentum. New experiments indicate that the temperature dependence of the spontaneous magnetization may not be described by the well known Bloch law (Köbler et al., 1999a).

Another interesting and often surprising point is that the spontaneous magnetoelastic effects in Gd compounds have been found to be of the same magnitude as in other rare earth compounds (Gratz and Lindbaum, 1994). This shows that the contribution of the exchange interaction to the magnetoelastic Hamiltonian is of equal importance as the crystal field contribution and varies over several orders of magnitude: as an example, in Gd_2In the spontaneous magnetoelastic effects are smaller than 10^{-4}, whereas GdNi exhibits spontaneous magnetostriction effects of more than one percent (Gratz and Lindbaum, 1998) and can therefore be classified as a GMS (giant magnetostriction) system. A further important family of GMS systems are the $Gd_5(Si_xGe_{1-x})_4$ compounds. In some of these compounds so-called *magnetostructural transitions* have been observed, i.e. the giant spontaneous as well as forced magnetoelastic effects can be connected with structural transitions (Morellon et al., 1998a, 2000).

It should be pointed out that also in compounds based on other rare earths it was necessary to consider not only the crystal field interactions, but also the contribution of the exchange interactions, in order to understand the observed magnetostrictive effects (e.g. in the case of $NdCu_2$ - see Rotter et al. (2002)). However, in Gd compounds this exchange contribution can be studied without any ambiguity arising from the crystal field interaction, because $L = 0$ for Gd^{3+}.

Due to the large absorption of thermal neutrons by the natural Gd isotope, neutron diffraction experiments are difficult. Therefore the magnetic structures are often unknown and in many cases no model for the spontaneous magnetostriction could be developed. A number of attempts have been made to extract information about the magnetic structure from specific heat experiments (Rotter et al., 2001b; Mallik and Sampathkumaran, 1998; Bouvier et al., 1991; Blanco et al., 1991) and recently magnetic x-ray scattering using synchrotron radiation has opened new possibilities (Detlefs et al., 1996; Rotter et al., 2000b).

The main subject of the present chapter is to review available experimental studies of spontaneous magnetoelastic effects in intermetallic Gd compounds. The aim is to show that the magnetic exchange interactions can lead to a wide variety of spontaneous magnetoelastic effects, including pronounced negative and positive magnetovolume effects as well as large anisotropic effects. Note: with *positive* (*negative*) effects we always mean that in the magnetically ordered state the corresponding lattice

parameter or the volume is *larger* (*smaller*) than the values obtained by extrapolation from the paramagnetic temperature range. This means: with *positive* or *negative* we mean the sign of the magnetostrictive strains, which are defined relative to the paramagnetic range (and not the sign of the magnetic contribution to the thermal expansion *coefficient*).

The concept of exchange-striction was already introduced by Callen and Callen (1965), however, up to now only few studies on this subject are available. In order to extract the influence of the magnetic exchange interactions, we consider only Gd compounds with partner elements, which show no or only very small induced magnetic moments. This means that we exclude for instance compounds with Co, Fe or Mn, whereas compounds with Ni showing only weak induced magnetic moments are included in our study. For a review of thermal expansion anomalies and spontaneous magnetostriction in rare-earth intermetallics with Co and Fe the reader is referred to the chapter of Andreev (1995). Invar effects in transition metals and alloys have been reviewed by Wasserman (1990). The reader is also referred to the review by Morin and Schmitt (1990), dealing generally with magnetoelastic effects in rare earth intermetallics, including two ion as well as single ion magnetic interactions, with a special emphasis on quadrupolar interactions. The present chapter is complementary to these reviews and concentrates on spontaneous magnetoelastic effects caused by the Gd-Gd magnetic exchange interaction in non-cubic systems. It should contribute to a more complete picture of magnetoelastic effects.

The chapter is organized as follows: Section 2 gives a short account of the most important experimental methods used for the measurement of magnetically induced effects on the crystal structure. The current state concerning the microscopic theory of magnetoelastic effects in Gd systems is reviewed in section 3. Then some selected results for cubic systems are presented, showing that not only symmetry conserving effects (section 4: magnetovolume effects) are possible, but also very small distortions of the symmetry (section 5). Then follows in section 6 to 9 the main part of the chapter, namely a review of spontaneous magnetoelastic effects in non-cubic systems from hexagonal to monoclinic, showing a wide variety of anisotropic (but symmetry conserving) effects, as well as magnetovolume effects. Finally, all the presented results are summarized and discussed in section 10.

2 Experimental methods

X-ray diffraction at variable temperatures, on the one hand, and thermal expansion measurements using dilatometric methods, on the other hand, are the two most important experimental methods for measuring spontaneous magnetoelastic effects. The main advantage of the x-ray diffraction method lies in the direct measurement of the lattice parameters, allowing the determination of anisotropic effects also in polycrystalline samples. Especially distortions of the crystal symmetry can easily be detected by this method. However, the resolution of x-ray diffraction is much smaller than that of dilatometry using the capacitance or interferometric method. When good and well oriented single crystals are available, the dilatometric method is very reliable and much more sensitive than x-ray diffraction in measuring isotropic effects (volume effects) as well as anisotropic effects. However, the detection of spontaneous distortions of the crystal symmetry is difficult when using dilatometric methods. A review of the most common types of capacitance dilatometers was given by Rotter et al. (1998). Depending on the temperature a resolution of $\Delta l/l$ from 10^{-10} to 10^{-9} is possible. The resolution of the x-ray diffraction method is only about 10^{-5} to 10^{-4}, i.e. when no effects are visible in the x-ray results, this means only that the effects are smaller than about this value. The high sensitivity makes the capacitance method one of the best tools for detecting phase transitions. But due to thermal hysteresis effects in the dilatometer materials absolute measurements of length differences for large temperature intervals are less reliable than with the x-ray method. In addition, in many cases the intrinsic strains differ from the length changes measured on a macroscopic sample, due to grain boundaries, microstresses and lattice defects. For a very detailed review of all experimental methods used for thermal expansion measurements in solids the reader is referred to Taylor et al. (1998).

3 Microscopic Theory of Magnetoelastic Effects in Gd compounds

In order to analyze spontaneous magnetoelastic effects quantitatively it is first necessary to separate the magnetic contributions to the thermal expansion (i.e. the magnetostrictive strains) from the lattice contribution. This is usually done by comparison with a nonmagnetic isostructural reference compound or by extrapolating the temperature variation of the lattice parameters from the paramagnetic range by assuming a simple Debye model for the lattice contribution (see e.g. Barron et al. (1980)). Because in most of the cases presented in this chapter the latter method has been applied, we give a short account. According to Grüneisen rules, and assuming a quasiharmonic approximation together with a simple Debye model for the phonons and a classical γT electronic specific heat contribution, the following formula for the nonmagnetic contribution to the thermal expansion can be derived (see e.g. Lindbaum (1994)):

$$\epsilon_{nonmag} = \epsilon_{el} + \epsilon_{phon} = K_1 T^2 + K_2 T D(\Theta_D/T) \tag{1}$$

with

$$D(z) = \frac{3}{z^3} \int_0^z \frac{x^3 dx}{e^x - 1} \tag{2}$$

Here K_1, K_2 and the Debye temperature Θ_D are parameters which can be obtained by fitting (1) and (2) to the thermal expansion in the paramagnetic temperature range. The electronic contribution in (1), $\epsilon_{el} = K_1 T^2$, is usually much smaller than the lattice contribution ϵ_{phon}, i.e. in most cases it makes no difference when only ϵ_{phon} is taken into account for determining the nonmagnetic contribution to the thermal expansion.

We now turn to the main issue of this paragraph. Usually the magnetostriction of solids is analyzed within the framework of a phenomenological model which takes account of the crystal symmetry (Clark, 1980). Whereas this serves for practical purposes it is not possible to derive expressions for the temperature and magnetic field dependence of the strains. For such an analysis it is necessary to develop a microscopic theory of magnetoelastic effects. Whereas a lot of results have been derived for the single ion magnetoelastic effects (for an overview see Morin and Schmitt (1990)), much less attention has been paid to the effect of exchange interactions. However, already in the 60's the influence of the exchange interactions on the microscopic magnetoelastic properties have been discussed for ferromagnets and cubic crystals (Callen, 1968; Clark et al., 1965; Callen and Callen, 1963). Single ion and isotropic exchange contributions to the magnetostriction have been analyzed theoretically by Callen and Callen (1965) and it was shown how to get explicit expressions for the magnetostriction in different symmetries.

In the following short review of the microscopic theory of magnetoelastic effects caused by the exchange interactions we follow Morin and Schmitt (1990) and generalize it to the case of arbitrary magnetic structures and give general expressions valid for any crystal symmetry. We will neglect

the influence of the crystal field. The analysis is restricted to first order effects assuming that the magnetoelastic energy is small compared to the magnetic exchange energy. Furthermore any dynamical coupling between the lattice and the magnetic exchange (magnon-phonon interaction) will be neglected and we consider only the long wavelength static limit.

The analysis is based on the bilinear two ion exchange interaction $\mathbf{J}_i \, \overline{\overline{\mathcal{J}}} \, (ij) \mathbf{J}_j$ between the total angular momenta $\mathbf{J}$ of rare earth atoms on the sites i and j. This exchange interaction shows an anisotropy, which in the case of Gd compounds is expected to be small and mainly due to the classical dipole interaction (Jensen and Mackintosh, 1991). The exchange parameters $\overline{\overline{\mathcal{J}}} \, (ij)$ of the exchange Hamiltonian depend on the position of the atoms in the crystal - leading to *magnetoelastic interactions* (Morin and Schmitt, 1990). It is possible to calculate the magnetostrictive strains ϵ^α, if we assume, that the Hamiltonian may be written as a sum of exchange, Zeeman and elastic contributions.

$$\mathcal{H} = \mathcal{H}_{\text{ex}} + \mathcal{H}_{\text{Ze}} + E_{\text{el}} \tag{3}$$

$$\mathcal{H}_{\text{ex}} = -\frac{1}{2} \sum_{i,j(i \neq j)} \mathbf{J}_i \, \overline{\overline{\mathcal{J}}} \, (ij, \overline{\overline{\epsilon}}) \mathbf{J}_j \tag{4}$$

$$\mathcal{H}_{\text{Ze}} = -\sum_i g_J \mu_B \mathbf{J}_i \mathbf{H} \tag{5}$$

$$E_{\text{el}} = \frac{1}{2} \sum_{\alpha\beta} c_{\alpha\beta} \epsilon^\alpha \epsilon^\beta \tag{6}$$

Note that for the components ϵ^α of the strain tensor $\overline{\overline{\epsilon}}$ and for the elastic constants $c_{\alpha\beta}$ Voigt's abbreviated notation is adopted (i.e. $\alpha = 1, 2, 3, 4, 5, 6$ denote $11, 22, 33, 12, 13, 23$ respectively) - see e.g. Barron et al. (1980).

Starting point is the Taylor expansion of the magnetic exchange parameters with respect to the components of the strain tensor $\overline{\overline{\epsilon}}$, leading to the so-called magnetoelastic Hamiltonian.

$$-\frac{1}{2} \sum_{ij} \mathbf{J}_i \, \overline{\overline{\mathcal{J}}}(ij, \overline{\overline{\epsilon}}) \mathbf{J}_j \approx -\frac{1}{2} \sum_{ij} \mathbf{J}_i \, \overline{\overline{\mathcal{J}}}(ij, \overline{\overline{\epsilon}} = 0) \mathbf{J}_j - \frac{1}{2} \sum_{ij}^{\alpha} \epsilon^\alpha \mathbf{J}_i \, \overline{\overline{\mathcal{J}}}_{(\alpha)}(ij) \mathbf{J}_j + \cdots \tag{7}$$

with

$$\overline{\overline{\mathcal{J}}}_{(\alpha)} \, (ij) = \left[\frac{\partial \, \overline{\overline{\mathcal{J}}} \, (ij, \overline{\overline{\epsilon}})}{\partial \epsilon^\alpha} \right]_{\epsilon = 0} \tag{8}$$

Usually the analysis is limited to the first order in the strain (harmonic approximation) and second order terms (anharmonic coupling) are neglected. This second order magneto-elasticity has not been analyzed for the compounds under consideration.

By definition the Gibbs free energy is given by

$$F = -k_B T \ln Z \tag{9}$$

with the partition sum

$$Z = Tr\{e^{-\mathcal{H}/k_BT}\} \tag{10}$$

Here k_B denotes the Boltzmann constant. In our first order approach the trace in (10) is calculated using the states of the unperturbed system, i.e. without taking into account the magnetoelastic interactions, by putting $\bar{\bar{\epsilon}}= 0$ in (3)-(6). In practice, these eigenstates of the unperturbed system may be calculated by a mean field approach (Jensen and Mackintosh, 1991; Rotter et al., 2001b).

We now insert the Hamiltonian $\mathcal{H}$ into (9) and (10) and minimize the free energy F with respect to the strains ϵ^α by putting zero the derivative

$$\frac{\partial F}{\partial \epsilon^\alpha} = 0 \tag{11}$$

Using the elastic compliances $s^{\alpha\beta}$ which are related to the elastic constants by (see e.g. Barron (1998))

$$\sum_{\gamma=1}^{6} c_{\beta\gamma} s^{\gamma\alpha} = \delta_{\alpha\beta} \tag{12}$$

equation (11) yields the final result

$$\epsilon^\alpha = \frac{1}{2} \sum_{\beta,ij} s^{\alpha\beta} \langle \mathbf{J}_i \, \bar{\bar{\mathcal{J}}}_{(\beta)}(ij) \mathbf{J}_j \rangle_{T,\mathbf{H}} \tag{13}$$

Equation (13) shows that the complete temperature and field dependence of the strains can be calculated from static correlation functions $\langle J_i^\gamma J_j^{\gamma'} \rangle_{T,\mathbf{H}}$ (γ, γ' =1,2,3 label the cartesian components of the angular momentum $\mathbf{J}$) where $\langle\rangle_{T,\mathbf{H}}$ denote thermal expectation values (Callen and Callen, 1965). As already mentioned above, a mean field theory may be used to evaluate (13) and calculate the magnetostriction.

In some cases it is more convenient to Fourier transform this expression (13):

$$\epsilon^\alpha = \frac{1}{2} \sum_{\beta,\mathbf{q}} s^{\alpha\beta} \langle \mathbf{J}_{-\mathbf{q}} \, \bar{\bar{\mathcal{J}}}_{(\beta)}(\mathbf{q}) \mathbf{J}_{\mathbf{q}} \rangle_{T,\mathbf{H}} \tag{14}$$

with the definitions

$$\mathbf{J}_i = \sum_{\mathbf{q}} \mathbf{J}_{\mathbf{q}} \exp(-i\mathbf{q}\mathbf{R}_j) \tag{15}$$

$$\bar{\bar{\mathcal{J}}}_{(\beta)}\,(ij) = \sum_{\mathbf{q}} \bar{\bar{\mathcal{J}}}_{(\beta)}\,(\mathbf{q}) \exp[-i\mathbf{q}(\mathbf{R}_i - \mathbf{R}_j)] \tag{16}$$

In the case, that the magnetoelastic interaction is dominated by the isotropic contribution (i.e. $\bar{\bar{\mathcal{J}}}_{(\beta)}$ reduces to a scalar $\mathcal{J}_{(\beta)}$), coming from the strain dependence of the Heisenberg interaction (compare

the analysis of $GdCu_2$ in section 8.6), equations (13) and (14) reduce to

$$\epsilon^{\alpha} = \frac{1}{2} \sum_{ij} \left(\sum_{\beta} s^{\alpha\beta} \mathcal{J}_{(\beta)}(ij) \right) \langle \mathbf{J}_i \mathbf{J}_j \rangle_{T,\mathbf{H}} \tag{17}$$

$$\epsilon^{\alpha} = \frac{1}{2} \sum_{\mathbf{q}} \left(\sum_{\beta} s^{\alpha\beta} \mathcal{J}_{(\beta)}(\mathbf{q}) \right) \langle \mathbf{J}_{-\mathbf{q}} \mathbf{J}_{\mathbf{q}} \rangle_{T,\mathbf{H}} \tag{18}$$

In principle the correlation functions $\langle\rangle_{T,\mathbf{H}}$ in expressions (14) and (18) can be evaluated, if the Fourier transform of the magnetic moments is known (for instance from neutron diffraction experiments). Re-inserting (14) or (18) into the magnetoelastic interaction (7) results in higher order terms of magnetic interactions, which we have neglected in our discussion. Although not analyzed in detail by theory, experimental data gives some clear indication of the importance of higher order terms in the Hamiltonian of Gd compounds in both, the strains ϵ^{α} and the momenta $\mathbf{J}_i$. A compound near a structural instability such as the $Gd_5(Si_xGe_{1-x})_4$ system can only be described by considering higher order terms in the elastic energy. Recently Köbler et al. (1998, 1999a) have pointed out the importance of fourth order exchange interactions in compounds with pure spin magnetism (i.e. biquadratic, three spin and four spin interactions) such as GdMg and GdAg.

Additional comment deserve magnetostriction measurements near the ordering temperature T_C reflecting critical phenomena. Few data for critical expansion is available, such as have been reported by Dolejsi and Swenson (1981) for the case of Gd metal. The thermal expansion coefficient in the critical region should assume the form $|(T - T_C)/T_C|^{-\alpha}$. The critical exponent α should be the same as for the specific heat and depend only on the universality class (dimensionality, No. of degrees of freedom) of the system. For Gd metal this universality class has been determined recently by Frey et al. (1997).

A last point which has to be discussed are the magnetovolume effects caused by magnetic moments in the conduction band or of the d-electrons of partner elements like Ni. A simple model, based on the Stoner model for itinerant magnetism, shows that the kinetic energy increase associated with magnetic ordering in a band leads to a magnetic pressure P_M, which can be expressed by the following formula (Janak and Williams, 1976):

$$P_M = \frac{1}{2DV} \frac{\partial \ln D}{\partial \ln V} M^2 \tag{19}$$

where D, V and M denote the electronic density of states at the Fermi energy, the volume and the magnetic moment, respectively. Since the density of states increases with increasing volume (i.e. $\frac{\partial \ln D}{\partial \ln V} > 0$), the magnetic pressure P_M is positive, leading to a magnetically induced increase of the volume.

With this outlook on topics of current research we conclude the theoretical part of this chapter and turn to the discussion of available experimental data.

4 Magnetovolume effects in cubic systems

In this section some examples for spontaneous magnetovolume effects in cubic Gd based compounds will be presented. As will be discussed in section 5, in cubic systems also distortions of the crystal symmetry have been observed. In all cases of our knowledge these distortions are, however, very small compared to strains which conserve the crystal symmetry and which will be the main topic of the rest of this chapter. The symmetry breaking effects are so small that they probably can only be observed in the highly symmetric cubic systems, where the detection of such distortions is easier.

4.1 $GdAl_2$

$GdAl_2$ crystallizes in the pure C15 structure (cubic Laves phase, $MgCu_2$ type, space group $Fd3m$) without vacancies on the Gd sites, which lead to a superstructure of C15 in case of $GdNi_2$ (see section 4.2).

The magnetic properties of the RAl_2 compounds have been extensively investigated in the past. Within this series, $GdAl_2$ has the highest Curie temperature ($T_C \approx 168$ K) and is considered as a good example of a Heisenberg ferromagnet (du Tremolet de Lacheisserie, 1988; Taylor and Coles, 1975). Neutron diffraction experiments at 4.2 K gave a rather small magnetic moment on the Gd sites (6.6 μ_B) with a 0.6 μ_B moment in the conduction band (Abell et al., 1983). The magnetic anisotropy is very small (as expected for an S-state ion) and both NMR data (Kaplan et al., 1973) and torque measurements (Burd and Lee, 1977) indicate [111] as the easy magnetization direction.

Measurements of the thermal expansion using a strain gauge method (Pourarian, 1980) showed a negative magnetovolume effect, in agreement with measurements of du Tremolet de Lacheisserie (1988) using a tube type dilatometer. However there are discrepancies concerning the size of the effect: du Tremolet de Lacheisserie (1988) obtained a 0 K value of $(\Delta V/V)_{mag} \approx -1.16 \times 10^{-3}$, which is twice as large as the value of Pourarian (1980). Our own x-ray powder diffraction measurements (see Fig. 1) show also a negative magnetovolume effect, with a 0 K value of $(\Delta V/V)_{mag} \approx -1.4 \times 10^{-3}$, in good agreement with du Tremolet de Lacheisserie (1988). This large negative magnetovolume effect is very interesting and has to be attributed solely to the volume dependence of the (indirect) Gd-Gd exchange interaction, since the induced itinerant magnetic moment in the conduction band should lead to a positive magnetovolume effect. The x-ray diffraction experiments revealed no detectable line splitting or broadening, showing that there is no change of the cubic symmetry within the detection limit of about 1×10^{-4}. From forced magnetostriction experiments on a single crystal, also reported by du Tremolet de Lacheisserie (1988), a very small spontaneous trigonal distortion of about $(\Delta l/l)_{111} \approx 2 \times 10^{-5}$ could be deduced.

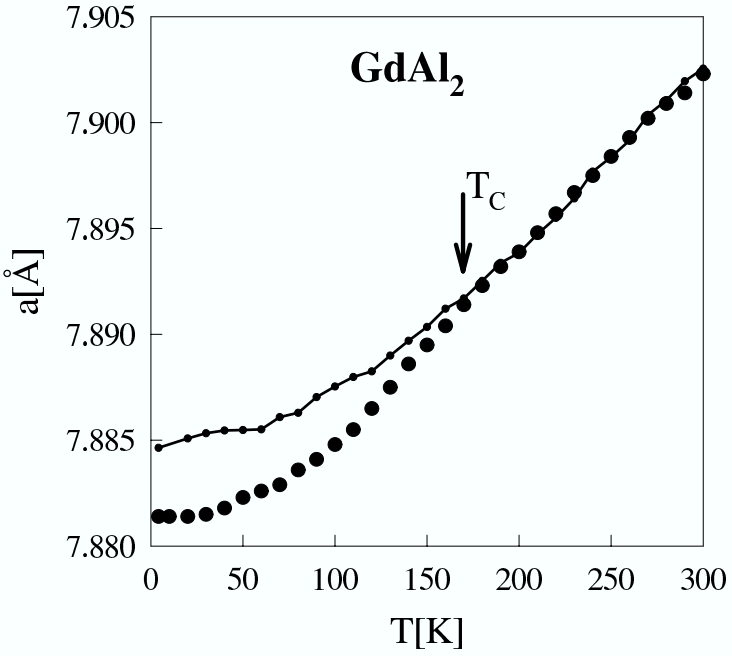

Fig. 1. Temperature variation of the cubic lattice parameter of $GdAl_2$ measured by x-ray powder diffraction (this work). The small points connected by a line indicate the corresponding values of the isostructural YAl_2 (nonmagnetic reference), scaled to coincide with $GdAl_2$ at 250 K, in order to allow a direct comparison.

4.2 GdNi$_2$

During the past decades (and frequently up to now) the RNi_2 compounds (R: rare earth element) have been reported to crystallize in the cubic Laves phase structure (C15). However, recent experimental as well as theoretical investigations showed that this is not true. Instead of showing the pure C15 structure, most of them (including $GdNi_2$) crystallize in a cubic superstructure of C15 with doubled lattice parameter due to ordered vacancies on the R sites. A single phase compound can only be obtained with the stoichiometry (1-δ):2 and can be described within space group $F\bar{4}3m$ with the 4a sites only partially occupied by the R atoms. The occupancy of the R 4a sites increases with decreasing radius of the R atom and reaches 1 for $LuNi_2$ (Latroche et al., 1990, 1993). This instability of the pure C15 structure in the RNi_2 compounds (i.e. the tendency towards the formation of vacancies) can be understood by space filling arguments. Recent theoretical investigations, based on *ab-initio* total energy calculations, showed that the vacancies at the R sites reduce the total energy, thus increasing the stability relative to the neighboring compounds in the R-Ni phase diagram (Lindbaum et al., 1999). The existence of ordered R-vacancies in the RNi_2 compounds is not only important for the understanding of the mechanisms stabilizing the crystal structure. They must also be taken into account when investigating other physical properties, like e.g. the magnetic structure. The ordered vacancies change the local environment of the R sites, leading to a symmetry change of the crystal field as well as the magnetic exchange interactions. As an example, recent investigations on $TbNi_2$ showed that the ordered vacancies on the Tb sites are responsible for a

temperature induced change of the magnetic structure at 14 K (Gratz et al., 1999a). An interesting property of the RNi_2 superstructures is a reversible temperature induced transition from ordered to disordered vacancies at high temperatures, first detected by anomalies in the transport properties and later directly observed by x-ray diffraction experiments (Gratz et al., 1996). Furthermore, recent high-pressure x-ray diffraction studies showed that there is also a pressure-induced order-disorder transition (Lindbaum et al., 2002).

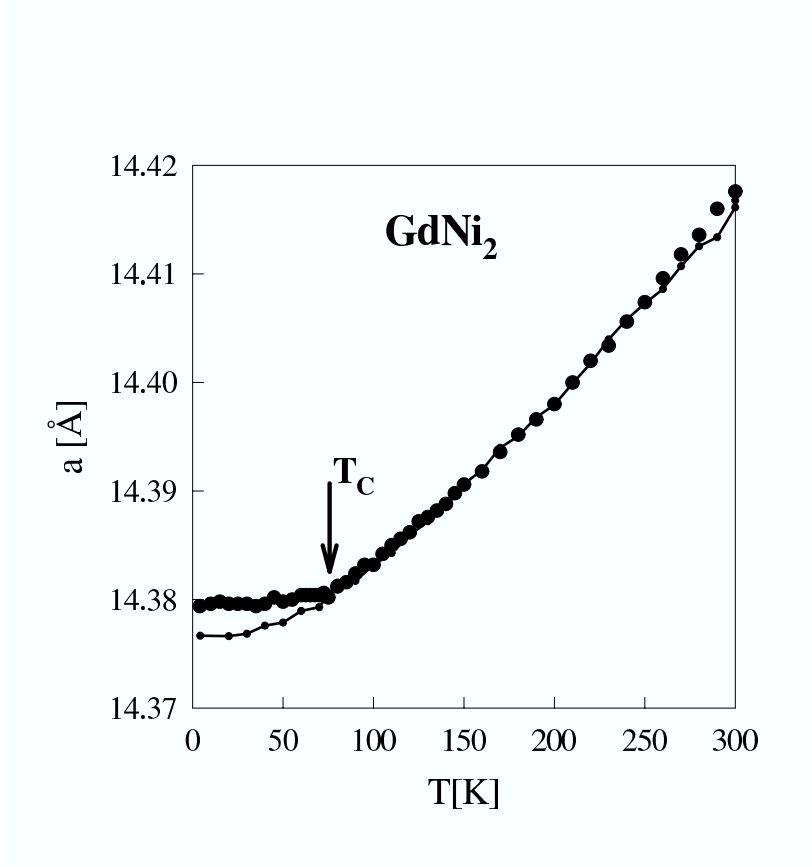

Fig. 2. Temperature variation of the cubic lattice parameter of the C15 superstructure of $GdNi_2$ measured by x-ray powder diffraction (this work). The small points connected by a line indicate the corresponding values of the isostructural YNi_2 (nonmagnetic reference), scaled to coincide with $GdNi_2$ at 150 K, in order to allow a direct comparison.

The magnetic properties of $GdNi_2$ have been largely investigated in the past (see e.g. Buschow (1977); Jesser and Clad (1986)). It orders ferromagnetically below $T_C \approx 74$ K and shows a weak Ni 3d polarization opposite to the 4f Gd moments. This weak itinerant Ni moment is a possible reason for the observed positive magnetovolume effect, which has been measured by low temperature x-ray powder diffraction (see Fig. 2), reaching a value of $(\Delta V/V)_{mag} \approx 0.6 \times 10^{-3}$ at 0 K (estimated by comparison with the nonmagnetic reference compound YNi_2). No line splitting or broadening of the x-ray lines could be observed below the magnetic ordering temperature. This means that a possible distortion of the cubic symmetry is smaller than 1×10^{-4}.

The RIn_3 systems crystallize in the cubic $AuCu_3$ type of structure and are known for salient features as valence fluctuations and the presence of various magnetic structures (see e.g. Lin et al. (1996) and references therein). $GdIn_3$ is antiferromagnetic with a Néel temperature T_N of about 43 K. Magnetization measurements on a single crystal by Staliński et al. (1979) showed, that the Néel temperature varies with the crystallographic axis along which the magnetic field is applied reaching the highest value along [100]. This observed variation of T_N suggests that the magnetic structure is a spiral antiferromagnetic one (Nagamiya, 1967). Grechnev et al. (1995) investigated the effect of pressure on the magnetic suszeptibility of RIn_3 compounds and performed also ab-initio calculations of the volume derivatives of the band structure and the exchange parameters. Their study supports the view that the RKKY-type R-R interaction is mainly mediated by the s- and p- electrons.

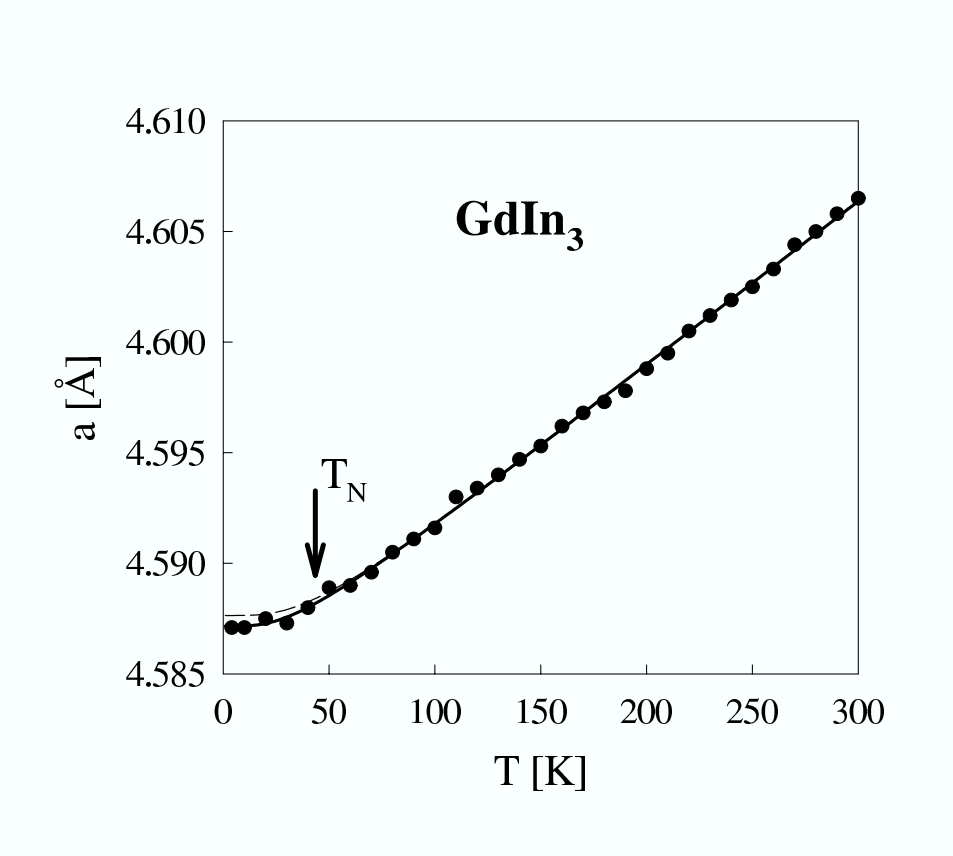

Fig. 3. Temperature variation of the cubic lattice parameter of $GdIn_3$ measured by x-ray powder diffraction (this work). The full line corresponds to a fit of a Debye model to the whole temparature range, the dashed line shows an extrapolation from the paramagnetic range obtained from fitting the Debye function only to the data points above T_N.

Fig. 3 shows the variation of the cubic lattice parameter, measured by x-ray powder diffraction. As can be seen, there is no volume effect or only a small negative one with an absolute value at 0 K smaller than 0.3×10^{-3}.

Further examples of cubic systems with very weak negative magnetovolume effects are $GdCu_2In$ and $GdPd_2In$, both crystallizing in the cubic Heusler structure $L2_1$ (Webster, 1969). Both compounds order antiferromagnetically below about 10 K with some complicated and up to now unknown magnetic structure (see e.g. Parsons et al. (1998); Taylor et al. (2000) and references therein). Specific heat measurements on both compounds show very similar results for the magnetic contributions (Parsons et al., 1998), but the corresponding effect on the crystal volume is 5 times larger in $GdCu_2In$ (measured by Taylor et al. (2000) on polycrystalline samples using a capacitance dilatometer). However, the estimated value of the magnetovolume effect at 0 K is very small in both. It is $(\Delta V/V)_{mag} \approx -10 \times 10^{-5}$ for $GdCu_2In$ and $(\Delta V/V)_{mag} \approx -2 \times 10^{-5}$ for $GdPd_2In$.

5 Spontaneous distortions of the crystal symmetry

Unfortunately, symmetry distortions have not been widely investigated in Gd compounds, because they are usually very small and therefore experiments are difficult. Some old data is available for cubic compounds. *Isotropic exchange interactions* which stay isotropic also under a strain such as Heisenberg and RKKY type do not lead to spontaneous symmetry distortions in *ferromagnetic* cubic systems (Morin and Schmitt, 1990). However, such distortions have been (indirectly) found in ferromagnetic systems from forced magnetostriction measurements on single crystals (e.g. a spontaneous tetragonal distortion $(\Delta l/l)_{001} \approx -3.7 \times 10^{-4}$ in GdZn by Rouchy et al. (1981), and a small spontaneous trigonal distortion $(\Delta l/l)_{111} \approx 2 \times 10^{-5}$ in $GdAl_2$ by du Tremolet de Lacheisserie (1988)). These distortions have to be attributed to the presence of *anisotropic exchange interactions* in these ferromagnetic compounds, but the origin of the exchange anisotropy has not yet been clarified.

In contrast to the cubic ferromagnets, in cubic *antiferromagnets* also isotropic exchange may lead to symmetry distortions, as for instance the small trigonal distortions in the antiferromagnetic compounds GdAs, GdSb and GdBi, ranging from 10^{-5} to 10^{-4}, which were directly measured by x-ray diffraction experiments by Hulliger and Stucki (1978). Diffraction in external fields would be necessary to show unambiguously if in these antiferromagnets the distortion is due to isotropic or anisotropic exchange interactions. The source of exchange anisotropy in Gd compounds is still topic of current investigations and in special cases, such as symmetry distortions of the cubic ferromagnets, measurements of magnetoelastic properties can make important contributions to this problem.

6.1 Gadolinium

Pure gadolinium crystallizes in the well known hexagonal close-packed (*hcp*) structure (see Fig. 4), which is described within the space group $P6_3/mmc$ with Gd on the 2c-sites (point symmetry $\bar{6}m2$).

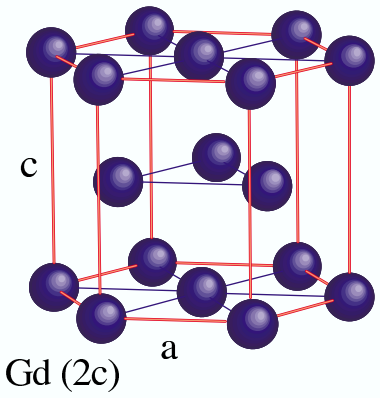

Fig. 4. *hcp* structure of gadolinium.

Gadolinium has the highest magnetic ordering temperature among all rare earth elements. The magnetic properties of Gd metal have been extensively studied (see e.g. McEwen (1978) and Dan'kov et al. (1998) and references therein). It shows ferromagnetic ordering below $T_C = 294$ K and remains ferromagnetic down to liquid helium temperature. The saturation moment is 7.55 μ_B per atom (Nigh et al., 1963), i.e. there is an additional moment of 0.55 μ_B compared to the 7 μ_B corresponding to a local 4f moment with $S = 7/2$. This additional moment is usually attributed to a conduction-electron polarization (see e.g. Cable and Wollan (1968)). The paramagnetic to ferromagnetic transition at T_C is of second order type and the universality class has been determined only recently by Frey et al. (1997). Neutron diffraction experiments performed by Cable and Wollan (1968) showed that from T_C down to the spin reorientation temperature $T_{SR} \approx 232$ K the moments are aligned along the hexagonal axis (i.e. c-direction). Below T_{SR} the moment direction departs from this direction and the angle between the hexagonal axis and the moment direction changes with temperature. Here it is worthwhile to mention that the magnetic properties of gadolinium are up to now a puzzle. In a recent *Nature* paper, Coey et al. (1999) reported that gadolinium is probably not really a ferromagnet between T_{SR} and T_C, but that the magnetic structure is some long-period modulated structure, similar to the incommensurate order found in erbium. This conclusion has been drawn from suszeptibility measurements around T_C and T_{SR}, but experiments for observing the long-period modulation are still missing. More recent suszeptibility and low field magnetization measurements performed by Kaul and Srinath (2000) confirm again the widely accepted view that gadolinium is a collinear ferromagnet between T_C and T_{SR}.

The thermal expansion of gadolinium has been studied several times (for a collection of data see

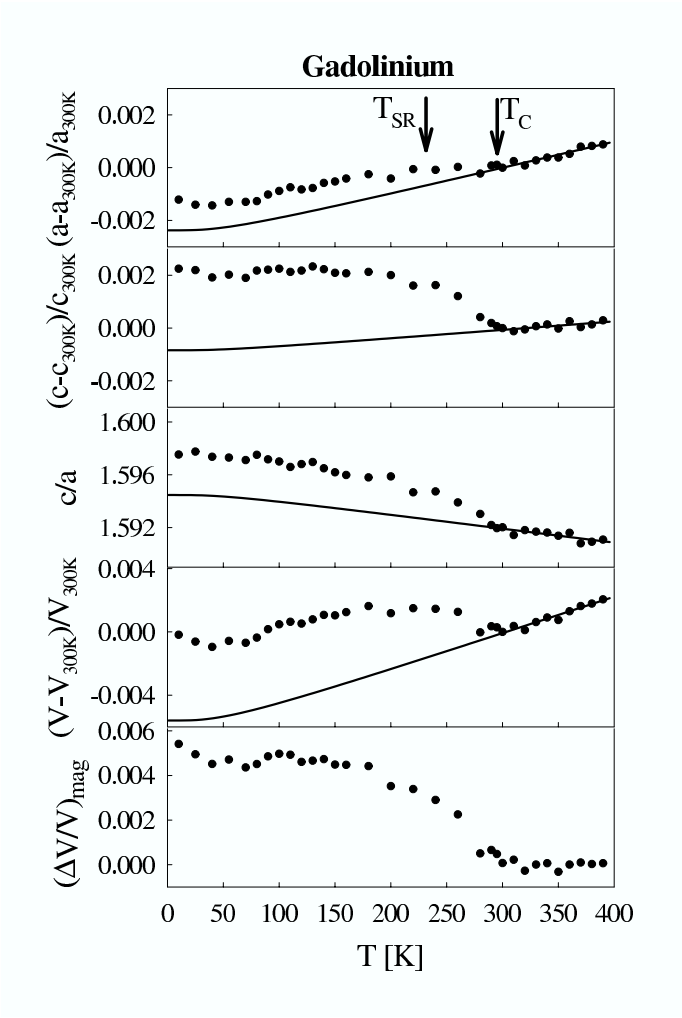

Fig. 5. Temperature variation of the hexagonal lattice parameters and of the volume of pure gadolinium measured by x-ray powder diffraction (this work). The values have been normalized to 300 K in order to show the relative changes. (The values at 300 K are $a = 3.632 \pm 0.002$ Å, $c = 5.782 \pm 0.002$ Å.) The lines represent the extrapolation of the lattice contribution from temperatures above T_C assuming a Debye temperature of 184 K (Bodriakov et al., 1998). The lowest part of the figure shows the magnetovolume effect, obtained by subtracting the lattice contribution from the volume expansion.

e.g. Touloukian et al. (1976)). Since there is some disagreement mainly concerning the temperature variation of the lattice parameter a, we remeasured the anisotropic thermal expansion of a polycrystalline Gd sample by means of x-ray diffraction between 10 K and 400 K. The result is shown in Fig. 5. As can be seen from the temperature variation of a and c there is a pronounced anisotropic magnetic contribution below T_C: The estimated values at 0 K of the magnetic contribution are $(\Delta a/a)_{mag} \approx 1.0 \times 10^{-3}$ and $(\Delta c/c)_{mag} \approx 3.0 \times 10^{-3}$. This leads to a clearly visible magnetically induced change of the c/a ratio of $(\Delta(c/a)/(c/a))_{mag} \approx 2.0 \times 10^{-3}$. However, what is much more peculiar is the big magnetovolume effect with a 0 K value of $(\Delta V/V)_{mag} \approx 5.0 \times 10^{-3}$. The size of this magnetovolume effect is comparable to R-Fe or R-Co compounds, like for instance RFe_2 and RCo_2, where the large magnetovolume effects of about 2 to 9 $\times 10^{-3}$ are attributed to the itinerant character of the magnetic moments of Co or Fe (see e.g. the review by Andreev (1995) p.68). The volume effects caused by localized magnetic moments are usually one order of magnitude smaller. A possible reason for the unexpected large positive magnetovolume effect in gadolinium is the large induced itinerant magnetic moment of about 0.55 μ_B in the conduction band (see above).

Intermetallic compounds of the general composition AB_5 have been extensively investigated as possible hydrogen storage media. Because of the ability of $LaNi_5$ to absorb large amounts of hydrogen (up to 6.7 atoms per formula unit - see van Voucht et al. (1970)) also $GdNi_5$- based systems have been investigated with respect to their hydrogen sorption properties (see e.g. Blažina et al. (1999) and Bobet et al. (1998)).

$GdNi_5$ crystallizes in the well known hexagonal $CaCu_5$ type (space group $P6/mmm$). As shown in Fig. 6, the structure is built up of two types of basal plane layers alternating along the c-axis, one at $z = 0$ composed of Gd (1a-sites with high point symmetry $6/mmm$) and Ni (2c-sites), the other one at $z = 1/2$ only composed of Ni atoms (3g-sites).

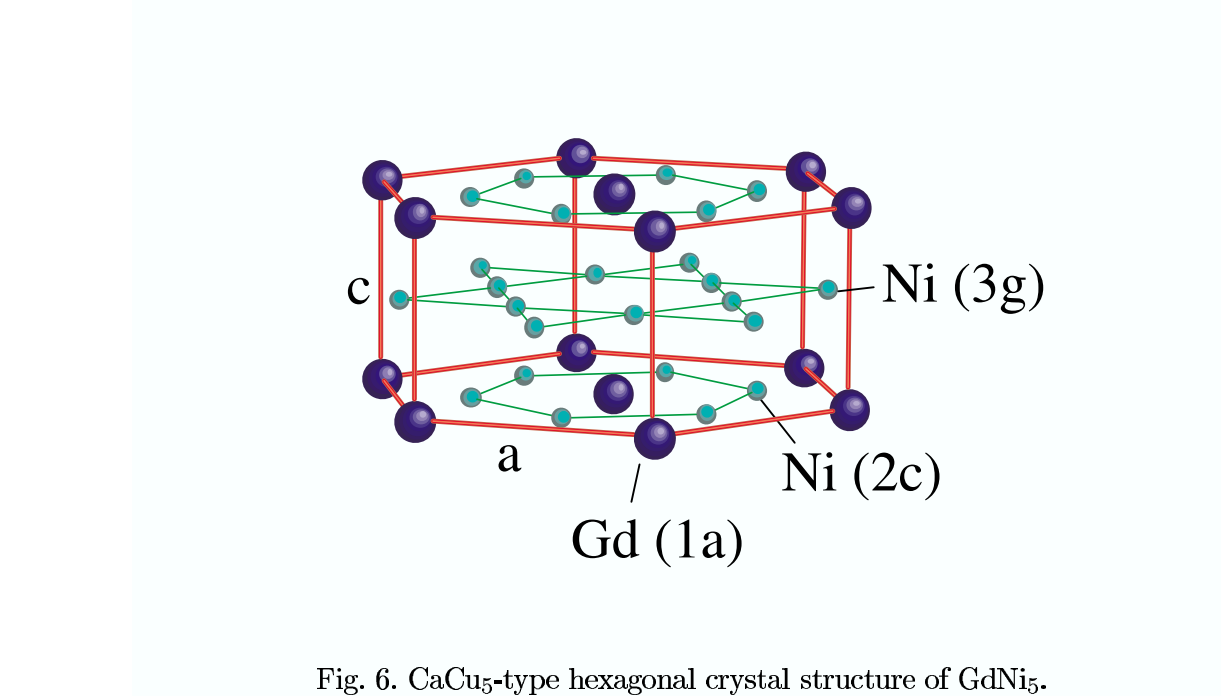

Fig. 6. $CaCu_5$-type hexagonal crystal structure of $GdNi_5$.

The magnetic properties of $GdNi_5$ have been intensively studied in the past and are now well understood (Franse and Radwański, 1993; Mulders et al., 2000). The magnetic interaction is strong compared to the other RNi_5 compounds (de Gennes scaling) with an ordering temperature of $T_c \approx$ 31 K. $GdNi_5$ is a ferrimagnet with ferromagnetically ordered Gd moments of 7 μ_B aligned parallel to the hexagonal axis. These Gd moments induce an antiparallel moment of 0.16 μ_B on the Ni atoms. There is a weak magnetic anisotropy caused by the dipolar interaction between the Gd moments (Yaouanc et al., 1996). In the past $GdNi_5$ has also been used as a testing ground for validating muon spin relaxation theories in magnetic materials (de Réotier and Yaouanc, 1997).

No spontaneous magnetostriction could be detected within the sensitivity of the x-ray diffraction experiments. As can be seen in Fig. 7 there is no significant difference in the temperature dependence of the lattice parameters between $GdNi_5$ and the nonmagnetic isostructural YNi_5. The reason for the vanishing or very small (i.e. $< 10^{-4}$) effects in this compound could be that only one atom among six is a Gd atom, leading to weak magnetic and magnetoelastic interactions. A further example for

a compound with a low concentration of Gd atoms, also showing weak or vanishing effects, is the tetragonal $GdNi_2B_2C$ (see section 7.3).

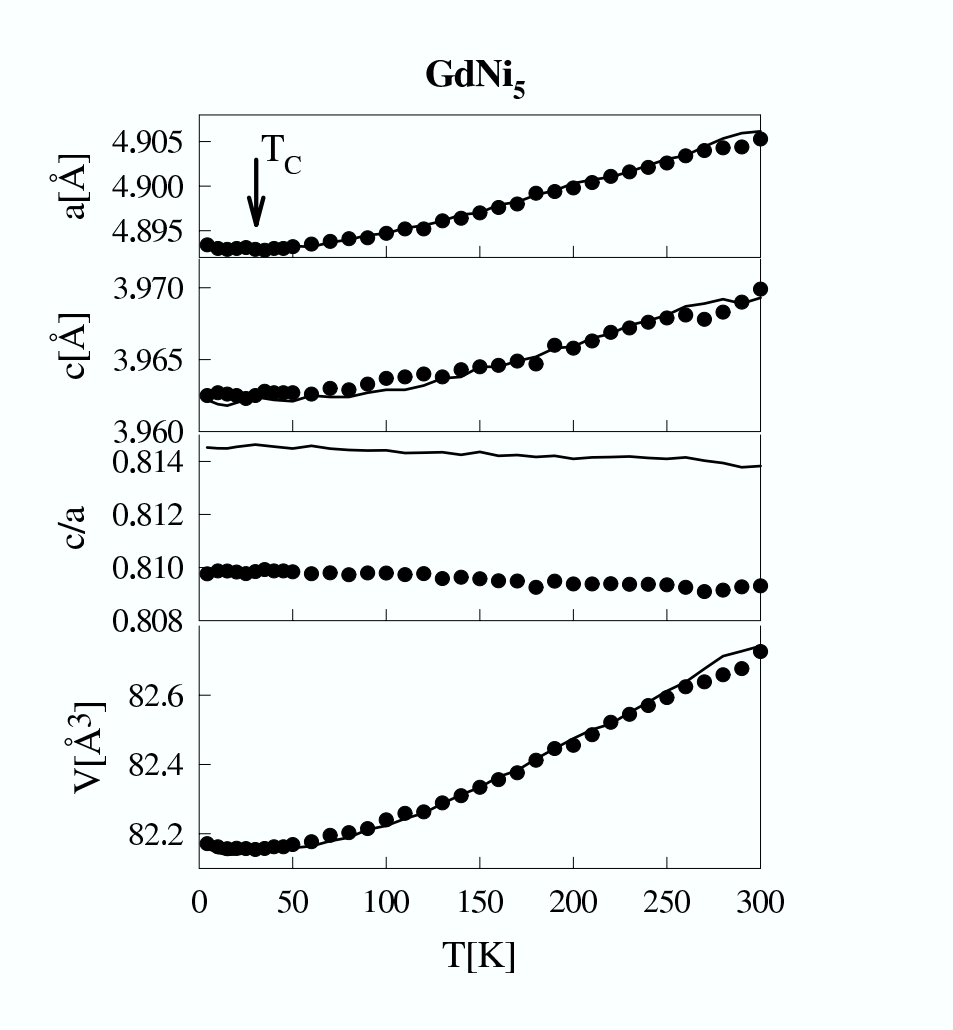

Fig. 7. Anisotropic thermal expansion of $GdNi_5$ measured by x-ray powder diffraction (this work). The lines indicate the corresponding values of the isostructural YNi_5 (nonmagnetic reference), scaled to coincide with $GdNi_5$ at 150 K for allowing a direct comparison (the c/a ratio has not been scaled).

6.3 Gd_2In

Gd_2In crystallizes in the hexagonal Ni_2In-type structure (space gr. $P6_3/mmc$), which has two crystallographically different sites for Gd (Palenzona, 1968). The unit cell of the structure is shown in Fig. 8. As can be seen from this figure the structure is composed of hexagonal layers with the stacking sequence ABACA. The A layers at $z = 0$ and $z = 1/2$ contain only Gd atoms on the cell corners (2a-sites with quasi-cubic point symmetry $\overline{3}m$). The B and C layers at $z = 1/4$ and $z = 3/4$ contain each one Gd atom (2d-sites with hexagonal point symmetry $\overline{6}m2$) and one In atom (2c-sites, also $\overline{6}m2$). Interestingly, the Gd sublattice forms a double hexagonal close packed structure (*dhcp*), which differs only by the stacking sequence of the hexagonal planes from a *hcp* structure formed by elemental gadolinium (see section 6.1). However, the distances of the Gd atoms are very different. The Gd

- Gd distance within the hexagonal planes is much larger in Gd_2In ($a \approx 3.63$ Å for gadolinium and $a \approx 5.41$ Å for Gd_2In), whereas the distances in direction of the hexagonal axis are much smaller (gadolinium: $c \approx 5.78$ Å, Gd_2In: $c/2 \approx 3.38$ Å).

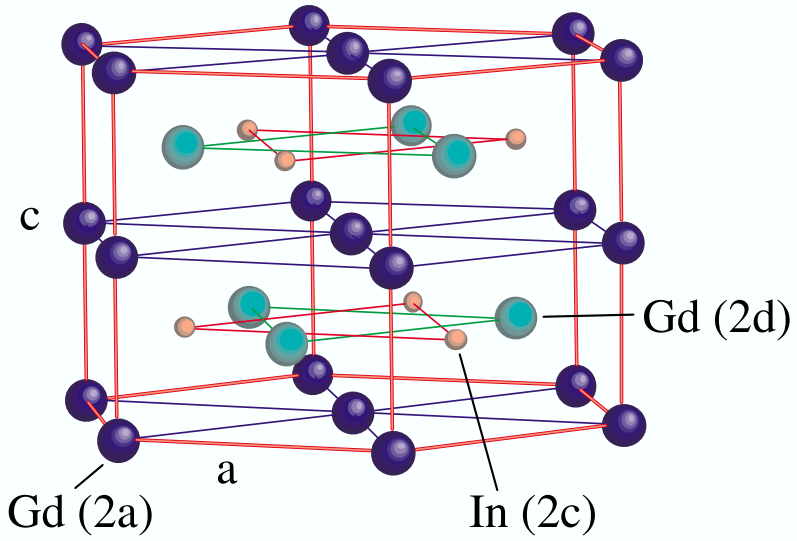

Fig. 8. Ni_2In-type hexagonal crystal structure of Gd_2In.

The magnetic properties of Gd_2In show interesting features: It becomes ferromagnetic below 190 K, but there is a second magnetic transition at about 100 K to an antiferromagnetic structure. Under a magnetic field this metamagnetic transition is shifted to lower temperatures and fields of about 1 Tesla can completely restore the ferromagnetic state (McAlister, 1984; Gamari-Seale et al., 1979; Jee et al., 1996). Jee et al. (1996) reported that the temperature- and magnetic field dependence of the magnetization shows that the system is not a simple ferromagnet between 100 and 190 K, but a helical ferromagnet. McAlister (1984) reported that magnetization, resistivity and magnetoresistivity measurements support the suggestion that the low temperature structure below 100 K could be a spiral antiferromagnetic structure. Measurements of the magnetization and magnetoresistance in the vicinity of the metamagnetic transition support that the low temperature structure is different from simple antiferromagnetic (Stampe et al., 1997). Ravot et al. (1993) reported a propagation vector (0,0,≈ 1/6), obtained by neutron powder diffraction experiments at 20 K.

As can be seen in Fig. 9 there is no spontaneous magnetostriction effect within the sensitivity of the x-ray diffraction experiments ($\approx 1 \times 10^{-4}$) at both magnetic transition temperatures of 190 K and 100 K, respectively. This is interesting and unexpected, since this compound is characterized by a strong Gd - Gd magnetic interaction, leading to the relatively high magnetic ordering temperature of 190 K. Despite this strong magnetic exchange interaction the c/a ratio as well as the volume are absolutely unaffected by the ordering of the Gd moments. Note that Gd_2In has the second highest magnetic ordering temperature of all systems reviewed in the present chapter after pure Gd metal

(see section 6.1), which shows pronounced anisotropic spontaneous magnetoelastic effects as well as a large positive magnetovolume effect. Further studies including field-induced magnetostriction experiments on single crystals are necessary in order to clarify why there is no pronounced spontaneous magnetostriction detectable in Gd_2In.

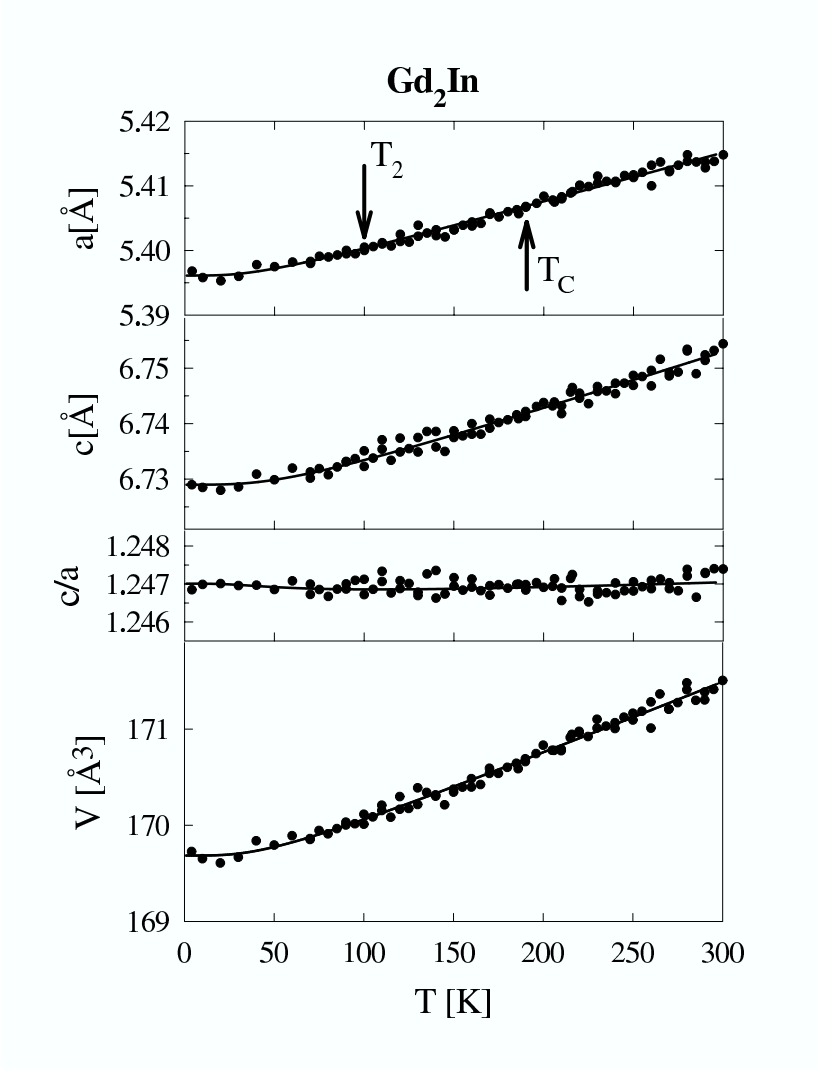

Fig. 9. Anisotropic thermal expansion of Gd_2In measured by x-ray powder diffraction (Gratz and Lindbaum, 1998). The lines are the result of fitting Debye functions. The arrows indicate the two magnetic transitions at 190 K and 100 K (see text).

The RCuAl (R = rare earth except for La and Eu) compounds belong to a large group of ternary intermetallics showing the ZrNiAl-type hexagonal structure with space group $P\bar{6}2m$ (Szytula, 1991). All the R atoms occupy equivalent positions (3g sites) with point symmetry mm only. The structure is built up of two types of basal plane layers (with and without R atoms) alternating along the c-axis (see Fig. 10).

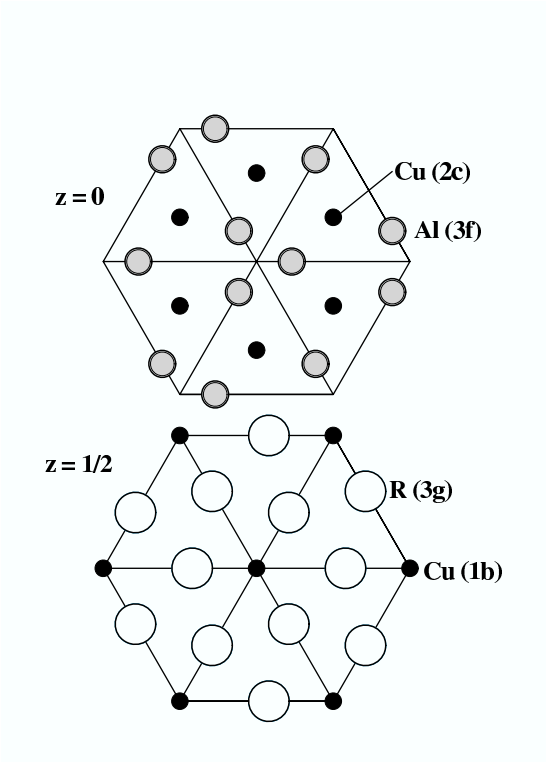

Fig. 10. ZrNiAl-type hexagonal crystal structure of RCuAl.

While the magnetic properties of the compounds with light R atoms are rather complex, ferromagnetic ordering has been deduced from magnetization measurements on polycrystalline samples for Gd and the other heavy R atoms. In the case of GdCuAl the magnetic ordering temperature is $T_C \approx$ 82 K. Javorský et al. (1998) reported a second magnetic transition at $T_R \approx 37$ K observed in specific heat and suszeptibility data. Powder x-ray diffraction experiments with an external magnetic field performed by Andreev et al. (1999) (for a description of the method see e.g. Gratz et al. (1999b)) showed that in GdCuAl the magnetic moments are aligned along the c-axis below T_C as well as below the second magnetic transition at T_R.

Measurements of the temperature dependence of the hexagonal lattice parameters using low-temperature x-ray powder diffraction (Andreev et al., 1999) show clear anomalies below the magnetic ordering temperature (82 K) in both the a(T) and c(T) curves (see Fig. 11). An estimation of the spontaneous magnetostriction by extrapolating from the paramagnetic range to low temperatures shows a monotonous increase of the magnetostriction which reaches quite large values at 0 K ($(\Delta a/a)_{mag} = -1.7\times10^{-3}$ and $(\Delta c/c)_{mag} = 3.0\times10^{-3}$). This leads to a pronounced change in the c/a ratio of $(\Delta(c/a)/(c/a))_{mag} \approx 4.7\times10^{-3}$, but only to a small volume effect ($(\Delta V/V)_{mag} \approx 2(\Delta a/a)_{mag} + (\Delta c/c)_{mag} = -0.4\times10^{-3}$), which is near the size of the experimental error. There was no measurable effect at the second mag-

netic transition at 37 K which has been observed by Javorský et al. (1998).

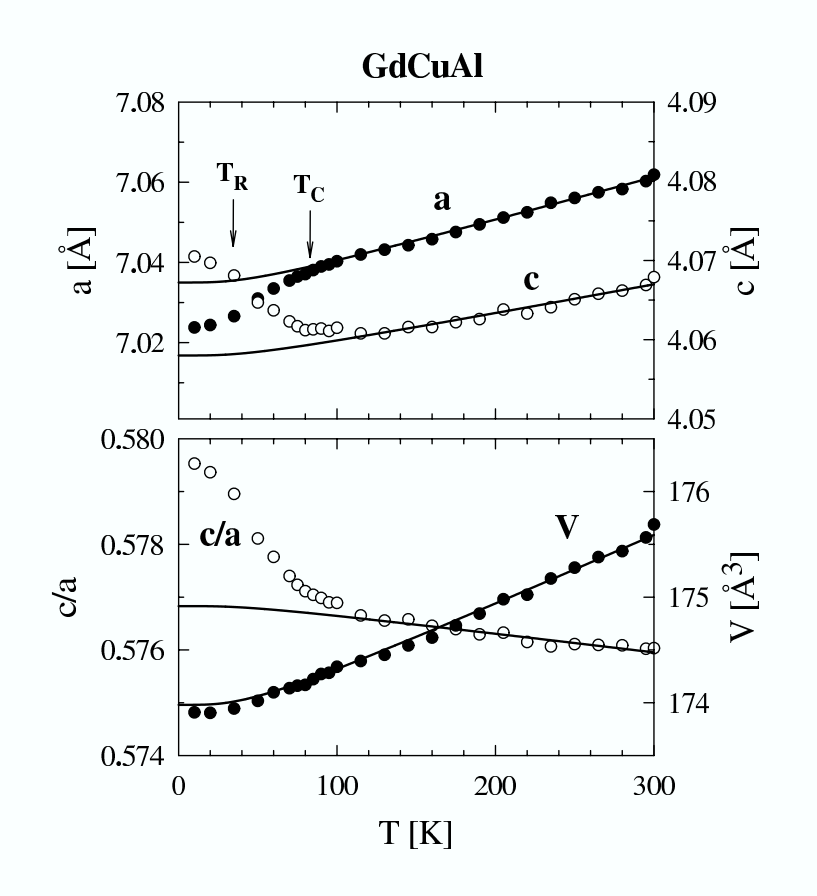

Fig. 11. Anisotropic thermal expansion of GdCuAl measured by x-ray powder diffraction (Andreev et al., 1999). The lines are extrapolations from the paramagnetic range. T_C and T_R indicate the magnetic ordering temperature and the second magnetic transition observed by Javorský et al. (1998), respectively.

GdNiAl crystallizes like GdCuAl in the hexagonal ZrNiAl-type structure, but a pronounced anomaly in the hexagonal lattice parameters at about 200 K has been observed and attributed to a transition between two slightly different forms of the ZrNiAl-type structure (Merlo et al., 1998). The atomic position parameters $x_{Gd} \approx 0.583$ and $x_{Al} \approx 0.232$, which are not fixed by space group symmetry, do not change significantly at this structural transition (Jarosz et al., 2000).

As reported by Merlo et al. (1998) and Javorský et al. (1995), GdNiAl orders ferromagnetically below about 60 K, and two other magnetic transitions occur at 30 and 14 K, which are probably due to the occurrence of antiferromagnetic order, but no further information concerning the easy axis in the ferromagnetic state and the magnetic structures below the two additional transitions could be found in literature. However, as reported by Merlo et al. (1998), a further magnetic transition has been observed in this compound in the paramagnetic range at about 180 K. Above this temperature the paramagnetic moment of Gd (obtained from a Curie-Weiss fit of suszeptibility data) agrees with the calculated free ion value, but below a 9 % higher value has been found. Merlo et al. (1998) suggest that this transition could be connected with the structural transformation at about 200 K, and that below this transition the slightly different interatomic distances could be responsible for a larger polarization of the conduction electrons.

The temperature variation of the lattice parameters, as measured by x-ray diffraction by Merlo

et al. (1998) and Jarosz et al. (2000), shows no significant anisotropic spontaneous magnetostriction, neither due to the ferromagnetic ordering between about 60 K and 30 K nor due to the two additional magnetic transitions at 30 and 14 K. This is in contrast to the behaviour of GdCuAl (see Fig. 11), where a pronounced change of the c/a ratio due to the magnetic ordering has been observed. But note that there is a clear positive volume anomaly with an estimated 0 K value of about $(\Delta V/V)_{mag} \approx 0.8 \times 10^{-3}$ in GdNiAl (Jarosz et al., 2000). This positive volume effect, which does not exist in GdCuAl, may be due to an induced itinerant magnetic moment at the Ni sites. In general the above comparison of the isostructural GdNiAl and GdCuAl shows that the magnetoelastic effects can be strongly influenced by the partner elements of Gd, i.e. exchanging Cu by Ni can change the behaviour completely.

6.5 GdCuSn

GdCuSn crystallizes in the hexagonal NdPtSb-type structure (Pacheco et al., 1998), which is an ordered form of the $CaIn_2$ type, which had been reported as the structure of GdCuSn before (Komarovskaja et al., 1983). The correct structure of GdCuSn is described within the space group $P6_3mc$ with Gd on the 2a-sites (point symmetry $3m$), Cu on the 2b-sites (also point symmetry $3m$) with $z_{Cu} \approx 0.81$ and Sn also on the 2b-sites with $z_{Sn} \approx 0.23$. The hexagonal unit cell of the structure is shown in Fig. 12.

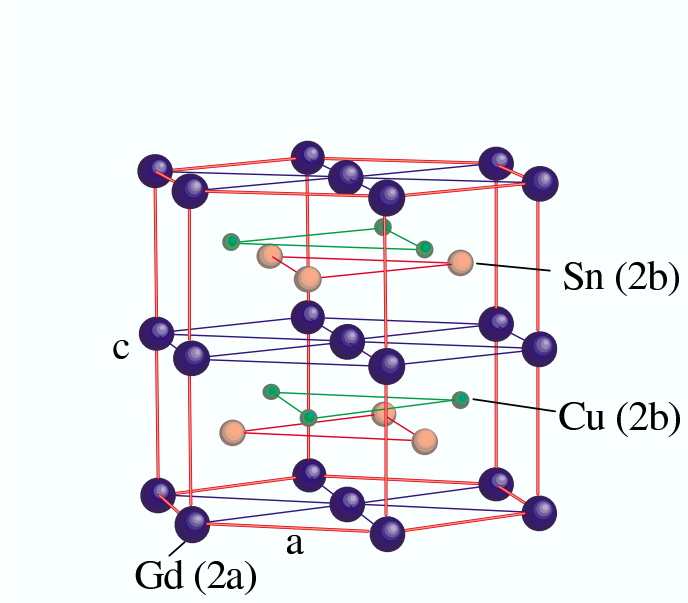

Fig. 12. *NdPtSb*-type hexagonal crystal structure of GdCuSn.

Already in 1977 bulk magnetic measurements showed that GdCuSn orders antiferromagnetically below about 24 K (Österreicher, 1977). Only a few years ago conclusions about the magnetic structure were drawn from Mössbauer experiments by analyzing the Gd and Sn resonance spectra (Bialic et al., 1997). The authors of this work suggest a magnetic structure described by the propagation vector (0,1/2,0) with antiferromagnetic order within the hexagonal Gd planes and ferromagnetic stacking along the c axis. Fig. 13 shows this magnetic structure schematically.

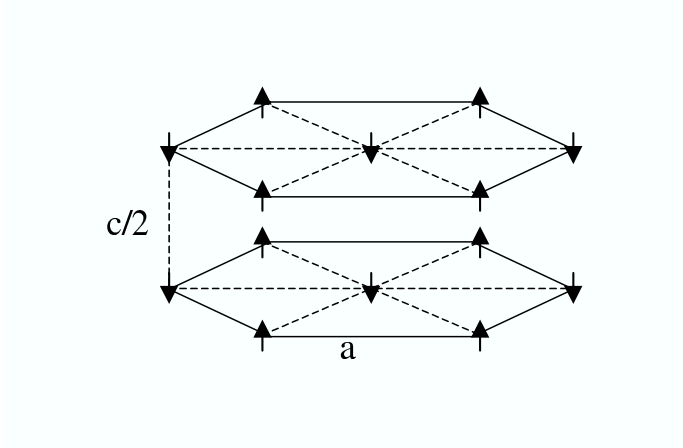

Fig. 13. Possible magnetic structure of GdCuSn (Bialic et al., 1997).

Fig. 14 shows the temperature dependence of the lattice parameters as well as of the volume of GdCuSn measured by low temperature x-ray diffraction. As can be seen there is a significant spontaneous anisotropic magnetostriction effect due to the magnetic ordering. An estimation of the magnetic contribution to the thermal expansion at 0 K by extrapolating from the paramagnetic range down to lowest temperatures gives the values $(\Delta a/a)_{mag} \approx 0.3\times10^{-3}$ and $(\Delta c/c)_{mag} \approx -1.1\times10^{-3}$. This leads to a clearly visible magnetically induced change of the c/a ratio of $(\Delta(c/a)/(c/a))_{mag} \approx -1.4\times10^{-3}$, and a negative volume magnetostriction ($(\Delta V/V)_{mag} \approx -0.5\times10^{-3}$). Therefore GdCuSn is, like $GdAl_2$ (section 4.1) and GdCuAl (section 6.4), an example for a compound where the Gd - Gd exchange interaction leads to a negative magnetovolume effect.

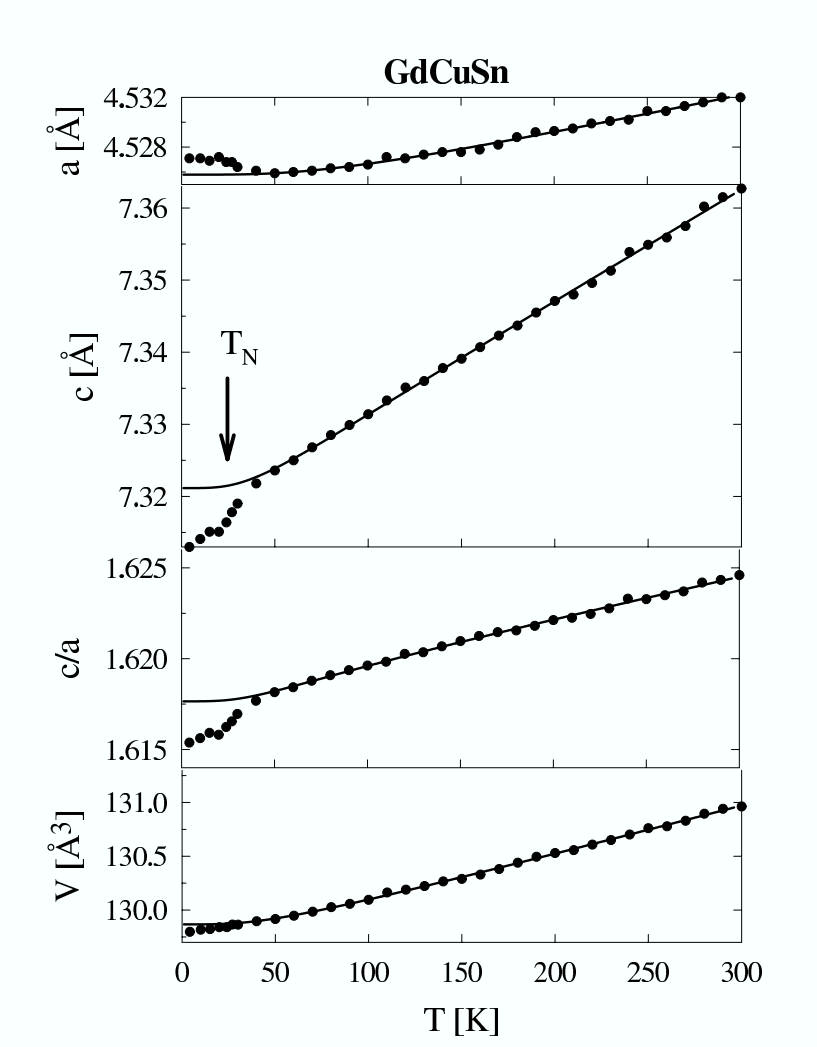

Fig. 14. Anisotropic thermal expansion of GdCuSn measured by x-ray powder diffraction (Gratz and Lindbaum, 1998). The lines represent the extrapolation of the lattice contribution from the paramagnetic range by fitting Debye functions.

7.1 $GdAg_2$ and $GdAu_2$

$GdAg_2$ and $GdAu_2$ crystallize in the tetragonal $MoSi_2$-type structure (Dwight et al., 1967). The space group is $I4/mmm$ with Gd on the 2a-sites (point symmetry $4/mmm$) and Ag(Au) on the $4e$ sites. The z atomic position parameter of the $4e$ sites (point symmetry $4mm$) is about 1/3. For $GdAg_2$ a value of $z_{Ag} = 0.327 \pm 0.004$ has been determined from neutron diffraction experiments (Gignoux et al., 1991). This structure can roughly be viewed as being composed of three tetragonally distorted body centered cubes along c-direction, as shown in Fig. 15.

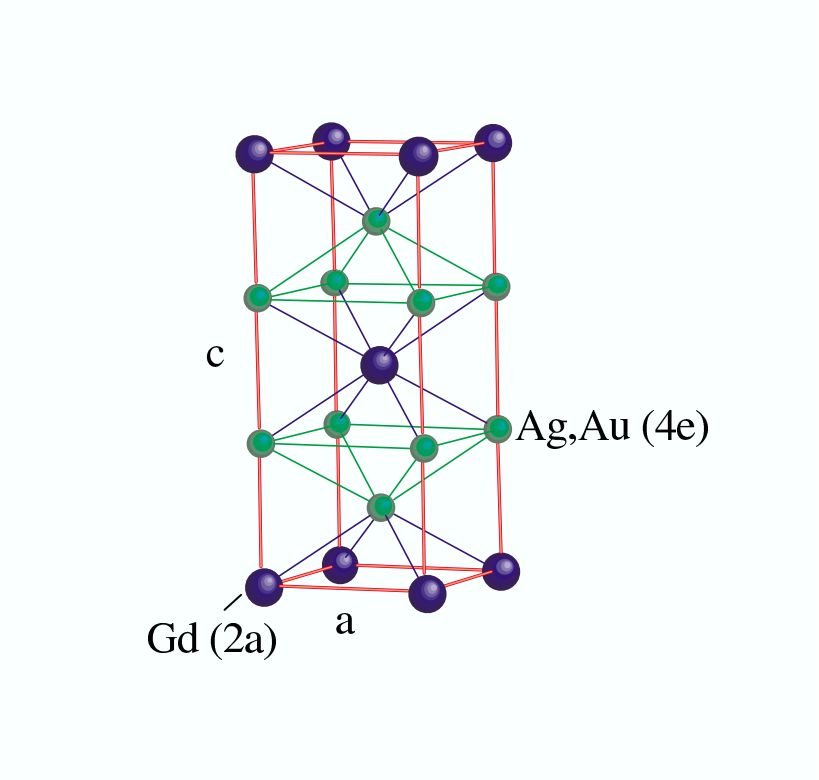

Fig. 15. Tetragonal $MoSi_2$-type structure of $GdAg_2$ and $GdAu_2$.

$GdAg_2$ has first been reported to order magnetically at about 27 K from resistivity measurements (Ohashi et al., 1975). Further studies by Gignoux et al. (1991) including specific heat, resistivity and magnetization measurements, as well as neutron powder diffraction experiments, showed that this compound orders antiferromagnetically below $T_N \approx 22.7$ K with two further first-order magnetic transitions at $T_{R1} \approx 21.2$ K and $T_{R2} \approx 10.8$ K. The neutron diffraction experiments showed that the magnetic order is incommensurate with a propagation vector of about (0.362,0,1) and that the moment direction seems to change from [110] below T_{R2} to [001] above T_{R2} (Due to the small temperature range between T_N and T_{R1} it was not possible to investigate the magnetic structure with neutron diffraction for this range). The observed first-order magnetic transitions in the ordered range have been attributed to anisotropic terms in the two-ion Gd-Gd exchange interaction. A further peculiarity, also mentioned by Gignoux et al. (1991) is that the magnetic ordering temperature of $GdAg_2$ is lower than in $TbAg_2$ ($T_N \approx 34.8$ K), violating the De Gennes law. This has been referred to a change in the conduction

band due to the boundary situation of $GdAg_2$ concerning the crystal structure, i.e. only the RAg_2 with heavy R, starting from Gd, show the $MoSi_2$ type of structure. Fig. 16 shows the temperature dependence of the lattice parameters as well as of the volume of $GdAg_2$ measured by low temperature x-ray diffraction. As can be seen there is a pronounced spontaneous anisotropic magnetostriction effect due to the magnetic ordering with no significant change at T_{R2}. An estimation of the magnetic contribution to the thermal expansion by extrapolating from the paramagnetic range down to 0 K gives the values $(\Delta a/a)_{mag} \approx 0.3 \times 10^{-3}$ and $(\Delta c/c)_{mag} \approx -0.6 \times 10^{-3}$. This leads to a clearly visible magnetically induced change of the c/a ratio of $(\Delta(c/a)/(c/a))_{mag} \approx -0.9 \times 10^{-3}$, but to no measurable volume magnetostriction within the sensitivity of the x-ray experiment ($|(\Delta V/V)_{mag}| < 0.1 \times 10^{-3}$).

$GdAu_2$ orders like $GdAg_2$ antiferromagnetically, but at a much higher ordering temperature of $T_N \approx$ 50 K (Tung et al., 1996). Neutron diffraction studies for determining the magnetic structure are in progress. Fig. 17 shows the temperature dependence of the lattice parameters as well as of the volume of $GdAu_2$, also measured by low temperature x-ray diffraction. In contrast to $GdAg_2$ there is no measurable spontaneous magnetoelastic effect at all. The magnetically induced change of c/a as well as the volume magnetostriction of $GdAu_2$ is smaller than the experimental resolution (i.e. $< 10^{-4}$). This different behaviour concerning the spontaneous magnetostriction may - like the different T_N (see above) - also be connected with conduction band properties, leading to a different $RKKY$ exchange coupling of the Gd moments.

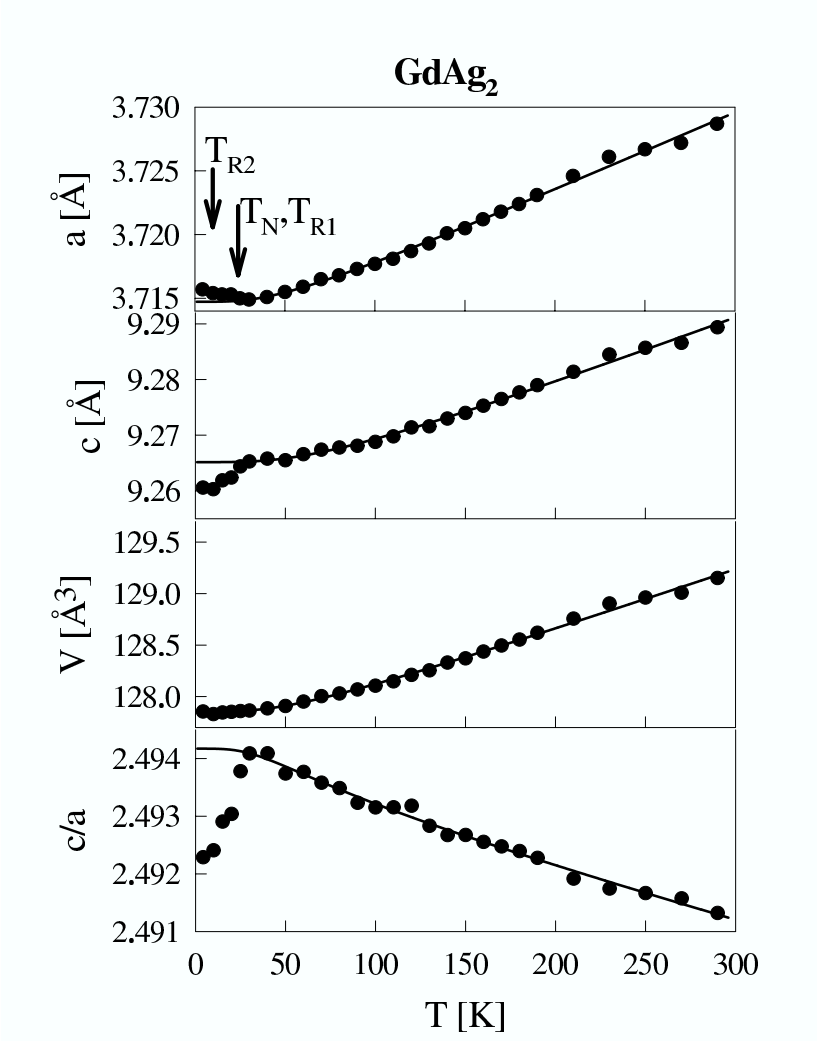

Fig. 16. Anisotropic thermal expansion of $GdAg_2$ measured by x-ray powder diffraction (this work). The lines represent the extrapolation of the lattice contribution from the paramagnetic range by fitting Debye functions. The arrows indicate the different magnetic transition temperatures (see text).

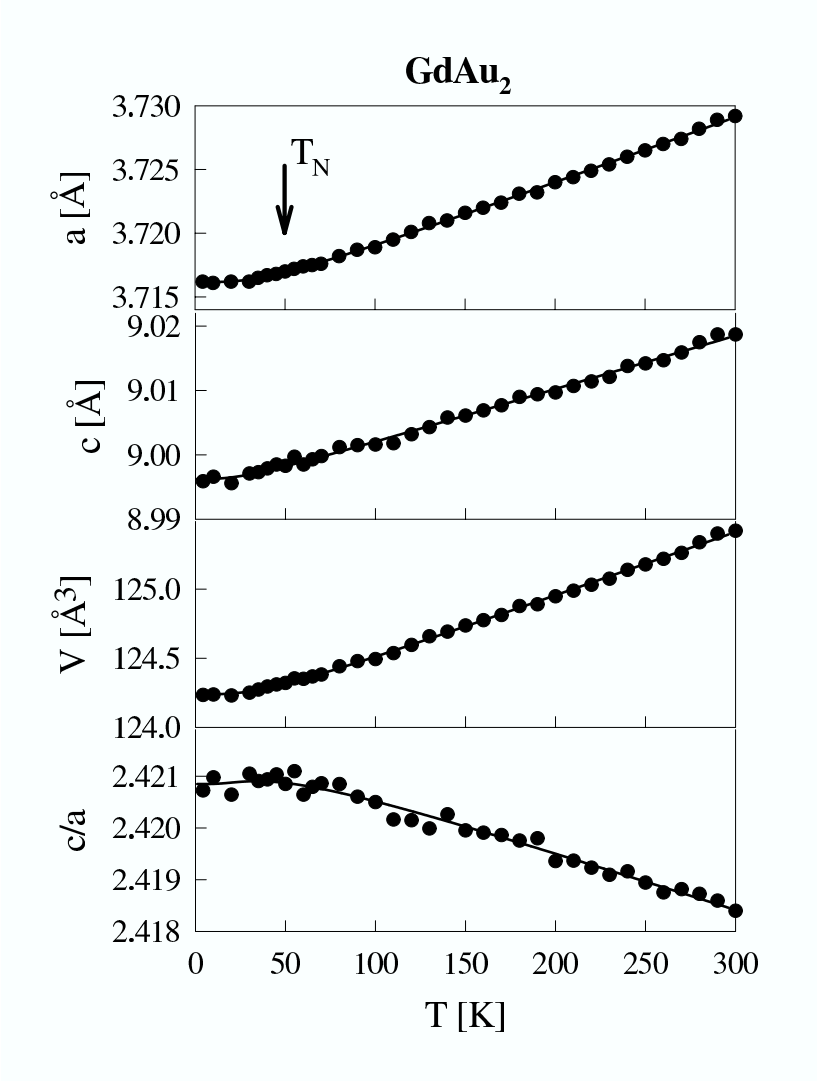

Fig. 17. Anisotropic thermal expansion of $GdAu_2$ measured by x-ray powder diffraction (this work). The lines represent the result of fitting Debye functions to the whole temperature range.

As reported by Kalychak et al. (1990) the R_2Cu_2In compounds (with exception of R=Eu and Yb) crystallize in the tetragonal Mo_2FeB_2 type of structure (space group $P4/mbm$). In case of the R_2Ni_2In compounds this structural type occurs only for R=La,Ce,Pr and Nd. The other R_2Ni_2In compounds including R=Gd show the orthorhombic Mn_2AlB_2 type of structure (space group $Cmmm$). But with an off-stoichiometric content of Ni ($R_2Ni_{2-x}In$ with $x = 0.22$) the tetragonal Mo_2FeB_2 type of structure is also formed for R=Sm to Lu. This means that Gd_2Cu_2In and $Gd_2Ni_{1.78}In$ have the same crystal structure, allowing again a direct comparison of the spontaneous magnetoelastic effects in two compounds, which differ only by one of the partner elements of Gd. Fig. 18 shows the arrangement of the atoms within the tetragonal unit cell. The Gd atoms occupy one type of crystallographic site, namely the $4h$-sites with only orthorhombic point symmetry mm (atomic position parameter $x_{Gd} \approx 0.18$). The Cu atoms occupy the $4g$-sites (mm, atomic position parameter $x_{Cu} \approx 0.38$) and the In atoms occupy the high-symmetry sites $2a$ with point symmetry $4/m$.

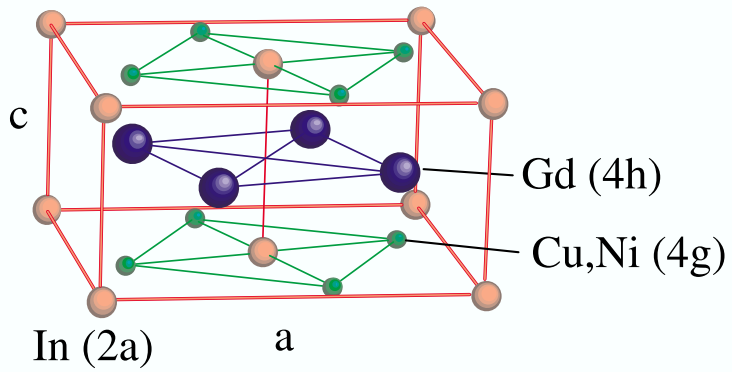

Fig. 18. Tetragonal structure of Gd_2Cu_2In and $Gd_2Ni_{2-x}In$.

Only three years ago Fisher et al. (1999) reported first about the magnetic properties of R_2Cu_2In compounds. Magnetization as well as electrical resistivity measurements showed that all the investigated magnetic compounds (R=Gd to Tm) order ferromagnetically with relatively high ordering temperatures, varying between 27 K for Ho_2Cu_2In and 86 K for Gd_2Cu_2In. The easy axis varies among the investigated compounds. For Gd_2Cu_2In it is parallel to the tetragonal c axis. For the isostructural $Gd_2Ni_{1.78}In$ no report concerning the magnetic properties could be found in literature. The only available information comes from unpublished suszeptibility measurements (Hilscher, 2001), indicating that $Gd_2Ni_{1.78}In$ orders antiferromagnetically below $T_N \approx 20$K.

Fig. 19 and Fig. 20 show the anisotropic thermal expansion obtained by x-ray powder diffraction for Gd_2Cu_2In and $Gd_2Ni_{1.78}In$, respectively. Within the sensitivity of the experiments no magnetovolume

effect can be observed in both compounds ($|(\Delta V/V)_{mag}| < 0.1 \times 10^{-3}$). But the comparison of the anisotropic effects shows pronounced differences. For Gd_2Cu_2In the estimation for the magnetic contribution to the thermal expansion by extrapolating from the paramagnetic range down to 0 K gives the values $(\Delta a/a)_{mag} \approx -1.9 \times 10^{-3}$ and $(\Delta c/c)_{mag} \approx +3.8 \times 10^{-3}$. This leads to a large magnetically induced change of the c/a ratio of $(\Delta(c/a)/(c/a))_{mag} \approx 5.7 \times 10^{-3}$. In the case of $Gd_2Ni_{1.78}In$ the observed anisotropic effects are much smaller ($(\Delta a/a)_{mag} \approx -0.2 \times 10^{-3}$, $(\Delta c/c)_{mag} \approx 0.4 \times 10^{-3}$, $(\Delta(c/a)/(c/a))_{mag} \approx 0.6 \times 10^{-3}$). This means that, like in the case of GdCuAl and GdNiAl (see section 6.4), the exchange of the Cu atoms by Ni atoms leads to a strong decrease of the anisotropic magnetoelastic effects. However, it has to be noted, that in the present case the change of the partner element of Gd leads also to a strong decrease of the magnetic Gd-Gd interaction itself, reflected in the pronounced decrease of the magnetic ordering temperature. This may also be a reason for the weaker spontaneous magnetostriction in the Ni compound.

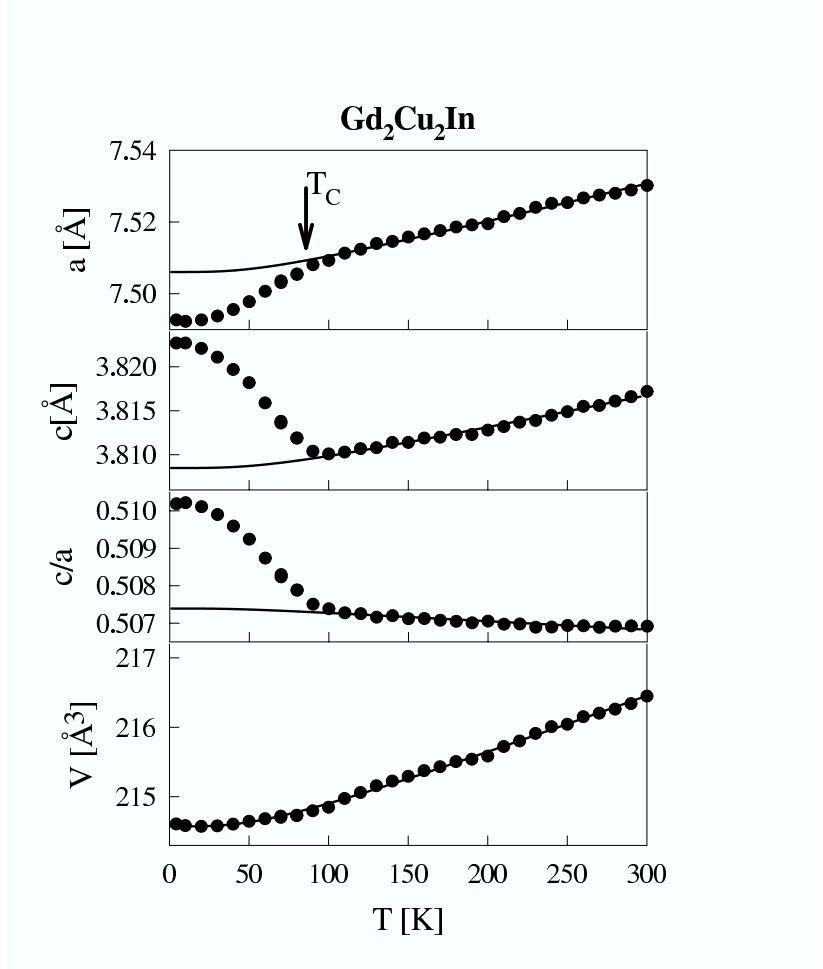

Fig. 19. Anisotropic thermal expansion of Gd_2Cu_2In measured by x-ray powder diffraction (this work). The lines represent the extrapolation of the lattice contribution from the paramagnetic range by fitting Debye functions.

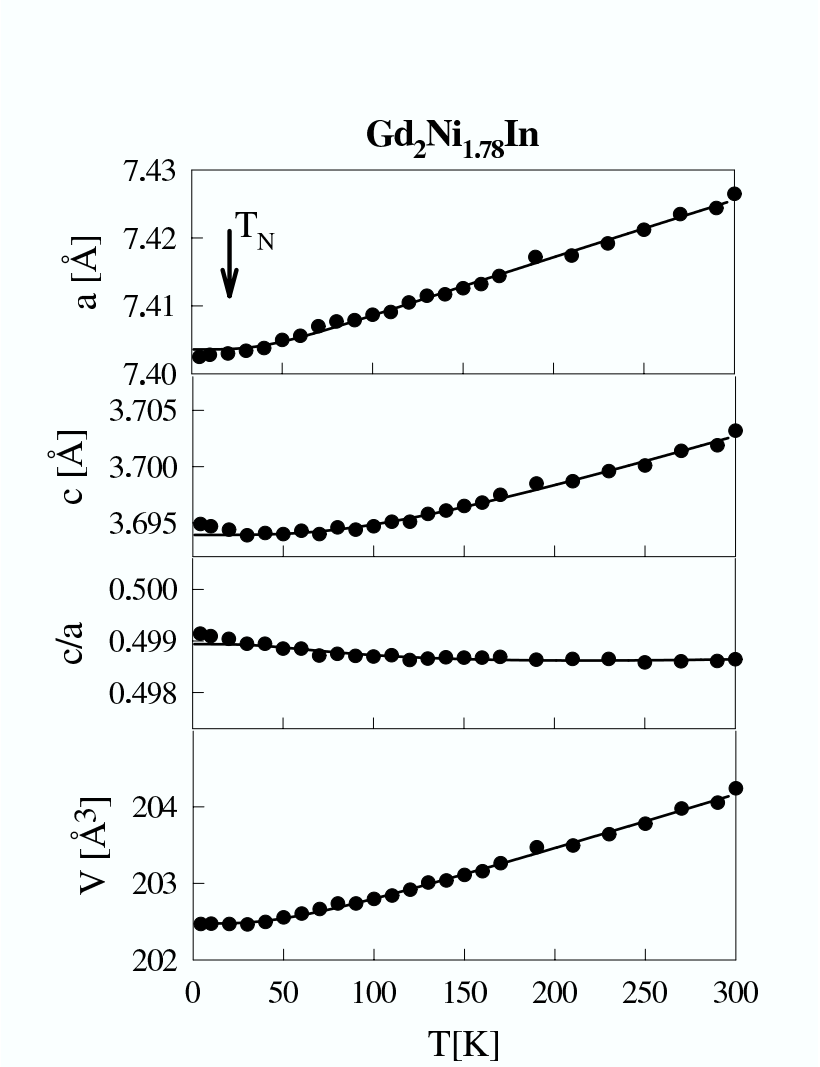

Fig. 20. Anisotropic thermal expansion of $Gd_2Ni_{1.78}In$ measured by x-ray powder diffraction (this work). The lines represent the extrapolation of the lattice contribution from the paramagnetic range by fitting Debye functions.

Since the discovery of the RT_2B_2C borocarbides (T = transition metal) much attention has been paid to the physical and structural properties of the whole series of isotypic compounds, because of the high superconducting transition temperatures and because of the interesting interplay between magnetic ordering and superconductivity. These compounds crystallize in the tetragonal $LuNi_2B_2C$ type of structure, which might be regarded as a variant of the $ThCr_2Si_2$ type with two additional carbon atoms in the tetragonal unit cell (Siegrist et al., 1994). The tetragonal unit cell of the structure is shown in Fig. 21. The space group is $I4/mmm$ with R on the $2b$ sites (high point symmetry $4/mmm$), Ni on the $4d$ sites, B on the $4e$ sites and C on the $2a$ sites. The only fractional coordinate not fixed by symmetry is z_B which takes a value of ≈ 0.14 in case of $GdNi_2B_2C$ (Belger et al., 1998; Lynn et al., 1997).

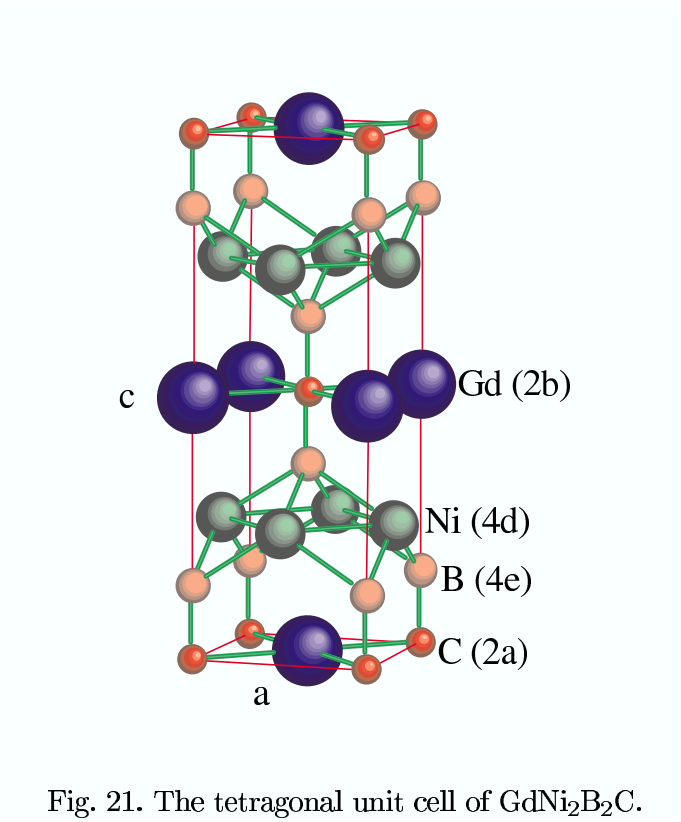

Fig. 21. The tetragonal unit cell of $GdNi_2B_2C$.

Detlefs et al. (1996) have investigated the magnetic structure of $GdNi_2B_2C$ with resonant and nonresonant magnetic x-ray-scattering techniques. These studies showed that between $T_N \approx$ 19-20 K and $T_R \approx 14$ K the magnetic structure is of the transverse sine-modulation type with an incommensurate propagation vector of ($\approx$0.55,0,0). The magnetic moments of Gd lie within the basic plane perpendicular to the propagation vector. Below T_R a component of the Gd moment develops along the c axis with the same propagation vector as the component in the basic plane. Further information on the magnetic structure below T_N has been gained by ^{155}Gd Mössbauer spectroscopy (Tomala et al., 1998), suggesting a bunched spiral-like magnetic structure with the moments rotating within the b-c plane. Despite the considerable efforts devoted to resolve the magnetic structures of $GdNi_2B_2C$, the absence of superconductivity in this compound remains an open question.

Concerning the spontaneous magnetostriction, $GdNi_2B_2C$ is a further example for only very weak effects. As can be seen in Fig. 22 there is no effect visible within the sensitivity of the x-ray diffraction experiments, neither in the volume nor in the c/a ratio. Measurements on a single crystal using capacitance dilatometry showed effects of about 5×10^{-5} (Massalami, 2002). These small effects are in accordance with the analysis of $ErNi_2B_2C$ (Doerr et al., 2002), where the magnetoelastic phenomena have been attributed to crystal field effects only (compare the different situation in the RCu_2 compounds which show a significant exchange contribution - see section 8.6). Like for $GdNi_5$ (see section 6.2), the reason for the small (i.e. $< 10^{-4}$) effects in this compound could also be that only one atom among six is a Gd atom, leading to weak magnetoelastic effects.

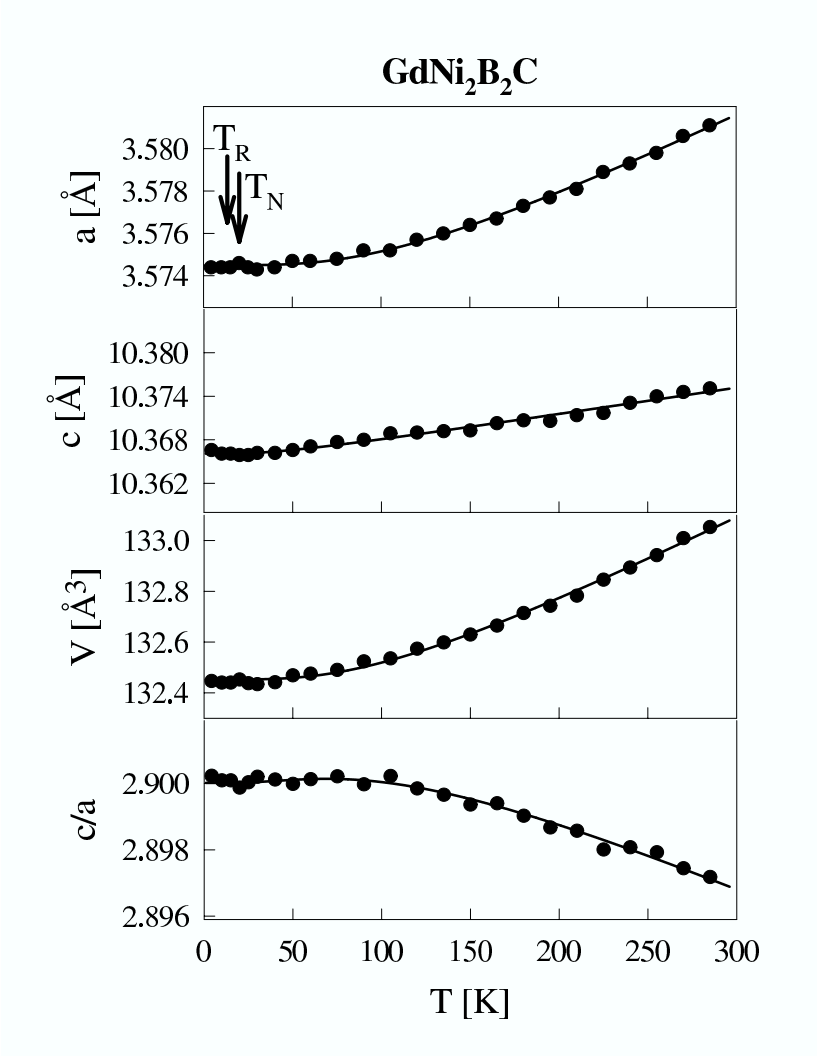

Fig. 22. Anisotropic thermal expansion of $GdNi_2B_2C$ measured by x-ray powder diffraction (this work). The lines indicate extrapolations from the paramagnetic range obtained by fitting Debye functions to the temperature range above T_N.

8.1 Magnetostructural transitions in $Gd_5(Si_xGe_{1-x})_4$ compounds

Recently, a giant magnetocaloric effect (MCE) has been discovered in the $Gd_5(Si_xGe_{1-x})_4$ pseudobinary system with $x \leq 0.5$ (Pecharsky and Gschneidner-Jr, 1997a,b,c, 1999). In the composition range $0.24 \leq x \leq 0.5$ the MCE is connected with a first-order transition from a high-temperature paramagnetic to a low-temperature ferromagnetic state, at temperatures ranging from 130K to 276K (Pecharsky and Gschneidner-Jr, 1997b). A recent study by Morellon et al. (1998a) on $Gd_5(Si_{0.45}Ge_{0.55})_4$ (i.e. $x = 0.45$) has revealed that on cooling this transition is accompanied by a structural transition from a monoclinic structure in the paramagnetic state to an orthorhombic structure in the ferromagnetic state. Furthermore this magnetostructural transition can be induced reversibly by an external magnetic field, leading to strong magnetoelastic effects (Morellon et al., 1998a) as well as to a giant negative magnetoresistance (Morellon et al., 1998b; Levin et al., 1999, 2000). In contrast to the compounds with $0.24 \leq x \leq 0.5$, the Ge-rich compounds with $x \leq 0.2$ order antiferromagnetically (or ferrimagnetically) at about 125 K (second-order transition) and then experience a further first-order transition to a low-temperature ferromagnetic state, connected with a giant MCE (Morellon et al., 1998a).

One example for the interesting magnetoelastic properties of the $Gd_5(Si_xGe_{1-x})_4$ pseudobinary system is the compound $Gd_5(Si_{0.1}Ge_{0.9})_4$ (i.e. $x = 0.1$). In contrast to the compounds with $0.24 \leq x \leq 0.5$, which show a monoclinic structure, this compound crystallizes in an orthorhombic structure (Gd_5Ge_4 type), which is similar to the Gd_5Si_4 type of the Si-rich compounds (Pecharsky and Gschneidner-Jr, 1997d). Both, the Gd_5Ge_4- and the Gd_5Si_4 type are described within space group *Pnma*, the Gd atoms occupy three different crystallographic sites (Gd1: 4c, Gd2: 8d, Gd3: 8d), and the Ge and Si atoms are statistically distributed over three sites (M1: 4c, M2: 4c, M3: 8d). The only difference between the two types lies in different fractional coordinates, which are not fixed by symmetry (for a comprehensive structural study of the $Gd_5(Si_xGe_{1-x})_4$ pseudobinary system see Pecharsky and Gschneidner-Jr (1997d) and Morellon et al. (2000)). For illustrating the magnetic and crystallographic properties of the $Gd_5(Si_xGe_{1-x})_4$ system, the magnetic and crystallographic temperature - composition phase diagram is shown in Fig. 23.

Ac-suszeptibility measurements by Morellon et al. (2000) showed, that (on heating) $Gd_5(Si_{0.1}Ge_{0.9})_4$ undergoes a first-order transition from a ferromagnetic to an antiferromagnetic state at $T_C = 81$ K, followed by a second-order transition to the paramagnetic state at $T_N = 127$ K. Measurements of the thermal dependence of the lattice parameters using x-ray powder diffraction, reported by the same authors and shown in Fig. 24, revealed a very pronounced spontaneous magnetostriction at the first-order ferromagnetic to antiferromagnetic transition at $T_C = 81$ K, whereas no significant effects could be observed at T_N. On cooling through T_C the following abrupt changes of the lattice parameters are visible: $(\Delta a/a)_{mag} \approx -16 \times 10^{-3}$, $(\Delta b/b)_{mag} \approx 3 \times 10^{-3}$, $(\Delta c/c)_{mag} \approx 7 \times 10^{-3}$

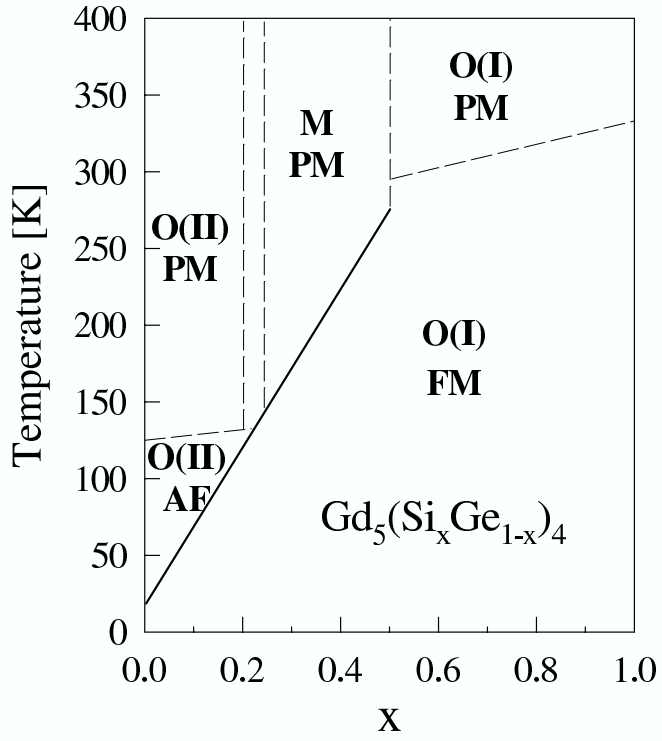

Fig. 23. Magnetic and crystallographic temperature - composition phase diagram of the $Gd_5(Si_xGe_{1-x})_4$ compounds (after Morellon et al. (2000)). FM, PM, AF label different magnetic phases (FM: ferromagnetic, PM: paramagnetic, AF: antiferromagnetic). O(I), M and O(II) label different crystallographic structures (O(I): orthorhombic Gd_5Si_4 structure, M: monoclinic structure, O(II): orthorhombic Gd_5Ge_4 structure). The solid line marks the first-order magnetostructural phase boundary.

and $(\Delta V/V)_{mag} \approx -6 \times 10^{-3}$. The change of the c/a ratio is $(\frac{\Delta(c/a)}{(c/a)})_{mag} \approx 23 \times 10^{-3}$. This means that the anisotropic effects are larger than 2 %, i.e. $Gd_5(Si_{0.1}Ge_{0.9})_4$ can be classified as a giant magnetostriction (GMS) compound (Engdahl, 1999).

Furthermore, Rietveld analysis of the x-ray powder patterns showed, that the spontaneous magnetostriction at T_C is connected with a significant change of some of the fractional coordinates (Morellon et al., 2000), leading mainly to a shifting of atoms in a-direction, where the magnetostriction is largest. The obtained atomic positions are very similar to the values determined for Gd_5Si_4 (Pecharsky and Gschneidner-Jr, 1997d). This means that the antiferromagnetic to ferromagnetic transition is not only accompanied by a giant magnetostriction of the lattice parameters, but also by a structural change. In order to illustrate this *magnetostructural* transition from the high-temperature Gd_5Ge_4 type to the low temperature Gd_5Si_4 type, Fig. 25 shows the orthorhombic unit cells, with atomic positions obtained from Rietveld fits below (30 K) and above (100 K) the transition. The main difference between the two orthorhombic structures is a common shifting (in a - direction) of the atoms in the upper half of the unit cell relative to the atoms in the lower half.

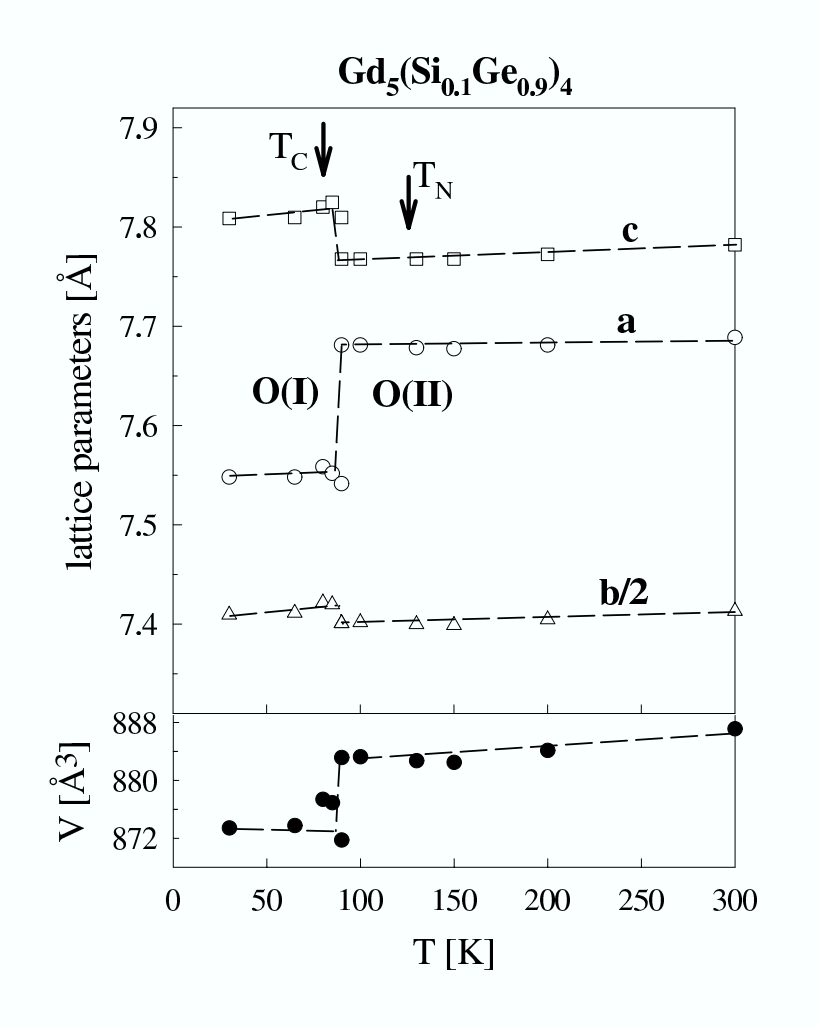

Fig. 24. Thermal dependence of the lattice parameters and the volume of $Gd_5(Si_{0.1}Ge_{0.9})_4$, measured by x-ray powder diffraction. The shown data have been extracted from Morellon et al. (2000). The dashed lines serve as a guide for the eyes.

Forced magnetostriction measurements using a strain gauge technique, also performed by Morellon et al. (2000), indicate that the magnetostructural transition can be induced reversibly by an external magnetic field. This means that there is a remarkable resemblance of the observed magnetostructural transition in $Gd_5(Si_{0.1}Ge_{0.9})_4$ with the transition in $Gd_5(Si_{0.45}Ge_{0.55})_4$ (Morellon et al., 1998a), where the transition is also dominated by a drastic reduction of the lattice parameter a. However, it has to be pointed out, that in $Gd_5(Si_{0.1}Ge_{0.9})_4$ no change of the symmetry is involved in the magnetostructural transition.

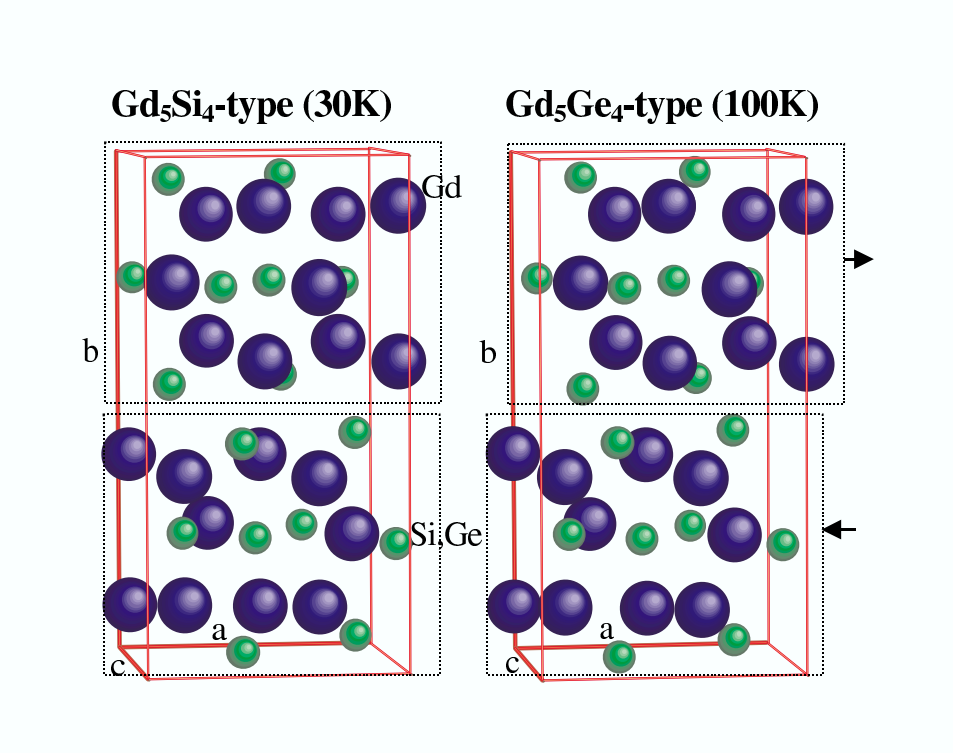

Fig. 25. Orthorhombic structures of $Gd_5(Si_{0.1}Ge_{0.9})_4$ below and above the magnetostructural transition. The dotted boxes and the arrows indicate roughly the shifting of the atoms in the Gd_5Ge_4 type (O(II)) compared to the Gd_5Si_4 type (O(I)).

GdNi crystallizes in the orthorhombic CrB type of structure (space group *Cmcm*). The Gd atoms are located on the 4*c* sites with point symmetry *mm* (0, $y_{Gd} \approx 0.14$, $\frac{1}{4}$). The Ni atoms also occupy the 4*c* sites with $y_{Ni} \approx 0.43$ (see e.g. Buschow (1980)). It is interesting to note that among the RNi compounds there exists a second type of orthorhombic structure. Only the compounds with R from La to Gd crystallize in the CrB type. The compounds with R from Dy to Tm and Y show the less symmetric FeB type with space group *Pnma* (see e.g. Burzo et al. (1990)). (As reported by Blanco et al. (1992) TbNi crystallizes in a monoclinic intermediate structure). Fig. 26 shows the orthorhombic unit cell and the atomic arrangement of the CrB type of structure. (The shown orthorhombic cell is not the primitive unit cell, since the lattice is base centered orthorhombic, i.e. there is an additional lattice point in the centre of the *a*-*b* planes.)

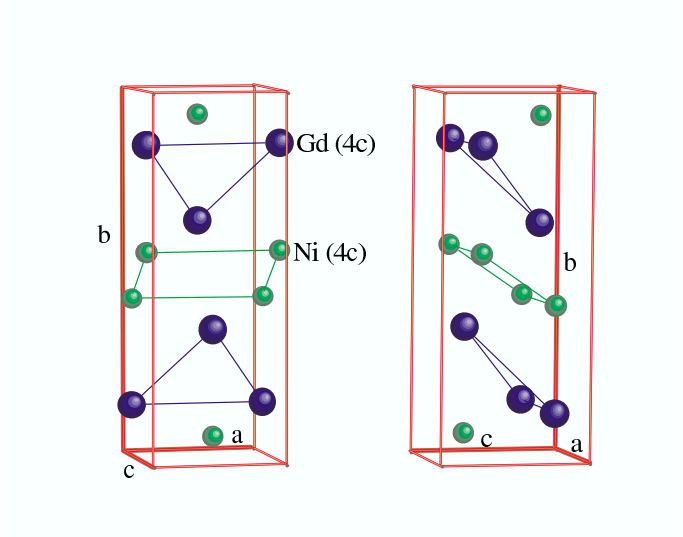

Fig. 26. Orthorhombic CrB-type structure of GdNi.

As shown by neutron diffraction experiments and magnetization measurements, GdNi is a simple collinear ferromagnet with the magnetic moments parallel to the *b*- axis below $T_c \approx 69$ K (Blanco et al., 1992). The magnetic moment at 4.2 K is $7.3 \pm 0.1\ \mu_B$. NMR spectra of this compound are also consistent with a direction of magnetization along the b-axis for this compound (de Jesus et al., 2000).

The spontaneous magnetostriction, obtained by x-ray powder diffraction, shows, like for $Gd_5(Si_{0.1}Ge_{0.9})_4$ (see section 8.1), very large anisotropic effects (see Fig. 27). The estimated values at 0 K in the different crystallographic directions are $(\Delta a/a)_{mag} \approx 4.0 \times 10^{-3}$, $(\Delta b/b)_{mag} \approx 5.4 \times 10^{-3}$, $(\Delta c/c)_{mag} \approx -8.2 \times 10^{-3}$ and $(\Delta V/V)_{mag} \approx 1.2 \times 10^{-3}$. Especially the spontaneous magnetically induced contraction in *c*- direction of almost 1 % is outstanding. The magnetically induced change of the c/b ratio reaches $(\frac{\Delta(c/b)}{(c/b)})_{mag} \approx -1.36 \times 10^{-2}$ and therefore GdNi has to be considered as a GMS compound (compare Engdahl (1999)). Whether the observed giant magnetostriction of the lattice parameters is connected with a change of the atomic positions, has not been determined, i.e. further studies are necessary in order to answer the question whether GdNi shows, like $Gd_5(Si_{0.1}Ge_{0.9})_4$, a magnetostructural transition and whether this transition can be induced by a magnetic field. The relatively

large positive volume effect could be due to an induced itinerant Ni moment (Paulose et al., 1996), what is confirmed by a comparison with GdPt (see section 8.5). A further hint for the existence of an induced Ni moment could be the temperature dependence of the magnetization, which deviates remarkably from the typical bahaviour of rare earth systems (see e.g. Walline and Wallace (1964)). The volume effect has also been measured by a strain gauge technique with a reported value of about 1.8×10^{-3} at 10 K (Espeso et al., 1994). In addition to the large positive volume effect below T_c, this strain gauge experiments showed a very small negative effect of about 10^{-5} around T_c, too small for being detectable with x-ray powder diffraction. The reason for this small additional effect is unclear.

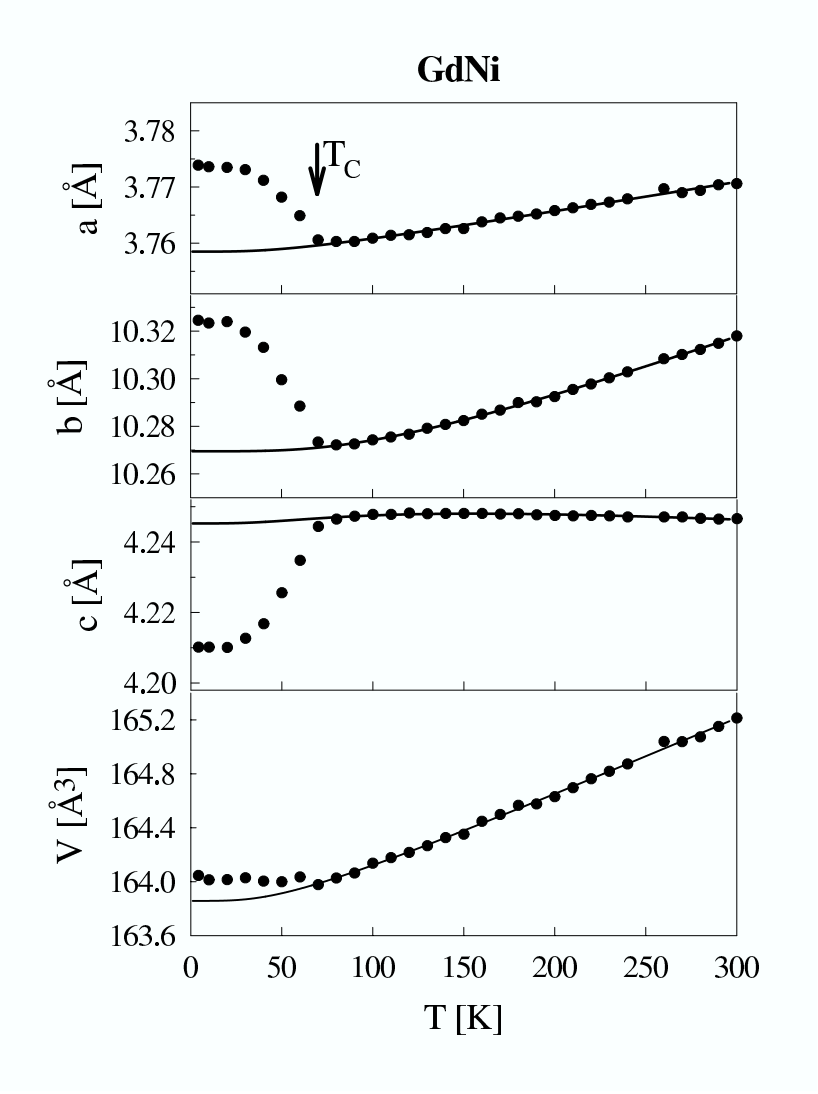

Fig. 27. Anisotropic thermal expansion of GdNi measured by x-ray powder diffraction (Gratz and Lindbaum, 1998). The lines represent extrapolations of the lattice contribution from the paramagnetic range, obtained by fitting Debye functions.

8.3 $GdNi_{1-x}Cu_x$

The assumption that an induced itinerant Ni moment plays an important role for the pronounced positive magnetovolume effect in GdNi, is supported by the fact that by substituting Ni by Cu the volume effect becomes smaller. For Cu concentrations x higher than 20 % the FeB type of structure is formed instead of the CrB type of structure. Magnetization measurements and neutron powder diffraction experiments showed that with 30 % Cu the system is, like GdNi, a simple collinear ferromagnet with a very similar ordering temperature of $T_c \approx 68$ K and with the magnetic moment direction parallel to the b-axis of the FeB structure (Blanco et al., 1992). However, the volume effect of $(\Delta V/V)_{mag} \approx 0.6 \times 10^{-3}$ at 10 K (Espeso et al., 1994) is about two to three times smaller than in GdNi. Furthermore, for Cu concentrations higher than 35 % the magnetic structure changes from ferromagnetic to antiferromagnetic (Gignoux and Gomez-Sal, 1976). The neutron diffraction studies by Blanco et al. (1992) showed that the compound with a Cu concentration of 60 % orders in a helimagnetic structure with a propagation vector (0,0,0.25) with the moments lying in the a-b plane ($T_N \approx 63$ K). The magnetovolume effect for this compound reaches a value of $(\Delta V/V)_{mag} \approx 0.8 \times 10^{-3}$ at 10 K (Espeso et al., 1994).

8.4 GdCu

The RCu series is characterized by a structural instability. The light rare-earth based compounds crystallize in the orthorhombic FeB-type structure, while the heavy ones do so in the cubic CsCl-type structure. GdCu is the first in the series to adopt this cubic structure at room temperature, but is unstable, showing a tendency to transform into the FeB type at low temperatures. But this martensitic structural transition occurs only in a bulk (polycrystalline) sample, whereas powdered samples keep the CsCl structure down to lowest temperatures (Blanco et al., 1999). Studying the spontaneous magnetoelastic effects in the orthorhombic FeB-type phase of GdCu is very interesting with respect to a comparison with the isostructural GdPt (see section 8.5).

As reported by Blanco et al. (1999), neutron diffraction patterns of powder and bulk polycrystalline samples of GdCu were obtained for both structures: In the cubic CsCl type of structure, which orders antiferromagnetically at $T_N \approx 150$ K, a propagation vector of (1/2 1/2 0) has been found with the moments probably parallel to the c-axis (note that other noncollinear magnetic structures might give rise to the same neutron-diffraction pattern). In the orthorhombic low temperature phase ($T_N \approx 45$ K) the available diffraction patterns suggest a magnetic propagation of (0 1/4 1/4) and a helimagnetic arrangement of the moments normal to the [011] direction. Furthermore it has been concluded that a simple RKKY model of an isotropic exchange interaction can be used to understand the stability of the magnetic structure in the cubic high temperature phase, whereas anisotropy in the magnetic interactions has to be taken into account for the orthorhombic low temperature phase.

Concerning the spontaneous magnetoelastic effects in GdCu the only available data are the lattice pa-

rameters, as obtained by Blanco et al. (1999) from the above mentioned neutron diffraction patterns at variable temperatures. Due to the relatively low resolution of these neutron diffraction experiments concerning the determination of the lattice parameters it is only possible to give qualitative results. Fig. 28 shows data for the orthorhombic FeB type, indicating a large anisotropic spontaneous magnetostriction with a negative sign in b direction (roughly -1×10^{-2}), accompanied by somewhat smaller positive effects in a (roughly 5×10^{-3}) and c (roughly 3×10^{-3}) direction. This behaviour of GdCu in the FeB type is similar to that of the isostructural GdPt (see section 8.5) and suggests, that the kind of magnetic ordering (GdPt: ferromagnetic, GdCu: antiferromagnetic) has no influence on the qualitative behaviour of the spontaneous magnetostriction.

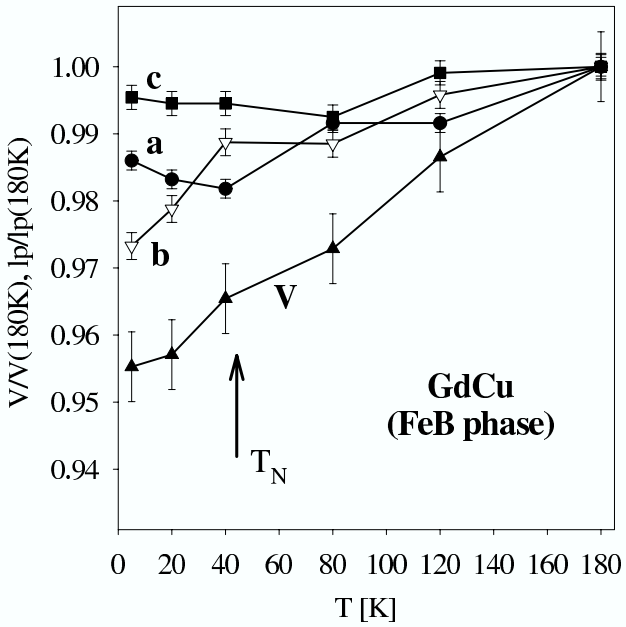

Fig. 28. Anisotropic thermal expansion of the orthorhombic FeB phase of GdCu obtained from neutron diffraction experiments on a bulk polycrystalline sample (Blanco et al., 1999). The lattice parameters (lp) at 180 K are: $a = 7.15 \pm 0.01$ Å, $b = 4.527 \pm 0.008$ Å, $c = 5.471 \pm 0.008$ Å.

8.5 GdPt

Like the RNi compounds, the RPt compounds crystallize in two different orthorhombic structures. The heavy RPt (R=Gd to Tm) show the FeB type of structure (space group *Pnma*), whereas the light RPt (R=La to Nd) show the more symmetric CrB type of structure with space group *Cmcm* (Dwight et al., 1965; Roy et al., 1978). The Gd atoms occupy the 4*c*-sites (x, $y = \frac{1}{4}$, z, point symmetry m) of the space group *Pnma* with $x_{Gd} \approx 0.180$ and $z_{Gd} \approx 0.133$. The Pt atoms also occupy the 4*c*-sites with $x_{Pt} \approx 0.036$ and $z_{Pt} \approx 0.623$. Fig. 29 shows the orthorhombic unit cell and the atomic arrangement of this structure type.

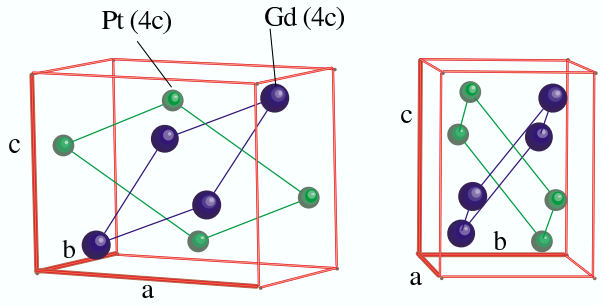

Fig. 29. Orthorhombic FeB-type structure.

The RPt compounds are ferromagnets with relatively low ordering temperatures (Castets et al., 1980, 1982). GdPt has the highest ordering temperature among all RPt compounds ($T_c \approx 68$ K).

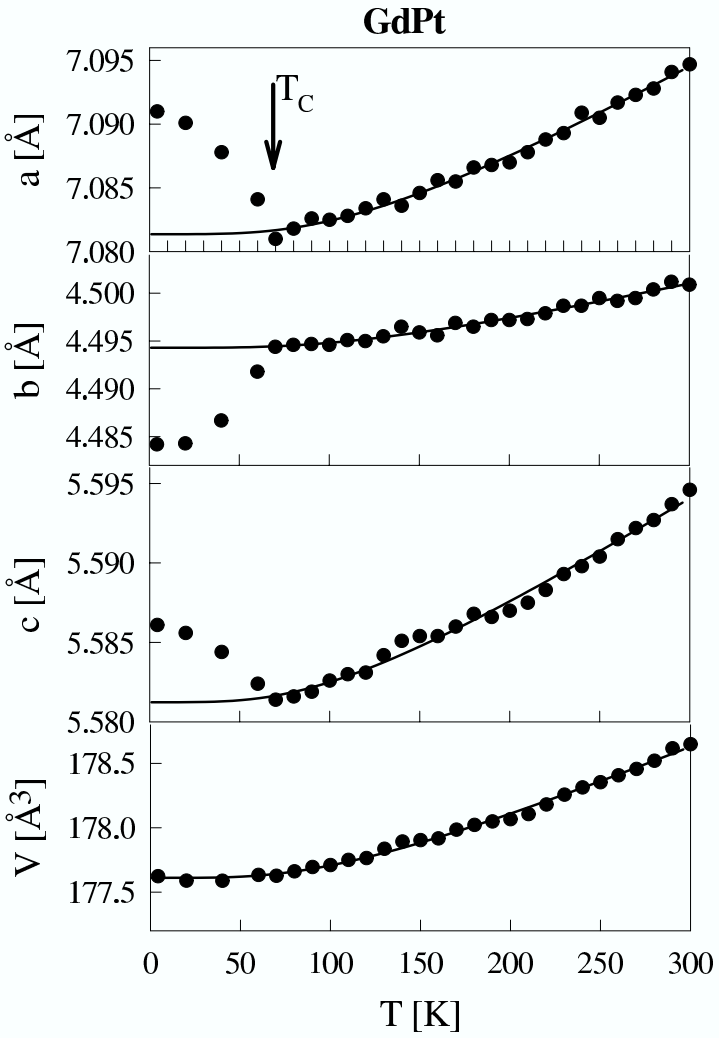

Fig. 30. Anisotropic thermal expansion of the orthorhombic GdPt measured by x-ray powder diffraction (this work). The lines represent extrapolations of the lattice contribution from the paramagnetic range, obtained by fitting Debye functions.

Fig. 30 shows the temperature dependence of the lattice parameters of GdPt, obtained by x-ray

powder diffraction. The estimated values of the spontaneous magnetoelastic effects at 0 K are $(\Delta a/a)_{mag} \approx 1.4 \times 10^{-3}$, $(\Delta b/b)_{mag} \approx -2.3 \times 10^{-3}$, $(\Delta c/c)_{mag} \approx 0.9 \times 10^{-3}$ and $|(\Delta V/V)_{mag}| < 0.1 \times 10^{-3}$. This means that the pronounced linear effects, which are dominated by a negative magnetostriction in b- direction, compensate each other, leading to a volume effect smaller than the experimental resolution. This is a further hint that the observed volume effect in GdNi (see section 8.2) is due to an induced itinerant Ni moment, since GdNi has a related crystal structure, almost the same magnetic ordering temperature and is also ferromagnetic.

8.6 $GdCu_2$

Among the presented systems in this chapter, $GdCu_2$ is one for which a variety of studies dealing with the magnetic properties and spontaneous as well as field-induced magnetostriction have been done in the past and also very recently (Rotter et al., 2001a). Since we think that this compound can be viewed as a model system for the investigation of magnetoelastic effects, it follows a relatively detailed description of magnetoelastic effects of $GdCu_2$.

8.6.1 Crystal Structure

All 1:2 compounds of lanthanides with Cu exhibit the orthorhombic $CeCu_2$-type structure (see e.g. Debray (1973), space group $Imma$, Ce on $4e$ sites with point symmetry mm, Cu on $8h$), with the exception of $LaCu_2$. $LaCu_2$ displays the related hexagonal AlB_2 structure with space group P_6/mmm (Storm and Benson, 1963). The orthorhombic $CeCu_2$ structure can be viewed as a distorted AlB_2-type structure (see Fig. 31). In some RCu_2 compounds a martensitic transition in high magnetic fields has been observed and associated with a conversion of the $CeCu_2$ to the AlB_2 type of structure (Svoboda et al., 1999). Furthermore for $LaCu_2$ a pressure induced transition from the AlB_2 type to the $CeCu_2$ type has been predicted by *ab-initio* total energy calculations and experimentally observed by high-pressure x-ray diffraction with a diamond anvil cell (Lindbaum et al., 2000, 1998). The atomic position parameters of $GdCu_2$, which are not fixed by space group symmetry, have been determined from neutron diffraction experiments and are discussed below (see section 8.6.3).

8.6.2 Magnetic Properties

Investigations of $GdCu_2$ in the magnetically ordered state ($T_N \approx 42$ K) revealed that in this compound no change of the magnetic structure exists in zero external magnetic field (Koyanagi et al., 1998; Luong and Franse, 1981; Luong et al., 1985). The magnetic entropy as calculated from the specific heat reaches its theoretical value of $R \ln 8$ at 47 K, just above T_N (Koyanagi et al., 1998). In high magnetic fields the anisotropy in the magnetization does not exceed a few percent (Borombaev et al., 1987). Recent measurements of the anisotropy in the magnetization of a single crystal (see Fig. 32) revealed an anomaly at T $\approx$ 10 K (Rotter et al., 2000b), the origin of which is still the topic of current research. Neutron scattering experiments on polycrystalline and single crystal samples (Rotter

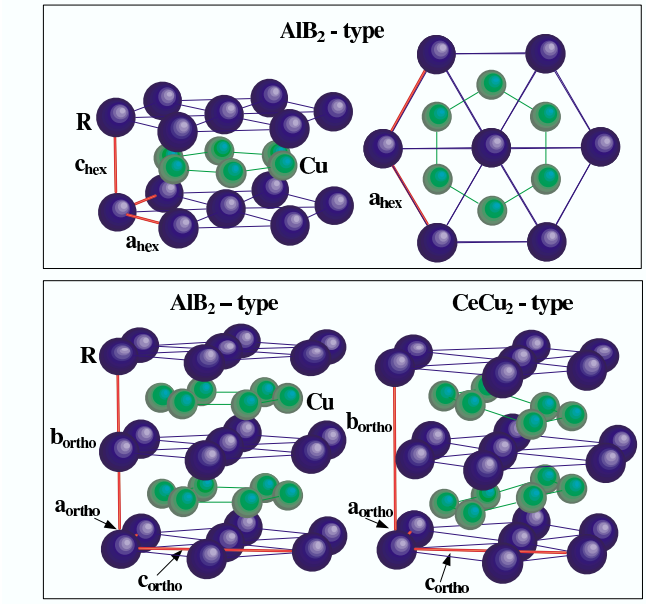

Fig. 31. The upper part shows the highly symmetric hexagonal AlB_2 type of structure. In the lower part the hexagonal cell of the AlB_2 structure is doubled along the hexagonal axis (left), which allows a direct comparison with the $CeCu_2$ type (right).

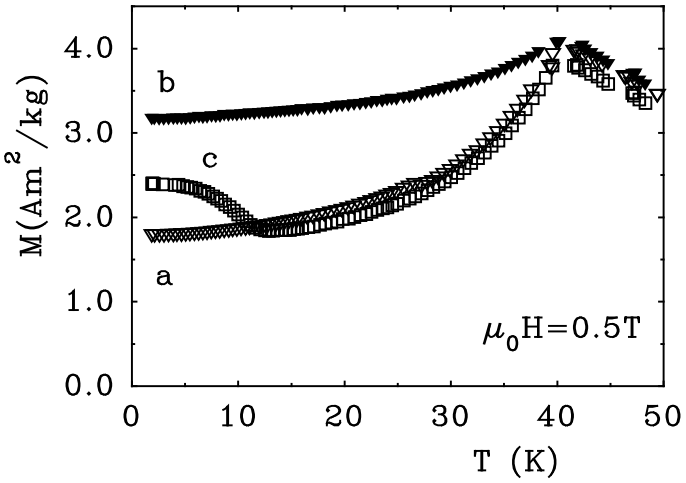

Fig. 32. Temperature dependence of the magnetization of $GdCu_2$ (Rotter et al., 2000b).

et al., 2000a), as well as magnetic scattering experiments using synchrotron radiation (Rotter et al., 2000b), showed that the modulation vector of the magnetic structure is $\mathbf{Q}_0$=(2/3 1 0) and that the type of ordering can be viewed as an *antiferromagnetic* modulation of the moments in *b* direction and a *cycloidal* propagation in *a* direction with a pitch angle of 120 degrees. The proposed magnetic structure of $GdCu_2$ is shown in Fig. 33. The magnetic unit cell consists of three structural unit cells aligned in *a* direction. From the projection into the *ac*–plane the cycloidal propagation in *a* direction can be seen. The filled and open symbols denote two different neighboring *ac* planes showing the

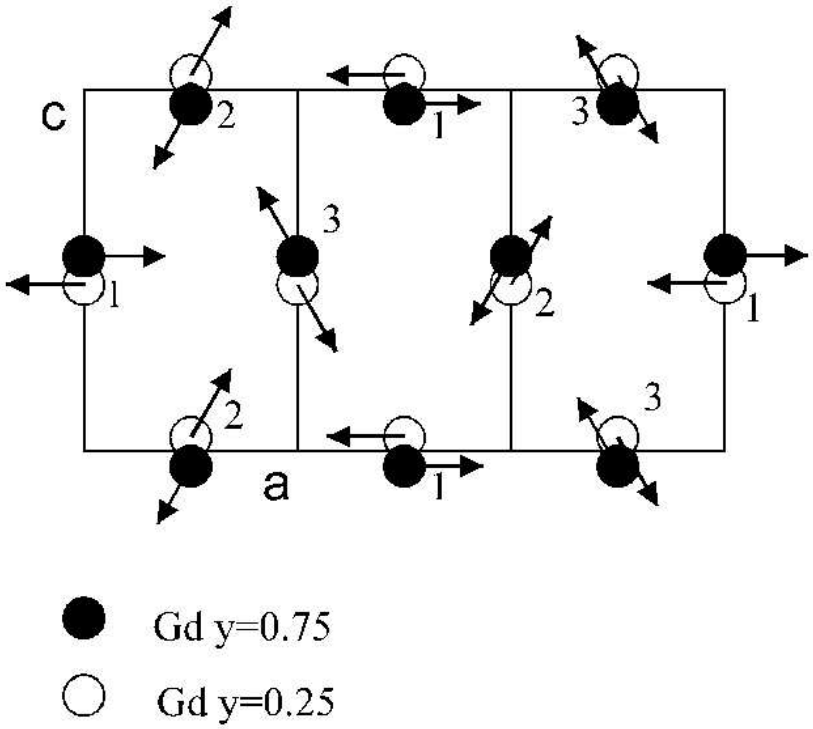

Fig. 33. Magnetic structure of $GdCu_2$, the different symbols denote atoms belonging to the same *ac* plane, for simplicity the copper atoms are not shown. The magnetic structure can be viewed as a superposition of three simple antiferromagnetic lattices as indicated by the numbers (Rotter et al., 2000a).

antiferromagnetic propagation in b direction. A Rietveld refinement of the powder data at 2 K gives a magnetic Gd moment of 6.9 μ_B (Rotter et al., 2000a).

8.6.3 Spontaneous magnetostriction

The thermal expansion of $GdCu_2$ has been measured already in 1985 on polycrystals by dilatometric experiments (Luong et al., 1985) and later by x-ray diffraction on powder (Gratz and Lindbaum, 1994) and single crystals (Borombaev et al., 1987). The most recent measurements have been performed on a single crystal produced by the Bridgeman method and using a capacitance dilatometer down to 500 mK in a magnetic field of 0-15 T. Fig. 34 shows the thermal expansion measured along the a-, b- and c-axis in zero field in comparison with results of powder x-ray diffraction (Rotter et al., 2001a; Gratz and Lindbaum, 1994). Below the ordering temperature T_N the thermal expansion shows a pronounced negative spontaneous magnetoelastic effect in the a-direction, and a positive one in the b- and c-direction. These anisotropic contributions cancel each other leading only to a small magnetovolume effect. The estimated 0 K values of the spontaneous magnetostriction, obtained by the powder x-ray diffraction experiments are $(\Delta a/a)_{mag} \approx -2.1 \times 10^{-3}$, $(\Delta b/b)_{mag} \approx 1.2 \times 10^{-3}$, $(\Delta c/c)_{mag} \approx 1.5 \times 10^{-3}$ and $(\Delta V/V)_{mag} \approx 0.6 \times 10^{-3}$.

In case of $GdCu_2$ not only the magnetoelastic effects on the lattice parameters have been investigated, but also the magnetically induced influence on the atomic positions. The atomic position parameters z_{Gd}, y_{Cu} and z_{Cu}, which are not fixed by space group symmetry, have been determined from the

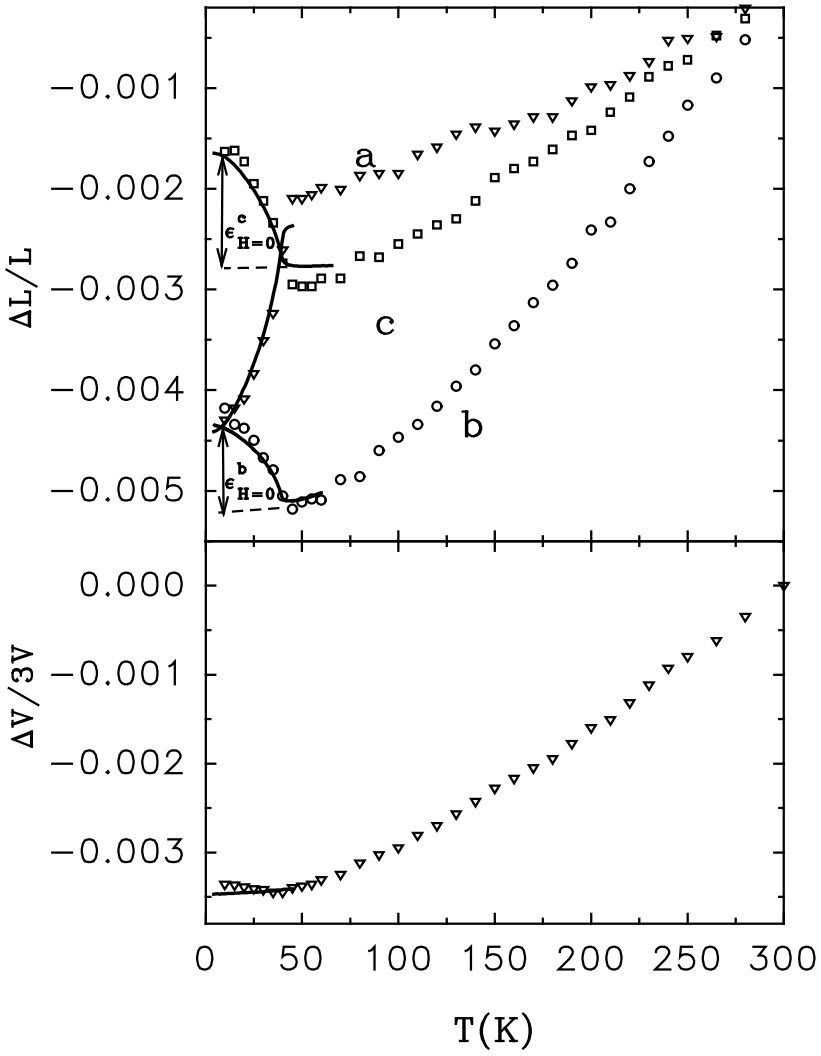

Fig. 34. Normalized thermal expansion of $GdCu_2$ along the orthorhombic a-, b- and c-direction (upper figure) and the volume expansion calculated from these data (bottom figure, the factor $\frac{1}{3}$ facilitates the comparison with the upper figure). The symbols denote the results of powder x-ray diffraction (Gratz and Lindbaum, 1994), the lines correspond to expansion measurements on a single crystal using the capacitance method (Rotter et al., 2001a). The values $\epsilon_{H=0}$ denote the relative length changes in the ordered state with respect to the nonmagnetic state.

neutron diffraction patterns at 2 and 60 K (shown in Rotter et al. (2000a)) by Rietveld analysis: At 2 K the obtained values are $z_{Gd} = 0.5403(8)$, $y_{Cu} = 0.0523(8)$ and $z_{Cu} = 0.1653(10)$. At 60 K (i.e. above $T_N \approx 42$ K) the values are: $z_{Gd} = 0.5429(6)$, $y_{Cu} = 0.0527(5)$ and $z_{Cu} = 0.1653(6)$. As can be seen there is only for Gd a significant difference in the atomic position between the paramagnetic and magnetically ordered state, whereas for Cu the differences are very small (as expected for a pure lattice contribution). This suggests that the observed shifting of the Gd atoms is due to the magnetic ordering.

8.6.4 Field induced magnetostriction

Fig. 35 shows the field induced magnetostriction for external fields along the a-, b- and c-axis (Rotter et al., 2001a). All measurements were done with increasing and decreasing field and they show only a

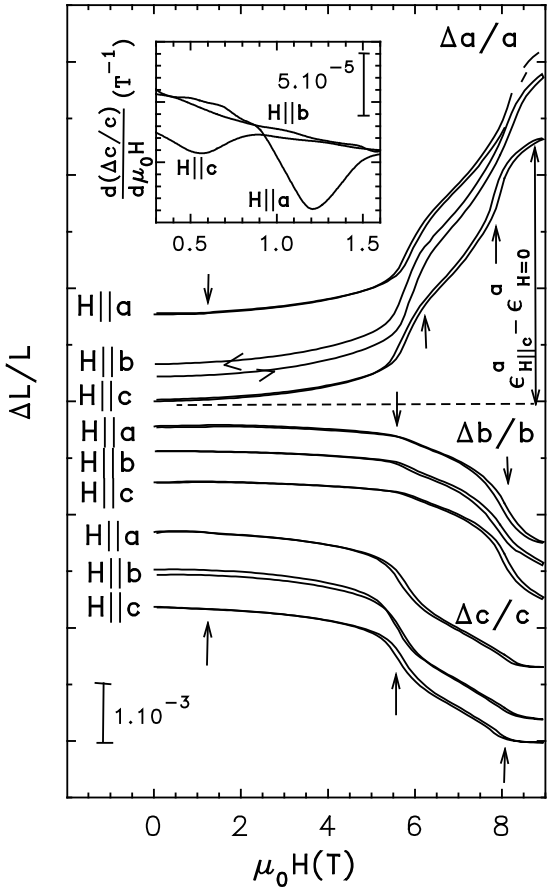

Fig. 35. Magnetostriction $\Delta a/a$, $\Delta b/b$ and $\Delta c/c$ of $GdCu_2$ for magnetic fields parallel to the orthorhombic a-, b- and c-axis at 4.2 K (Rotter et al., 2001a). The arrows indicate the position of phase transitions. For each curve the hysteresis is shown. The inset shows the low field data of the derivative of $\Delta c/c$ with respect to the magnetic field.

small hysteresis. Below $\mu_0 H = 5$ T the magnetostrictive effects are rather small. Above this value two remarkable kinks occur at 5.5 T and 8.0 T, approximately, which are connected to the two magnetic phase transitions which were also found in magnetization measurements (Borombaev et al., 1987). Above 8.0 T the system is in the induced ferromagnetic state and no further transitions could be seen when continuing some of the scans up to 15 T (Rotter et al., 2001a). From all the data it is evident that the field induced magnetostriction is strongly different for the different crystallographic axes (leading again to a very small volume effect) but is nearly independent of the magnetic field direction. The only difference between the different field directions was found examining the low field behavior more closely (compare inset in fig. 35, there the derivatives of the $\Delta c/c$ curves are shown as an example), showing some small differences between the curves. A transition at 0.6 T and 1.2 T is observed for fields parallel to a and c, respectively. No phase transition is observed for $\mathbf{H}||b$. This is in accordance with the findings from the magnetization experiments on a single crystal (Borombaev et al., 1987) and can be attributed to the fact, that in zero field the moments are confined to the ac-plane.

8.6.5 Discussion

A model for describing the magnetoelastic properties of $GdCu_2$ has been proposed by Rotter et al. (2001a), following the ideas outlined in section 3. Using equations (13) and (14) the magnetostriction has been calculated. By a comparison of the model with the experimentally determined spontaneous (Fig. 34) and field-induced magnetostriction (Fig. 35), it could be shown that the magnetoelastic interaction is dominated by the next neighbor exchange interaction in *b*- direction (for a detailed explanation see Rotter et al. (2001a)). In *b*- direction the Gd atoms have the shortest distances and are arranged in zig-zag like chains.

Another point which has to be discussed is the possible origin of the magnetoelastic interaction. Note the experimental result that the strains do not depend on the direction of the magnetic field (compare fig. 35), i.e. $\epsilon_{\mathbf{H}||a} \approx \epsilon_{\mathbf{H}||b} \approx \epsilon_{\mathbf{H}||c} \equiv \epsilon_{\mathrm{sat}}$. It follows, that the derivatives of the diagonal components of the exchange interaction tensor with respect to any strain ϵ are equal (Rotter et al., 2001a). Such a behaviour may be attributed to the fact that the magnetoelastic interaction in $GdCu_2$ is dominated by the isotropic exchange and thus can be described by equations (17) and (18). The anisotropic exchange interaction which leads to the observed magnetic structure with moments restricted to the *ac*-plane is small and does not contribute to the magnetoelastic interaction. When aligning the moments ferromagnetically with a magnetic field of about 9 Tesla (see figure 35), the signs of the magnetoelastic strains $\Delta a/a$, $\Delta b/b$ and $\Delta c/c$ are reversed (compared to the spontaneous magnetostriction), in agreement with the supposed model. However, this does not change the fact that the sign of the magnetostriction in *a*-direction remains opposite to the other two directions.

Finally, it has to be mentioned that, in addition to the magnetically induced effects on the lattice parameters, there is also a shifting of the Gd atoms within the unit cell. As discussed above, the relative atomic position parameter z_{Gd} changes by about -0.003 due to the magnetic ordering.

8.7 $GdZn_2$

$GdZn_2$ crystallizes in the orthorhombic $CeCu_2$ type of structure (see section 8.6), but shows in contrast to the isostructural $GdCu_2$ ferromagnetic order with $T_c \approx 68$ K (Debray et al., 1970). As discussed in section 8.6, $GdCu_2$ shows a cycloidal antiferromagnetic structure, whereas $GdZn_2$ is a simple ferromagnet (Debray et al., 1970). Due to this difference concerning the magnetic structure it seems very interesting to compare the two compounds with respect to the spontaneous magnetoelastic effects.

Fig. 36 shows the spontaneous magnetostriction of $GdZn_2$, measured by x-ray powder diffraction (Ohta et al., 1995). The measurements indicate, like in $GdCu_2$, a negative spontaneous magnetostriction in *a*- direction and a positive in *b*- and *c*- direction, but the effect in *a* direction is very small and at the limit of the resolution of the experiment. The estimated values at 0 K are: $(\Delta a/a)_{mag} \approx -0.2 \times 10^{-3}$, $(\Delta b/b)_{mag} \approx 1.4 \times 10^{-3}$, $(\Delta c/c)_{mag} \approx 1.9 \times 10^{-3}$ and $(\Delta V/V)_{mag} \approx 3.1 \times 10^{-3}$. This means that, in-

terestingly, the spontaneous magnetoelastic effects in $GdZn_2$ are qualitatively very similar to $GdCu_2$, although the magnetic structures are very different. However, the quantitative comparison of the spontaneous magnetoelastic effects shows pronounced differences. The contraction in a- direction is almost zero or at least much smaller than in $GdCu_2$, whereas the expansion in the other directions is similar, leading to a much larger volume effect.

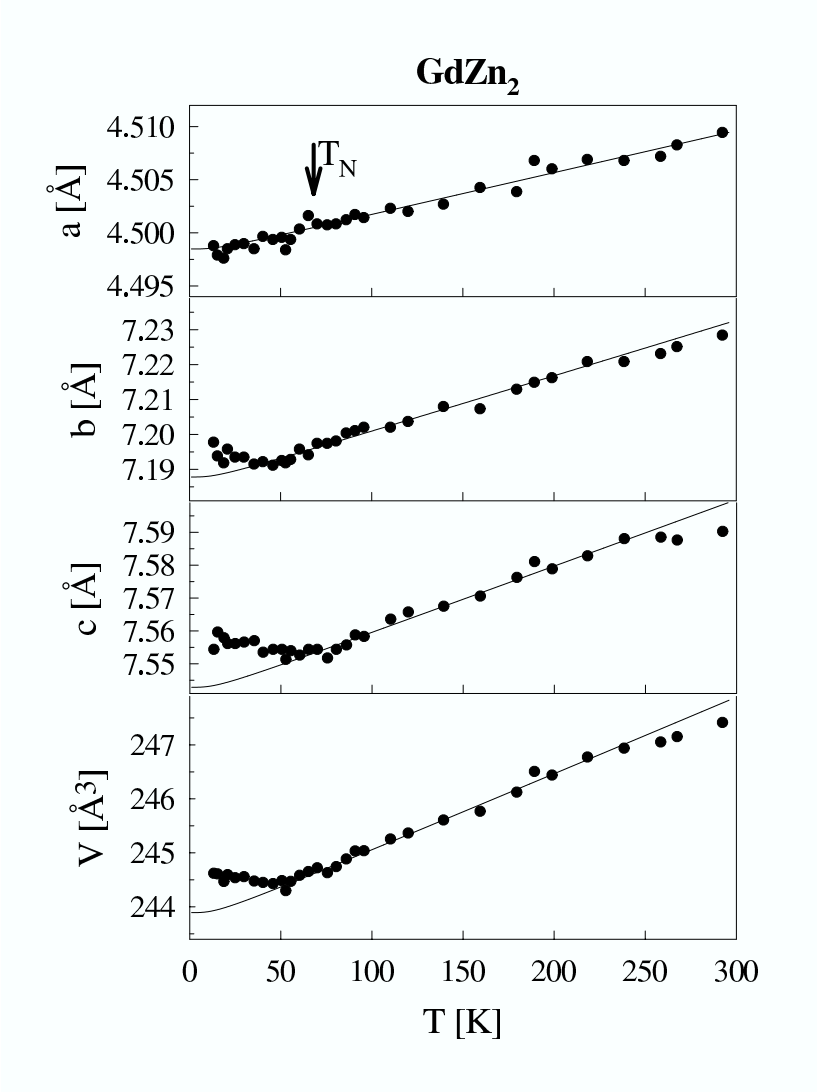

Fig. 36. Anisotropic thermal expansion of the orthorhombic $GdZn_2$, measured by x-ray powder diffraction (the data points have been extracted from Ohta et al. (1995)). The lines represent extrapolations of the lattice contribution from the paramagnetic range.

8.8 $Gd(Cu_{1-x}Ni_x)_2$

A further possibility to study the influence of the magnetic structure on the spontaneous magnetoelastic effects is the comparison of $GdCu_2$ with the solid solution $Gd(Cu_{1-x}Ni_x)_2$. This is possible since up to a Ni content of about 40% the $CeCu_2$ type of structure remains stable. On the other hand there is a pronounced change of the magnetic properties due to the Ni substitution. The magnetic ordering temperature increases from 42 K (x=0) up to about 110 K for x=0.3 and, interestingly,

the magnetic structure changes from antiferromagnetic to ferromagnetic above a Ni concentration of about $x = 0.15$ (Poldy and Kirchmayr, 1974; Gratz and Poldy, 1977).

Measurements of the spontaneous magnetostriction of the ferromagnetic compound $Gd(Cu_{0.8}Ni_{0.2})_2$ ($T_c \approx 95$ K) by x-ray diffraction (Borombaev and Markosyan, 1987) show, like for $GdZn_2$, qualitatively the same results as for the antiferromagnetic $GdCu_2$, i.e. a contraction in a- direction and an expansion in the other directions. This means that again the spontaneous magnetoelastic effects remain qualitatively the same, when changing from the complicated antiferromagnetic structure of $GdCu_2$ to a simple ferromagnetic one. But again a quantitative comparison shows pronounced differences. The estimated values at 0 K for $Gd(Cu_{0.8}Ni_{0.2})_2$ are $(\Delta a/a)_{mag} \approx -3.5 \times 10^{-3}$, $(\Delta b/b)_{mag} \approx 4.9 \times 10^{-3}$, $(\Delta c/c)_{mag} \approx 0.8 \times 10^{-3}$ and $(\Delta V/V)_{mag} \approx 2.2 \times 10^{-3}$. In contrast to the pure $GdCu_2$ (see section 8.6) the spontaneous magnetostriction is dominated by a very large effect in b- direction. The (positive) volume effect is, like in the ferromagnetic $GdZn_2$, much larger than in $GdCu_2$. Possibly, the ferromagnetic order in $Gd(Cu_{0.8}Ni_{0.2})_2$ and $GdZn_2$ is responsible for a larger volume effect. But note that in the case of $Gd(Cu_{0.8}Ni_{0.2})_2$ it could also be an induced itinerant Ni moment which is responsible for the larger volume effect.

8.9 Gd_3Ni and Gd_3Rh

Gd_3Ni and Gd_3Rh crystallize in the Fe_3C type of structure, which is described in the space group *Pnma*. The Gd atoms occupy two different crystallographic sites, namely the 4*c* sites (point symmetry *m*) and the 8*d* sites (point symmetry 1), whereas the Ni (Rh) atoms are only located on the 4*c* sites. Fig. 37 shows the unit cell and the atomic arrangement of this structure type. As an example the atomic position parameters of Gd_3Ni at room temperature as reported by Kusz et al. (2000) are given: Gd(1): 4*c* sites (≈0.033, 1/4, ≈0.859); Gd(2): 8*d* sites (≈0.678, ≈0.435, ≈0.175); Ni: 4*c* sites (≈0.388, 1/4, ≈0.059). As reported by Talik and Neumann (1994) and Talik and Ślebarski (1995) the two compounds Gd_3Ni and Gd_3Rh show some complicated antiferromagnetic structure with ordering temperatures of $T_N \approx 100$ K and $T_N \approx 112$ K, respectively.

The spontaneous magnetostriction has been measured by single crystal x-ray diffraction between 10 and 300 K (Kusz et al., 2000). As can be seen from Figs. 38 and 39, both compounds show pronounced linear as well as volume effects. Gd_3Ni is characterized by a large positive spontaneous magnetostriction in a-direction (the estimated value at 0 K is $(\Delta a/a)_{mag} \approx 2.9 \times 10^{-3}$), whereas the effects in b- and c- direction are about two times smaller ($(\Delta b/b)_{mag} \approx 1.3 \times 10^{-3}$, $(\Delta c/c)_{mag} \approx -1.3 \times 10^{-3}$). The resulting volume effect of $(\Delta V/V)_{mag} \approx 2.9 \times 10^{-3}$ is about twice as large as in the earlier discussed GdNi. Gd_3Rh, on the other hand, is characterized by a negative spontaneous magnetostriction in a-direction (estimated value at 0 K $(\Delta a/a)_{mag} \approx -2.5 \times 10^{-3}$) and by an almost uniform expansion of the b-c plane ($(\Delta b/b)_{mag} \approx 2.0 \times 10^{-3}$, $(\Delta c/c)_{mag} \approx 2.6 \times 10^{-3}$). The resulting volume effect of $(\Delta V/V)_{mag} \approx 2.1 \times 10^{-3}$ is smaller than in Gd_3Ni. A possible reason for this difference could be that in the case of Gd_3Ni an induced itinerant Ni moment enhances the positive volume

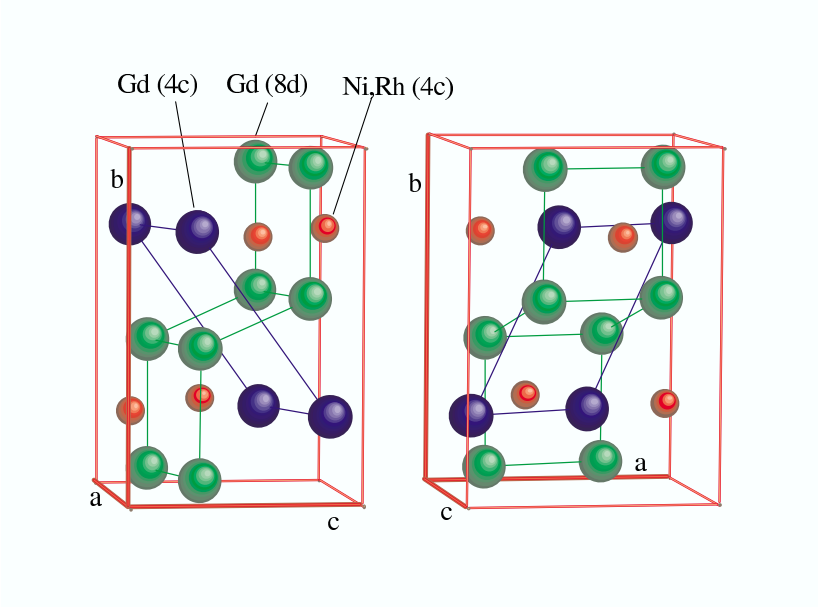

Fig. 37. Orthorhombic Fe_3C-type structure of Gd_3Ni and Gd_3Rh.

magnetostriction.

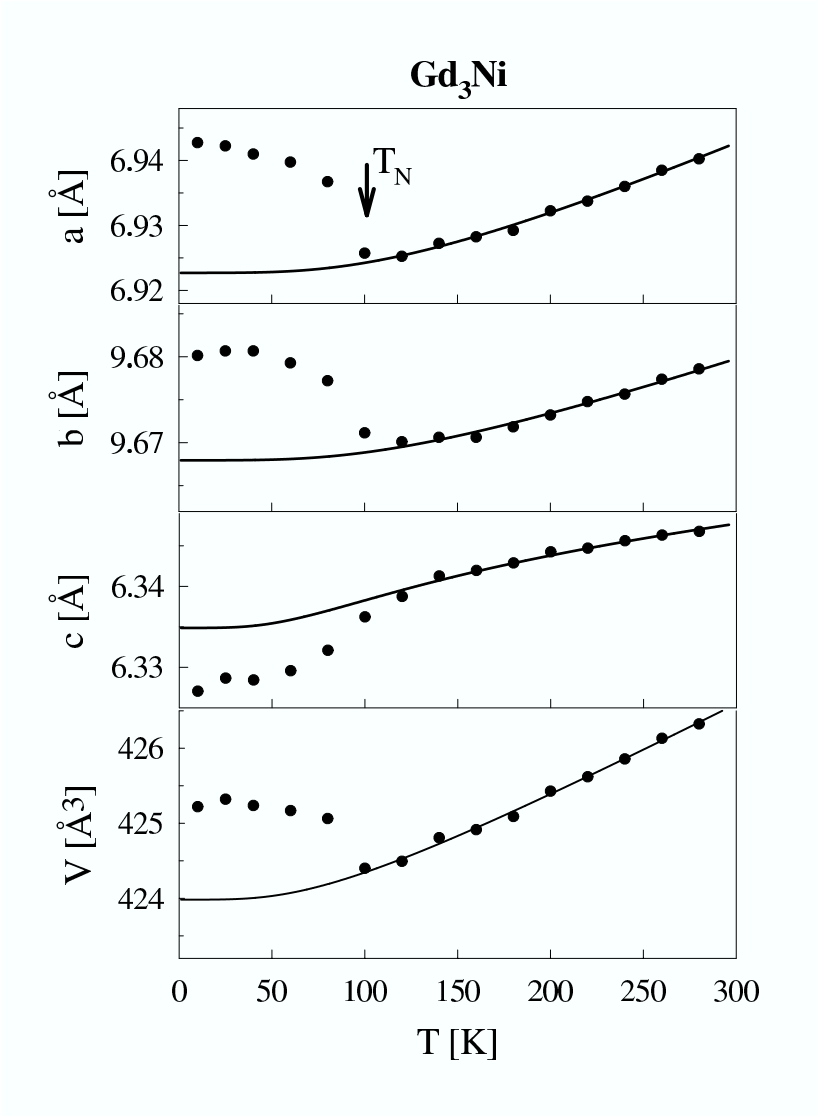

Fig. 38. Anisotropic thermal expansion of the orthorhombic Gd_3Ni, measured by single crystal x-ray diffraction (the data points have been extracted from Kusz et al. (2000)). The lines represent extrapolations of the lattice contribution from the paramagnetic range.

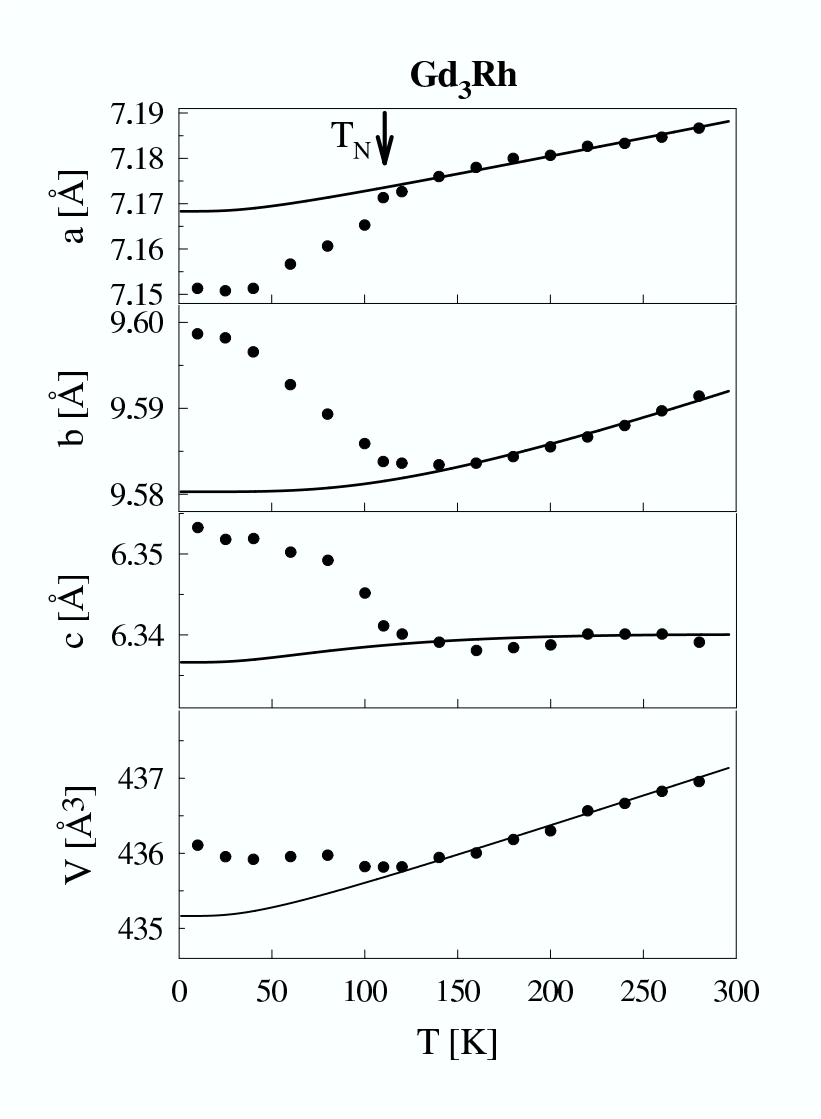

Fig. 39. Anisotropic thermal expansion of the orthorhombic Gd_3Rh, measured by single crystal x-ray diffraction (the data points have been extracted from Kusz et al. (2000)). The lines represent extrapolations of the lattice contribution from the paramagnetic range.

The magnetostriction in high T_C–superconductors have been investigated on polycrystalline samples of $GdBa_2Cu_3O_{7-\delta}$ using the capacitance method (Zieglowski, 1988). This compound orders antiferromagnetically below $T_N = 2.2$ K. The spontaneous magnetostriction is not sensitive to the superconductivity showing that magnetic order and superconductivity are decoupled in this compound. Varying the superconducting properties by a temperature treatment of the sample showed, that in contrast to the spontaneous magnetostriction the field induced magnetostriction is strongly dependent on the superconducting properties.

9 Monoclinic systems

Only two examples with monoclinic structures could be found. One is the already discussed $Gd_5(Si_xGe_{1-x})_4$ system in the concentration range $0.24 \leq x \leq 0.5$ (see section 8.1).

A second is the compound Gd_5Ir_2, investigated by Kusz et al. (2000), which has a monoclinic structure related to the orthorhombic structures of Gd_3Ni and Gd_3Rh (see section 8.9). The authors reported the temperature dependence of the orthorhombic lattice parameters, showing only for the b - direction a significant magnetostriction. The temperature dependence of the monoclinic angle has not been reported.

10 Summary and conclusions

As shown in the preceding sections, there is a wide variety of spontaneous magnetoelastic effects in Gd - based systems, from very small (below 10^{-4}) up to effects larger than 10^{-2} (GMS). Not only the anisotropic spontaneous magnetostriction can reach very large values (such as the GMS of $(\frac{\Delta(c/b)}{(c/b)})_{mag} = -1.36 \times 10^{-2}$ in GdNi or of $(\frac{\Delta(c/a)}{(c/a)})_{mag} = 2.3 \times 10^{-2}$ in $Gd_5(Si_{0.1}Ge_{0.9})_4$), but also the magnetovolume effects can be unexpectedly large (e.g.: $(\frac{\Delta V}{V})_{mag} = +0.5 \times 10^{-2}$ in pure Gd metal). The occurrence of GMS in Gd compounds shows that not only the crystal field (as pointed out by Engdahl (1999)), but also the exchange interaction has to be considered as a source of GMS. In the tables 1 and 2 the spontaneous magnetoelastic effects of the systems presented in this chapter are summarized.

Table 1

Summary of the spontaneous magnetostriction in non-cubic systems *showing pronounced anisotropic* effects, ordered with respect to the size of the effects. The presented values are the estimated values at 0 K. x,n indicate the experimental method (x-ray, neutron) Note: < means that the absolute value is smaller than this value, which is about the resolution of the experimental technique. (h),(t),(o) indicate the crystal system (hexagonal, tetragonal, orthorhombic). In addition $T_{C(N)}$, the propagation vector and the direction of the magnetic moment are tabulated.

	meth.	$\Delta a/a$ $[10^{-3}]$	$\Delta b/b$ $[10^{-3}]$	$\Delta c/c$ $[10^{-3}]$	$\Delta V/V$ $[10^{-3}]$	$T_{C(N)}$	Prop.	Moment direction
$Gd_5(Si_{0.1}Ge_{0.9})_4$ (o)	x[a]	−16	+3	+7	−6	$T_C = 81$K	(0 0 0)[1]	
GdNi (o)	x[b]	+4.0	+5.4	−8.2	+1.2	$T_C = 69$K	(0 0 0)	[0 1 0][2]
GdCu (FeB) (o)	n[c]	5 ± 3	-10 ± 3	3 ± 3	-2 ± 5	$T_N = 45$K	$(0\,\frac{1}{4}\,\frac{1}{4})$	[x,y,z=-y][3]
$Gd(Cu_{0.8}Ni_{0.2})_2$ (o)	x[d]	−3.5	+4.9	+0.8	+2.2	$T_C = 95$K	(0 0 0)[4]	
Gd_2Cu_2In (t)	x[e]	−1.9		+3.8	< 0.1	$T_C = 86$K	(0 0 0)	[0 0 1][5]
Gd_3Rh (o)	x[f]	−2.5	+2.0	+2.6	+2.1	$T_N = 112$K[6]		
GdCuAl (h)	x[g]	−1.7		+3.0	−0.4	$T_C = 82$K	(0 0 0)	[0 0 1][7]
Gd_3Ni (o)	x[f]	+2.9	+1.3	−1.3	+2.9	$T_N = 100$K[8]		
GdPt (o)	x[e]	+1.4	−2.3	+0.9	< 0.1	$T_C = 68$K	(0 0 0)[9]	
$GdCu_2$ (o)	x[h]	−2.1	+1.2	+1.5	+0.6	$T_N = 42$K	$(\frac{2}{3}\,1\,0)$	[x 0 z][10]
$GdZn_2$ (o)	x[i]	−0.2	+1.4	+1.9	+3.1	$T_C = 68$K	(0 0 0)[11]	
Gd (h)	x[e]	+1.0		+3.0	+5.0	$T_C = 294$K	(0 0 0)	>232K:[0 0 1][12]
GdCuSn (h)	x[b]	+0.3		−1.1	−0.5	$T_N = 24$K	$(0\,\frac{1}{2}\,0)$	[0 0 1][13]
$GdAg_2$ (t)	x[e]	+0.3		−0.6	< 0.1	$T_N = 23$K	(0.362 0 1)	>10.8K:[0 0 1] <10.8K:[1 1 0][14]
$Gd_2Ni_{2-x}In$ (t)	x[e]	−0.2		+0.4	< 0.1	$T_N = 20$K[15]		

References for magnetostriction measurements:

[a] Morellon et al. (2000) [b] Gratz and Lindbaum (1998), [c] Blanco et al. (1999), [d] Borombaev and Markosyan (1987), [e] this work, [f] Kusz et al. (2000), [g] Andreev et al. (1999), [h] Gratz and Lindbaum (1994), [i] Ohta et al. (1995)

References for magnetic properties:

[1] Morellon et al. (2000), [2] Blanco et al. (1992), [3] Blanco et al. (1999), [4] Poldy and Kirchmayr (1974), [5] Fisher et al. (1999), [6] Talik and Neumann (1994), [7] Andreev et al. (1999), [8] Talik and Ślebarski (1995), [9] Castets et al. (1980, 1982), [10] Rotter et al. (2000b,a), [11] Debray et al. (1970), [12] Cable and Wollan (1968), [13] Bialic et al. (1997), [14] Gignoux et al. (1991), [15] Hilscher (2001)

Table 2

Summary of the spontaneous magnetostriction (estimated values at 0 K) of the systems with *very small* or *not determined* (n.d.) *anisotropic* effects. The table is ordered with respect to the size of the observed volume effects. x,d indicate the x-ray or dilatometric method. Note: < means that the absolute value is smaller than this value, which is about the resolution of the experimental technique. (c),(h),(t),(o) indicate the crystal system (cubic, hexagonal, tetragonal, orthorhombic). In addition $T_{C(N)}$, the propagation vector and the direction of the magnetic moment are tabulated.

	meth.	$\Delta a/a$ $[10^{-3}]$	$\Delta b/b$ $[10^{-3}]$	$\Delta c/c$ $[10^{-3}]$	$\Delta V/V$ $[10^{-3}]$	$T_{C(N)}$	Prop.	Moment direction
$GdAl_2$ (c)	x[a]				-1.4	$T_C = 168K$	(0 0 0)	[1 1 1][1]
	d[b]				-1.16			
GdNiAl (h)	x[c]	$\approx +0.3$		$\approx +0.3$	$+0.8$	$T_C = 60K$	>30K:(0 0 0)[2]	
$GdNi_{0.4}Cu_{0.6}$ (o)	d[d]	n.d.	n.d.	n.d.	$+0.8$	$T_N = 63K$	(0 0 0.25)	[x y 0][3]
$GdNi_{0.7}Cu_{0.3}$ (o)	d[d]	n.d.	n.d.	n.d.	$+0.6$	$T_C = 68K$	(0 0 0)	[0 1 0][3]
$GdNi_2$ (c)	x[a]				$+0.6$	$T_C = 74K$	(0 0 0)[4]	
$GdCu_2In$ (c)	d[e]				-0.10	$T_N = 10K$[5]		
$GdPd_2In$ (c)	d[e]				-0.02	$T_N = 10K$[5]		
$GdIn_3$ (c)	x[a]				≈ -0.3	$T_N = 43K$[6]		
$GdNi_5$ (h)	x[a]	< 0.1		< 0.1	< 0.1	$T_C = 31K$	(0 0 0)	[0 0 1][7]
Gd_2In (h)	x[f]	< 0.1		< 0.1	< 0.1	$T_C = 190K$	>100K:hel.FM[8]	
							<100K:$(0\,0\,\frac{1}{6})$[9]	
$GdAu_2$ (t)	x[a]	< 0.1		< 0.1	< 0.1	$T_N = 50K$[10]		
$GdNi_2B_2C$ (t)	x[a]	< 0.1		< 0.1	< 0.1	$T_N = 20K$	(0.55 0 0)	>14K:[0 1 0]
								<14K:[0 y z][11]

References for magnetostriction measurements:

[a] this work, [b] du Tremolet de Lacheisserie (1988), [c] Jarosz et al. (2000), [d] Espeso et al. (1994), [e] Taylor et al. (2000), [f] Gratz and Lindbaum (1998)

References for magnetic properties:

[1] Kaplan et al. (1973); Burd and Lee (1977), [2] Merlo et al. (1998); Javorský et al. (1995), [3] Blanco et al. (1992), [4] Buschow (1977); Jesser and Clad (1986), [5] Parsons et al. (1998); Taylor et al. (2000), [6] Staliński et al. (1979), [7] Franse and Radwański (1993); Mulders et al. (2000), [8] Jee et al. (1996), [9] Ravot et al. (1993), [10] Tung et al. (1996), [11] Detlefs et al. (1996); Tomala et al. (1998)

As can be seen from these tables, for any kind of the magnetic ordering (i.e. ferromagnetic or antiferromagnetic) examples exist with large and small effects. However, there is a tendency to larger effects in ferromagnetic systems.

Second, the observed effects depend strongly on the partner elements of Gd, which can be seen from a comparison of isostructural systems, like for instance GdCuAl and GdNiAl, Gd_2Cu_2In and $Gd_2Ni_{2-x}In$, or $GdAg_2$ and $GdAu_2$. Such comparisons show, that changing one of the partner elements can have a strong influence on the spontaneous magnetostriction. How far the qualitative behaviour of the spontaneous magnetostriction is determined by the type of crystal structure, remains unclear: A comparison of the $CeCu_2$-type compounds $GdCu_2$, $Gd(Cu_{0.8}Ni_{0.2})_2$ and $GdZn_2$, having different magnetic structures, shows that the qualitative behaviour of the magnetostriction is always the same, i.e. the sign of the magnetostriction in a-direction is opposite to those of b- and c-direction. This holds also true when changing the magnetic structure of $GdCu_2$ from antiferromagnetic to ferromagnetic by applying a magnetic field. Furthermore also the comparison of the FeB-type compounds GdCu (antiferromagnetic) and GdPt (ferromagnetic) supports the conclusion, that the qualitative behaviour of the spontaneous magnetostriction is connected with the crystal structure. But on the other hand the compounds Gd_3Ni and Gd_3Rh, which are both antiferromagnetic and have the same crystal structure, show different qualitative behaviour of the spontaneous magnetostriction. In case of Gd_3Ni it is the magnetostriction in c- direction, which has opposite sign compared to the other directions, wheras in Gd_3Rh it is the a-direction.

Third, it is obvious that in systems with a small number of Gd atoms (e.g. $GdNi_5$ and $GdNi_2B_2C$) the effects are very small, since the magnetic as well as magnetoelastic interactions are weaker in systems with low Gd concentration. This is supported by the studies on $GdCu_2$, showing that at least in case of this compound the magnetostriction is dominated by the next neighbor exchange interaction (i.e. in case of a compound with low Gd concentration smaller effects have to be expected due to the smaller number of next neighbors). But note that systems with high Gd concentration do not necessarily have large effects. In Gd_2In, for instance, two of three atoms are Gd, leading to strong magnetic interactions, reflected in the high ferromagnetic ordering temperature of 190 K, but the associated magnetoelastic effects are smaller than 10^{-4}.

$Gd_5(Si_{0.1}Ge_{0.9})_4$ is one representative of the $Gd_5(Si_xGe_{1-x})_4$ compounds, where a magnetic transition is not only connected with a giant magnetostriction of the lattice parameters, but also with an instability of other structural parameters. Furthermore this magnetostructural transition can be induced reversibly by a magnetic field and is connected with a giant magnetocaloric effect (Morellon et al., 2000, 1998a). This example shows that the measurement of the spontaneous magnetostriction could be very useful for finding systems showing magnetostructural transitions and giant magnetocaloric effects.

What is not shown in the tables, are spontaneous distortions of the crystal symmetry, which are usually very small (i.e. $< 10^{-4}$) and have only be observed in cubic systems, where the detection of symmetry distortions is easier. To our knowledge the largest symmetry breaking effect has been

observed for cubic GdZn by Rouchy et al. (1981), namely a tetragonal distortion of $(\Delta l/l)_{001} \approx -3.7 \times 10^{-4}$ (see section 5).

One of the maybe most interesting and unexpected observations concerning spontaneous magnetoelastic effects in Gd compounds are the large magnetovolume effects, ranging from $(\frac{\Delta V}{V})_{mag} = +5.0 \times 10^{-3}$ in pure Gd metal to $(\frac{\Delta V}{V})_{mag} = -6 \times 10^{-3}$ in $Gd_5(Si_{0.1}Ge_{0.9})_4$. The size of the magnetovolume effect in pure Gd is comparable to typical systems with Fe or Co, where the observed positive magnetovolume effects are associated with the itinerant character of the Fe or Co moments. In all Gd systems, presented in this chapter and showing pronounced magnetovolume effects (i.e. absolute value larger than 0.5×10^{-3}), these effects are always positive (only with the exception of $GdAl_2$ and $Gd_5(Si_{0.1}Ge_{0.9})_4$). This suggests that the polarization of the conduction electrons or the d-electrons of partner atoms like Ni, induced by the molecular field of the Gd moments, play an important role for the magnetovolume effects in Gd systems. This is also supported by the fact that the largest positive magnetovolume effects are observed in ferromagnetic systems, where the Gd molecular field inducing a polarization of the s, p or d electrons, is largest. As an example, the contribution of the induced itinerant moment can be demonstrated by substituting Cu for Ni in GdNi: by replacing 30 % of the Ni atoms by Cu, neither the type of the magnetic ordering (ferromagnetic), nor the Curie temperature is changed, but the magnetovolume effect is reduced from $+1.2 \times 10^{-3}$ in GdNi to $+0.6 \times 10^{-3}$ in $GdNi_{0.7}Cu_{0.3}$, because, in contrast to the Cu d-electrons, the Ni d-electrons can be polarized by the Gd molecular field. A second example, which demonstrates not only the role of an induced Ni moment but also of the type of magnetic ordering, is the comparison of the antiferromagnetic $GdCu_2$ with the isostructural, but ferromagnetic $Gd(Cu_{0.8}Ni_{0.2})_2$. In the latter the magnetovolume effect is almost four times larger. However, one should not forget about the large *negative* magnetovolume effects in $Gd_5(Si_{0.1}Ge_{0.9})_4$ and $GdAl_2$. In the case of $GdAl_2$ the large negative magnetovolume effect has to be attributed to the volume dependence of the (indirect) Gd-Gd exchange interaction since an induced itinerant magnetic moment should lead to a positive magnetovolume effect. This means that not only an itinerant magnetic moment, but also the volume dependence of the (indirect) Gd-Gd exchange interaction can lead to pronounced magnetovolume effects $> 10^{-3}$. In the case of $Gd_5(Si_{0.1}Ge_{0.9})_4$ the magnetostriction is connected with a magnetostructural transition and the large negative magnetovolume effect is probably due to the rearrangement of the atoms in the unit cell.

Finally, we would like to point out the importance of investigations of the *field-induced* magnetostriction in Gd compounds. Such investigations are very important for a quantitative analysis of the spontaneous magnetostriction, what has for instance been shown by the studies on $GdCu_2$. The lack of systematic studies of the field-induced magnetostriction in Gd compounds may be one reason why only in a few cases a quantitative description of the spontaneous magnetoelastic effects in Gd compounds have been performed.

Acknowledgements

This work has been supported by the Austrian Academy of Sciences (APART 10739), by the Austrian Science Fund FWF (Project P14932), and by the Deutsche Forschungsgemeinschaft DFG (SFB 463). Further we would like to thank E. Gratz (TU Vienna) for fruitful discussions.

References

Abell, J. S., J. X. Boucherle, R. Osborn, B. D. Rainford and J. Schweizer, 1983, J. Magn. Magn. Mat. **31-34**, 247.

Andreev, A., P. Javorský and A. Lindbaum, 1999, Journal of Alloys and Compounds **290**, 10.

Andreev, A. V., 1995, In: Buschow, K. H. J. (Ed.), Handbook of Magnetic Materials. Vol. 8. Elsevier Sci. Pub., p. 59.

Barron, T. H. K., 1998, In: Ho, C. Y. (Ed.), Thermal Expansion of Solids. Vol. I-4. CINDAS Data Series on Material Properties, ASM International, Ch. 1, p. 1.

Barron, T. H. K., J. G. Collins and G. K. White, 1980, Adv. Phys. **29**, 609.

Belger, A., U. Jaenicke-Rössler, D. Lipp, B. Wehner, P. Paufler and G. Behr, 1998, Physica C **306**, 277.

Bialic, D., R. Kruk, R. Kmieć and K. Tomala, 1997, Journal of Alloys and Compounds **257**, 49.

Blanco, J. A., J. I. Espeso, J. García-Soldevilla, J. C. Gómez-Sal, M. R. Ibarra, C. Marquina and H. E. Fischer, 1999, Phys. Rev. B **59**, 512.

Blanco, J. A., D. Gignoux and D. Schmitt, 1991, Phys. Rev. B **43**, 13145.

Blanco, J. A., J. C. Gómez-Sal, J. Rodríguez-Fernandez, D. Gignoux, D. Schmitt and J. Rodríguez-Carvajal, 1992, J. Phys.: Condens. Matter **4**, 8233.

Blažina, Z., B. Šorgić and A. Drašner, 1999, J.Phys.: Condens. Matter **11**, 3105.

Bobet, J.-L., S. Pechev, B. Chevalier and B. Darriet, 1998, Journal of Alloys and Compounds **267**, 136.

Bodriakov, V. Y., A. A. Povzner and S. A. Nikitin, 1998, Eur. Phys. J. B **4**, 441.

Borombaev, M. K., R. Z. Levitin, A. S. Markosyan, V. A. Reimer, A. V. Sinitsyn and Z. Smetana, 1987, Z. Sov. Phys. JETP **66**, 866.

Borombaev, M. K. and A. S. Markosyan, 1987, Fiz. Met. Metalloved. **63**, 714.

Bouvier, M., P. Lethuillier and D. Schmitt, 1991, Phys. Rev. B **43**, 13137.

Burd, J. and E. W. Lee, 1977, J. Phys. C **10**, 4581.

Burzo, E., A. Chelkowski and H. Kirchmayr, 1990, In: Wijn, H. P. J. (Ed.), Landolt-Boernstein Group III. Vol. 19d2. Springer Berlin Heidelberg New York.

Buschow, K. H. J., 1977, Rep. Prog. Phys. **40**, 1179.

Buschow, K. H. J., 1980, In: Wohlfarth, E. P. (Ed.), Ferromagnetic Materials. Vol. 1. Elsevier Sci. Pub., p. 297.

Cable, J. W. and E. O. Wollan, 1968, Phys. Rev. **165**, 733.

Callen, E., 1968, J. Appl. Phys. **39**, 519.

Callen, E. and H. B. Callen, 1963, Phys. Rev. **129**, 578.

Callen, E. and H. B. Callen, 1965, Phys. Rev. **139**, A455.

Castets, A., D. Gignoux and J. C. Gómez-Sal, 1980, J. Solid State Chem. **31**, 197.

Castets, A., D. Gignoux, J. C. Gómez-Sal and E. Roudaut, 1982, Solid State Commun. **44**, 1329.

Clark, A. E., 1980, In: Wohlfarth, E. P. (Ed.), Ferromagnetic Materials. Vol. 1. Elsevier Sci. Pub., Amsterdam,The Netherlands, p. 531.

Clark, A. E., B. F. DeSavage and R. Bozorth, 1965, Phys. Rev. **138**, A216.

Coey, J. M. D., V. Skumryev and K. Gallagher, 1999, Nature **401**, 35.

Dan'kov, S. Y., A. M. Tishin, V. K. Pecharsky and K. A. Gschneidner-Jr, 1998, Phys.Rev. B **57**, 3478.

de Jesus, V. L. B., I. S. Oliveira, P. C. Riedi and A. P. Guimaraes, 2000, J. Magn. Magn. Mat. **212**, 125.

de Réotier, P. D. and A. Yaouanc, 1997, J.Phys.: Condens. Matter **9**, 9113.

Debray, D., 1973, Journal of the Less-Common Metals **30**, 237.

Debray, D. K., W. E. Wallace and E. Ryba, 1970, J. Less-Common Met. **22**, 19.

Detlefs, C., A. I. Goldmann, C. Stassis, P. C. Canfield, B. K. Cho, J. P. Hill and D. Gibbs, 1996, Phys. Rev. B **53**, 6355.

Doerr, M., M. Rotter, M. El-Massalami, S. Sinning, H. Takeya and M. Loewenhaupt, 2002, J. Phys.: Condens. Matter **submitted**.

Dolejsi, D. A. and C. A. Swenson, 1981, Phys. Rev. B **24**, 6326.

du Tremolet de Lacheisserie, E., 1988, J. Magn. Magn. Mat. **73**, 289.

Dwight, A. E., R. A. Conner and J. W. Donwey, 1965, Acta Crystallogr. **18**, 835.

Dwight, A. E., J. W. Downey and R. A. Conner, 1967, Acta Crystallogr. **22**, 745.

Engdahl, G., 1999, Handbook of Giant Magnetostrictive Materials (Academic Press London) .

Espeso, J. I., J. Rodríguez-Fernández, J. C. Gómez-Sal and J. A. Blanco, 1994, IEEE Transactions on Magnetics **30(2)**, 1009.

Fisher, I. R., Z. Islam and P. C. Canfield, 1999, J. Magn. Magn. Mat. **202**, 1.

Fontcuberta, J., A. Seffar, A. Hernando, J. C. Gómez-Sal and J. M. Rojo, 1997, J. Appl. Phys. **81**, 3887.

Franse, J. J. M. and R. J. Radwański, 1993, In: Buschow, K. H. J. (Ed.), Handbook of Magnetic Materials. Vol. 7. Elsevier, Amsterdam, p. 307.

Frey, E., F. Schwabl, S. Henneberger, O. Hartmann, R. Wäppling, A. Kratzer and G. M. Kalvius, 1997, Phys. Rev. Lett. **79**, 5142.

Gamari-Seale, H., T. Anagnostopoulos and J. K. Yakinthos, 1979, J.Appl.Phys. **50**, 434.

Gignoux, D. and J. C. Gomez-Sal, 1976, J. Magn. Magn. Mat. **1**, 203.

Gignoux, D., P. Morin and D. Schmitt, 1991, J. Magn. Magn. Mat. **102**, 33.

Gratz, E., E. Goremychkin, M. Latroche, G. Hilscher, M. Rotter, H. Müller, A. Lindbaum, H. Michor, V. Paul-Boncour and T. Fernandez-Diaz, 1999a, J. Phys.: Condens. Matter **11**, 7893.

Gratz, E., A. Kottar, A. Lindbaum, M. Mantler, M. Latroche, V. Paul-Boncour, M. Acet, C. Barner,

W. B. Holzapfel, V. Pacheco and K. Yvon, 1996, J. Phys.: Condens. Matter **8**, 8351.

Gratz, E. and A. Lindbaum, 1994, J. Magn. Magn. Mat. **137**, 115.

Gratz, E. and A. Lindbaum, 1998, J. Magn. Magn. Mat. **177-181**, 1077.

Gratz, E., A. Lindbaum and P. Pototschnig, 1999b, J. Magn. Magn. Mat. **196-197**, 286.

Gratz, E. and C. A. Poldy, 1977, Phys. Stat. Sol. (b) **82**, 159.

Grechnev, G. E., A. S. Panfilov, I. V. Svechkarev, K. H. J. Buschow and A. Czopnik, 1995, Journal of Alloys and Compounds **226**, 107.

Hernando, A., J. M. Rojo, J. C. Gómez-Sal and J. M. Novo, 1996, J. Appl. Phys. **79**, 4815.

Hilscher, G., 2001, unpublished .

Hulliger, F. and F. Stucki, 1978, Int. Phys. Conf. Ser. **37**, 92.

Janak, J. F. and A. R. Williams, 1976, Phys. Rev. B **14**, 4199.

Jarosz, J., E. Talik, T. Mydlarz, J. Kusz, H. Böhm and A. Winiarski, 2000, J. Magn. Magn. Mat. **208**, 169.

Javorský, P., L. Havela, V. Sechovský, H. Michor and K. Jurek, 1998, Journal of Alloys and Compounds **264**, 38.

Javorský, P., N. Tuan, M. Divis, L. Havela, P. Svoboda, V. Sechovský and G. Hilscher, 1995, J. Magn. Magn. Mat. **140-144**, 1139.

Jee, C. S., C. L. Lin, T. Mihalisin and X. Q. Wang, 1996, J.Appl.Phys. **79**, 5403.

Jensen, J. and A. R. Mackintosh, 1991, Rare Earth Magnetism (Clarendon Press Oxford) .

Jesser, R. and R. Clad, 1986, J. Magn. Magn. Mat. **54-57**, 710.

Kalychak, Y. M., V. I. Zaremba, V. M. Baranyak, P. Y. Zavalii, V. Bruskov, L. Sysa and O. Dmytrakh, 1990, Inorg. Mater. **26**, 74.

Kaplan, N., E. Dormann, K. H. J. Buschow and D. Lebenbaum, 1973, Phys. Rev. B **7**, 40.

Kaul, S. N. and S. Srinath, 2000, Phys. Rev. B **62**, 1114.

Köbler, U., A. Hoser, M. Kawakami, T. Chatterji and J. Rebizant, 1999a, J. Magn. Magn. Mater. **205**, 343.

Köbler, U., D. Hupfeld, W. Schnelle, K. Mattenberger and T. Brückel, 1999b, J. Magn. Magn. Mat. **205**, 90.

Köbler, U., R. M. Mueller, W. Schnelle and K. Fischer, 1998, J. Magn. Magn. Mater. **188**, 333.

Komarovskaja, L. P., R. V. Skolozdra and I. V. Filatova, 1983, Dop. Akad. Nauk Ukr. RSR **A45(1)**, 82.

Koyanagi, A., Y. Yoshida, Y. Kimura, R. Settai, K. Sugiyama and Y. Onuki, 1998, J. Phys. Soc. Jpn. **67**, 2510.

Kusz, J., H. Böhm and E. Talik, 2000, J. Appl. Cryst. **33**, 213.

Latroche, M., V. Paul-Boncour and A. Percheron-Guegan, 1993, Z. Phys. Chem. **179**, 261.

Latroche, M., V. Paul-Boncour, A. Percheron-Guegan and J. C. Achard, 1990, J. Less-Common Met. **161**, L27.

Levin, E. M., V. K. Pecharsky and K. A. Gschneidner-Jr, 1999, Phys. Rev. B **60**, 7993.

Levin, E. M., V. K. Pecharsky, K. A. Gschneidner-Jr and P. Tomlinson, 2000, J. Magn. Magn. Mater. **210**, 181.

Lin, C. L., T. Yuen and T. Mihalisin, 1996, Phys. Rev. B **54**, 9254.

Lindbaum, A., 1994, Ph.D. thesis, Technische Universität Wien.

Lindbaum, A., E. Gratz and S. Heathman, 2002, Phys. Rev. B **in press**.

Lindbaum, A., J. Hafner and E. Gratz, 1999, J. Phys.: Condens. Matter **11**, 1177.

Lindbaum, A., J. Hafner, E. Gratz and S. Heathman, 1998, J. Phys.: Condens. Matter **10**, 2933.

Lindbaum, A., S. Heathman, G. Kresse, M. Rotter, E. Gratz, A. Schneidewind, G. Behr, K. Litfin, T. LeBihan and P. Svoboda, 2000, J. Phys.: Condens. Matter **12**, 3219.

Luong, N. H. and J. J. M. Franse, 1981, phys. stat. sol. **66**, 399.

Luong, N. H., J. J. M. Franse and T. D. Hien, 1985, J. Phys. F.: Met. Phys. **15**, 1751.

Lynn, J. W., S. Skanthakumar, Q. Huang, S. K. Sinha, Z. Hossain, L. C. Gupta, R. Nagarajan and C. Godart, 1997, Phys. Rev. B **55**, 6584.

Mallik, R. and E. Sampathkumaran, 1998, Phys. Rev. B **58**, 9178.

Massalami, M., 2002, private communication .

McAlister, S. P., 1984, J.Phys.F: Met. Phys. **14**, 2167.

McEwen, K. A., 1978, In: Gschneidner-Jr, K. A. and L. R. Eyring (Eds.), Handbook on the Physics and Chemistry of Rare Earths. Vol. 1. North-Holland, Amsterdam, p. 411.

Merlo, F., S. Cirafici and F. Canepa, 1998, Journal of Alloys and Compounds **266**, 22.

Morellon, L., P. A. Algarabel, M. R. Ibarra, J. Blasco, B. Garcia-Landa, Z. Arnold and F. Albertini, 1998a, Phys. Rev. B **58**, R14721.

Morellon, L., J. Blasco, P. A. Algarabel and M. R. Ibarra, 2000, Phys. Rev. B **62**, 1022.

Morellon, L., J. Stankiewicz, B. Garcia-Landa, P. A. Algarabel and M. R. Ibarra, 1998b, Appl. Phys. Lett. **73**, 3462.

Morin, P. and D. Schmitt, 1990, In: Buschow, K. H. J. and E. P. Wohlfarth (Eds.), Ferromagnetic Materials. Vol. 5. Elsevier Sci. Pub., p. 1.

Mulders, A. M., C. T. Kaiser, P. C. M. Gubbens, A. Amato, F. N. Gyax, M. Pinkpank, A. Schenck, P. D. de Réotier, A. Yaouanc, K. H. J. Buschow, F. Kayzel and A. Menovsky, 2000, Physica B **289-290**, 451.

Nagamiya, T., 1967, Solid State Phys. **20**, 305.

Nigh, H. E., S. Legvold and F. H. Spedding, 1963, Phys. Rev. **132**, 1092.

Ohashi, M., T. Kaneko and S. Miura, 1975, J. Phys. Soc. Jpn. **38**, 588.

Ohta, S., T. Kitai and T. Kaneko, 1995, J. Phys.: Condens. Matter **7**, 6809.

Österreicher, H., 1977, J. Less-Common Met. **55**, 131.

Pacheco, J. V., K. Yvon and E. Gratz, 1998, Z. Kristallogr. **213**, 510.

Palenzona, A., 1968, J.Less-Common Met **16**, 379.

Parsons, M. J., J. Crangle, K. U. Neumann and K. R. A. Ziebeck, 1998, J. Magn. Magn. Mat. **184**, 184.

Paulose, P. L., S. Patil, R. Mallik, E. Sampathkumaran and V. Nagarajan, 1996, Physica B **223&224**, 382.

Pecharsky, V. K. and K. A. Gschneidner-Jr, 1997a, Phys. Rev. Lett. **78**, 4494.

Pecharsky, V. K. and K. A. Gschneidner-Jr, 1997b, Appl. Phys. Lett. **70**, 3299.

Pecharsky, V. K. and K. A. Gschneidner-Jr, 1997c, J. Magn. Magn. Mater. **167**, l179.

Pecharsky, V. K. and K. A. Gschneidner-Jr, 1997d, J. Alloys Compd. **260**, 98.

Pecharsky, V. K. and K. A. Gschneidner-Jr, 1999, J. Magn. Magn. Mater. **200**, 44.

Poldy, C. A. and H. Kirchmayr, 1974, Phys. Stat. Sol. (b) **65**, 553.

Pourarian, F., 1980, J. Phys. Chem. Solids **41**, 123.

Ravot, D., O. Gorochov, T. Roisnel, G. Andre, F. Bourre-Vigneron and J. A. Hodges, 1993, Int. J. Mod. Phys. B **7**, 818.

Rotter, M., M. Doerr, M. Loewenhaupt, A. Lindbaum, H. Müller, J. Enser and E. Gratz, 2001a, J. Magn. Mag. Mat. **236**, 267.

Rotter, M., M. Doerr, M. Loewenhaupt and P. Svoboda, 2002, J. Appl. Phys. **91**, in press.

Rotter, M., A. Lindbaum, E. Gratz, H. Müller, G. Hilscher, H. Sassik, H. E. Fischer, M. T. Fernandez-Diaz, R. Arons and E. Seidl, 2000a, J. Magn. Magn. Mat. **214**, 281.

Rotter, M., M. Loewenhaupt, M. Doerr, A. Lindbaum and H. Michor, 2001b, Phys. Rev. B **64**, 014402.

Rotter, M., H. Müller, E. Gratz, M. Doerr and M. Loewenhaupt, 1998, Rev. Sci. Instrum. **69**, 2742.

Rotter, M., A. Schneidewind, M. Loewenhaupt, M. Doerr, A. Stunault, A. Hiess, A. Lindbaum, E. Gratz, G. Hilscher and H. Sassik, 2000b, Physica B **284-288**, 1329.

Rouchy, J., P. Morin and E. du Tremolet du Lacheisserie, 1981, J. Magn. Magn. Mat. **23**, 59.

Roy, J. L., J. M. Moreau, D. Paccard and E. Parthe, 1978, Acta Crystallogr. B **34**, 9.

Siegrist, T., H. W. Zandbergen, R. J. Cava, J. J. Krajewski and W. F. Peck, 1994, Nature **367**, 254.

Staliński, B., A. Czopnik, N. Iliew and T. Mydlarz, 1979, Journal de Physique **C5**, 149.

Stampe, P. A., X. Z. Zhou, H. P. Kunkel, J. A. Cowen and G. Williams, 1997, J.Phys.: Condens. Matter **9**, 3763.

Storm, A. R. and K. E. Benson, 1963, Acta Cryst. **16**, 701.

Svoboda, P., M. Doerr, M. Loewenhaupt, M. Rotter, T. Reif, F. Bourdarot and P. Burlet, 1999, Europhys. Lett. **48**, 410.

Szytula, A., 1991, In: Buschow, K. H. J. (Ed.), Handbook of Magnetic Materials. Vol. 6. North-Holland, Amsterdam, p. 85.

Talik, E. and M. Neumann, 1994, Physica B **193**, 207.

Talik, E. and A. Ślebarski, 1995, J. of Alloys and Compounds **223**, 87.

Taylor, J. W., H. Capellmann, K. U. Neumann and K. R. A. Ziebeck, 2000, Eur. Phys. J. B **16**, 233.

Taylor, R. E., T. H. K. Barron, A. Cezairliyan, P. S. Gaal, T. Hahn, C. Y. Huang, R. K. Kirby, H. A. McKinstry, S. T. McKinstry, A. P. Miiller, B. D. Rothrock, G. Ruffino, C. A. Swenson and G. K. White, 1998, Thermal expansion of solids, CINDAS Data Series on Material Properties, Volume I-4, ASM International 1998, edited by C.Y. Ho .

Taylor, R. H. and B. R. Coles, 1975, J. Phys. F **5**, 121.

Tomala, K., J. P. Sanchez, P. Vulliet and P. C. Canfield, 1998, Phys. Rev. B **58**, 8534.

Touloukian, Y. S., R. K. Kirby, R. E. Taylor and P. D. Desai, 1976, In: Thermophysical Properties of Matter (Thermal Expansion). Vol. 12. Plenum Publishing New York - Washington.

Tung, L. D., K. H. J. Buschow, J. J. M. Franse and N. P. Thuy, 1996, J. Magn. Magn. Mat. **154**, 96.

van Voucht, J. H. N., F. A. Kuijpers and H. C. A. M. Bruning, 1970, Philips Res.Rep. **25**, 133.

Walline, R. E. and W. E. Wallace, 1964, J. Chem. Phys. **41**, 1587.

Wasserman, E. F., 1990, In: Buschow, K. H. J. and E. P. Wohlfarth (Eds.), Ferromagnetic Materials. Vol. 5. Elsevier Sci. Pub., p. 237.

Webster, P. J., 1969, Contemp. Phys. **10**, 559.

Yaouanc, A., P. D. de Réotier, P. C. M. Gubbens, A. M. Mulders, F. E. Kayzel and J. J. M. Franse, 1996, Phys.Rev. B **53**, 350.

Zieglowski, J., 1988, Ph.D. thesis, Universität zu Köln.

Noncollinear amplitude-modulated magnetic order in Gd compounds

M. Rotter,* M. Loewenhaupt, and M. Doerr
Institut für Angewandte Physik, Technische Universität Dresden, D-01062 Dresden, Germany

A. Lindbaum and H. Michor
Institut für Experimentalphysik, Technische Universität Wien, Wiedner Hauptstraße 8-10, A-1040 Wien, Austria
(Received 10 October 2000; revised manuscript received 5 February 2001; published 4 June 2001)

In the present work a model within the mean-field theory is developed in order to analyze the specific heat of magnetically ordered systems. This model allows to draw conclusions about the type of magnetic structure from the specific heat near the magnetic transition. The known description of collinear amplitude-modulated and equal-moment magnetism has been extended to account for noncollinear amplitude-modulated (NCAM) antiferromagnetic order by introducing an anisotropic exchange interaction. Experimental evidence for NCAM order is expected from measurements of the specific-heat anomaly at the ordering temperature and from magnetic scattering experiments. The specific heat of $GdCu_2$ was measured and analyzed within the model and a good agreement is reached. Furthermore, the specific heat of other noncollinear Gd antiferromagnets near the ordering temperature has been calculated and is compared to available experimental data.

DOI: 10.1103/PhysRevB.64.014402 PACS number(s): 75.50.Ee, 75.10.−b, 75.25.+z

I. INTRODUCTION

In 1991 a mean-field (MF) model has been developed for the magnetic order in compounds with negligible single-ion anisotropy.[1] There the exchange interaction was assumed to be isotropic. Within this description, equal-moment (EM) magnetic structures have been analyzed and the specific heat has been calculated. By taking into account some weak anisotropy of the exchange coupling or crystal field the stabilization of collinear amplitude-modulated (AM) magnetic structures with regard to other possible states with equal moments (e.g., helical or cycloidal) could be shown. It was found that the specific-heat discontinuity at the ordering temperature is reduced for AM compounds relative to that expected in the case of EM magnetism. In addition, a connection between the shape of the specific-heat curves and the exchange constants was predicted. The results of the model were compared to specific-heat measurements on a number of Gd compounds ($GdCu_2Si_2$, $GdNi_2Si_2$, $GdGa_2$, $GdCu_5$).

The purpose of this paper is to develop a theoretical model for noncollinear amplitude-modulated (NCAM) systems. Such intermediate behavior is expected if the anisotropy of the exchange interactions is included *explicitly* into the theory. AM and EM order are derived as special cases in this model. To keep the formalism self-contained the standard MF treatment of the Hamiltonian is rewritten following the notation in Ref. 1 and extending it where necessary. The results of the model are compared to experimental specific-heat data of a number of Gd compounds. For this purpose the specific heat of $GdCu_2$ was measured additionally and analyzed in detail. Other available experimental data are discussed within the framework of the generalized model.

II. FORMALISM

The subsequent analysis is based on an anisotropic bilinear two-ion exchange interaction $\bar{\bar{\mathcal{J}}}(ij)$ between the total angular momenta $\mathbf{J}(i)$ of the rare-earth atoms at different sites i and j. It must be emphasized that in general the magnetic exchange is anisotropic, for instance due to the classical dipole-dipole interaction. In our notation two lines (=) above a symbol denote a tensor and $(\,)^T$ denotes the transposition of a vector (bold-faced symbols denote vectors). Then the Hamiltonian of the magnetic interaction can be written as

$$\mathcal{H}=-\frac{1}{2}\sum_{\substack{i,j=1\\(i\neq j)}}^{N}\mathbf{J}^T(i)\bar{\bar{\mathcal{J}}}(ij)\mathbf{J}(j). \tag{1}$$

This approach is only valid, when crystal field, multi-ion and higher-order interactions can be neglected. Therefore, Gadolinium and its compounds are good candidates to check the theoretical model (see below). We will use a MF theory and thereby neglect magnetic fluctuations above the ordering temperature T_N. Except for the critical region this is a valid approximation,[2] because Gd^{3+} has a large spin moment and in most cases the exchange is of long range. Introducing thermal averages of the magnetic moment of the rare earth $\langle\mathbf{M}(i)\rangle=g_J\mu_B\langle\mathbf{J}(i)\rangle$ we may define the following effective exchange field

$$\mathbf{H}_{\mathrm{ex}}(i)=(g_J\mu_B)^{-2}\sum_{j(\neq i)}\bar{\bar{\mathcal{J}}}(ij)\langle\mathbf{M}(j)\rangle. \tag{2}$$

Note that in Eq. (2) the multiplication of the interaction tensor $\bar{\bar{\mathcal{J}}}(ij)$ with the moment vector $\langle\mathbf{M}(j)\rangle$ results in a vector that contributes to the exchange field $\mathbf{H}_{\mathrm{ex}}(i)$. In a MF theory the Hamiltonian (1) is approximated by (compare Ref. 1)

$$\mathcal{H}\sim\mathcal{H}_{\mathrm{MF}}=-\sum_i\mathbf{M}^T(i)\mathbf{H}_{\mathrm{ex}}(i)+\frac{1}{2}\sum_i\langle\mathbf{M}^T(i)\rangle\mathbf{H}_{\mathrm{ex}}(i). \tag{3}$$

We now introduce Fourier transforms of the moments $\langle \mathbf{M}(j) \rangle$, the exchange fields $\mathbf{H}_{\mathrm{ex}}(i)$, and of the exchange tensor $\bar{\bar{\mathcal{J}}}(ij)$ by

$$\mathbf{M}_{n\mathbf{Q}} = \frac{1}{N} \sum_i \langle \mathbf{M}(i) \rangle e^{-in\mathbf{Q}\mathbf{R}_i}, \tag{4}$$

$$\mathbf{H}_{n\mathbf{Q}} = \frac{1}{N} \sum_i \mathbf{H}_{\mathrm{ex}}(i) e^{-in\mathbf{Q}\mathbf{R}_i}, \tag{5}$$

$$\bar{\bar{\mathcal{J}}}(n\mathbf{Q}) = \sum_j \bar{\bar{\mathcal{J}}}(ij) e^{-in\mathbf{Q}(\mathbf{R}_i - \mathbf{R}_j)}, \tag{6}$$

where $\mathbf{Q}$ is the propagation vector of the magnetic structure under consideration. The magnetic moments can be written as

$$\langle \mathbf{M}(i) \rangle = \sum_{n(\neq 0)} \mathbf{M}_{n\mathbf{Q}} e^{in\mathbf{Q}\mathbf{R}_i}. \tag{7}$$

Note, that n runs from $-\infty$ to $+\infty$ in the sum in Eq. (7) if the propagation $\mathbf{Q}$ is incommensurate. If $\mathbf{Q}$ is commensurate, n numbers all nonequivalent wave vectors $n\mathbf{Q}$. Using the Fourier transforms (4)–(6) Eq. (2) becomes

$$\mathbf{H}_{n\mathbf{Q}} = (g_J \mu_B)^{-2} \bar{\bar{\mathcal{J}}}(n\mathbf{Q}) \mathbf{M}_{n\mathbf{Q}}. \tag{8}$$

We may write the internal energy per ion (which is equal to the thermal average of $\mathcal{H}$)[3]

$$U = \frac{\langle \mathcal{H}_{\mathrm{MF}} \rangle}{N} = -\frac{1}{2} (g_J \mu_B)^{-2} \sum_{n(\neq 0)} \mathbf{M}^T_{-n\mathbf{Q}} \bar{\bar{\mathcal{J}}}(n\mathbf{Q}) \mathbf{M}_{n\mathbf{Q}}. \tag{9}$$

III. BEHAVIOR OF THE SPECIFIC HEAT NEAR THE NÉEL TEMPERATURE T_N

In the following, the MF approach is taken as a reasonable interpolation near the Néel temperature T_N. This results in a model that can be solved and compared to experimental results (keeping in mind that within the critical region fluctuations will be present). The behavior of the specific heat may be obtained analytically by using an expansion of the magnetic moment on each site i as a function of the corresponding exchange field and the reduced variable $t = (1 - T/T_N)^{1/2}$ (a "^" on top of a vector denotes the corresponding unit vector)

$$\begin{aligned} \langle \mathbf{M}(i) \rangle &= \hat{\mathbf{H}}_{\mathrm{ex}}(i) g_J \mu_B J \mathcal{B}_J(g_J \mu_B H_{\mathrm{ex}}(i)/k_B T) \\ &= \frac{C^{(1)}}{T} \mathbf{H}_{\mathrm{ex}}(i) + \frac{C^{(3)}}{T^3} \mathbf{H}_{\mathrm{ex}}(i) [H_{\mathrm{ex}}(i)]^2 + \cdots \\ &= \frac{C^{(1)}}{T_N} \mathbf{H}_{\mathrm{ex}}(i)(1 + t^2 + t^4 + \cdots) + \frac{C^{(3)}}{T_N^3} \mathbf{H}_{\mathrm{ex}}(i) \\ &\quad \times [H_{\mathrm{ex}}(i)]^2 (1 + 3t^2 + 6t^4 + \cdots) + \cdots. \end{aligned} \tag{10}$$

Here $\mathcal{B}_J(x)$ is the Brillouin function and the $C^{(n)}$ are the Curie constants of nth order (for Gadolinium $J = 7/2$, $g_J = 2$), see Ref. 1:

$$C^{(1)} = (g_J \mu_B)^2 J(J+1)/(3k_B), \tag{11}$$

$$C^{(3)} = -(g_J \mu_B)^4 J(J+1)(2J^2 + 2J + 1)/(90 k_B^3).$$

The expansion (10) is possible, because near the ordering temperature $T \sim T_N$ all magnetic moments are expected to be much smaller than the saturation moment. Therefore also the exchange fields $\mathbf{H}_{\mathrm{ex}}(i)$ will be smaller than $k_B T/g_J \mu_B$ (in a limited temperature range near T_N).

Replacing $\langle \mathbf{M}(i) \rangle$ and $\mathbf{H}_{\mathrm{ex}}(i)$ in Eq. (10) by their Fourier expansion [Eqs. (4) and (5)], substituting $\mathbf{H}_{n\mathbf{Q}}$ by Eq. (8) and identifying the corresponding Fourier components on both sides of the equation provides a nonlinear system of equations in $\mathbf{M}_{\mathbf{Q}}, \mathbf{M}_{3\mathbf{Q}}, \ldots$. This system can be solved by expanding the $\mathbf{M}_{n\mathbf{Q}}$**'s** in ascending (odd) powers of t and by identifying the corresponding terms in $t, t^3, \ldots$, i.e., the nth harmonic $\mathbf{M}_{n\mathbf{Q}}$ is expanded as

$$\mathbf{M}_{n\mathbf{Q}} = \mathbf{M}_{n1} t + \mathbf{M}_{n3} t^3 + \mathbf{M}_{n5} t^5 + \cdots. \tag{12}$$

For $n = 1$ and first order in t the following eigenvalue problem of $\bar{\bar{\mathcal{J}}}(\mathbf{Q})$ is derived:[4]

$$\bar{\bar{\mathcal{J}}}(\mathbf{Q}) \mathbf{M}_{11} = \frac{(g_J \mu_B)^2 T_N}{C^{(1)}} \mathbf{M}_{11}. \tag{13}$$

Given the exchange $\bar{\bar{\mathcal{J}}}(\mathbf{Q})$, this eigenvalue problem may be solved for different wave vectors $\mathbf{Q}$. Maximizing the largest eigenvalue $\lambda(\mathbf{Q})$ with respect to $\mathbf{Q}$ gives the ordering wave vector $\mathbf{Q}_0$ of the system, the ordering temperature $T_N = \lambda(\mathbf{Q}_0) C^{(1)}/(g_J \mu_B)^2$ and the eigenvector $\mathbf{M}_{11}$.[5] The components of this eigenvector determine the type of magnetic structure just below the ordering temperature. However, by using the first-order terms in t, only the direction of $\mathbf{M}_{11}$ can be calculated [by solving the eigenvalue problem (13)] but not its length.

The length of $\mathbf{M}_{11}$ is found to be characteristic for the discussed type of magnetic order (AM, NCAM, and EM) and can be calculated by comparing the components of third order in t (see the Appendix), the result is

$$|\mathbf{M}_{11}|^2=\begin{cases}\dfrac{-(C^{(1)})^3}{C^{(3)}[2+|\hat{\mathbf{M}}_{11}^T\hat{\mathbf{M}}_{11}|^2]} & \mathbf{Q}_0\neq 0,\notin \mathrm{BZB},\\ \dfrac{-(C^{(1)})^3}{C^{(3)}} & \mathbf{Q}_0=0 \ \text{ or } \ \mathbf{Q}_0\in \mathrm{BZB}.\end{cases} \tag{14}$$

Equation (14) shows, that the length of $\mathbf{M}_{11}$ (i.e., the magnitude of the ordered moment just below T_N) is determined by the Curie constants $C^{(1)},C^{(3)}$ and the product $|\hat{\mathbf{M}}_{11}^T\hat{\mathbf{M}}_{11}|$, which may vary between 0 (EM order) and 1 (AM order) depending on the (real and imaginary) components of $\hat{\mathbf{M}}_{11}$ as determined by the eigenvalue problem (13). In general the order will be NCAM (see the examples given in Sec. IV and V). In Eq. (14) the ferromagnetic case (i.e., $\mathbf{Q}_0=0$) and the simple antiferromagnetic case (i.e., $\mathbf{Q}_0\in$ BZB, BZB =[symmetry points on the Brillouin zone boundary]) have been treated separately, because in these cases the AM and EM (and NCAM) description of the ordering process is equivalent.[6]

In addition to Eq. (14) the third-order terms in t provide an expression for the third harmonic of the magnetic moment (for $\mathbf{Q}_0\neq 0,\notin$ BZB, see the Appendix):

$$\mathbf{M}_{3\mathbf{Q}_0}=t^3\left(1-\frac{C^{(1)}}{T_N(g_J\mu_B)^2}\bar{\bar{\mathcal{J}}}(3\mathbf{Q}_0)\right)^{-1}\mathbf{M}_{11}\times\frac{C^{(3)}}{[C^{(1)}]^3}(\mathbf{M}_{11}^T\mathbf{M}_{11}). \tag{15}$$

Equation (15) shows that the size of the third harmonic depends also on the product $|\hat{\mathbf{M}}_{11}^T\hat{\mathbf{M}}_{11}|$ and becomes zero for EM order. Therefore, any deviation from EM order can be determined by measuring the intensity on the third harmonic in a magnetic scattering experiment. However, such measurements are very difficult, since the magnetic moment near the ordering temperature is usually very small and at lower temperatures the moments tend to saturate thereby destroying NCAM order.

Using Eqs. (9), (13), and (14) the magnetic contribution to the specific heat for temperatures just below T_N can be calculated as

$$C^{\mathrm{mag}}\Big|_{T\to T_N}=\frac{\partial U}{\partial T}\Big|_{T\to T_N}=\begin{cases}-\dfrac{\mathbf{M}_{-11}^T\bar{\bar{\mathcal{J}}}(\mathbf{Q}_0)\mathbf{M}_{11}+\mathbf{M}_{11}^T\bar{\bar{\mathcal{J}}}(-\mathbf{Q}_0)\mathbf{M}_{-11}}{2(g_J\mu_B)^2}\dfrac{\partial t^2}{\partial T}\Big|_{T\to T_N}=\dfrac{|\mathbf{M}_{11}|^2}{C^{(1)}} & \\ \quad=\dfrac{1}{C^{(1)}}\left[\dfrac{\partial|\mathbf{M}_{\mathbf{Q}_0}|}{\partial t}\Big|_{T\to T_N}\right]^2=\dfrac{-(C^{(1)})^2}{C^{(3)}[2+|\hat{\mathbf{M}}_{11}^T\hat{\mathbf{M}}_{11}|^2]} & \mathbf{Q}_0\neq 0,\notin \mathrm{BZB}\\ -\dfrac{\mathbf{M}_{-11}^T\bar{\bar{\mathcal{J}}}(\mathbf{Q}_0)\mathbf{M}_{11}}{2(g_J\mu_B)^2}\dfrac{\partial t^2}{\partial T}\Big|_{T\to T_N}=\dfrac{|\mathbf{M}_{11}|^2}{2C^{(1)}}=\dfrac{1}{2C^{(1)}}\left[\dfrac{\partial|\mathbf{M}_{\mathbf{Q}_0}|}{\partial t}\Big|_{T\to T_N}\right]^2=-\dfrac{(C^{(1)})^2}{2C^{(3)}} & \mathbf{Q}_0=0\\ -\dfrac{\mathbf{M}_{11}^T\bar{\bar{\mathcal{J}}}(\mathbf{Q}_0)\mathbf{M}_{11}+\mathbf{M}_{11}^T\bar{\bar{\mathcal{J}}}(-\mathbf{Q}_0)\mathbf{M}_{-11}}{4(g_J\mu_B)^2}\dfrac{\partial t^2}{\partial T}\Big|_{T\to T_N}=\dfrac{|\mathbf{M}_{11}|^2}{2C^{(1)}} & \\ \quad=\dfrac{1}{2C^{(1)}}\left[\dfrac{\partial|\mathbf{M}_{\mathbf{Q}_0}|}{\partial t}\Big|_{T\to T_N}\right]^2=-\dfrac{(C^{(1)})^2}{2C^{(3)}}. & \mathbf{Q}_0\in \mathrm{BZB}\end{cases} \tag{16}$$

The specific heat near the ordering temperature shows a discontinuity that corresponds to the size of the derivative of the ordered magnetic moment with respect to t. The jump in the molar heat capacity c^{mag} ($c^{\mathrm{mag}}=N_AC^{\mathrm{mag}}$, $N_A=6.0221\times10^{23}$/mol denotes the Avogadro constant) at T_N may vary between $[-(C^{(1)})^2/3C^{(3)}]N_A=13.43$ J/K mol and $[-(C^{(1)})^2/2C^{(3)}]N_A=20.15$ J/K mol [corresponding to AM and EM magnetic structures, respectively—calculated with $J=7/2$ using Eq. (11)]. Using high-quality specific-heat measurements it is therefore possible to estimate the size of the magnetic contribution at T_N and attempt to obtain information about the type of magnetic structure just below the ordering temperature from the size of the product $|\hat{\mathbf{M}}_{11}^T\hat{\mathbf{M}}_{11}|^2$. In the following part of this paper some examples will be given.

Note that in Eq. (16) the ferromagnetic ($\mathbf{Q}_0=0$) and simple antiferromagnetic case ($\mathbf{Q}_0\in$ BZB) give specific-heat values as expected for EM order (although the AM and EM descriptions are equivalent for these special values of $\mathbf{Q}_0$). Furthermore, it is worth considering the case where the exchange anisotropy is only due to the classical dipole-dipole interaction: if the basis of the crystallographic structure con-

TABLE I. Magnetic contribution to the molar heat capacity near the magnetic ordering temperature for some Gd compounds. The propagation vector and the moment direction derived from magnetic-scattering experiments is given for comparison. The last column contains the type of magnetic order as suggested by these experiments (see text).

	$c^{\mathrm{mag}}\|_{T\to T_N}$ [J/K mol]	Moment direction	$\mathbf{Q}_0$	Type
Gd	15–25 [Ref. 13]	[001]	(0 0 0)	→EM=NCAM=AM
$GdCu_2Si_2$	15–18 [Ref. 14]	[010]	(1/2 0 1/2) ∈ BZB	→EM=NCAM=AM [Ref. 15]
$GdCu_2$	20	[x0z]	(2/3 1 0)	EM
$GdCu_2Ge_2$	18–22 [Ref. 7], [Ref. 16]			EM
$GdBa_2Cu_3O_{7-\delta}$	14–22 [Ref. 17]	[001]	(1/2 1/2 1/2) ∈ BZB	→EM=NCAM=AM [Ref. 18]
GdAg	19–21	[001]	(1/2 1/2 0) ∈ BZB	→EM=NCAM=AM [Ref. 19]
$GdCo_2Si_2$	19–20 [Ref. 7]			EM
GdS	17–20 [Ref. 20]			NCAM
$GdAu_2Si_2$	14–18 [Ref. 7]			NCAM
$GdCo_2Ge_2$	16–17 [Ref. 16]			NCAM
$GdPd_2Ge_2$	14–16 [Ref. 7]			NCAM
$GdNi_2B_2C$	12–16 (at 20 K) [Ref. 21], [Ref. 22] 1 (at 14 K)	[010]	(0.55 0 0) [Ref. 23]	AM[a]
$GdNi_2Ge_2$	12–14 (at 28 K) [Ref. 16] 3 (at 15 K) [Ref. 16]			AM
GdAuGe	10 (at 17 K) [Ref. 24] 3 (at 15 K)			AM
$GdRu_2Ge_2$	7–9 (at 32 K) [Ref. 25] 3 (at 28 K)			AM
$GdAg_2Si_2$	6–7 (at 17 K) [Ref. 7] 6–7 (at 11 K)			AM
GdMg	7–9 (at 105 K) [Ref. 26] 4–6 (at 90 K)			AM
$GdCu_5$	3–4 [Ref. 14]		(1/3 1/3 0.223)	
Gd_2PdSi_3	4–6 [Ref. 27], [Ref. 28]			
$GdGa_2$	13–14 [Ref. 14]		(0.39 0.39 0)	AM
$GdNi_2Si_2$	10–11 [Ref. 14]	[010]	(0.207 0 0.903) [Ref. 15]	AM
$GdFe_2Ge_2$	14–15 [Ref. 16]			AM
$GdPt_2Ge_2$	10–13 [Ref. 7]			AM
$GdNi_2Sn_2$	10–15 [Ref. 7]			AM
$GdPd_2In$	11 [Ref. 29], [Ref. 30]			AM
$GdCu_2In$	9–11 [Ref. 29], [Ref. 30]			AM

[a]Note that below $T_R \sim 0.7T_N$ there is a spin reorientation into a NCAM state.

sists only of one Gd atom, then $\bar{\bar{\mathcal{J}}}(\mathbf{Q})$ is real for any $\mathbf{Q}$ and therefore either AM or (if $\mathbf{Q}_0=0$ or $\mathbf{Q}_0 \in$ BZB) simple collinear EM order is predicted.

It has been pointed out that the analysis of specific heat may lead to important conclusions about the magnetic structure near the ordering temperature. However, in many cases critical fluctuations make it difficult to obtain reliable MF values for $C^{\mathrm{mag}}|_{T\to T_N}$. In addition, the sample quality is an important issue since impurities and microstrains may lead to changes of the specific heat near the magnetic ordering temperature. In Sec. V the specific heat is discussed for some Gd compounds.

For Gd the conclusions from specific-heat data are in some respect as important as results from scattering experiments.[1,7] Candidates for NCAM order are proposed for further study.

IV. THE CASE OF $GdCu_2$

To give an example of how NCAM order might occur, the case of $GdCu_2$ is discussed in more detail. Up to now it seems to be the only Gd compound exhibiting EM order that is noncollinear (compare Table I). Recent neutron-scattering experiments on $GdCu_2$ indicate a noncollinear magnetic structure.[8] The heat capacity has been measured on polycrystals[9] and single crystals.[10] For $c^{\mathrm{mag}}_{GdCu_2}|_{T\to T_N}$ at the ordering temperature a value of 15 J/K mol has been reported in Refs. 1 and 9 and was taken as evidence for an AM magnetic structure. However, from more recent measurements on a single crystal a larger value of 20 J/K mol can be estimated.[10] Therefore, the heat capacity has been remeasured on a high quality single crystal with the aim to get additional reliable data and compare it to the model. The single crystal was produced by a Bridgeman method, details

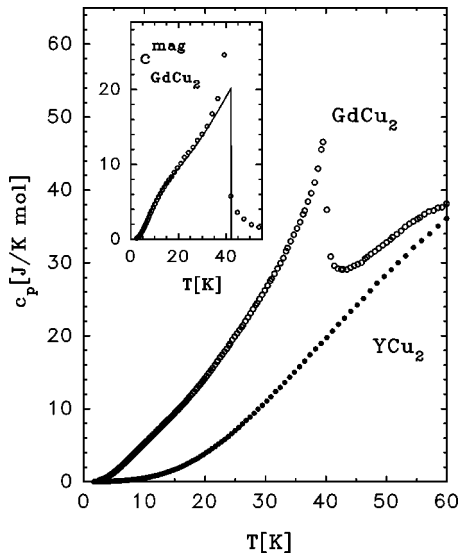

FIG. 1. Molar heat capacity c_P of a $GdCu_2$ single crystal in zero magnetic field in comparison with the isostructural nonmagnetic reference compound YCu_2. The inset shows the magnetic contribution c^{mag} (circles) as derived from these data in comparison with results of a numerical calculation (full line) described in the text.

are given in Refs. 8 and 11. Heat capacity was measured by a conventional quasiadiabatic heat-pulse technique. The molar heat capacity c_P of $GdCu_2$ is shown in Fig. 1 in comparison with the data of YCu_2. One peak has been observed at 42 K corresponding to the Néel temperature in accordance with measurements on polycrystals.[12] Taking into account the part caused by critical fluctuations around T_N we estimate from these data a MF heat capacity jump of 20 J/K mol, approximately, confirming the results of Ref. 10.

It has been shown[8] in a simple model of $GdCu_2$ with a propagation vector $\mathbf{Q}_0=(2/3\,1\,0)$, that the eigenvector corresponding to possible magnetic structures is given by

$$\mathbf{M}_{11}=|\mathbf{M}_{11}|(2+2\sigma\sqrt{1+\sigma^2}+2\sigma^2)^{-1/2}\begin{pmatrix} i \\ 0 \\ \sigma+\sqrt{1+\sigma^2}\end{pmatrix}. \tag{17}$$

Here σ is a parameter that denotes the ratio of some off-diagonal and diagonal components of the exchange tensor

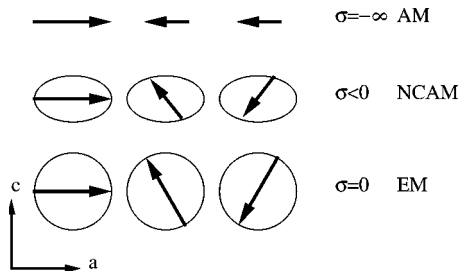

FIG. 2. Types of moment propagation for different values of the parameter σ (see text).

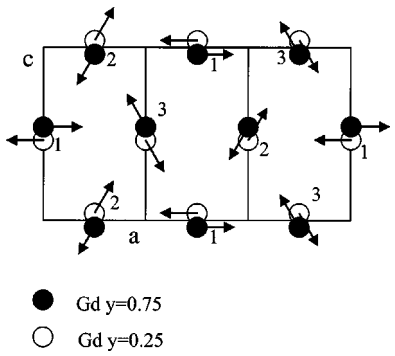

FIG. 3. Magnetic structure of $GdCu_2$. The filled and open circles denote two different neighboring *ac* planes showing the antiferromagnetic propagation in *b* direction. For simplicity the copper atoms are not shown. The magnetic structure can be viewed as a superposition of three simple antiferromagnetic lattices as indicated by the numbers.

(see Ref. 8 for details). For the magnetic structure corresponding to this eigenvector, the magnitude of the magnetic moment varies with its angle according to an "elliptic" (i.e., NCAM) propagation (see Fig. 2, the magnetic structure shown in Fig. 3 corresponds to $\sigma=0$). By inserting the eigenvector (17) into Eqs. (14)–(16) it is possible to calculate the magnitude of the linear term in the expansion of the magnetic moment (12)

$$|\mathbf{M}_{11}|^2=\frac{-(C^{(1)})^3}{C^{(3)}[2+\gamma^2]} \quad \text{with} \quad \gamma^2\equiv|\hat{\mathbf{M}}_{11}^T\hat{\mathbf{M}}_{11}|^2=\frac{\sigma^2}{1+\sigma^2}. \tag{18}$$

Consequently the magnetic contribution to the specific heat at T_N is then calculated from Eq. (16) to be

$$C^{mag}|_{T\to T_N}=\frac{-(C^{(1)})^2}{C^{(3)}[2+\gamma^2]} \tag{19}$$

For $|\sigma|\ll 1$ the eigenvector $(i\,0\,1)$ corresponds to the cycloidal propagation (shown in Fig. 2, bottom). For this eigenvector the product $\hat{\mathbf{M}}_{11}^T\hat{\mathbf{M}}_{11}$ is zero and the anomaly in the molar heat capacity at T_N is calculated to be

$$c^{mag}_{GdCu_2}|_{T\to T_N}=N_A C^{mag}|_{T\to T_N}$$
$$=\frac{-(C^{(1)})^2}{2C^{(3)}}N_A=20.15 \text{ J/mol K}. \tag{20}$$

This result is expected for EM structures [compare the discussion of Eq. (16) and Ref. 1] and is in accordance with our experimental data of the heat capacity.

The proposed cycloidal propagation ($\sigma=0$) is in accordance with neutron-scattering experiments performed at $T=4$ K.[8] The corresponding magnetic structure of $GdCu_2$ is

shown in Fig. 3. This type of ordering can be viewed as an *antiferromagnetic* modulation of the moments in *b* direction and a *cycloidal* EM propagation in *a* direction with a pitch angle of 120°. The propagation vector is $\mathbf{Q}_0=(2/3\,1\,0)$. There are two different domains possible, one with a left-handed and another with a right-handed cycloid. The magnetic unit cell consists of three structural unit cells along *a* direction. From the projection into the *ac* plane the cycloidal propagation in *a* direction can be seen.

Assuming that the magnetic structure is the same (EM) at all temperatures the specific heat can be calculated numerically at all temperatures below T_N by solving self-consistently Eqs. (4)–(10). In the inset of Fig. 1 the result of such a calculation is shown by the full line. It compares well to the experimental data except for the critical region, where strong critical fluctuations are present, which are not considered in the MF model.

Moreover, considering temperatures near T_N the neutron technique at present is not sensitive enough to detect a small amplitude modulation $\sigma\neq 0$ of the magnetic moment. Using Eq. (15) it is possible to calculate the magnitude of the third harmonic. The terms linear in t are zero

$$|\mathbf{M}_{31}|^2=0 \tag{21}$$

and therefore the third harmonic increases as $\mathbf{M}_{3\mathbf{Q}_0}=\mathbf{M}_{33}t^3$ with $\mathbf{M}_{33}\|\mathbf{M}_{11}$ and

$$|\mathbf{M}_{33}|^2=\left|\left[1-\frac{C^{(1)}}{T_N(g_J\mu_B)^2}\bar{\bar{\mathcal{J}}}(3\mathbf{Q}_0)\right]^{-1}\hat{\mathbf{M}}_{11}\right|^2 \times\frac{\gamma[C^{(1)}]^6}{(2+\gamma^2)^{3/2}\sqrt{-C^{(3)}}}. \tag{22}$$

It might be possible to determine a small deviation from the cycloidal EM propagation near T_N by measuring the intensity on the third harmonic in a synchrotron experiment using the high sensitivity of resonant magnetic x-ray scattering techniques.

At present it is not clear, what is the reason for the observed anisotropy in the exchange interactions of $GdCu_2$. A numerical calculation of the anisotropy of the classical dipole-dipole exchange indicates degenerate eigenvalues in Eq. (13). Probably this degeneracy is lifted by some small additional interaction, which has not been included in the current model and stabilizes the observed magnetic structure. We strongly suggest further theoretical investigations on this subject.

V. DISCUSSION OF OTHER Gd COMPOUNDS

In Table I the heat-capacity data for several Gd compounds are compiled in combination with available data on the magnetic structure. In some cases such as Gd metal strong critical fluctuations near the ordering temperature make it difficult to estimate correctly the MF value of $c^{\mathrm{mag}}|_{T\to T_N}$ and therefore a reliable interval of values is given instead of an accurate value in Table I.

Most compounds exhibiting EM order show strong critical fluctuations (such as Gd, GdS, $GdCu_2Ge_2$, $GdCu_2Si_2$) and order in a simple collinear structure. No Gd compound with a single Gd ion in the crystallographic basis has been reported to show noncollinear EM order. This is in agreement with the predictions of classical dipole-dipole exchange.[31]

Numerical calculations[32] showed that the anisotropy of the classical dipole-dipole exchange fails to describe the moment direction in the case of Gd whereas it describes it correctly in the cases of GdAg, $GdCu_2Si_2$, $GdBa_2Cu_3O_{7-\delta}$, $GdNi_2Si_2$, and $GdNi_2B_2C$.

In the case of $GdAg_2Si_2$ the ordering process is very complex leading to two relatively small discontinuities of 6 and 7 J/K mol at 11 and 17 K, respectively.[7] A similar behavior is found for GdMg, GdAuGe, $GdRu_2Ge_2$, and $GdNi_2Ge_2$. Also in $GdNi_2B_2C$ and $GdPd_2Ge_2$ a second phase transition below the ordering temperature has been reported. Such a behavior has been attributed to higher-order exchange interactions.[26] $GdCu_5$ does not exhibit any anomaly at T_N, but a broad maximum at about $T_N/2$. Also in Gd_2PdSi_3, $GdNi_2Si_2$ and $GdGa_2$ there is no *sharp* transition at the ordering temperature.

Ignoring for the moment these difficulties in the interpretation of specific-heat data, we find strong candidates for NCAM order—$GdAu_2Si_2$, $GdCo_2Ge_2$, and $GdPd_2Ge_2$. We strongly suggest to perform scattering experiments on these compounds in the vicinity of the ordering temperature to find more evidence for the formation of NCAM structures. Considering the experimental difficulties in finding small deviations from an EM structure (as described above for the case of $GdCu_2$) and that only in a few cases scattering experiments have been reported, it is possible, that in many of the mentioned cases NCAM order might be found, perhaps within a small temperature region.

VI. SUMMARY

We have proposed anisotropic exchange as a reason for the formation of NCAM structures in Gd compounds. The specific heat of noncollinear Gd antiferromagnets has been calculated and compared to available experimental data. Some candidates for the formation of NCAM order are suggested and proposed for further study by scattering experiments. The magnetic structure near the ordering temperature is very sensitive to small details of the exchange interaction. A complete set of precise diffraction data for several Gd compounds is necessary to clarify what might be the origin of anisotropy in the exchange interaction of Gd compounds and if classical dipole-dipole exchange can describe it.

ACKNOWLEDGMENTS

Part of this work was performed within the program of the Sonderforschungsbereich 463 (funded by the Deutsche Forschungsgemeinschaft). We acknowledge support by the Austrian Science Foundation (FWF) Project No. P-11581-PHY. We want to acknowledge the extremely fruitful discussions

with W. Schnelle about the specific-heat experiments and with K. Becker, C. Kuehnert, B. Yavorsky, J. Blanco, and J. Jensen concerning the theoretical part of this work.

APPENDIX

Here the derivation of Eq. (14) is discussed in detail. Introducing the Fourier transforms [Eqs. (4) and (5)] in Eq. (10) and comparing the components of third order in t results in the following system of equations (for $n=1,3,5,7,...$)

$$\mathbf{M}_{n3}=\frac{C^{(1)}}{T_N(g_J\mu_B)^2}\bar{\bar{\mathcal{J}}}(n\mathbf{Q}_0)(\mathbf{M}_{n1}+\mathbf{M}_{n3})+\frac{C^{(3)}}{T_N^3(g_J\mu_B)^6}\times\sum_{m,r=\pm1}\bar{\bar{\mathcal{J}}}([n-m-r]\mathbf{Q}_0)\mathbf{M}_{(n-m-r)1}\times[M^T_{m1}\bar{\bar{\mathcal{J}}}^T(m\mathbf{Q}_0)\bar{\bar{\mathcal{J}}}(r\mathbf{Q}_0)\mathbf{M}_{r1}]. \tag{A1}$$

Note that the sum in Eq. (A1) contains only one term if $\mathbf{Q}_0=0$ and a prefactor of $\frac{1}{4}$ has to be added to this sum if $\mathbf{Q}_0\in$ BZB. For $n=1$ Eq. (A1) may be rewritten using Eq. (13):

$$\left(\bar{\bar{1}}-\frac{C^{(1)}}{T_N(g_J\mu_B)^2}\bar{\bar{\mathcal{J}}}(\mathbf{Q}_0)\right)\mathbf{M}_{13}=\begin{cases}\mathbf{M}_{11}\left[1+\dfrac{2C^{(3)}}{[C^{(1)}]^3}(\mathbf{M}^T_{-11}\mathbf{M}_{11})\right]+\dfrac{C^{(3)}}{[C^{(1)}]^3}\mathbf{M}_{-11}(\mathbf{M}^T_{11}\mathbf{M}_{11}) & \mathbf{Q}_0\neq0,\notin\text{BZB}\\ \mathbf{M}_{11}\left[1+\dfrac{C^{(3)}}{[C^{(1)}]^3}(\mathbf{M}^T_{-11}\mathbf{M}_{11})\right] & \mathbf{Q}_0=0\\ \mathbf{M}_{11}\left[1+\dfrac{C^{(3)}}{2[C^{(1)}]^3}(\mathbf{M}^T_{-11}\mathbf{M}_{11})\right]+\dfrac{C^{(3)}}{4[C^{(1)}]^3}(\mathbf{M}_{11}+\mathbf{M}_{-11})(\mathbf{M}^T_{11}\mathbf{M}_{11}) & \mathbf{Q}_0\in\text{BZB}.\end{cases} \tag{A2}$$

Comparing the left side of this vector equation to the eigenvalue problem (13) the bracket is equivalent to the projection operator $\bar{\bar{\mathcal{P}}}(\mathbf{Q}_0)$ into the plane normal to the eigenvector $\mathbf{M}_{11}$.

$$\bar{\bar{\mathcal{P}}}(\mathbf{Q}_0)=\left(\bar{\bar{1}}-\frac{\bar{\bar{\mathcal{J}}}(\mathbf{Q}_0)}{\lambda(\mathbf{Q}_0)}\right). \tag{A3}$$

Therefore, the left side vanishes if Eq. (A2) is multiplied by $\mathbf{M}^{\dagger}_{11}=\mathbf{M}^T_{-11}$ leading to[33]

$$0=\begin{cases}|\mathbf{M}_{11}|^2\left[1+\dfrac{2C^{(3)}}{[C^{(1)}]^3}|\mathbf{M}_{11}|^2\right]+\dfrac{C^{(3)}}{[C^{(1)}]^3}|\mathbf{M}_{11}|^4|\hat{\mathbf{M}}^T_{11}\hat{\mathbf{M}}_{11}|^2 & \mathbf{Q}_0\neq0,\notin\text{BZB}\\ |\mathbf{M}_{11}|^2\left[1+\dfrac{C^{(3)}}{[C^{(1)}]^3}|\mathbf{M}_{11}|^2\right] & \mathbf{Q}_0=0\\ |\mathbf{M}_{11}|^2\left[1+\dfrac{C^{(3)}}{2[C^{(1)}]^3}|\mathbf{M}_{11}|^2\right]+\dfrac{C^{(3)}}{2[C^{(1)}]^3}|\mathbf{M}_{11}|^4 & \mathbf{Q}_0\in\text{BZB}.\end{cases} \tag{A4}$$

The nonzero solution of this equation corresponds to the moment $|\mathbf{M}_{11}|^2$ for $T<T_N$ as given in Eq. (14). Note that in general $\mathbf{M}^T_{11}\mathbf{M}_{11}$ is not equivalent to $|\mathbf{M}_{11}|^2$ ($|\mathbf{M}_{11}|^2=\mathbf{M}^{\dagger}_{11}\mathbf{M}_{11}$), because $\mathbf{M}_{11}$ is a complex vector.

For $n=3$ in Eq. (A1) we get the following expression for the third harmonic of the magnetic moment (here $\mathbf{Q}_0\neq0,\notin$ BZB)

$$\mathbf{M}_{33}=\frac{C^{(3)}}{[C^{(1)}]^3}\bar{\bar{\mathcal{P}}}^{-1}(3\mathbf{Q}_0)\mathbf{M}_{11}(\mathbf{M}^T_{11}\mathbf{M}_{11}) \tag{A5}$$

from which Eq. (15) can be deduced.

*Electronic address: rotter@physik.tu-dresden.de

[1] J. A. Blanco, D. Gignoux, and D. Schmitt, Phys. Rev. B **43**, 13 145 (1991).

[2] I. Affleck, J. Phys.: Condens. Matter **1**, 3047 (1989).

[3] Note: if the reduced wave vector corresponding to $n\mathbf{Q}$ lies on the zone boundary of the first Brillouin zone, it contributes only partly to the sum in Eqs. (7) and (9).

[4] For $|n|>1$ and first order in t the Eq. $\bar{\bar{\mathcal{J}}}(n\mathbf{Q})\mathbf{M}_{n1}=[(g_J\mu_B)^2T_N/C^{(1)}]\mathbf{M}_{n1}$ is derived. For arbitrary $\bar{\bar{\mathcal{J}}}(n\mathbf{Q})$ and T_N calculated by Eq. (13) only the solution $\mathbf{M}_{n1}=0$ is possible. However, if for some special reason such as symmetry the eigenvalue problem of some $\bar{\bar{\mathcal{J}}}(n\mathbf{Q})$ leads to the same eigenvalue as Eq. (13), multiple $\mathbf{Q}$ structures or frustration is the consequence. In this article we will neglect this possibility and assume

$\mathbf{M}_{n1}=0$ for all $|n|>1$ and $\mathbf{Q}\neq\mathbf{Q}_0$.

[5] For $n=-1$ the complex-conjugate problem has to be solved, because from the Fourier transform (6) follows $\bar{\bar{\mathcal{J}}}(\mathbf{Q})=\bar{\bar{\mathcal{J}}}(-\mathbf{Q})^*$ and therefore $\mathbf{M}_{-11}=\mathbf{M}_{11}^*$.

[6] Note: for $\mathbf{Q}_0=0$ the terms containing a sum over $\pm\mathbf{Q}$ in the expansion of Eq. (10) reduce to one term only. For $\mathbf{Q}_0\in$ BZB a factor $\frac{1}{2}$ has to be considered in the Fourier expansions, because the terms containing $\mathbf{Q}_0$ only contribute partly to the sums in Eqs. (7) and (9).

[7] R. Mallik and E. Sampathkumaran, Phys. Rev. B **58**, 9178 (1998).

[8] M. Rotter, A. Lindbaum, E. Gratz, H. Müller, G. Hilscher, H. Sassik, H. E. Fischer, M. T. Fernandes-Diaz, R. Arons, and E. Seidl, J. Magn. Magn. Mater. **214**, 281 (2000).

[9] N. H. Luong, J. J. M. Franse, and T. D. Hien, J. Phys. F: Met. Phys. **15**, 1751 (1985).

[10] A. Koyanagi, Y. Yoshida, Y. Kimura, R. Settai, K. Sugiyama, and Y. Onuki, J. Phys. Soc. Jpn. **67**, 2510 (1998).

[11] M. Rotter, A. Schneidewind, M. Loewenhaupt, M. Doerr, A. Stunault, A. Hiess, A. Lindbaum, E. Gratz, G. Hilscher, and H. Sassik, Physica B **284-288**, 1329 (2000).

[12] M. K. Borombaev, R. Z. Levitin, A. S. Markosyan, V. A. Reimer, A. V. Sinitsyn, and Z. Smetana, Zh. Eksp. Teor. Fiz. **93**, 1517 (1987) [Sov. Phys. JETP **66**, 866 (1987)].

[13] S. Y. Dankov, A. M. Tishin, V. K. Pecharsky, and K. A. Gschneidner, Phys. Rev. B **57**, 3478 (1998).

[14] M. Bouvier, P. Lethuillier, and D. Schmitt, Phys. Rev. B **43**, 13 137 (1991).

[15] J. M. Barandiaran, D. Gignoux, D. Schmitt, J. C. Gomez-Sal, J. R. Fernandez, P. Chieux, and J. Schweizer, J. Magn. Magn. Mater. **73**, 233 (1988).

[16] N. P. Duong, K. H. J. Buschow, E. Brück, L. T. Tai, and T. D. Hien, in *Trends in Material Science and Technology*, edited by F. Bekker, N. D. Chien, J. J. M. Franse, T. D. Hien, N. T. Hien, and N. P. Thuy (Hanoi National University Publishing House, Hanoi, 1999), pp. 142-145.

[17] B. W. Lee, J. M. Ferreira, Y. Dalichaouch, M. S. Torikachvili, K. N. Yang, and M. B. Maple, Phys. Rev. B **37**, 2368 (1988).

[18] D. McK. Paul, H. A. Mook, A. W. Hewat, B. C. Sales, L. A. Boatner, J. R. Thompson, and M. Mostoller, Phys. Rev. B **37**, 2341 (1988).

[19] T. Chattopadhyay, G. J. McIntyre, and U. Köbler, Solid State Commun. **100**, 117 (1996).

[20] U. Köbler, D. Hupfeld, W. Schnelle, K. Mattenberger, and T. Brückel, J. Magn. Magn. Mater. **205**, 90 (1999).

[21] G. Hilscher and H. Michor, in *Studies of High Temperature Superconductors*, edited by A. V. Narlikar (Nova Science Publishers, New York, 1999), Vol. 28, pp. 241-286.

[22] K. Tomala, J. P. Sanchez, P. Vulliet, P. C. Canfield, Z. Drzazga, and A. Winiarska, Phys. Rev. B **58**, 8534 (1998).

[23] C. Detlefs, A. I. Goldmann, C. Stassis, P. C. Canfield, B. K. Cho, J. P. Hill, and D. Gibbs, Phys. Rev. B **53**, 6355 (1996).

[24] B. J. Gibson, W. Schnelle, R. Pöttgen, K. Bartkowski, and R. K. Kremer, Czech. J. Phys. **46**, 2573 (1996).

[25] A. Garnier, D. Gignoux, D. Schmitt, and T. Shigeoka, Physica B **222**, 80 (1996).

[26] U. Köbler, R. M. Müller, W. Schnelle, and K. Fischer, J. Magn. Magn. Mater. **188**, 333 (1998).

[27] R. Mallik, E. V. Sampathkumaran, M. Strecker, and G. Wortmann, Europhys. Lett. **41**, 315 (1998).

[28] S. R. Saha, H. Sugawara, T. D. Matsuda, H. Sato, R. Mallik, and E. V. Sampathkumaran, Phys. Rev. B **60**, 12 162 (1999).

[29] M. J. Parsons, J. Crangle, K. U. Neumann, and K. R. A. Ziebeck, J. Magn. Magn. Mater. **184**, 184 (1998).

[30] J. W. Taylor, H. Capellmann, K. U. Neumann, and K. R. A. Ziebeck, Eur. Phys. J. B **16**, 233 (2000).

[31] In this case the exchange interaction $\bar{\bar{\mathcal{J}}}(\mathbf{Q})$ is real and symmetric $[\bar{\bar{\mathcal{J}}}(\mathbf{Q})=\bar{\bar{\mathcal{J}}}^T(\mathbf{Q})]$, it has real eigenvalues and it follows that $\hat{\mathbf{M}}_{11}^T\hat{\mathbf{M}}_{11}=1$ (AM). Note that this rule only holds, if the classical dipole-dipole interaction is able to lift the degeneracy of the upmost eigenvalue of $\bar{\bar{\mathcal{J}}}(\mathbf{Q})$.

[32] M. Rotter (unpublished).

[33] Note: in the case of simple antiferromagnetism (i.e., $\mathbf{Q}_0\in$ BZB) the exchange interaction $\bar{\bar{\mathcal{J}}}(\mathbf{Q})$ is real and symmetric $[\bar{\bar{\mathcal{J}}}(\mathbf{Q})=\bar{\bar{\mathcal{J}}}^T(\mathbf{Q})]$, it has real eigenvalues and it follows that the eigenvector $\mathbf{M}_{11}=\mathbf{M}_{-11}$ is also real.

The Dipole Interaction and Magnetic Anisotropy in Gadolinium Compounds

M. Rotter*
Institut für Physikalische Chemie, Universität Wien, A–1090 Wien, Austria and
Institut für Festkörperphysik, Technische Universität Dresden, D–01062 Dresden, Germany

M. Loewenhaupt and M. Doerr
Institut für Festkörperphysik, Technische Universität Dresden, D–01062 Dresden, Germany

A. Lindbaum, H. Sassik
Institut für Festkörperphysik, Technische Universität Wien,
Wiedner Hauptstraße 8–10, A–1040 Wien, Austria

K. Ziebeck
Department of Physics, Loughborough University, Loughborough, LE 11 3TK, U. K.

B. Beuneu
Laboratoire Léon Brillouin, CEA-CNRS, Saclay, 91191 Gif sur Yvette Cedex, France
(Dated: August 14, 2003)

The influence of the dipole interaction on the magnetic anisotropy of Gd compounds is investigated. Available data on ferromagnets and antiferromagnets with different crystal structures are discussed and complemented by new neutron scattering experiments on $GdCu_2In$, $GdAu_2Si_2$, $GdAu_2$ and $GdAg_2$. If the propagation vector of the magnetic structure is known, the orientation of the magnetic moments as caused by the dipole interaction can be predicted by a straightforward numerical method for compounds with a single Gd atom in the primitive unit cell. The moment directions found by magnetic diffraction on $GdAu_2Si_2$, $GdAu_2$, $GdAg_2$, $GdCu_2Si_2$, $GdNi_2B_2C$, $GdNi_2Si_2$, $GdBa_2Cu_3O_7$, $GdNi_5$, GdCuSn, $GdCu_2In$, $GdCu_4In$ and GdX (X=Ag, Cu, S, Se, Sb, As, Bi, P) are compared to the predicted directions resulting in an almost complete accordance. Therefore, the dipole interaction is identified as the dominating source of anisotropy for most Gd-compounds. The numerical method can be applied to a large number of other compounds with zero angular momentum.

PACS numbers: 75.30.Gw Magnetic Anisotropy
Keywords: Neutron diffraction, Gd compounds

I. INTRODUCTION

The sources of magnetic anisotropy of rare earth compounds are single ion, dipolar and exchange anisotropy. The largest contribution usually comes from single ion anisotropy, unless the angular momentum is zero ($L = 0$) such as in the case of Gd^{3+}. The exchange anisotropy may be large for $L \neq 0$ due to the spin-orbit interaction [1]. The small but finite magnetic anisotropy of $L = 0$ rare earth compounds is topic of various speculations about it's origin: An important contribution can come from the dipole interaction [2]. Also crystal field and exchange effects coming from higher multiplets have been discussed as the source [3, 4]. Recently, the role of biquadratic exchange for the magnetic properties of these ($L = 0$) compounds has been pointed out [5]. Different methods for the study of the anisotropy of the exchange interaction (i.e. the determination of the exchange tensor) have been suggested [6]. This is still an experimental challenge for neutron scattering but only few quantitative results have been reported [7–10].

It is well accepted, that the dipole interaction drives the anisotropy of Gd metal [2, 11–14]. It's influence leads to a modification of the critical dynamics and the corresponding universality class has been identified [15, 16]. Recent first principles calculations [17] indicate an equally large contribution arising from the spin orbit coupling of the conduction bands.

In Gd compounds few investigations of the anisotropy of magnetic interactions have been performed and no systematic study is available, especially on antiferromagnets. Recently the ferromagnet $GdNi_5$ has been analyzed by muon spin resonance [18]. In the past electron paramagnetic resonance in some Gd systems diluted with La or Y has been used to determine the exchange anisotropy between Gd ions [19]. $GdBa_2Cu_3O_7$ has been diluted by Y and electron spin resonance spectra support the dominance of the dipolar anisotropy in this compound [3].

In this paper we present a systematic study of Gd compounds with one Gd atom in the primitive unit cell. In these compounds the direction of the magnetic moments can be predicted from the knowledge of the propagation vector. We will show that it is possible to draw conclusions about the dominant interaction driving the mag-

*Electronic address: rotter@physik.tu-dresden.de

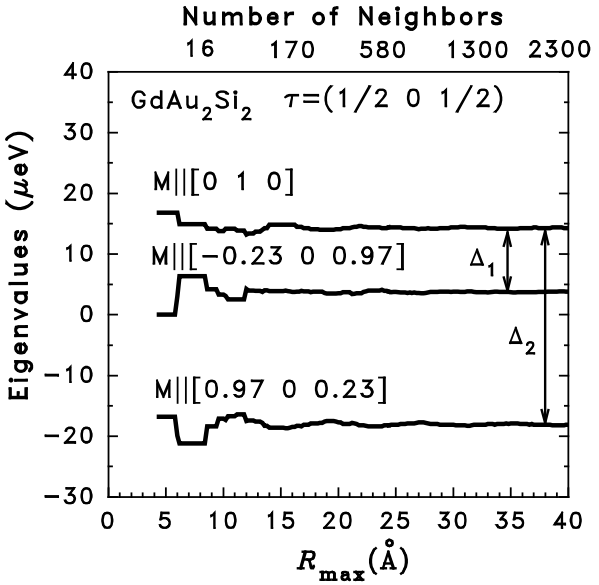

FIG. 1: Convergence behavior of the eigenvalues of $\mathcal{J}_{\alpha\beta}(\tau)$ of $GdAu_2Si_2$ with respect to the maximum distance $R_{\max}$ of neighbors considered. The different lines correspond to eigenvalues with eigenvectors representing moment directions parallel to $\mathbf{e}_0 = [0\,1\,0]$, $\mathbf{e}_1 = [-0.23\,0\,0.97]$ and $\mathbf{e}_2 = [.97\,0\,0.23]$ (mind: in order to show that these vectors are orthonormal, the components are given with respect to euclidian coordinate system, not with respect to crystallographic lattice. The orientation is $x||a$, $y||b$ and $z||c$). Δ_1 and Δ_2 indicate differences of eigenvalues, which are a measure of the dipolar anisotropy.

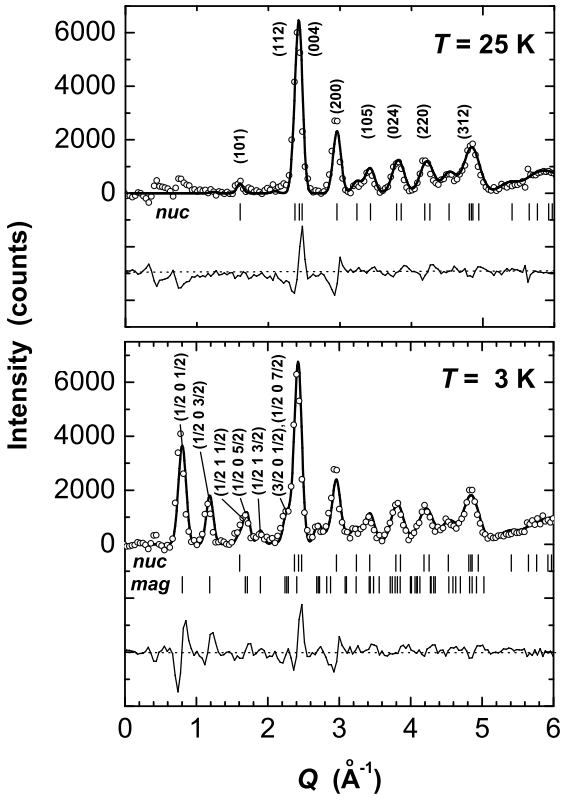

FIG. 2: Neutron diffraction patterns of $GdAu_2Si_2$ at $T = 25$ K and 3 K. The lines correspond to the calculated pattern, below each pattern the difference between calculated and measured intensity is shown. The positions of nuclear peaks and the magnetic satellites with strong intensity are indicated by the vertical bars.

netic anisotropy.

II. DIPOLAR MODEL

If the propagation vector τ of a magnetic compound has been determined from neutron or magnetic X-ray diffraction data, it is possible to calculate that orientation of the magnetic moments in the ordered state, that is favored by the dipole interaction. For a detailed description of the analytical method, which is strictly valid near the ordering temperature, we refer to [20]. Here we outline only the main steps of the calculation:

A general two ion coupling which depends only on the dipolar moments of the $4f$ electrons is

$$\mathcal{H} = -\frac{1}{2}\sum_{ij} J_i^\alpha \mathcal{J}_{\alpha\beta}(ij) J_j^\beta \qquad (1)$$

In this expression (1) the $4f$ moment of the i^{th} Gd^{3+} ion is represented by the three components of the angular momentum operator J_i^α ($\alpha = 1, 2, 3$).

In order to calculate the orientation of the magnetic moments, it is necessary to calculate the Fourier transform $\mathcal{J}_{\alpha\beta}(\tau)$ of the interaction tensor $\mathcal{J}_{\alpha\beta}(ij)$

$$\mathcal{J}_{\alpha\beta}(\tau) = \sum_j \mathcal{J}_{\alpha\beta}(ij) e^{-i\tau(\mathbf{R}_i - \mathbf{R}_j)} \qquad (2)$$

For the following calculations we used the dipole interaction as given by

$$\mathcal{J}_{\alpha\beta}(ij) = (g_J\mu_B)^2 \frac{3(R_i^\alpha - R_j^\alpha)(R_i^\beta - R_j^\beta) - \delta_{\alpha\beta}|\mathbf{R}_i - \mathbf{R}_j|^2}{|\mathbf{R}_i - \mathbf{R}_j|^5} \qquad (3)$$

Here $\mathbf{R}_i$ denotes the lattice vector of the i^{th} Gd ion, g_J the Landé factor and μ_B the Bohr magneton.

The sum in equation (2) is evaluated numerically neglecting the contributions for distances between Gd ions that are larger than a maximum distance $R_{\max}$. The next step is to diagonalize the Fourier transform $\mathcal{J}_{\alpha\beta}(\tau)$. The predicted moment direction is given by the eigenvector corresponding to the largest eigenvalue.

Note that any *isotropic* contribution to the exchange interaction (such as Heisenberg or RKKY type interactions) is usually much larger and therefore deter-

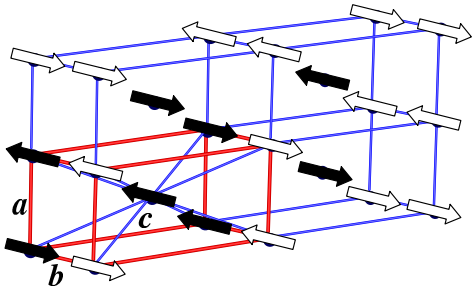

FIG. 3: Magnetic unit cell of $GdAu_2Si_2$ (domain with $\tau = (1/2 \quad 0 \quad 1/2)$ and magnetic moments parallel to [0 1 0]). For clarity we show only the Gd sublattice.

mines the ordering temperature but will not influence the *anisotropic* behavior including the orientation of the magnetic moments. It should also be mentioned, that if high accuracy for the components of the Fourier transform $\mathcal{J}_{\alpha\beta}(\tau)$ is needed, analytical methods have to be used for the calculation [11]. Because of the long range of the interaction, the numerical procedure may converge slowly. This is important in some special cases, when the propagation vector and the geometry of the lattice cause a very small anisotropy of the dipole interaction and other interactions or surface effects may influence the orientation of the magnetic moments [21].

As an example fig. 1 illustrates the issue of convergence of the eigenvalues for the body centered tetragonal lattice of $GdAu_2Si_2$. For the calculation the propagation vector $\tau = (1/2 \quad 0 \quad 1/2)$ has been used, which has been determined from the neutron diffraction experiment described in the following. Δ_1 and Δ_2 denote differences of eigenvalues, which are a measure of the dipolar anisotropy between the three orthogonal directions shown in fig. 1. The largest eigenvalue of $\mathcal{J}_{\alpha\beta}(\tau)$ corresponds to the eigenvector [010]. Therefore the calculation predicts that the magnetic moments are aligned along the [010] direction.

III. NEUTRON DIFFRACTION

In order to enlarge the available set of scattering data on Gd compounds we have collected data on some cubic and tetragonal Gd systems using the 7C2 - hot source diffractometer of the LLB, Saclay with a neutron wavelength of 0.58 Å . The absorption of the samples was reduced by using a double wall cylindric sample holder (outer diameter 12 mm, inner diameter 10 mm). In the following we outline in detail the experimental results and show how they correspond to the predictions of the dipolar model.

A. $GdAu_2Si_2$

$GdAu_2Si_2$ orders antiferromagnetically at $T_N = 12$ K [22]. This system has been chosen because the analysis of the specific heat suggests a non-collinear amplitude modulated magnetic structure [20]. Powder diffraction patterns taken at 25 K and 3 K are shown in fig. 2 (for each pattern the background signal has been subtracted). The pattern at 25 K in the magnetically disordered state can be indexed according to the tetragonal $ThCr_2Si_2$ structure with $a = 0.4245$ nm and $c = 1.0165$ nm. At 3 K the magnetic lines (for $Q < 2$ Å^{-1}) can be indexed with the propagation vector $\tau = (1/2 \quad 0 \quad 1/2)$.

The propagation vector and the orientation of the magnetic moments have been varied and the calculated diffraction patterns have been compared to the experimental data. Modules of the *McPhase* software [23] have been used for these computations. The absorption has been calculated for our experimental geometry according to the method given in [24]. It was found to be of minor importance compared to the Lorentz factor in the low angle range, where the magnetic intensities have been refined. For the calculation of the intensity profile a Gaussian lineshape with an angle dependent linewidth was applied. Due to the limited resolution the fit is not very sensitive to small changes of the propagation vector. However, the magnetic intensities are very sensitive to the orientation of the magnetic moments.

The best fit of the intensities could be achieved with moments of 6.2 μ_B oriented parallel to [0 1 0], i.e. transversal to the propagation vector $\tau = (1/2 \quad 0 \quad 1/2)$. The magnetic unit cell is shown in fig. 3. Due to the tetragonal symmetry there exist two domains.

Note that the propagation $\tau = (1/2 \quad 0 \quad 1/2)$ must lead to an equal moment structure and is not compatible with the non-collinear amplitude modulated structure indicated by the specific heat [20]. Consequently either the propagation at temperatures near T_N must differ from $(1/2 \quad 0 \quad 1/2)$ or critical fluctuations should be taken into account in more detail to improve the interpretation of the specific heat in this system.

The dipolar model (section II) was applied to $GdAu_2Si_2$ in order to investigate the influence of the dipole interaction. The Fourier transform $\mathcal{J}_{\alpha\beta}(\tau)$ was calculated by applying equ. (1)-(3) to the case of $GdAu_2Si_2$ as shown in fig. 1. The largest eigenvalue corresponds to the moment direction [0 1 0]. This is in agreement with the results of the diffraction experiment and indicates that the dipole interaction is the dominant source of anisotropy in this system. The experimental magnetic diffraction pattern and the pattern calculated from the dipolar model are compared in fig. 4. For the other compounds of this study a similar analysis has been performed.

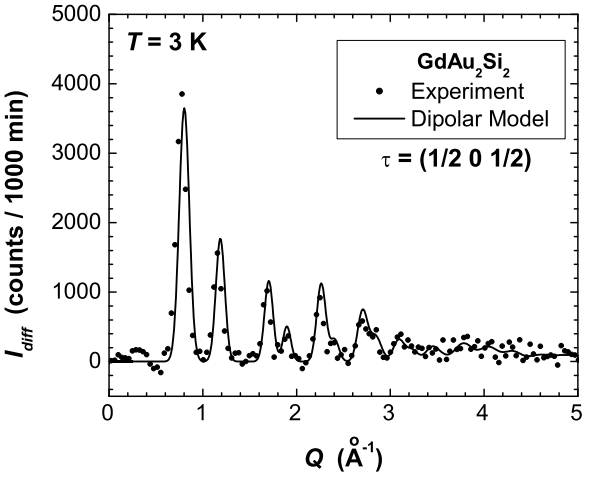

FIG. 4: Magnetic neutron diffraction pattern (data points) of $GdAu_2Si_2$ as determined from the difference of measurements at $T = 4$ K and 25 K. The lines correspond to the pattern calculated from the dipolar model described in the text.

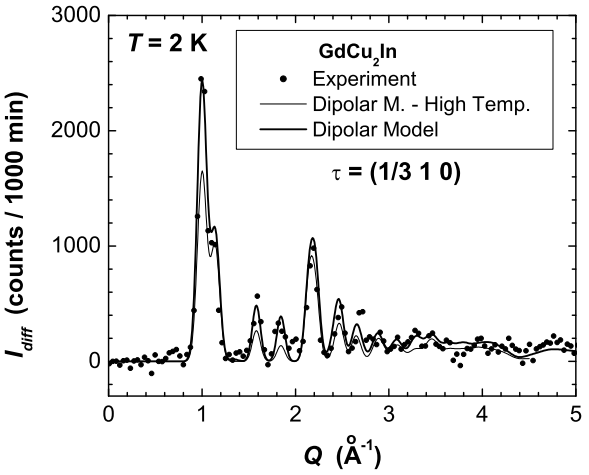

FIG. 5: Magnetic neutron diffraction pattern (data points) of $GdCu_2In$ as determined from the difference of measurements at $T = 2$ K and 20 K. The lines correspond to the pattern calculated from the dipolar model described in the text. Extending the temperature range of the model (the high temperature expansion is shown by a thin line) to low temperatures by numerical methods (thick line) improves the description of the experimental data (see text).

B. $GdCu_2In$

$GdCu_2In$ crystallizes in the cubic Heusler structure $L2_1$ [25] (lattice constant $a = 0.662$ nm at 2 K). It orders antiferromagnetically below $T_N \sim 10$ K with some complicated and up to now unknown magnetic structure [26, 27]. Thermal expansion was measured [27] on polycrystalline samples using a capacitance dilatometer. The estimated value of the magneto-volume effect at 0 K is small ($(\Delta V/V)_{mag} \approx -1 \times 10^{-4}$).

We investigated the magnetic structure of the Heusler compound $GdCu_2In$ by neutron diffraction and find complex antiferromagnetism. The propagation vector and the orientation of the magnetic moments have been varied and the calculated magnetic diffraction patterns have been compared to the experimental data taken at $T = 2$ K. Fig. 5 shows the difference pattern of measurements at 20 K and 2 K. The best fit could be achieved with a propagation of $\tau = (1/3\ \ 1\ \ 0)$ and a moment direction perpendicular to [001].

The dipolar model (see section II) predicts for this propagation a collinear amplitude modulated magnetic structure with moments parallel to [100]. This moment direction is consistent with the experimental result. But, the quantitative agreement of the powder pattern of this calculated magnetic structure with the experiment is not completely satisfying (see thin lines in fig. 5). The reason for this discrepancy is a slight modification of the magnetic structure at lower temperatures which cannot be modeled because the calculation procedure outlined in section II is strictly valid only for temperatures near T_N.

In order to remove this restriction of the model a large effort was undertaken to extend the theoretical analysis to low temperatures by numerical methods [28]. In a first step *isotropic* short range exchange interaction constants have been set up such as to give a maximum of the Fourier transform at (1/3 1 0) and to reflect the experimental Néel temperature (for details on this procedure see [9]). From these conditions equations for the isotropic exchange parameters follow which can be fulfilled only if more than three neighbors are considered. Therefore, in the model calculation we used the following four nearest neighbor interaction constants, which are associated with the neighbors at (1/2 1/2 0) (-0.0333 meV), (1 0 0) (0.012 meV), (1/2 1/2 1) (0.004 meV) and (2 0 0) (-0.002 meV). In addition to these short range isotropic exchange constants the dipolar interaction as given by equ. (3) was taken into account for distances up to 4 nm. The program *McPhase* [23],[43] was used to calculate the temperature dependence of the magnetic structure. At low temperature a non-collinear magnetic structure is predicted by the calculation. When increasing the temperature to 0.9 T_N a spin reorientation associated with a change of the magnetic structure from non-collinear to collinear (with moments parallel to [010] in agreement with the analytical approach - section II) has been computed.

The experimental magnetic diffraction pattern of $GdCu_2In$ at 2 K is in good agreement with the predictions by the model based on isotropic short range exchange plus classical dipolar interactions (see fig. 5). Note, that a magnetic moment of 6.0 μ_B/Gd has been used in the calculation.

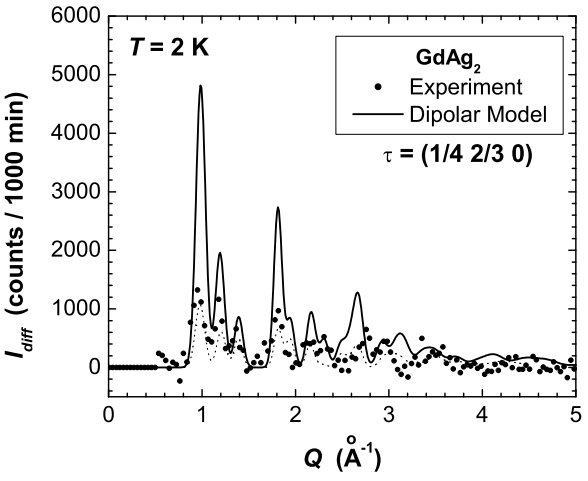

FIG. 6: Magnetic neutron diffraction pattern (data points) of $GdAg_2$ as determined from the difference of measurements at $T = 2$ K and 35 K. The straight line corresponds to the pattern calculated from the dipolar model described in the text. The dotted line corresponds to Rietveld type fits, which have been used to determine the magnetic propagation vector.

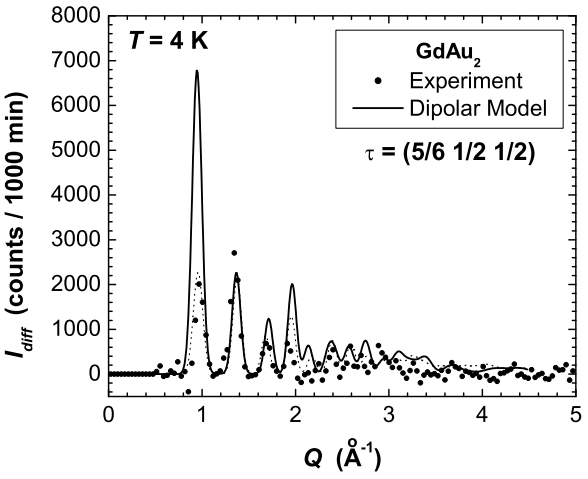

FIG. 7: Magnetic neutron diffraction pattern (data points) of $GdAu_2$ as determined from the difference of measurements at $T = 4$ K and 70 K. The straight line corresponds to the pattern calculated from the dipolar model described in the text. The dotted line corresponds to Rietveld type fits, which have been used to determine the magnetic propagation vector.

C. $GdAg_2$ and $GdAu_2$

$GdAg_2$ and $GdAu_2$ crystallize in the tetragonal $MoSi_2$-type structure [29]. The space group is $I4/mmm$ with Gd on the 2a-sites (point symmetry $4/mmm$) and Ag(Au) on the 4*e* sites. This structure can roughly be viewed as being composed of three tetragonally distorted body centered cubes along *c*-direction ($GdAg_2$: a =0.3716 nm, c =0.926 nm, $GdAu_2$: a =0.3716 nm, c =0.8996 nm). The z atomic position parameter of the 4*e* sites (point symmetry $4mm$) is about 1/3. For $GdAg_2$ a value of $z_{Ag} = 0.327 \pm 0.004$ has been determined from neutron diffraction experiments [30].

$GdAg_2$ has first been reported to order magnetically at about 27 K from resistivity measurements [31]. Further studies [30, 32] including specific heat, resistivity , thermal expansion and magnetization measurements as well as first neutron powder diffraction experiments, showed that this compound orders antiferromagnetically below $T_N \approx 23$ K with two further first-order magnetic transitions at $T_{R1} \approx 21$ K and $T_{R2} \approx 11$ K. The observed first-order magnetic transitions in the ordered range have been attributed to anisotropic terms in the two-ion Gd-Gd exchange interaction. A further peculiarity is that the magnetic ordering temperature of $GdAg_2$ is lower than in $TbAg_2$ ($T_N \approx 35$ K), violating the De Gennes law. Recently, the role of biquadratic exchange for the magnetic properties of these ($L = 0$) compounds has been pointed out [5]. This has been referred to a change in the conduction band due to the boundary situation of $GdAg_2$ concerning the crystal structure, i.e. only the RAg_2 compounds with heavy rare earth, starting from Gd, show the $MoSi_2$ type of structure [30].

In the previous neutron diffraction experiments by Gignoux et al. [30] magnetic satellites have been found below the ordering temperature. However, the data has to be doubted, because at the position of the (002) nuclear reflection no intensity has been found at any temperature in contrast to expectations from the reported crystallographic structure. Therefore also the magnetic scattering at low angles has to be doubted and we decided to remeasure $GdAg_2$.

Indeed our new data are in excellent agreement with the reported crystallographic structure including intensity on the (002) nuclear reflection. Fig. 6 shows the magnetic diffraction pattern as determined from the difference of measurements at 2 K and 35 K. Fitting suggests a propagation of $\tau = (1/4\ \ 2/3\ \ 0)$ (dotted lines). The best fit of the 2 K pattern with this propagation corresponds to an amplitude modulated structure with moments in [110] direction. The prediction of classical dipolar exchange (just below the ordering temperature) is a moment direction along [0.98,0.20,0], which is more or less along a direction.

In order to make a correct theoretical prediction of the squaring up at temperatures far below T_N a *McPhase* calculation has been performed similar to the case of $GdCu_2In$. At 2 K a cycloid in the ac plane is predicted. However, the magnetic pattern calculated in this way is in clear disagreement with the experimental pattern (see fig. 6).

$GdAu_2$ orders like $GdAg_2$ antiferromagnetically, but at a much higher ordering temperature of $T_N \approx 50$ K [33]. In contrast to $GdAg_2$ there is no measurable spontaneous

magnetoelastic effect at all. The magnetically induced change of c/a as well as the volume magnetostriction of $GdAu_2$ is smaller than 10^{-4} [32]. The results of our neutron diffraction study for determining the magnetic structure are shown in fig. 7. The best fit gives a propagation of $\tau = (5/6 \;\; 1/2 \;\; 1/2)$ with an equal moment cycloid with moments perpendicular to [011].

However, the classical dipolar interaction predicts collinear moments parallel to [100] for this propagation (near the ordering temperature). At lower temperatures a *McPhase* calculation gives an equal moment cycloid with moments perpendicular to [0,0.98,-0.2]. The predicted intensities do not correspond to the experimental data.

Provided that the propagations are correct (small deviations from the assumed propagation vectors will not alter the result) the experimental data indicates, that in $GdAg_2$ and $GdAu_2$ the classical dipolar model for the anisotropy of the two ion interactions cannot describe the experimental moment direction sufficiently. Note that in both cases the dipolar anisotropy is rather small (see table I) and therefore other sources of anisotropy may become important.

IV. DISCUSSION

For generalization we now consider other available data for compounds with one Gd atom per primitive crystallographic unit cell. Table I shows a list of the compounds which have been investigated and which we have subjected to our model analysis. Most of the experimental data have been derived from neutron diffraction. The moment directions taken from the experiment are compared to the calculation and agree for almost all cases under investigation.

In order to give a measure for the dipolar anisotropy for every compound the differences Δ_1 and Δ_2 of eigenvalues of $\mathcal{J}_{\alpha\beta}(\tau)$ (compare fig. 1) are given in the last column of table I. For orientation also the eigenvectors $\mathbf{e}_1$ and $\mathbf{e}_2$ are listed, which correspond to the hard moment directions. The values of Δ_1 and Δ_2 show, that the dipolar anisotropy varies over one order of magnitude. It is largest for the 1:1 compounds (short Gd-Gd distances) and smallest for $GdNi_5$. It is small also in those few cases where the dipolar model fails ($GdAg_2$ and $GdAu_2$). Note that *cubic ferromagnets* such as GdMg [5] have not been listed, because in this case the dipolar anisotropy is zero by symmetry. To our knowledge no experimental determination of the moment direction (easy axis) has been reported in this very interesting class of compounds.

In conclusion, in this paper we have shown that in many Gd compounds the observed anisotropy originates from the dipole interaction. Thus the compounds under consideration might behave according to the dipolar universality class as described in [15, 16] for the case of Gd metal. Although the magnetic anisotropy of Gd compounds is usually much smaller than that of the other rare earth compounds, it can be predicted with much higher accuracy from first principles. However, care must be taken if the dipolar anisotropy energy Δ_1 (as defined in our model - section II) is less than 10 μeV. Then other sources of anisotropy become important, which still have to be identified for the compounds under consideration.

Acknowledgments

We are grateful to the valuable comments of U. Köbler and P. Maier on the manuscript and J. P. Ambroise for helpful assistance at LLB, Saclay. Part of this work was performed within the program of the Sonderforschungsbereich 463 (funded by the Deutsche Forschungsgemeinschaft). We acknowledge financial support by the Austrian Science Fund (FWF) project No. P-14932-PHY, by the Austrian Academy of Sciences (APART 10739) and by the European Commission in the frame of the HPRI access program.

TABLE I: Magnetic anisotropies of several Gd compounds in comparison with the prediction from the dipole interaction. The second column describes the experimental method (n - neutron diffraction, x - magnetic X-ray scattering, m- Moessbauer spectroscopy, μSR- muon spin relaxation). In the third column the ordering temperatures are given. The fourth column contains the propagation vector, and the fifth the experimentally derived moment direction at low temperature (moment direction coordinates $[m_x m_y m_z]$ refer to Euclidean coordinate system with $x||a$, $y||b$ and $z||c$). In many cases the experimental data are in agreement with the prediction from the dipole interaction given in column six, exceptions are $GdAg_2$ and $GdAu_2$. The last column contains the differences Δ_1 and Δ_2 of the eigenvalues of $\mathcal{J}_{\alpha\beta}(\tau)$, which are a measure of the dipolar anisotropy. The corresponding eigenvectors are given in brackets (compare fig.1).

Experiment					**Theory**	
Compound	Method	Ordering Temperature (K)	Propagation Vector τ	Experimental Moment Direction	Calculated Moment Direction	Dipolar Anisotropy $\Delta_1^{[e_1]}\|\Delta_2^{[e_2]}$ (μeV)
cubic						
GdAg (*bcc*)	n[34]	134	(1/2 1/2 0)	[0 0 1]	[0 0 1]	$36^{[100]}\|36^{[010]}$
GdCu (*bcc*)	n[35]	150	(1/2 1/2 0)	[0 0 1]	[0 0 1]	$41^{[100]}\|41^{[010]}$
GdX (*fcc*,X=S,P,Se)	n[36, 37]	50,28,60	(3/2 3/2 3/2)	$\perp$[1 1 1]	$\perp$[1 1 1]	$0\|53,50,48^{[111]}$
(X=As,Sb,Bi)	n[36, 37]	15.2,32,19	(3/2 3/2 3/2)	$\perp$[1 1 1]	$\perp$[1 1 1]	$0\|47,39,37^{[111]}$
$GdCu_2In$	n[this work]	10	(1/3 1 0)	$\perp$[0 0 1]	[1 0 0]^a	$2.9^{[001]}\|12.3^{[010]}$
$GdCu_4In$	n[38]	7	(0 1/2 1)	[0 1 0]	[0 1 0]	$4.9^{[100]}\|4.9^{[001]}$
hexagonal						
$GdNi_5$	μSR[18]	32	(0 0 0)	[0 0 1]	[0 0 1]	$7.5^{[100]}\|7.5^{[010]}$
GdCuSn^b	m[39]	24	(0 1/2 0)	[0 0 1]	[0 0 1]	$12^{[100]}\|50^{[010]}$
tetragonal						
$GdAg_2$	n[this work]	22.7	(1/4 2/3 0)	[1 1 0]	[0.98 0.20 0]^c	$4.3^{[001]}\|12.3^{[-0.20\ 0.98\ 0]}$
$GdAu_2$	n[this work]	50	(5/6 1/2 1/2)	$\perp$[0 1 1]	[1 0 0]^d	$7^{[0\ 0.20\ 0.98]}\|35^{[0\ 0.98\ -0.20]}$
$GdAu_2Si_2$	n[this work]	12	(1/2 0 1/2)	[0 1 0]	[0 1 0]	$11^{[-0.22\ 0\ 0.97]}\|32^{[0.97\ 0\ 0.22]}$
$GdCu_2Si_2$	n[40]	12.5	(1/2 0 1/2)	[0 1 0]	[0 1 0]	$13^{[-0.2\ 0\ 0.98]}\|38^{[0.98\ 0\ 0.2]}$
$GdNi_2Si_2$	n[40]	14.5	(0.207 0 0.903)	[0 1 0]	[0 1 0]	$14^{[-0.99\ 0\ 0.13]}\|34^{[0.13\ 0\ 0.99]}$
$GdNi_2B_2C$	n,x[41]	20	(0.55 0 0)	[0 1 0]	[0 1 0]	$21^{[001]}\|50^{[100]}$
orthorhombic						
$GdBa_2Cu_3O_7$	n[42]	2.2	(1/2 1/2 1/2)	[0 0 1]	[0 0 1]	$14^{[010]}\|15^{[100]}$

[a]note: extending the theory to $T \to 0$ by a *McPhase* calculation gives a non-collinear equal moment structure with moments $\perp$[0 0 1] in agreement with the experiment.

[b]note: only the Gd sublattice has one Gd atom per unit cell. The full structure has two Gd atoms per primitive unit cell.

[c]note: extending the theory to $T \to 0$ by a *McPhase* calculation gives a non-collinear equal moment structure with moments $\perp$[0 1 0].

[d]note: extending the theory to $T \to 0$ by a *McPhase* calculation gives a non-collinear equal moment structure with moments $\perp$[0,0.98,-0.2].

[1] K. W. H. Stevens, *Magnetic Ions in Crystals* (Princeton University Press, 1997).

[2] J. Jensen and A. R. Mackintosh, *Rare Earth Magnetism* (Clarendon Press Oxford, 1991).

[3] F. Simon, A. Rockenbauer, T. Feher, A. Janossy, C. Chen, A. J. S. Chowdhury, and J. W. Hodby, Phys. Rev. **B 59**, 12072 (1999).

[4] R. W. Cochrane, C. Y. Wu, and W. P. Wolf, Phys. Rev. **B 8**, 4348 (1973).

[5] U. Köbler, R. M. Müller, P. J. Brown, and K. Fischer, J. Phys.: Cond. Mat. **13**, 6835 (2001).

[6] W. P. Wolf, J. de Phys. **32**, C1 (1971).

[7] A. Loidl, K. Knorr, J. K. Kjems, and B. Luethi, Z. Phys. **B 35**, 253 (1979).

[8] B. Halg and A. Furrer, Phys. Rev. **B 34**, 6258 (1986).

[9] M. Rotter, M. Loewenhaupt, S. Kramp, T. Reif, N. M. Pyka, W. Schmidt, and R. v. d. Kamp, Europ. Phys. J. **B 14**, 29 (2000).

[10] M. Rotter, M. Doerr, M. Loewenhaupt, U. Witte, P. Svoboda, J. Vejpravová, H. Sassik, C. Ritter, D. Eckert, A. Handstein, et al., Phys. Rev. **B 64**, 134405 (2001).

[11] N. M. Fujiki, K. De'Bell, and D. J. W. Geldart, Phys. Rev. **B 36**, 8512 (1987).

[12] D. J. W. Geldart, P. Hargraves, N. M. Fujiki, and R. A. Dunlap, Phys. Rev. Lett. **62**, 2728 (1989).

[13] J. M. Coey, V. Skumryev, and K. Gallagher, Nature **401**, 35 (1999).

[14] S. N. Kaul and S. Srinath, Phys. Rev. **B 62**, 1114 (2000).

[15] S. Henneberger, E. Frey, P. G. Maier, F. Schwabl, and G. M. Kalvius, Phys. Rev. **B 60**, 9630 (1999).
[16] S. Srinath and S. N. Kaul, Phys. Rev. **B 60**, 12166 (1999).
[17] M. Colarieti-Tosti, S. I. Simak, R. Ahuja, L. Nordström, O. Eriksson, and M. S. S. Brooks, J. Magn. Magn. Mat. (2003), proceedings of the International Conference on Magnetism - Rome 2003.
[18] A. Yaouanc, P. DalmasdeRéotier, P. C. M. Gubbens, A. M. Mulders, F. E. Kayzel, and J. J. M. Franse, Phys. Rev. **B 53**, 350 (1996).
[19] M. T. Hutchings, R. J. Birgeneau, and W. P. Wolf, Phys. Rev. **168**, 1026 (1968).
[20] M. Rotter, M. Loewenhaupt, M. Doerr, A. Lindbaum, and H. Michor, Phys Rev. **B 64**, 014402 (2001).
[21] A. Aharony and M. E. Fisher, Phys. Rev. **B 8**, 3323 (1973).
[22] R. Mallik and E. V. Sampathkumaran, Phys. Rev. **B 58**, 9178 (1998).
[23] M. Rotter, J. Magn. Magn. Mat. (2003), in print.
[24] D. Schmitt and B. Ouladdiaf, J. Appl. Cryst. **31**, 620 (1998).
[25] P. J. Webster, Contemp. Phys. **10**, 559 (1969).
[26] M. J. Parsons, J. Crangle, K. U. Neumann, and K. R. A. Ziebeck, J. Magn. Magn. Mat. **184**, 184 (1998).
[27] J. W. Taylor, H. Capellmann, K. U. Neumann, and K. R. A. Ziebeck, Eur. Phys. J. **B 16**, 233 (2000).
[28] M. Rotter, M. Doerr, M. Loewenhaupt, A. Lindbaum, K. Ziebeck, and B. Beuneu, Physica B (2003), submitted.
[29] A. Dwight, J. Downey, and R. Conner, Acta Crystallogr. **22**, 745 (1967).
[30] D. Gignoux, P. Morin, and D. Schmitt, J. Magn. Magn. Mat. **102**, 33 (1991).
[31] M. Ohashi, T. Kaneko, and S. Miura, J. Phys. Soc. Jpn. **38**, 588 (1975).
[32] A. Lindbaum and M. Rotter, in *Magnetic Materials*, edited by K. H. J. Buschow (Elsevier Sci. Pub., Amsterdam,The Netherlands, 2002), vol. 14, pp. 307–362.
[33] L. D. Tung, K. H. J. Buschow, J. J. M. Franse, and N. P. Thuy, Journ. Magn. Magn. Mat. **154**, 96 (1996).
[34] T. Chattopadhyay, G. J. McIntyre, and U. Köbler, Sol. Stat. Com. **100**, 117 (1996).
[35] J. A. Blanco, J. I. Espeso, J. I. GarcíaSoldevilla, J. C. GómezSal, M. R. Ibarra, C. Marquina, and H. E. Fischer, Phys. Rev. **B 59**, 512 (1999).
[36] T. R. McGuire, R. J. Gambino, S. J. Pickart, and H. A. Alperin, J. of Appl. Phys. **40**, 1009 (1969).
[37] F. Hulliger, J. Magn. Magn. Mat. **8**, 183 (1978).
[38] H. Nakamura, N. Kim, M. Shiga, R. Kmiec, K. Tomala, E. Ressouche, J. P. Sanchez, and B. Malaman, J.Phys.: Cont. Mat. **11**, 1095 (1999).
[39] D. Bialic, R. Kruk, R. Kmieć, and K. Tomala, Journal of Alloys and Compounds **257**, 49 (1997).
[40] J. M. Barandiaran, D. Gignoux, D. Schmitt, J. C. Gomez-Sal, J. R. Fernandez, P. Chieux, and J. Schweizer, J. Mag. Magn. Mat. **73**, 233 (1988).
[41] C. Detlefs, A. I. Goldman, C. Stassis, P. C. Canfield, B. K. Cho, J. P. Hill, and D. Gibbs, Phys. Rev. **B 53**, 6355 (1996).
[42] D. M. Paul, H. A. Mook, A. W. Hewat, B. C. Sales, L. A. Boatner, J. R. Thompson, and M. Mostoller, Phys. Rev. **B 37**, 2341 (1988).
[43] www.mcphase.de

Eur. Phys. J. B **14**, 29–42 (2000)

THE EUROPEAN PHYSICAL JOURNAL B

EDP Sciences

Anisotropic magnetic exchange in orthorhombic RCu_2 compounds (R = rare earth)

M. Rotter[1,a], M. Loewenhaupt[2], S. Kramp[2,5], T. Reif[3], N.M. Pyka[4], W. Schmidt[5], and R. van de Kamp[6]

[1] Institut für Experimentalphysik, Technische Universität Wien, Wiedner Hauptstraße 8–10, 1040 Wien, Austria
[2] Institut für Angewandte Physik, Technische Universität Dresden, 01062 Dresden, Germany
[3] Institut für Festkörperforschung, Forschungszentrum Jülich, 52425 Jülich, Germany
[4] TU München, Zentrale Betriebseinheit FRM - II, 85747 Garching, Germany
[5] Institut Laue Langevin, BP 156 38042 Grenoble Cedex 9, France
[6] Hahn Meitner Institut, 14109 Berlin, Germany

Received 21 April 1999

Abstract. The magnetic excitations in the field induced ferromagnetic phase F3 of a $NdCu_2$ single crystal were investigated by means of inelastic neutron scattering experiments. A mean field model using the random phase approximation in connection with anisotropic magnetic bilinear R-R (R denotes a rare earth) exchange interactions is proposed to account for the observed dispersion. The relevance of this model to the analysis of the magnetic ordering process in other RCu_2 compounds is discussed.

PACS. 75.30.Et Exchange and superexchange interactions

1 Introduction

The magnetic structures of $NdCu_2$ in zero field and for magnetic fields parallel to the b axis of the orthorhombic crystal have been the topic of extensive studies [1–3]. For the corresponding magnetic phase diagram and the description of the different magnetic phases we refer the reader to the given references. The investigation of the magnetic excitations is an important dynamical counterpart to the determination of the static magnetic structure, leading to conclusions about the magnetic ground state and the detailed form of the magnetic interactions. By measuring the field and temperature dependence of the magnetic excitations it is possible to refine theoretical models for the magnetic ordering process.

In $NdCu_2$ the zero field phase AF1 consists of a complicated stacking of 10 ferromagnetic bc planes in a direction leading to an excitation spectrum with 20 branches within an energy range from 0.6 to 2.0 meV [4,5]. The presently available resolution of neutron spectrometry, however, is not sufficient to determine all branches unambiguously unless detailed theoretical predictions are available. For these reasons the magnetic excitations have been measured in the field induced ferromagnetic state, where only two branches appear that can be easily resolved by experiment and that can be calculated very fast by an analytical formula that can be used for a fit.

The paper is organized in the following way: In the first section the details of the neutron scattering experiments will be described, then the results are presented followed by a discussion of the symmetry of the magnetic interactions and an outline of the method used to calculate the magnetic excitations. A quantitative analysis of the experimental data is performed, followed by a discussion about its relevance to other RCu_2 compounds in the final section of the paper.

[a] e-mail: martin_rotter@hotmail.com

2 Experiments

The inelastic neutron scattering (INS) experiments have been performed on a large $NdCu_2$ single crystal ($5 \times 7.5 \times 5.2$ mm^3) that was also used for the magnetic structure determination and is described elsewhere [2]. The majority of the INS measurements was carried out on the IN12 triple-axis spectrometer at the Institut Laue-Langevin, Grenoble, using vertical and horizontal magnetic fields of 3 T. Additional experiments have been performed on the V2 triple-axis spectrometer at the BER2-reactor of the Hahn-Meitner-Institut, Berlin, equipped with a horizontal cryomagnet operated at 3 Tesla. Monochromator and analyzer of both spectrometers were made of pyrolytic-graphite (002) crystals. The IN12 spectrometer has been run in constant-momentum-transfer (constant-**Q**) mode with variable incident-neutron energy, bent monochromator and flat analyzer. No filter has been used because higher order contaminations are filtered out by the bent neutron guide. When working with vertical magnetic field ((010)-scattering plane) the scattered-neutron

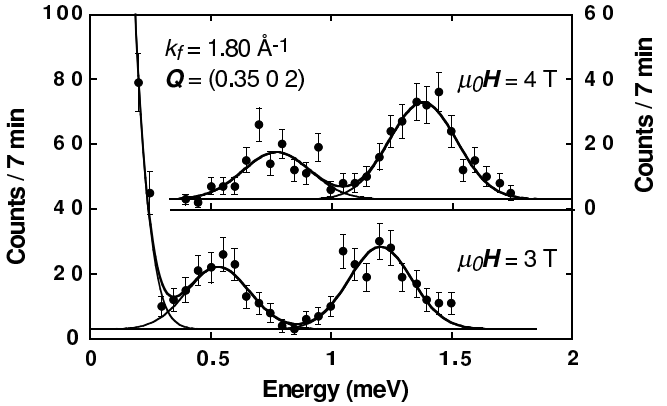

Fig. 1. Magnetic excitations of $NdCu_2$ for $\mathbf{Q}$ = (0.35 0 2). At this wave vector the minimal energy of the dispersion was measured. The upper scan shows the shift of the magnetic excitations when increasing the applied magnetic field.

energy was kept fixed at $k_f = 1.8$ Å^{-1} (6.7 meV). In horizontal field ((001)-scattering plane) the final neutron energy has been varied between $k_f = 1.7$ Å^{-1} (6.0 meV) and 2.1 Å^{-1} (9.2 meV) in order to get access to some **Q**-vectors in (h00)-direction. This variation was necessary because of geometrical restrictions due to the construction principle of the horizontal cryomagnet. Nevertheless, only a few points near the zone boundary could be measured in (h10)-direction on IN12. The study of the (h00)-direction could be completed at the V2 spectrometer using a new horizontal cryomagnet with only two, relatively small blind spots. This experiment was carried out in constant-**Q** mode with fixed scattered-neutron energies of $k_f = 1.1$ Å^{-1} (2.5 meV), 1.4 Å^{-1} (4.1 meV) and 1.55 Å^{-1} (5.0 meV). A cooled Be-filter was placed in front of the analyzer. Monochromator and analyzer have been used in focusing geometry.

3 Results

The measurements have been carried out along the principle symmetry directions (h00), (0k0) and (00l) at T = 1.8 K and B = 3 T. Under these conditions the lattice parameters have been determined to $a = 4.385$ Å, $b = 6.997$ Å and $c = 7.385$ Å. Due to the two Nd^{3+} ions per unit cell in the ferromagnetically ordered phase two magnon branches are expected from the crystal field (CF) ground state doublet. With magnon energies < 2 meV these excitations are well separated from transitions to the higher CF-levels [6].

As an example, Figure 1 shows a constant-**Q** spectrum at the reciprocal lattice vector $\mathbf{Q}$ = (0.35 0 2). The two excitations with energies 0.53 meV and 1.21 meV are clearly separated. The magnetic origin of the measured excitations has been checked by increasing the magnetic field from 3 T to 4 T. Due to the Zeeman contribution the energy of the two excitations shifts by about 0.2 meV to 0.77 and 1.38 meV (see Fig. 1). Energy scans at other

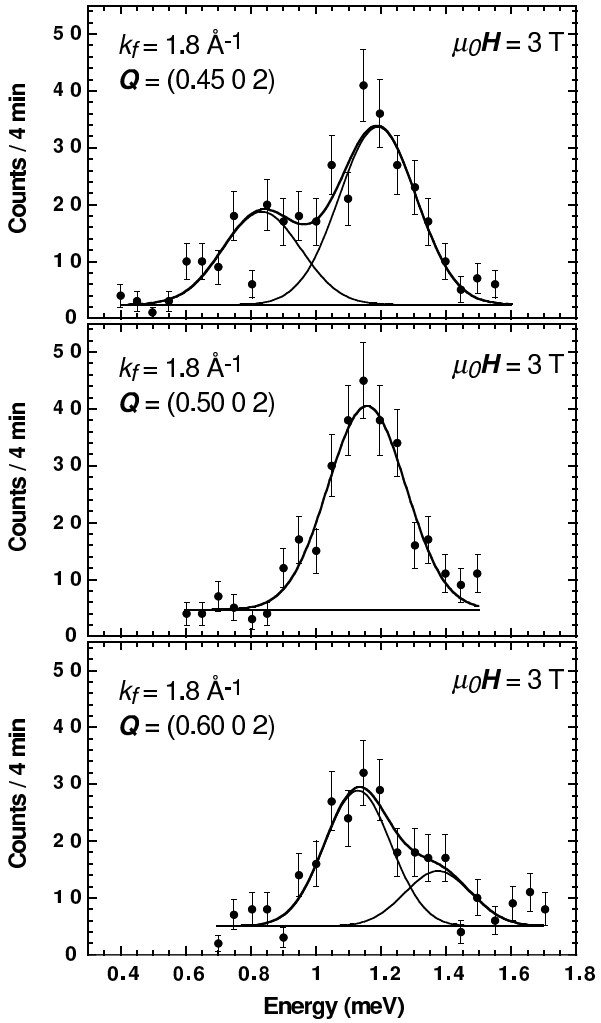

Fig. 2. Constant **Q** scans along (h 0 2) showing the crossing of the two modes at (0.5 0 2).

points along the symmetry directions of the reciprocal lattice revealed, that the scan shown in Figure 1 corresponds to an absolute minimum of the dispersion. Note that the position of the spin wave minimum does not coincide with the ordering wave vector $\boldsymbol{\tau}$ = (0.6 0 0) of the antiferromagnetic zero-field phase AF1.

Three subsequent scans along the (h 0 2) direction are shown in Figure 2. At $\mathbf{Q}$ = (0.45 0 2) the lower excitation has moved up to 0.83 meV, whereas the upper did not change. The scans at (0.5 0 2) and (0.6 0 2) indicate, that a stronger, nondispersive mode at about 1 meV is crossed by a weak, dispersive mode at (0.5 0 2).

Energy scans performed along (h 0 1) revealed only one, weakly dispersive branch above 1 meV. It is the same branch, which is observable along (h 0 2), but there the second branch appears as well.

To investigate the behavior of the two modes separately, scattering experiments in the ab plane were performed at the V2 spectrometer using a new horizontal cryomagnet with large accessible angular range. For **Q** in the reciprocal ab plane only one excitation can be

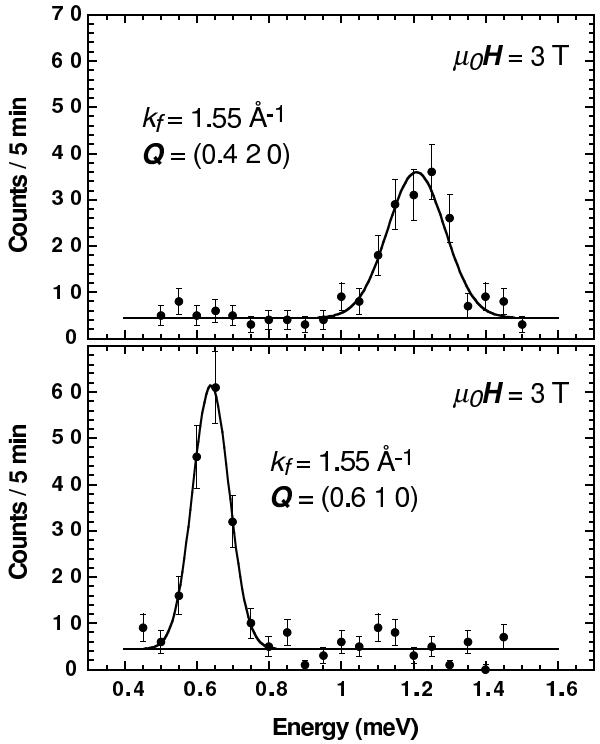

Fig. 3. Constant **Q** scans at two equivalent positions in the reciprocal *ab* plane of $NdCu_2$ measured in the horizontal field configuration. Only one excitation may be observed under these conditions (see text).

measured, because the second excitation has no intensity due to the structure factor. This property is due to the fact, that the projection of the $CeCu_2$ – type structure into the *ab* plane can be described by a primitive rectangular two dimensional lattice. Figure 3 exemplifies this situation at the two equivalent positions (0.4 2 0) and (0.6 1 0). It is instructive to compare the two excitations observed along (h 0 2) to equivalent points along (h 1 0) and (h 2 0): along (h 1 0) the strongly dispersive mode can be measured, whereas along (h 2 0) only the weakly dispersive excitation can be observed.

Unfortunately, even with the new horizontal cryomagnet on the V2 spectrometer not all **q** values were accessible ($\mathbf{q} = \mathbf{Q} - \boldsymbol{\tau}$ with $\boldsymbol{\tau}$ being a reciprocal lattice vector). However, the dispersive branch could clearly be followed from the zone boundary at (0 1 0) up to (0.6 1 0). Crossings of the two modes have been found at $\mathbf{q}$ = (0.2 0 0) and $\mathbf{q}$ = (0.53 0 0).

The results of all scans performed along the symmetry directions of the reciprocal lattice are summarized in Figure 7 and will be discussed in comparison with the calculated dispersion in Section 5. The energies of the two modes at the Γ point have been determined at (0 0 2) to 1.18 meV and 1.63 meV.

4 The MF-RPA model for magnetic excitations

For the calculation of the magnetic excitations in systems with low symmetry great care has to be taken about the anisotropy of the magnetic interactions. In general there are several sources of magnetic anisotropy: single ion and two ions, the most investigated being single ion anisotropy originating from crystal fields. The two ions anisotropy is often considered to be of minor importance and therefore neglected, *i.e.* an isotropic Heisenberg type of magnetic exchange is assumed, especially for high symmetry compounds where anisotropic exchange constants are partly zero for reason of symmetry.

In the orthorhombic RCu_2 compounds there is evidence that the strong single ion anisotropy [7] alone cannot explain the behavior of the magnetic excitations. The importance of anisotropy in two ions exchange interactions has been investigated in some cubic and hexagonal systems, see *e.g.* the case of TbP [8], RSb [9] and Pr [10]. In Pr and TbP the anisotropy of bilinear exchange could be demonstrated by a splitting of otherwise degenerate excitations, in CeSb this anisotropy results in a soft mode at another position than the ordering wave vector of the system. The latter, outstanding feature was found also in the present investigation on $NdCu_2$ and strongly underlines the presence of anisotropic exchange interactions. There is also another, more quantitative argument for the importance of anisotropic exchange in $NdCu_2$, which due to its length is presented in Appendix A.

After having commented the experimental evidence for anisotropic exchange, the most general bilinear exchange interaction allowed by symmetry will now be discussed.

The RCu_2 compounds crystallize in the $CeCu_2$ structure (space group *Imma*, D_{2h}^{28}), which can be thought of as an orthorhombic distortion of the hexagonal AlB_2 structure [11] (space group P_6mmm, D_{6h}^1, note that $LaCu_2$ crystallizes in this hexagonal structure). The orthorhombic *b* axis corresponds to the hexagonal axis and the *ac* plane to the hexagonal plane. Figure 4 shows the $CeCu_2$ structure in a projection into the *ac* plane, so that this correspondence can be seen clearly.

Table 1 gives the interaction tensor for the most general case of 4 equivalent neighbors (all situated in one *ab* plane) and, in addition to that, 3 more special cases. Any two ions contribution to the exchange can be classified according to the 4 cases in Table 1. *E.g.* for ions separated only in *c* direction the exchange is diagonal (this follows from the mirror symmetry of the *ac* and *bc* planes). For all other types of neighbors exchange with off diagonal elements is allowed by the orthorhombic symmetry.

In the following calculation all off-diagonal terms in the exchange will be neglected. This results in short analytical expressions for the magnetic excitation energies, but it must be kept in mind, that this approach might be too simple when comparing the calculation with the experiment.

In addition to this simplification a further restriction is used in the fitting of the exchange parameters

Table 1. General bilinear magnetic interaction tensors between Nd^{3+} ions in $NdCu_2$.

exchange tensor $\bar{\bar{\mathcal{J}}}(ij)$	distance $\mathbf{R}_i - \mathbf{R}_j$
$\begin{pmatrix} \mathcal{J}^{aa} & \mathcal{J}^{ab} & \mathcal{J}^{ac} \\ \mathcal{J}^{ba} & \mathcal{J}^{bb} & \mathcal{J}^{bc} \\ \mathcal{J}^{ca} & \mathcal{J}^{cb} & \mathcal{J}^{cc} \end{pmatrix}, \begin{pmatrix} \mathcal{J}^{aa} & -\mathcal{J}^{ab} & -\mathcal{J}^{ac} \\ -\mathcal{J}^{ba} & \mathcal{J}^{bb} & \mathcal{J}^{bc} \\ -\mathcal{J}^{ca} & \mathcal{J}^{cb} & \mathcal{J}^{cc} \end{pmatrix}$	$\begin{pmatrix} R^a \\ R^b \\ R^c \end{pmatrix}, \begin{pmatrix} -R^a \\ R^b \\ R^c \end{pmatrix}$
$\begin{pmatrix} \mathcal{J}^{aa} & \mathcal{J}^{ab} & -\mathcal{J}^{ac} \\ \mathcal{J}^{ba} & \mathcal{J}^{bb} & -\mathcal{J}^{bc} \\ -\mathcal{J}^{ca} & -\mathcal{J}^{cb} & \mathcal{J}^{cc} \end{pmatrix}, \begin{pmatrix} \mathcal{J}^{aa} & -\mathcal{J}^{ab} & \mathcal{J}^{ac} \\ -\mathcal{J}^{ba} & \mathcal{J}^{bb} & -\mathcal{J}^{bc} \\ \mathcal{J}^{ca} & -\mathcal{J}^{cb} & \mathcal{J}^{cc} \end{pmatrix}$	$\begin{pmatrix} -R^a \\ -R^b \\ R^c \end{pmatrix}, \begin{pmatrix} R^a \\ -R^b \\ R^c \end{pmatrix}$
$\begin{pmatrix} \mathcal{J}^{aa} & 0 & \mathcal{J}^{ac} \\ 0 & \mathcal{J}^{bb} & 0 \\ \mathcal{J}^{ca} & 0 & \mathcal{J}^{cc} \end{pmatrix}, \begin{pmatrix} \mathcal{J}^{aa} & 0 & -\mathcal{J}^{ac} \\ 0 & \mathcal{J}^{bb} & 0 \\ -\mathcal{J}^{ca} & 0 & \mathcal{J}^{cc} \end{pmatrix}$	$\begin{pmatrix} R^a \\ 0 \\ R^c \end{pmatrix}, \begin{pmatrix} -R^a \\ 0 \\ R^c \end{pmatrix}$
$\begin{pmatrix} \mathcal{J}^{aa} & 0 & 0 \\ 0 & \mathcal{J}^{bb} & \mathcal{J}^{bc} \\ 0 & \mathcal{J}^{cb} & \mathcal{J}^{cc} \end{pmatrix}, \begin{pmatrix} \mathcal{J}^{aa} & 0 & 0 \\ 0 & \mathcal{J}^{bb} & -\mathcal{J}^{bc} \\ 0 & -\mathcal{J}^{cb} & \mathcal{J}^{cc} \end{pmatrix}$	$\begin{pmatrix} 0 \\ R^b \\ R^c \end{pmatrix}, \begin{pmatrix} 0 \\ -R^b \\ R^c \end{pmatrix}$
$\begin{pmatrix} \mathcal{J}^{aa} & 0 & 0 \\ 0 & \mathcal{J}^{bb} & 0 \\ 0 & 0 & \mathcal{J}^{cc} \end{pmatrix}$	$\begin{pmatrix} 0 \\ 0 \\ R^c \end{pmatrix}$

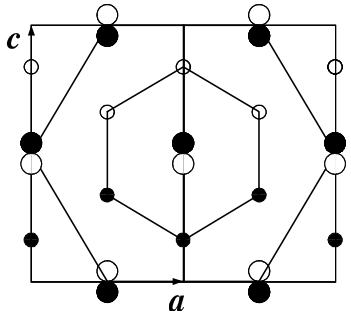

Fig. 4. Structure of $NdCu_2$ projected into the ac plane. The correspondence of the orthorhombic $CeCu_2$ structure to the hexagonal AlB_2 structure is indicated. The big circles indicate the Nd atoms at $y_{Nd} = 0.25$ (filled) and $y_{Nd} = 0.75$ (open), the small circles indicate the Cu atoms at $y_{Cu} = 0.0511$ and 0.4489 (filled) and $y_{Cu} = 0.5511$,0.9489 (open).

to the experimental data. It is assumed that the magnetic exchange constants "do not see" the orthorhombic distortion of the hexagonal lattice (compare Fig. 4) and in addition the exchange is isotropic for magnetic moments in the ac plane (*i.e.* $\mathcal{J}^{aa} = \mathcal{J}^{cc}$, $\mathcal{J}^{ac} = 0$). This assumption is asserted also by the analysis of other RCu_2 compounds, for instance $DyCu_2$. A high magnetic field along the c direction of $DyCu_2$ leads to a big hysteresis with a sudden increase of the saturation moment to the value of 8.5 $\mu_B/f.u.$ [12]. Afterwards the magnetic and magneto elastic behavior of the c axis resembles closely that of the original a axis (and *vice versa*). Therefore this behavior is called "conversion of the easy axis from a to c". The magnetic phase diagram after this axis conversion has been studied in detail for fields along c [13] and agrees in all details (within 0.5 K and 0.1 T) with that of the original a axis. Preliminary neutron scattering experiments in the converted state indicate, that the ordering wave vector does not change after the axis conversion [14]. This experimental evidence underlines the assumption, that in RCu_2 compounds the exchange is isotropic in the ac plane within a few μeV. Another case of interest in this respect is $GdCu_2$: In this compound the magnetic structure is compatible with hexagonal symmetry, it is just the lattice which shows an orthorhombic distortion. However, the lattice becomes more hexagonal at the ordering temperature, as can be seen by the change of the a/c ratio [15]. These results justify the assumption that the exchange is isotropic in the ac plane.

Assuming hexagonal symmetry Figure 5 shows the different types of neighbors. The numbers indicate, which of the exchange constants are related by orthorhombic symmetry only.

Bearing in mind the assumptions about the magnetic exchange the detailed calculation of the low energy magnetic excitations in the field induced ferromagnetic phase of $NdCu_2$ is performed in the mean field (MF)-random phase approximation (RPA). This method has the advantage compared to linearized spin wave theory that it is very easy to introduce the magnetic single ion anisotropy caused by the crystal field [16]. The magnetic anisotropy, both of single ion and two ions type, produces a gap in the excitation spectra.

The starting point of the calculation is the following Hamiltonian, consisting of a single ion and a two ions part:

$$H = \sum_{i,lm} B_l^m O_l^m(\mathbf{J}_i) - g_J \mu_B \sum_i \mathbf{J}_i \mathbf{B} - \frac{1}{2} \sum_{ij} \mathbf{J}_i \bar{\bar{\mathcal{J}}}(ij) \mathbf{J}_j. \quad (1)$$

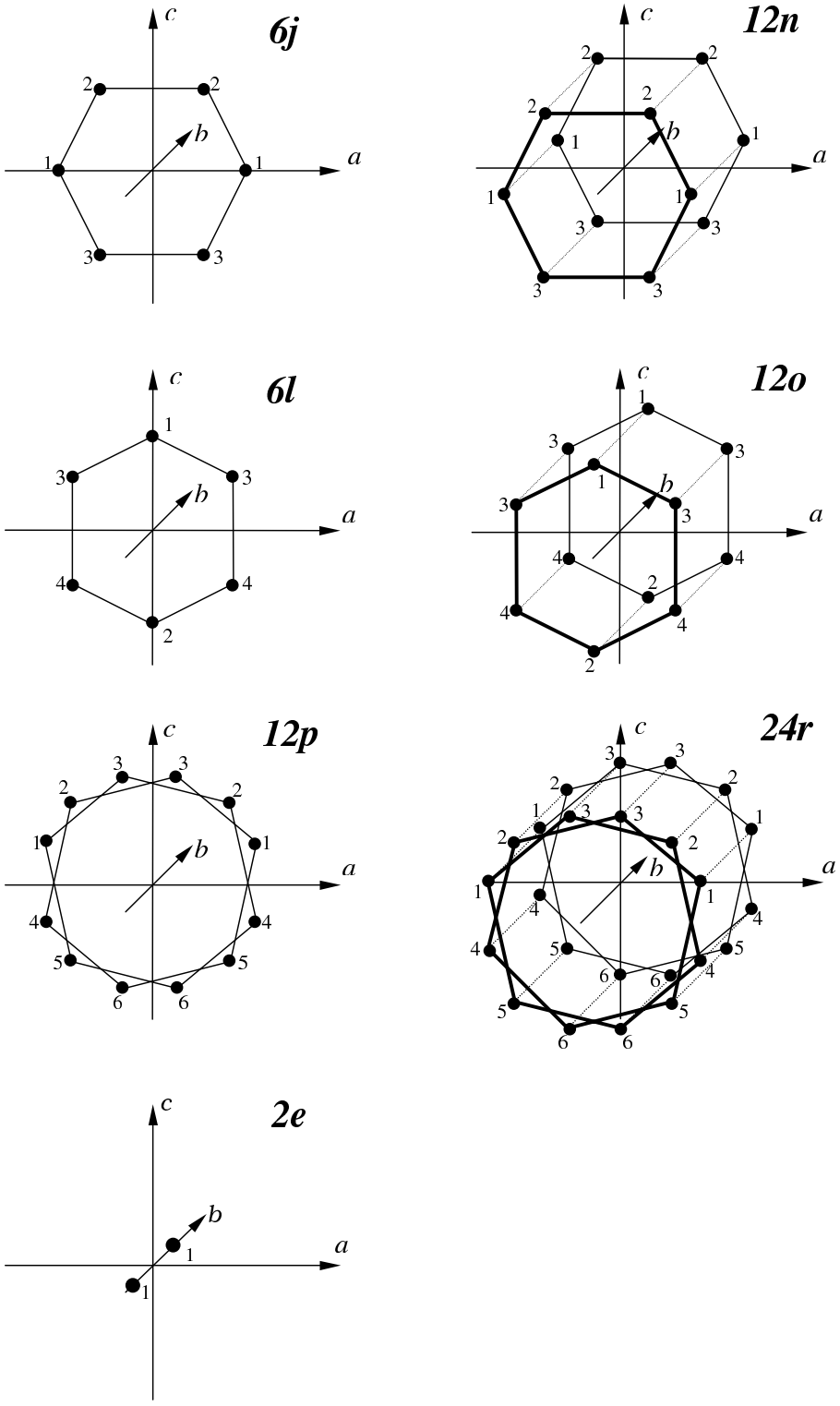

Fig. 5. Different types of bilinear exchange interactions in RCu_2 compounds assuming hexagonal symmetry of the exchange. The numbers indicate which of the exchange constants are related by orthorhombic symmetry only.

$$\bar{\bar{\mathcal{J}}}(\mathbf{Q}) = \begin{pmatrix} \bar{\bar{\mathcal{J}}}_{\mathrm{S}}(\mathbf{Q}) & \bar{\bar{\mathcal{J}}}_{\mathrm{D}}(\mathbf{Q})\exp[\mathrm{i}\mathbf{Q}(\mathbf{r}_1-\mathbf{r}_2)] \\ \bar{\bar{\mathcal{J}}}^{*}_{\mathrm{D}}(\mathbf{Q})\exp[-\mathrm{i}\mathbf{Q}(\mathbf{r}_1-\mathbf{r}_2)] & \bar{\bar{\mathcal{J}}}_{\mathrm{S}}(\mathbf{Q}) \end{pmatrix} \tag{13}$$

$$\bar{\bar{\mathcal{J}}}_{\mathrm{S}}(\mathbf{Q}) = \sum_{j}^{i,j \text{ same sublattice}} \bar{\bar{\mathcal{J}}}(ij)\exp[-\mathrm{i}\mathbf{Q}(\mathbf{R}_i-\mathbf{R}_j)] \tag{14}$$

$$\bar{\bar{\mathcal{J}}}_{\mathrm{D}}(\mathbf{Q}) = \sum_{j}^{i,j \text{ different sublattice}} \bar{\bar{\mathcal{J}}}(ij)\exp[-\mathrm{i}\mathbf{Q}(\mathbf{R}_i-\mathbf{R}_j)]. \tag{15}$$

In this expression the first term describes the crystal field [17], the second the Zeeman energy and the third the anisotropic bilinear exchange. At very low temperatures the magnetic properties may be calculated by considering only the ground state doublet $|\pm\rangle$ of the crystal field split multiplet.

In [4] the crystal field parameters have been estimated to $B_2^0 = 117\ \mu$eV, $B_2^2 = 134\ \mu$eV, $B_4^0 = 1.92\ \mu$eV, $B_4^2 = 0.87\ \mu$eV, $B_4^4 = 1.69\ \mu$eV, $B_6^0 = 0.0476\ \mu$eV, $B_6^2 = 0.0116\ \mu$eV, $B_6^4 = 0.0421\ \mu$eV and $B_6^6 = 0.366\ \mu$eV. The corresponding ground state doublet is given by $|\pm\rangle = -0.0487|\pm 9/2\rangle - 0.891|\mp 7/2\rangle + 0.373|\pm 5/2\rangle + 0.23|\mp 3/2\rangle - 0.111|\pm 1/2\rangle$. However, the following analysis does neither depend on any particular choice of crystal field parameters nor on the form of the ground state.

The Hamiltonian (1) may be projected into the ground state doublet yielding (for external fields B parallel to the b axis, the coordinates are chosen such that $a||x$,$c||y$,$b||z$)

$$\begin{aligned} H = E_0 &- g_{\mathrm{J}}\mu_{\mathrm{B}}\sum_i \begin{pmatrix} M & 0 \\ 0 & -M \end{pmatrix}_i B \\ &- \frac{1}{2}\sum_{ij} \begin{pmatrix} 0 & A \\ A & 0 \end{pmatrix}_i \mathcal{J}^{aa}(ij) \begin{pmatrix} 0 & A \\ A & 0 \end{pmatrix}_j \\ &- \frac{1}{2}\sum_{ij} \begin{pmatrix} M & 0 \\ 0 & -M \end{pmatrix}_i \mathcal{J}^{bb}(ij) \begin{pmatrix} M & 0 \\ 0 & -M \end{pmatrix}_j \\ &- \frac{1}{2}\sum_{ij} \begin{pmatrix} 0 & C \\ -C & 0 \end{pmatrix}_i \mathcal{J}^{cc}(ij) \begin{pmatrix} 0 & C \\ -C & 0 \end{pmatrix}_j \end{aligned} \tag{2}$$

$$A = \langle +|J^a|-\rangle \qquad A^* = A \tag{3}$$

$$\pm M = \langle \pm|J^b|\pm\rangle \qquad M^* = M \tag{4}$$

$$C = \langle +|J^c|-\rangle \qquad C^* = -C. \tag{5}$$

A mean field (MF) is introduced and the splitting of the ground state $\Delta = E_- - E_+$ is calculated selfconsistently according to the following relations (taking into account interdoublet mixing to second order in B^{eff} as described in [3] Eqs. (8, 9)).

$$B^{\mathrm{eff}} = B + \frac{1}{g_{\mathrm{J}}\mu_{\mathrm{B}}}\mathcal{J}^{bb}(\mathbf{q}=0)\langle J^b\rangle \tag{6}$$

with the thermal expectation value defined as

$$\langle J^b\rangle = M^+ n_+ + M^- n_- \tag{7}$$

$$M^{\pm} = \pm M(1 \pm \alpha B^{\mathrm{eff}}) \tag{8}$$

$$E_\pm - E_0 = \mp g_{\mathrm{J}}\mu_{\mathrm{B}} M(1 \pm \alpha B^{\mathrm{eff}}/2)B^{\mathrm{eff}} \tag{9}$$

$$n_\pm = \frac{\exp(-E_\pm/k_{\mathrm{B}}T)}{\exp(-E_+/k_{\mathrm{B}}T) + \exp(-E_-/k_{\mathrm{B}}T)}\,. \tag{10}$$

In this expression $n_\pm$ are the thermal population numbers of the two states $|\pm\rangle$ split by the effective field B^{eff}. The Fourier transform of the exchange tensor $\bar{\bar{\mathcal{J}}}(ij)$ (*i.e.* $\mathcal{J}^{bb}(\mathbf{q}=0)$) is defined in equation (A.3).

The frequency dependent single ion susceptibility $\bar{\bar{\chi}}_0(\omega)$ can be calculated for the MF ground state doublet

$$\bar{\bar{\chi}}_0(\omega) = \begin{pmatrix} \frac{nA^2\Delta}{\Delta^2-\hbar^2\omega^2} & 0 & \frac{nAC\hbar\omega}{\Delta^2-\hbar^2\omega^2} \\ 0 & \chi_0^{bb} & 0 \\ -\frac{nAC\hbar\omega}{\Delta^2-\hbar^2\omega^2} & 0 & -\frac{nC^2\Delta}{\Delta^2-\hbar^2\omega^2} \end{pmatrix} \tag{11}$$

with the abbreviation $n = 2(n_- - n_+) \stackrel{T\to 0}{\longrightarrow} 2$. χ_0^{bb} is zero for $\omega \neq 0$ and will therefore be neglected in the following calculation.

A first estimate for the order of the excitation energies are the singularities of this single ion susceptibility (*i.e.* at $\hbar\omega = \Delta$). To describe the dispersion correctly the two-atomic basis in this compound is taken into account and RPA is performed (compare [16]) to calculate the susceptibility $\bar{\bar{\chi}}(\mathbf{Q},\omega)$

$$\bar{\bar{\chi}}(\mathbf{Q},\omega) = \left[\begin{pmatrix} \bar{\bar{\chi}}_0(\omega) & 0 \\ 0 & \bar{\bar{\chi}}_0(\omega) \end{pmatrix}^{-1} - \bar{\bar{\mathcal{J}}}(\mathbf{Q})\right]^{-1}. \tag{12}$$

This is an equation of 6×6 matrices (for each of the Nd atoms in the basis of the crystal there is a single ion excitation matrix). The Fourier transform of the coupling is given by

see equations (13, 14, 15) above.

In this expression the $\mathbf{R}_i$ are the position vectors of the Nd^{3+} ions, $(\mathbf{r}_1 - \mathbf{r}_2)$ designates the position of one Nd sublattice with respect to the other Nd sublattice. According to the fluctuation dissipation theorem (see [16])

the neutron cross-section is then given by summing over the components of $\overline{\overline{\chi}}''(\mathbf{Q},\omega) = (\overline{\overline{\chi}}(\mathbf{Q},\omega) - \overline{\overline{\chi}}^{\dagger}(\mathbf{Q},\omega))/2\mathrm{i}$

$$\frac{\mathrm{d}\sigma}{\mathrm{d}E'\mathrm{d}\Omega} = \frac{K}{1-\exp(-\hbar\omega/k_\mathrm{B}T)} \sum_{\substack{\alpha\beta\ldots \text{ spatial indices} \\ ss'\ldots \text{ sublattice indices}}} \times \chi''_{\substack{\alpha\beta \\ ss'}}(\mathbf{Q},\omega)\exp[-\mathrm{i}\mathbf{Q}(\mathbf{r}_s - \mathbf{r}_{s'})](\delta_{\alpha\beta} - \hat{Q}_\alpha\hat{Q}_\beta)$$

$$K = \frac{k_\mathrm{f}}{k_\mathrm{i}} N \frac{1}{\pi}\left(\frac{\hbar\gamma e^2}{mc^2}\right)^2 \left\{\frac{1}{2} g_\mathrm{J} F(Q)\right\}^2. \quad (16)$$

In this expression k_i and k_f denote the wave vector of the incoming and of the scattered neutron, respectively, $F(Q)$ is the magnetic form factor of Nd^{3+} in the dipole approximation, N the number of scattering Nd atoms, $\gamma = g_\mathrm{n}/2\hbar$ the gyromagnetic ratio of the neutron and $e^2/mc^2 = 2.82$ fm is the classical electron radius.

The excitation energies can be calculated by analyzing the poles of this cross-section. If the exchange is assumed to be isotropic in the ac plane, $\overline{\overline{\mathcal{J}}}_\mathrm{S}(\mathbf{Q})$ and $\overline{\overline{\mathcal{J}}}_\mathrm{D}(\mathbf{Q})$ are diagonal and the aa and cc components are equal. Using the notation $\mathcal{J}_\mathrm{D}(\mathbf{Q}) = \mathcal{J}_\mathrm{D}^{aa}(\mathbf{Q}) = \mathcal{J}_\mathrm{D}^{cc}(\mathbf{Q})$, $\mathcal{J}_\mathrm{S}(\mathbf{Q}) = \mathcal{J}_\mathrm{S}^{aa}(\mathbf{Q}) = \mathcal{J}_\mathrm{S}^{cc}(\mathbf{Q})$ (but still assuming that $\mathcal{J}_\mathrm{S}^{aa}(\mathbf{Q}) \neq \mathcal{J}_\mathrm{S}^{bb}(\mathbf{Q})$ and $\mathcal{J}_\mathrm{D}^{aa}(\mathbf{Q}) \neq \mathcal{J}_\mathrm{D}^{bb}(\mathbf{Q})$) it is possible to derive an analytical expression for the cross-section of the magnetic excitations by combining equations (11–16):

$$\frac{\mathrm{d}\sigma}{\mathrm{d}E'\mathrm{d}\Omega} = \frac{2Kn}{1-\exp(-\hbar\omega/k_\mathrm{B}T)} \Im\left(\frac{f\hbar^2\omega^2 + g}{\hbar^4(\omega_1^2-\omega^2)(\omega_2^2-\omega^2)}\right)$$

$$f = (1-\hat{Q}_a^2)A^2(\Re(v)-s) - C^2(1-\hat{Q}_c^2)(\Re(u)-r)$$

$$g = (1-\hat{Q}_a^2)A^2(s^2 - v^\star v)[r + \Re(u)] - (1-\hat{Q}_c^2)C^2(r^2 - u^\star u)[s + \Re(v)]$$

$$r = \Delta - nA^2\mathcal{J}_\mathrm{S}(\mathbf{Q})$$

$$s = \Delta + nC^2\mathcal{J}_\mathrm{S}(\mathbf{Q})$$

$$u = nA^2\mathcal{J}_\mathrm{D}(\mathbf{Q})$$

$$v = -nC^2\mathcal{J}_\mathrm{D}(\mathbf{Q}). \quad (17)$$

In this expression $\Re$ and $\Im$ denote real and imaginary parts. The excitation energies $\hbar\omega_1$ and $\hbar\omega_2$ are given by

$$[\hbar\omega_{\frac{1}{2}}]^2 = \{\Delta - nA^2[\mathcal{J}_\mathrm{S}(\mathbf{Q}) \mp |\mathcal{J}_\mathrm{D}(\mathbf{Q})|]\} \times \{\Delta + nC^2[\mathcal{J}_\mathrm{S}(\mathbf{Q}) \mp |\mathcal{J}_\mathrm{D}(\mathbf{Q})|]\}. \quad (18)$$

The corresponding intensities I_1 and I_2 can be calculated from the residua of equation (17) – note that any factors arising from the scattering geometry of a triple axis spectrometer are not included in the following expression:

$$I_{\frac{1}{2}} = \frac{Kn}{2\hbar\omega_{\frac{1}{2}}(1-\exp(-\hbar\omega_{\frac{1}{2}}/k_\mathrm{B}T))}\left(1 \mp \frac{\Re[\mathcal{J}_\mathrm{D}(\mathbf{Q})]}{|\mathcal{J}_\mathrm{D}(\mathbf{Q})|}\right) \times \{(1-\hat{Q}_a^2)A^2(s \pm |v|) - (1-\hat{Q}_c^2)C^2(r \pm |u|)\}. \quad (19)$$

Note that $\mathcal{J}_\mathrm{S}(\mathbf{Q})$ and $\mathcal{J}_\mathrm{D}(\mathbf{Q})$ transform under a translation about $(1\ \ 1\ \ 0)$ as $\mathcal{J}_\mathrm{S}(\mathbf{Q} + (1\,1\,0)) = \mathcal{J}_\mathrm{S}(\mathbf{Q})$ and $\mathcal{J}_\mathrm{D}(\mathbf{Q} + (1\,1\,0)) = -\mathcal{J}_\mathrm{D}(\mathbf{Q})$. Inserting this property into equations (18, 19) one finds, that $\hbar\omega_1(\mathbf{Q} + (1\,1\,0)) = \hbar\omega_1(\mathbf{Q})$ and $\hbar\omega_2(\mathbf{Q} + (1\,1\,0)) = \hbar\omega_2(\mathbf{Q})$. Neglecting the $\mathbf{Q}$ dependence of K for the moment (which is small due to the magnetic form factor), we see, that the intensities of the two excitations are exchanged by this translation, *i.e.* $I_1(\mathbf{Q} + (1\,1\,0)) = I_2(\mathbf{Q})$ and $I_2(\mathbf{Q} + (1\,1\,0)) = I_1(\mathbf{Q})$.

If neutron experiments are performed in the reciprocal ab plane, $\mathcal{J}_\mathrm{D}(\mathbf{Q})$ is real and according to equation (19) either $I_1(\mathbf{Q})$ or $I_2(\mathbf{Q})$ is zero. Only one excitation can be observed for a given wave vector $\mathbf{Q}$, the other branch can be measured at $\mathbf{Q} + (1\,1\,0)$.

However, such favorable experimental conditions can be used only to measure the dispersion for $l = 0$. For $l \neq 0$ the calculation always predicts two excitations.

5 Numerical analysis of the magnetic excitations in $NdCu_2$

For the transition matrix elements A and C defined in equation (3) the values $A = 2.00$ and $C = i1.6$ have been used. This is in reasonable agreement with the values deduced from magnetization at 8 K [7] (*i.e.* $A = 2.1$, $C = i1.5$) and those derived from the published crystal field parameters [4] (*i.e.* $A = 2.0$, $C = i1.5$). Scaling of both of these parameters scales the amplitude of the dispersion. Changing the relation of the values of A to C affects the form of the dispersion: the steepness of the low energy modes is increased while the high energy modes become flatter if A and C become very different (see Eq. (18)).

For the determination of Δ and B^eff the following parameters have been used in equations (2–10): $M = 2.27$, $\alpha = 0.03\ \mathrm{T}^{-1}$ and $\mathcal{J}^{bb}(\mathbf{q} = 0) = 24.6\ \mu$eV (*i.e.* the same as in [3]). Solving equations (2–10) selfconsistently with respect to Δ and B^eff for $B = 3T$ gives $\Delta = 0.861$ meV and $B^\mathrm{eff} = 4.50$ T.

Using the above value for Δ, only an insufficient fit of the observed dispersion could be achieved. To improve the fit, Δ was varied (yielding $\Delta = 1.106$ meV) and the standard deviation (described below by Eq. (20)) could be reduced to 20% of its former value. This indicates, that the value of Δ derived from the study of the magnetic phase diagram [3] at 3 T external field is too low, suggesting that $\mathcal{J}^{bb}(q = 0)$ has to be modified. A consistent description can be obtained with $\mathcal{J}^{bb}(q = 0) = 44\ \mu$eV, $B^\mathrm{eff} = 5.78$ T and $\Delta = 1.106$ meV. The new value for $\mathcal{J}^{bb}(q = 0)$ can be used as an input for refining the calculation of the exchange parameters $\mathcal{J}^{bb}(ij)$ describing the magnetic phase diagram (compare [3]).

The exchange parameters $\mathcal{J}^{aa}(ij) = \mathcal{J}^{cc}(ij)$ have been obtained by performing a least square fit of the calculated to the measured dispersion using a simulated annealing algorithm [18]. The following expression was minimized ($E_1(\mathbf{Q})$ and $E_2(\mathbf{Q})$ denote the measured modes, $s_1(\mathbf{Q})$ and $s_2(\mathbf{Q})$ some statistical weighting factors and

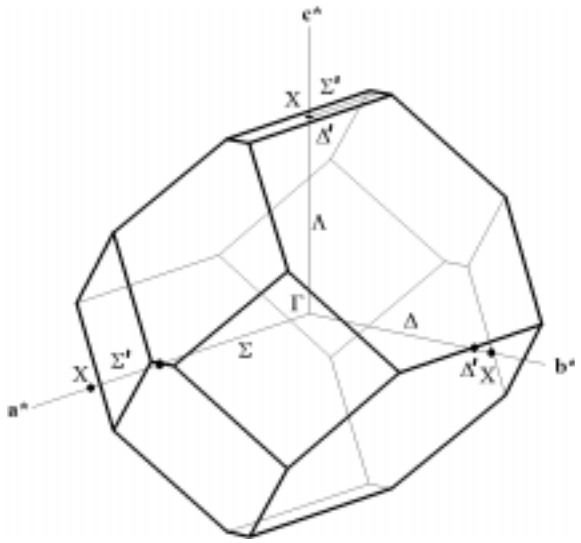

Fig. 6. First Brillouin zone of $NdCu_2$, the Γ–point, the X–point and the main symmetry directions are indicated.

$\Theta(x)$ the step function):

$$\sum_{\mathbf{Q}\in\{\text{measured constant Q-scans}\}} s_1(\mathbf{Q})[\hbar\omega_1(\mathbf{Q}) - E_1(\mathbf{Q})]^2 + s_2(\mathbf{Q})[\hbar\omega_2(\mathbf{Q}) - E_2(\mathbf{Q})]^2 + \sum_{\substack{i=1,2,\mathbf{Q}\in\{\text{1st Brillouin zone}\} \\ |\mathbf{Q}-(0.65\,1\,0)|>0.15\ \text{Å}^{-1}}} \Theta(0.73\ \text{meV} - \hbar\omega_i(\mathbf{Q})) \times \frac{1+\Theta(0.63\ \text{meV} - \hbar\omega_i(\mathbf{Q}))}{2}[\hbar\omega_i(\mathbf{Q}) - 0.73\ \text{meV}]^2. \quad (20)$$

The second sum in equation (20) ensures, that the minimum of the dispersion relation at $\mathbf{q} = (0.65\,1\,0)$ is a global minimum. In this sum only $\mathbf{q}$ vectors in the first Brillouin zone with positive h, k and l have been considered, because the excitation energies in the other parts of the zone are related by symmetry (compare Eq. (18)). The error in the fitted exchange parameters was estimated from the experimental error in the measurement. Assuming an average experimental error of 0.15 meV leads to a variation of (20) by about 0.14 meV^2. This variation corresponds to a variation of the fitting parameters within the range of the error bars shown in Figure 8. Note that an error estimation obtained in this way does not take into account the fact, that there might be several isolated solutions in other regions of the parameter space. Figure 6 shows the first Brillouin zone and the main symmetry directions of the reciprocal lattice. The primed letters denote the extension of a symmetry line from the zone boundary to the X–point. Note that for the related hexagonal lattice the Brillouin zone would have the shape of a simple honeycomb with $\Sigma'/\Sigma = 1/2$.

Using a set of fitted parameters and formula (18) the excitation energies have been calculated. Figure 7 shows, how the calculated excitation energies compare to the experimental data. The dispersion along Λ shows a fast oscillation with $\mathbf{q}$ indicating the long range of the exchange. It was necessary to include the neighbor $\mathbf{r} = (0, 0, 2c)$ (distance: 15 Å) into the model to explain this oscillating behavior (or alternatively assume non hexagonal exchange resulting in a model with even more parameters and different signs of parameters which in hexagonal description should be equal). This high frequency in Fourier space was also observed in the magnetic excitations of $PrCu_2$ [19]. In Σ direction the position of the minimum in the dispersion and the mode crossing are in excellent agreement with the available experimental data. Also the two weakly dispersive modes along Δ compare well to the calculation.

In addition to the peak positions which are shown in Figure 7, the intensities have been evaluated and compared to the calculation (19). The contribution of the polarization factors $(1 - \hat{Q}_a^2)$ and $(1 - \hat{Q}_c^2)$ dominates and results in strong intensities for $\mathbf{Q} \parallel b$. The relative intensity of the two modes is correctly described by the model. For instance along the $(h\ \ 0\ \ 1)$ direction the intensity of the dispersive mode is only 10 percent of the intensity of the other mode. Along $(h\ \ 0\ \ 2)$ both modes have about the same intensity (difference less than 30 percent – compare the experimental data in Fig. 2). A calculation assuming hexagonal symmetry of the structure gives only one excitation. Comparing such a calculation to the experiment showed, that whenever two excitations are observed, the weaker excitation (*i.e.* the upper mode along $(0\ \ 0\ \ l)$ and the strongly dispersive mode along $(h\ \ 0\ \ 1)$ and $(h\ \ 0\ \ 2)$) is expected to disappear in hexagonal symmetry.

More accurate experimental data would be needed for a comparison of small details in the variation of the intensity, which are due to the oscillations in $\mathcal{J}_S(\mathbf{Q})$ and $\mathcal{J}_D(\mathbf{Q})$.

Figure 8 shows the dependence of the fitted exchange constants $\mathcal{J}^{aa} = \mathcal{J}^{cc}$ on the interatomic distance. The different types of neighbors are indicated by different symbols. Because of the orthorhombic distortion of the lattice the distance varies within some sets of exchange constants, which have been kept equal in the fit process because of the nearly hexagonal symmetry. The exchange constants of type $2e$, indicated by the filled triangles in Figure 8 appear rather large. If these constants are set to a smaller value, the quality of the fit deteriorates dramatically. The large contribution might be connected with the fact, that the parameters of type $2e$ describe the exchange between Nd^{3+} ions situated in a zig zag chain in b direction with very short distance, whereas for all other types of interactions one or more Cu atoms are situated in or near the connecting line. The dashed line in Figure 8 represents the magnitude of the classical dipole – dipole interaction, the solid line

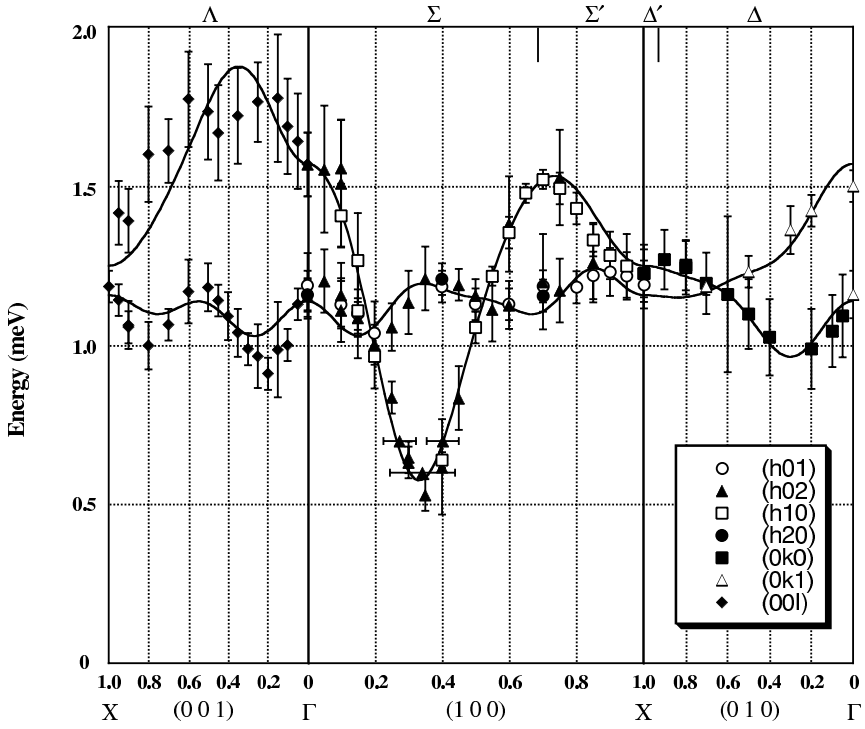

Fig. 7. **Q**-dependence of the magnetic excitations in the field induced ferromagnetic phase of $NdCu_2$ at $\mu_0 H \parallel b = 3$ T, the lines show the dispersion as calculated by the MF-RPA model described in the text.

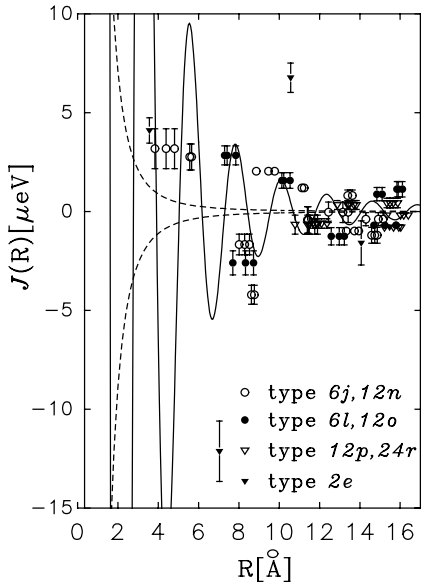

Fig. 8. Dependence of the fitted exchange constants on the interatomic distance. The different types of neighbors are indicated by different symbols. The full lines show the indirect exchange interaction as given by a free electron model described in the text. The dashed lines show the magnitude of the classical dipolar exchange (*i.e.* $+2(g_J\mu_B)^2/R^3$ and $-5(g_J\mu_B)^2/2R^3$).

shows the indirect exchange interaction as given by a free electron model [16]. The corresponding formulas are

$$\mathcal{J}^{\alpha\beta}(ij) = (g_J\mu_B)^2 \frac{3(R_i^\alpha - R_j^\alpha)(R_i^\beta - R_j^\beta) - |\mathbf{R}_i - \mathbf{R}_j|^2}{|\mathbf{R}_i - \mathbf{R}_j|^5} \tag{21}$$

for the classical dipole exchange and

$$\mathcal{J}^{\alpha\beta}(ij) = \delta_{\alpha\beta} 12\pi\nu |j_0|^2 \bar{\mathcal{N}}(\tilde{\epsilon}_F) \times \frac{\sin(2k_F|\mathbf{R}_i - \mathbf{R}_j|) - 2k_F|\mathbf{R}_i - \mathbf{R}_j|\cos(2k_F|\mathbf{R}_i - \mathbf{R}_j|)}{2k_F|\mathbf{R}_i - \mathbf{R}_j|^4} \tag{22}$$

for the indirect exchange interaction in a simple isotropic model (RKKY) [16]. In the above expression ν denotes the number of conduction electrons/f.u. (*i.e.* $\nu = 5 = 3[\mathrm{Nd}] + 2 \times 1[\mathrm{Cu}]$), j_0 the effective *s*-*f* exchange integral (*i.e.* $j_0 \sim (g_J - 1)0.1$ eV), $k_F = 1.395$ Å^{-1} the Fermi wave vector in a free electron model [20] and $\bar{\mathcal{N}}(\tilde{\epsilon}_F)$ the density of electronic states/f.u. (*i.e.* ~ 2.8 eV^{-1}; this value corresponds to the specific heat γ–value in YCu_2 of 6.7 mJ/mol K^2). To compare with the experimentally determined exchange constants the indirect exchange (RKKY) had to be scaled by a factor 0.06.

The classical dipolar exchange is comparable to the indirect RKKY exchange only for neighbors up to 6 Å, especially for next neighbors in the quasi – hexagonal *ac* plane. It is obviously non diagonal (this fact is neglected in the present analysis of the magnetic excitations) and therefore might drive the formation of the noncollinear magnetic structure observed in $GdCu_2$ [15].

Figure 9 shows the Fourier transform of the exchange interaction constants $\mathcal{J}^{bb}(\mathbf{Q})$ (as determined by the magnetic phase diagram [3], compare equation (A.3)) and $\mathcal{J}^{aa}(\mathbf{Q}) = \mathcal{J}^{cc}(\mathbf{Q}) = \mathcal{J}_S(\mathbf{Q}) + \mathcal{J}_D(\mathbf{Q})$ (as determined by the magnetic excitations in the field induced ferromagnetic phase F3). The difference of the dashed and full line

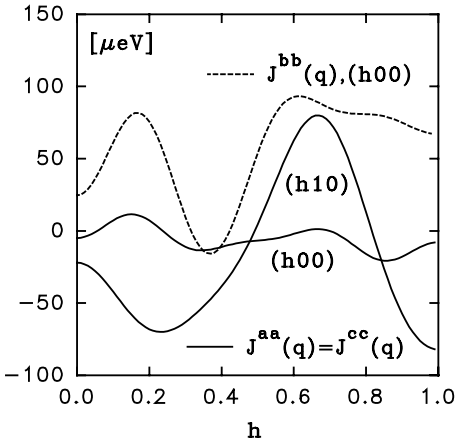

Fig. 9. Fourier transform of the fitted exchange interaction of $NdCu_2$ for moments in the quasi – hexagonal plane ($\mathcal{J}^{aa}(\mathbf{Q}) = \mathcal{J}^{cc}(\mathbf{Q})$) and for moments in b direction ($\mathcal{J}^{bb}(\mathbf{Q})$). Note that the curve of $\mathcal{J}^{bb}(\mathbf{Q})$ has been taken from the parameters used to describe the phase diagram in [3] and should be modified at $Q = 0$ according to the present analysis discussed in the text.

in (h 0 0) direction is a measure of the anisotropy of the exchange. The wavelength of the oscillations with $\mathbf{q}$ is inversely related to the range of the exchange interactions, indicating the importance of distant neighbor interactions in $NdCu_2$.

6 Magnetic order in other RCu_2 compounds

Having analyzed the exchange in such detail for $NdCu_2$ one question is obvious: Is it possible to interpret the ordering process of other RCu_2 compounds (R = Ce, Pr, Sm, Gd, Tb, Dy, Ho, Er, Tm) on the basis of these parameters?

The exchange parameters given in Figure 8 can be used to make a prediction for the ordering temperature and the magnetic structure of some other RCu_2 compounds on the basis of a MF theory. For simplicity we assume, that the CF anisotropy of the rare earth moments can be described by considering an anisotropic two level system (except in the case of Gd, where CF effects can be neglected). The anisotropy of this two level system is estimated by the saturation value of the magnetic moment components $\mu^{\rm sat}_{a,b,c} = g_{\rm J}\mu_{\rm B}M_{a,b,c}$ in the three orthorhombic axes (the corresponding matrix elements of $\mathbf{J}$, *i.e.* $M_{a,b,c}$ have been calculated from the available experimental data and are listed in the third column of Table 2 for some RCu_2 compounds).

To calculate the ordering temperatures for different possible magnetic structures the two ions exchange interactions of the present analysis of $NdCu_2$ are used. Assuming an indirect exchange interaction, $\overline{\overline{\mathcal{J}}}_{\rm Spin}(\mathbf{q})$ should be comparable among the different rare earths [16]. $\overline{\overline{\mathcal{J}}}_{\rm Spin}(\mathbf{q})$ is defined by

$$\overline{\overline{\mathcal{J}}}(\mathbf{q}) \equiv (g_{\rm J}-1)^2\ \overline{\overline{\mathcal{J}}}_{\rm Spin}(\mathbf{q}). \qquad (23)$$

Next we calculate the maximum of the Fourier transform of the exchange interaction $\mathcal{J}^{bb}(\mathbf{Q})$ and $\mathcal{J}^{aa}(\mathbf{Q}) = \mathcal{J}^{cc}(\mathbf{Q})$.

For $\mathcal{J}^{aa}(\mathbf{Q}) = \mathcal{J}^{cc}(\mathbf{Q})$ the maximum of the exchange corresponds to the minimum of the dispersion in $NdCu_2$ at $\mathbf{Q} \sim (2/3\,1\,0)$. From the present analysis of the magnetic excitations we find $\mathcal{J}^{aa}(\mathbf{Q} = (2/3\,1\,0)) = 79\ \mu$eV (using the parameters shown in Fig. 8). This value is scaled according to equation (23) for other RCu_2 compounds and listed in column 4 of Table 2. The maximum of $\mathcal{J}^{bb}(\mathbf{Q})$ will be at about $\mathbf{Q} \sim (2/3\,0\,0)$, corresponding to the type of magnetic order found in $NdCu_2$. From the Néel temperature $T_{\rm N} = 6.5$ K we estimate $\mathcal{J}^{bb}(\mathbf{Q} = (2/3\,0\,0)) = 93\ \mu$eV (see Fig. 9, [3]). Also this value is scaled according to equation (23) and listed in column 4 of Table 2 for other RCu_2 compounds.

With this input it is now possible to calculate ordering temperatures for moments in a or c direction

$$k_{\rm B}T^a_{\rm N} = M_a^2\mathcal{J}^{aa}(\mathbf{Q} = (2/3\,1\,0)) \qquad (24)$$

$$k_{\rm B}T^c_{\rm N} = M_c^2\mathcal{J}^{cc}(\mathbf{Q} = (2/3\,1\,0)) \qquad (25)$$

and for moments in b direction

$$k_{\rm B}T^b_{\rm N} = M_b^2\mathcal{J}^{bb}(\mathbf{Q} = (2/3\,0\,0)). \qquad (26)$$

Note that the ordering wave vector $\mathbf{Q}$ is different for magnetic moments within the ac plane and parallel to the b direction due to the different position of the maximum in $\mathcal{J}^{aa}(\mathbf{Q}) = \mathcal{J}^{cc}(\mathbf{Q})$ and $\mathcal{J}^{bb}(\mathbf{Q})$, respectively. Equations (24–26) are valid also for negligible CF anisotropy (*i.e.* $M_a \sim M_b \sim M_c$) and can be used to calculate the ordering temperatures $T^\alpha_{\rm N}$ for the two types of modulation. Naturally, only the largest value for the ordering temperature will be of physical relevance (compare [16]).

In Table 2 the calculated ordering temperatures for the different moment directions and ordering wave vectors are compared to experimental data. The calculation of the ordering temperature was performed according to equations (24–26), except for the case of Gd, where the CF splitting is negligible. For Gd the well-known formula $3k_{\rm B}T^\alpha_{\rm N} = J(J+1)\mathcal{J}^{\alpha\alpha}(\mathbf{Q})$ was used.

Of course, from such simple modeling a complete explanation of all details cannot be expected. However, in most cases the calculation is in reasonable agreement with available experimental data.

Whenever $T^a_{\rm N}$ or $T^c_{\rm N}$ show the largest value, the predicted magnetic modulation vector $\mathbf{Q}$ is equal to (2/3 1 0) (*e.g.* for $TbCu_2$ and $DyCu_2$ – see Tab. 2). For the compounds where $T^b_{\rm N}$ has been calculated to be larger than $T^a_{\rm N}$ and $T^c_{\rm N}$, $\mathbf{Q} \sim (2/3\,0\,0)$ is the predicted modulation vector. In most cases this is true.

It is of interest to compare the exchange parameters used in this paper to those obtained by Iwata *et al.* [21] for $TbCu_2$ and $DyCu_2$: In Table 3 the reduced exchange parameters of $TbCu_2$ and $DyCu_2$, which have been defined in [21], are compared to those calculated from our set for $NdCu_2$ (shown in Fig. 8).

Table 2. Calculated and experimentally observed ordering temperatures and wave vectors for some RCu_2 compounds. The saturation moment is estimated from magnetization experiments. It is used to calculate the ordering temperature for different possible magnetic structures (*i.e.* (2/3 1 0) with a or c as the easy axis, (2/3 0 0) with b as the easy axis). If the observed structure does not agree with the calculated one it is marked by a "≠".

	J	g_J	$M_a = A$ $M_b = M$ $M_c = C/i$	$\mathcal{J}^{aa}(2/3\,1\,0)$ $\mathcal{J}^{bb}(2/3\,0\,0)$ $\mathcal{J}^{cc}(2/3\,1\,0)$ [μeV]	T_N^a T_N^b T_N^c [K]	T_N^{exp}[K]	τ^{exp}
$CeCu_2$	$\frac{5}{2}$	$\frac{6}{7}$	1.9 0.6 [30] 1.3	21.7 25.5 21.7	**0.9** ≠ 0.1 0.4	3.5 [31]	$(1\,1\,0)$[2]
$PrCu_2$	4	$\frac{4}{5}$	1.9 0.9 [32] 0.4	42.5 50.0 42.5	**1.8** 0.5 0.08	[33][3]	-
$NdCu_2$	$\frac{9}{2}$	$\frac{8}{11}$	2.0 2.5 [7] 1.6	79 93 79	3.7 **6.7** 2.3	6.5 [2]	(0.618 0 0)
$SmCu_2$	$\frac{5}{2}$	$\frac{2}{7}$	0.1 0.3 [34] ?	542 638 542	0.06 **0.67** ?	23 [6]	?
$GdCu_2$	$\frac{7}{2}$	2	-	1062 1250 1062	65 **76** ≠ 65	40 [15]	(2/3 1 0) [15]
$TbCu_2$	6	$\frac{3}{2}$	5.9 0.4 [32] 1.3	266 313 266	**107** 0.6 5.2	54 [25]	(2/3 1 0) [24]
$DyCu_2$	$\frac{15}{2}$	$\frac{4}{3}$	7.4 3.8 [32] 1.9	118 139 118	**75** 23 4.9	27 [13]	(2/3 1 0) [26]
$HoCu_2$	8	$\frac{5}{4}$	6.4 4.6 [32] 2.7	66.4 78.1 66.4	**31.5** 19.2 5.6	10 [25]	(2/3 1 0) [27][4]
$ErCu_2$	$\frac{15}{2}$	$\frac{6}{5}$	0.4 7.1 [32] 0.9	42.5 50.0 42.5	0.08 **29.2** 0.40	12 [25]	(0.615 0 0) [28][5]
$TmCu_2$	6	$\frac{7}{6}$	0.7 5.9 [29] 0.9	29.5 34.7 29.5	0.2 **14.0** 0.3	6 [25]	(5/8 0 0) [29][6]

[2] Note that in $CeCu_2$ the chemical and the magnetic unit cell is identical except for the fact that the magnetic moments of the Ce ions on the two positions are coupled antiferromagnetically. This may either be described by a propagation vector (0 0 0) and a 180° phase shift or by a propagation vector (1 1 0).
[3] *i.e.* in $PrCu_2$ the magnetic order is screened by quadrupolar order at 7.5 K.
[4] for $HoCu_2$ a propagation of (1/3 0 0) has been reported [27] for the high temperature phase between 7.4 and 10 K, this is equivalent to an indexing with a propagation vector (2/3 1 0), the moments are aligned in a direction.
[5] in $ErCu_2$ a propagation of (0.385 0 0) was discussed in [28], however satellites have also been found at (0.385 0 1) = (1 0 1)–(0.615 0 0).
[6] the data of $TmCu_2$ presented in [29] can be indexed according to (5/8 0 0).

In [21] the parameters of $TbCu_2$ and $DyCu_2$ have been adjusted to reproduce the correct Néel temperature within a mean field theory (compare Eq. (24); however, in [21] the effect of all crystal field states has been considered). The magnitude of the Néel temperature T_N is determined by a linear combination of these parameters, which is compared at the bottom of Table 3. The value derived from the present analysis of $NdCu_2$ exceeds only slightly the values for the other compounds.

Using the model described by [21] and the parameters derived from the present analysis of $NdCu_2$ (third column in Tab. 3), the critical field for the spin flip to the ferromagnetic phase has been calculated for $DyCu_2$ to 6.1 T. It exceeds the experimental value of 2.0 T [13,21].

7 Conclusion

The dispersion of the magnetic excitations in the field induced ferromagnetic phase F3 of $NdCu_2$ can be described by a MF-RPA model with anisotropic magnetic bilinear R-R exchange interactions. An attempt to analyze

Table 3. Comparison of the exchange constants determined from the phase diagrams of $TbCu_2$ and $DyCu_2$ in [21] with the model presented here for $NdCu_2$.

	$TbCu_2$ [21]	$DyCu_2$ [21]	$NdCu_2$
J_1 [K]	2.65	2.09	2.47
J_2 [K]	−1.00	−1.26	−2.79
J_3 [K]	3.16	2.78	3.49
J_4 [K]	−1.69	−1.67	−3.61
$J_1 - J_2 + J_3 - J_4$[K] $(\propto T_N/(g_J-1)^2)$	8.5	7.8	12.36
$J_0 = 2J_1 + 2J_2 + J_3 + J_4$[K] $(\propto \mathcal{J}_{\rm Spin}(q=0))$	4.77	2.77	−0.77

the magnetic ordering process in other RCu_2 compounds on the basis of this model shows:

1. The direction, into which the ordered magnetic moments point, is mainly determined by the crystal field, because the CF interaction is much bigger than the R-R exchange interaction.
2. The exchange interaction between neighbors in b direction dominates, probably because the interatomic distance between these R atoms is small and therefore the magnetic interaction is not screened by any Cu atoms.
3. Because of the anisotropy of the exchange the two R^{3+} ions in the primitive chemical unit cell may couple antiferromagnetically, if the moments are aligned along the a direction, but ferromagnetically, if the moments are aligned along the b direction. Therefore, the ordering wave vector is not the same for all RCu_2 compounds. It is approximately $\mathbf{Q} \sim (2/3\,1\,0)$, if the easy axis is the a or the c axis and $\mathbf{Q} \sim (2/3\,0\,0)$ if b is the easy axis.

We appreciate the fruitful discussions with A. Lindbaum, M. Ellerby, A. Metz and J. Jensen concerning the theoretical part of this work. Some of us (S.K. and M.R.) would like to acknowledge the support of the Hahn–Meitner–Institut (PECO). Part of this work was supported by the Austrian science foundation (FWF) project No 11239-PHY, the single crystal has been financed by the FWF project No 8913-PHY. Part of this work was performed within the program of the Sonderforschungsbereich 463 (funded by the Deutsche Forschungsgemeinschaft). We acknowledge funding of IN12 experiments by the German Research Ministry BMBF under project No. 05-300-CJB-6.

Appendix A

Here a more quantitative argument for the importance of anisotropic exchange in $NdCu_2$ will be presented. It is based on the analysis of the magnetic structures of this compound [3]. Figure 10 shows the free energy of the different magnetic structures in a magnetic field parallel to the b-direction. For every magnetic structure the free energy at zero temperature is given by a line, the slope of which is determined by the total magnetic moment of the

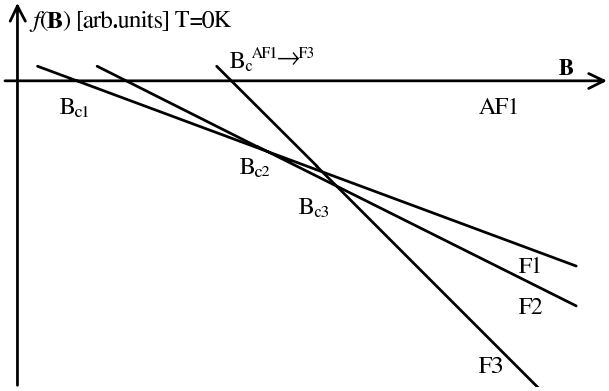

Fig. 10. Model: Magnetic free energy f at zero temperature as a function of the magnetic field B for the different structures AF1, F1, F2, F3 (neglecting the contribution of higher CF levels).

structure. The position of the line is determined by the special moment arrangement of this structure [3]. Therefore, if the magnetic structure and the transition fields B_{c1}, B_{c2} and B_{c3} are known from experiment, the position of all lines in Figure 10 can be determined (see [3]). Also the value of the critical field B_c^{AF1-F3} can be calculated, although this critical field cannot be observed directly in experiments. Thus the value of B_c^{AF1-F3} has been determined to 1.965 T [3]. At this field the free energy of F3 equals the free energy of AF1 and this fact may be used to make important conclusions about the magnetic exchange in this compound.

We will assume that the exchange is isotropic and show that this leads to contradictions with the experimentally observed magnitude of the excitation energy within the mean field (MF) – random phase approximation (RPA) model.

The magnetic energy of the zero field phase AF1 (per formula unit) can be calculated directly from the exchange interaction

$$f_{\rm AF1} = -\frac{1}{2N}\sum_{i,j}\langle \mathbf{J}_i\rangle_{\rm AF1}\overline{\overline{\mathcal{J}}}(ij)\langle \mathbf{J}_j\rangle_{\rm AF1}. \qquad \text{(A.1)}$$

In this expression the $\overline{\overline{\mathcal{J}}}(ij)$ represents the exchange tensors between Nd ion number i and j (at position $\mathbf{R}_i$ and

$\mathbf{R}_j$) and the $<\mathbf{J}_i>_{\mathrm{AF1}}$ represent the thermal expectation values of the angular momentum operator for the special spin configuration of AF1 in a crystal of N Nd-atoms.

For $\mathbf{q} \perp \mathbf{c}$ equation (A.1) can be Fourier transformed to give

$$f_{\mathrm{AF1}} = -\frac{1}{2} \sum_{\mathbf{q}\perp\mathbf{c}\in 1.\mathrm{BZ}} \langle \mathbf{J}(-\mathbf{q})\rangle_{\mathrm{AF1}} \bar{\bar{\mathcal{J}}}(\mathbf{q}) \langle \mathbf{J}(\mathbf{q})\rangle_{\mathrm{AF1}} \quad \text{(A.2)}$$

with the Fourier transform of the exchange and the spin arrangement defined as

$$\bar{\bar{\mathcal{J}}}(\mathbf{q}) = \sum_j \bar{\bar{\mathcal{J}}}(ij) \exp[-\mathrm{i}\mathbf{q}(\mathbf{R}_i - \mathbf{R}_j)] \quad \text{(A.3)}$$

$$\langle \mathbf{J}(\mathbf{q})\rangle_{\mathrm{AF1}} = \frac{1}{N} \sum_j \langle \mathbf{J}_j\rangle_{\mathrm{AF1}} \exp(-\mathrm{i}\mathbf{q}\mathbf{R}_j). \quad \text{(A.4)}$$

At zero temperature the expectation values in equation (A.3) ($\langle \mathbf{J}_j\rangle_{\mathrm{AF1}} = \pm M\hat{\mathbf{b}}$, the sign depending on j) can be evaluated from the magnetic structure of AF1 (collinear antiferromagnetic stacking of ferromagnetic bc-planes with the moment arrangement ↑↑↓↓↑↓↓↑↑↓). Then equation (A.2) simply reads

$$f_{\mathrm{AF1}} = -M^2 \Big\{ \mathcal{J}^{bb}(\boldsymbol{\tau})(0.647)^2 + \mathcal{J}^{bb}(3\boldsymbol{\tau})(0.247)^2 + \frac{1}{2}\mathcal{J}^{bb}(5\boldsymbol{\tau})(0.200)^2 \Big\}. \quad \text{(A.5)}$$

Here $\boldsymbol{\tau}$ =(0.6 0 0) designates the ordering wave vector of AF1. The factor 1/2 for the higher harmonic $5\boldsymbol{\tau}$ results from the fact that the zone boundaries have to be counted only half in the expansion (A.2).

For the free energy of the ferromagnetic phase F3 the total magnetic moment is not zero. In an external magnetic field B oriented parallel to the b-direction the Zeeman energy has to be considered in addition to the exchange interaction, yielding:

$$f_{\mathrm{F3}} = -g_{\mathrm{J}}\mu_{\mathrm{B}} MB - \mathcal{J}^{bb}(\mathbf{q}=0)M^2/2. \quad \text{(A.6)}$$

As stated above the free energies f_{AF1} and f_{F3} are equal at $B_{\mathrm{c}}^{\mathrm{AF1-F3}} = 1.965$ T. This leads to the relation

$$M^2\{\mathcal{J}^{bb}(\boldsymbol{\tau})(0.647)^2 + \mathcal{J}^{bb}(3\boldsymbol{\tau})(0.247)^2 + \frac{1}{2}\mathcal{J}^{bb}(5\boldsymbol{\tau})(0.200)^2\} = g_{\mathrm{J}}\mu_{\mathrm{B}} MB_{\mathrm{c}}^{\mathrm{AF1-F3}} + \mathcal{J}^{bb}(\mathbf{q}=0)M^2/2. \quad \text{(A.7)}$$

To continue the investigation of the exchange, the value of the Néel temperature $T_{\mathrm{N}} = 6.5$ K has to be explained. In a MF theory this is given by (k_{B} denotes Boltzmanns constant)

$$k_{\mathrm{B}} T_{\mathrm{N}} = M^2 \mathcal{J}^{bb}(\boldsymbol{\tau}). \quad \text{(A.8)}$$

The small shift of $\boldsymbol{\tau}$ with temperature [3] has been neglected in this expression. The structure AF1 can only be stable, if the Fourier transform of the exchange $\mathcal{J}^{bb}(\mathbf{q})$ has its maximum at $\mathbf{q} = \boldsymbol{\tau}$ (*i.e.* $\mathcal{J}^{bb}(\boldsymbol{\tau}) > \mathcal{J}^{bb}(3\boldsymbol{\tau})$, $\mathcal{J}^{bb}(\boldsymbol{\tau}) > \mathcal{J}^{bb}(5\boldsymbol{\tau})$) [16]. Replacing in the left side of equation (A.7) the higher harmonics $\mathcal{J}^{bb}(3\boldsymbol{\tau})$ and $\mathcal{J}^{bb}(5\boldsymbol{\tau})$ by $\mathcal{J}^{bb}(\boldsymbol{\tau}) = k_{\mathrm{B}}T_{\mathrm{N}}/M^2$ gives the relation

$$2k_{\mathrm{B}}T_{\mathrm{N}} \left\{ (0.647)^2 + (0.247)^2 + \frac{1}{2}(0.200)^2 \right\} > 2g_{\mathrm{J}}\mu_{\mathrm{B}} MB_{\mathrm{c}}^{\mathrm{AF1-F3}} + \mathcal{J}^{bb}(\mathbf{q}=0)M^2. \quad \text{(A.9)}$$

By inserting reasonable values for $M = 2.54$ (this corresponds to the moment per Nd at 3 T external field – compare [3]), $T_{\mathrm{N}} = 6.5$ K (*i.e.* $\mathcal{J}^{bb}(\boldsymbol{\tau}) = 0.093$ meV) and $B_{\mathrm{c}}^{\mathrm{AF1-F3}} = 1.965$ T an upper limit for the sum of all coupling parameters (*i.e.* $\mathcal{J}^{bb}(\mathbf{q}=0)$) can be deduced:

$$\mathcal{J}^{bb}(\mathbf{q}=0) < 0.0215 \text{ meV}. \quad \text{(A.10)}$$

This may be used to find an upper limit for the splitting of the ground state doublet in F3 at 3 T, which in a MF-theory is given by

$$\Delta = 2g_{\mathrm{J}}\mu_{\mathrm{B}} MB + 2M^2\mathcal{J}^{bb}(\mathbf{q}=0) < 0.214 \text{ meV/T} \times 3\text{T} + 2 \times 0.139 \text{ meV} = 0.920 \text{ meV}. \quad \text{(A.11)}$$

Using equation (18) and specializing it for the case of isotropic exchange ($\mathcal{J}^{aa} = \mathcal{J}^{bb} = \mathcal{J}^{cc} = \mathcal{J}$) allows to estimate the excitation energy of the lower magnetic excitation at the wave vector $\boldsymbol{\tau}$ to (for the derivation of this formula see the main text)

$$[\hbar\omega_2(\boldsymbol{\tau})]^2 = (\Delta - 2A^2\mathcal{J}(\boldsymbol{\tau}))(\Delta + 2C^2\mathcal{J}(\boldsymbol{\tau})). \quad \text{(A.12)}$$

Putting in values for A and C (Ref. [7]: $A = 2.1$, $C = 1.5i$) and estimating again $\mathcal{J}(\boldsymbol{\tau})$ from the Néel temperature gives

$$[\hbar\omega_2(\boldsymbol{\tau})]^2 = (\Delta - 0.76\,\mathrm{meV})(\Delta - 0.39\,\mathrm{meV}). \quad \text{(A.13)}$$

If we compare this to the estimation (A.11) ($\Delta < 0.92$ meV), we can conclude that the soft mode excitation $\hbar\omega_2(\boldsymbol{\tau})$ has to lie below 0.08 meV, which is one order of magnitude lower than the measured excitation energy of about 1 meV. Therefore the assumption of isotropic exchange leads to fundamental contradictions with the experiment.

Note that the numerical values in equations (A.7–A.13) are based on the original analysis of the magnetic phase diagram [3] and are in contrast to the new fitted value of $\mathcal{J}^{bb}(\mathbf{q}=0) = 0.044$ meV and $\Delta = 1.106$ meV described in the main text. The most convincing explanation for this discrepancy is the limited validity of the mean field theory near the ordering temperature. Usually the mean field approach predicts an ordering temperature which is too big in comparison with the experiment. Critical fluctuations reduce this ordering temperature (compare for instance Monte-Carlo calculations on Ising models [22,23]). To account for this effect a bigger value for T_{N} has to be inserted into equation (A.9). Taking for example $T_{\mathrm{N}} = 8$ K leads to $\Delta < 1.184$ meV (instead of (A.11)) and $\hbar\omega_2(\boldsymbol{\tau}) < 0.336$ meV – but also these values rule out the possibility of isotropic exchange.

References

1. R.R. Arons, M. Loewenhaupt, Th. Reif, E. Gratz, J. Phys.-Cond. **6**, 6789 (1994).
2. M. Loewenhaupt, T. Reif, R. Arons, E. Gratz, M. Rotter, B. Lebech, Z. Phys. B **96**, 491 (1995).
3. M. Loewenhaupt, T. Reif, P. Svoboda, S. Wagner, M. Waffenschmidt, H.V. Löhneysen, E. Gratz, M. Rotter, B. Lebech, T. Hauss, Z. Phys. B **101**, 499 (1996).
4. E. Gratz, M. Loewenhaupt, M. Divis, W. Steiner, E. Bauer, N. Pillmayr, H. Müller, H. Novotny, B. Frick, J. Phys.-Cond. **3**, 9297 (1991).
5. M. Loewenhaupt, T. Reif, W. Hahn, B. Frick, J. Magn. Magn. Mat. **177-181**, 1050 (1998).
6. E. Gratz, N. Pillmayr, E. Bauer, H. Müller, B. Barbara, M. Loewenhaupt, J. Phys.-Cond. **2**, 1485 (1990).
7. P. Svoboda, M. Divis, A.V. Andreev, N.V. Baranov, M.I. Bartashevich, P.E. Markin, J. Magn. Magn. Mat. **104-107**, 1329 (1992).
8. A. Loidl, K. Knorr, J.K. Kjems, B. Luethi, Z. Phys. B **35**, 253 (1979).
9. B. Haelg, A. Furrer, Phys. Rev. B **34**, 6258 (1986).
10. J. Jensen, J. Magn. Magn. Mat. **29**, 47 (1982).
11. P. Ahmet, M. Abliz, R. Settai, K. Sugiyama, Y. Onuki, T. Takeuchi, K. Kindo, S. Takayanagi, J. Phys. Soc. Japan **65**, 1077 (1996).
12. Y. Hashimoto, K. Kindo, T. Takeuchi, K. Senda, M. Date, A. Yamagishi, Phys. Rev. Lett. **72**, 1922 (1994).
13. M. Loewenhaupt, M. Doerr, L. Jahn, T. Reif, C. Sierks, M. Rotter, H. Müller, Physica B **246-247**, 472 (1998).
14. T. Reif, Ph.D. thesis, Universität zu Köln (1998).
15. M. Rotter, A. Lindbaum, E. Gratz, H. Müller, G. Hilscher, H. Sassik, H.E. Fischer, M.T. Fernandes-Diaz, R. Arons, E. Seidl, J. Phys.-Cond. (submitted).
16. J. Jensen, A.R. Mackintosh, *Rare Earth Magnetism* (Clarendon Press, Oxford, 1991).
17. K.W.H. Stevens, Proc. Phys. Soc. A **65**, 209 (1952).
18. S. Kirkpatrick, C.D. Gelatt, M.P. Vecchi, Science **220**, 671 (1983).
19. S. Kawarazaki, Y. Kobashi, M. Sato, Y. Miyako, J. Phys.-Cond. **7**, 4051 (1995).
20. K. Poldy, H. Kirchmayer, Phys. Stat. Solidi B **65**, 553 (1974).
21. N. Iwata, Y. Hashimoto, T. Kimura, T. Shigeoka, J. Magn. Magn. Mat. **81**, 354 (1989).
22. W. Selke, M.E. Fisher, Phys. Rev. B **20**, 257 (1979).
23. W. Selke, Z. Phys. B **29**, 133 (1978).
24. V. Sima, Z. Smetana, B. Lebech, E. Gratz, J. Magn. Magn. Mat. **54-57**, 1357 (1986).
25. B. Lebech, Z. Smetana, V. Sima, J. Magn. Magn. Mat. **70**, 97 (1987).
26. Y. Koike, N. Metoki, Y. Morii, Y. Yoshida, R. Settai, Y. Onuki, J. Phys. Soc. Japan **66**, (1997).
27. Z. Smetana, V. Sima, B. Lebech, J. Magn. Magn. Mat. **59**, 145 (1986).
28. Y. Hashimoto, H. Kawano, H. Yoshizawa, S. Kawano, T. Shigeoka, J. Magn. Magn. Mat. **140-144**, 1131 (1995).
29. M. Heidelmann, Ph.D. thesis, Universität zu Köln (1992).
30. R. Trump, Ph.D. thesis, Universität zu Köln (1991).
31. V. Nunez, R. Trump, P.J. Brown, T. Chattopadhyay, M. Loewenhaupt, F. Tasset, J. Phys.-Cond. **4**, 1115 (1992).
32. Y. Hashimoto, J. Sci. Hiroshima Univ. **43**, 157 (1979).
33. R. Settai, S. Araki, P. Ahmet, M. Abliz, K. Sugiyama, Y. Onuki, T. Goto, H. Mitamura, T. Goto, S. Takayanagi, J. Phys. Soc. Japan **67**, 636 (1998).
34. K. Maezawa, S. Wakabayashi, K. Sato, Y. Isikawa, T. Kaneko, G. Kido, Y. Nakagawa, Physica B **155**, 276 (1989).

ELSEVIER

Journal of Magnetism and Magnetic Materials 214 (2000) 281–290

Journal of magnetism and magnetic materials

www.elsevier.com/locate/jmmm

The magnetic structure of $GdCu_2$

M. Rotter[a,*], A. Lindbaum[b], E. Gratz[c], G. Hilscher[c], H. Sassik[c], H.E. Fischer[d], M.T. Fernandez-Diaz[d], R Arons[e], Erwin Seidl[f]

[a]*Institut für Angewandte Physik, Technische Universität Dresden, Mommsenstr 13, D-01062 Dresden, Germany*
[b]*European Commission (Joint Research Centre) Institute for Transuranium Elements, Postfach 2340, D-76125 Karlsruhe, Germany*
[c]*Institut für Experimentalphysik, Technische Universität Wien, Wiedner Hauptstraße 8–10, A–1040 Wien, Austria*
[d]*Institut Laue Langevin, F-38042 Grenoble, France*
[e]*Forschungszentrum Jülich, D-052425 Jülich, Germany*
[f]*Atominstitut der Österreichischen Universitäten, Schüttelstraße 115, A-1020 Wien, Austria*

Received 14 December 1999; received in revised form 11 February 2000

Abstract

The magnetic properties of $GdCu_2$ have been investigated. Neutron scattering experiments have been performed on powder and single-crystal samples to determine the magnetic structure. A non-collinear, cycloidal propagation fits best to the experimental data. The results are discussed in the framework of a mean field model. Low-field magnetization measurements indicate an anisotropy which is in agreement with the proposed magnetic structure.

PACS: 75.25. + 75.30

Keywords: Magnetic structure; Elastic neutron scattering; Anisotropic magnetic exchange; Magnetization

1. Introduction

Among the RM_2 intermetallic compounds (R = rare earth, M = transition metal) the $MgCu_2$-type structure (space group Fd3m) exists for all 3d metals from Mn to Ni. However, the 1 : 2 compounds with Cu exhibit the orthorhombic $CeCu_2$-type structure (space group Imma, D_{2h}^{28}, Ce at 4e sites, Cu at 8h), with the exception of $LaCu_2$. $LaCu_2$ displays the related hexagonal AlB_2 structure (space group P_6/mmm, D_{6h}^{1}) [1]. The orthorhombic $CeCu_2$ structure can be viewed as a distorted AlB_2-type structure. In some RCu_2 compounds a martensitic transition in high magnetic fields has been observed and associated with a conversion of the $CeCu_2$ to the AlB_2 type of structure [2].

Initial magnetic investigations on RCu_2 have been performed by Sherwood et al. for all lanthanides [3]. They observed metamagnetic behavior from which they deduced that these compounds order antiferromagnetically (AF). This was first confirmed by neutron diffraction measurements by Brun et al. [4] who interpreted their results on $TbCu_2$ in terms of collinear antiferromagnetism at

*Corresponding author. Tel.: + 49-351-463-4460; fax: + 49-351-463-3199.
E-mail address: rotter@physik.tu-dresden.de (M. Rotter).

0304-8853/00/$ - see front matter
PII: S0304-8853(00)00051-2

4.2 K with spins directed along the a direction. From specific heat, thermal expansion [5] and neutron diffraction [6] it has been found that in most of the RCu_2 intermetallics one or more first- or second-order transitions exist below the corresponding Néel temperature [7]. It is evident that in addition to the exchange interaction the crystal field is also important for the question of which magnetic structure is stable at a given temperature. It seems that in a first approximation the interplay between anisotropic exchange and the crystal field and their temperature dependence are responsible for whether there is a change of the magnetic structure observable in the ordered state or not. Among the magnetic RCu_2, $GdCu_2$ is the only compound without crystal field influence on the 4f states because Gd^{3+} is an S-state ion with $L = 0$. Investigations of $GdCu_2$ in the magnetically ordered state ($T_N = 42$ K) revealed that in this compound no change of magnetic structure exists in zero external magnetic field [8–10]. The magnetic entropy as calculated from the specific heat reaches its theoretical value of $R \ln 8$ at 47 K, just above T_N [8]. In high magnetic fields the anisotropy in the magnetization does not exceed a few percents [11]. Measurements of the dHvA branches in the field-induced ferromagnetic state indicate, that the Fermi surface is altered by the magnetic exchange interaction [8]. At lower fields the interpretation of dHvA measurements is difficult, because the magnetic structure of this compound has not been determined.

In the present paper we report an experimental investigation of $GdCu_2$ with the aim to clarify what magnetic structure appears if in a RCu_2 compound only the exchange interaction is responsible for the magnetic structure.

Already in 1974 a model calculation based on isotropic RKKY exchange interactions was performed and a magnetic structure with ferromagnetic *bc* planes and a cycloidal propagation in *a* direction with a pitch angle of 35° between neighboring *bc* planes was predicted [12]. This very rough estimate is in a surprising qualitative agreement with our results. The main difference to our results is, that we find antiferromagnetic *bc* planes.

2. Experimental

$GdCu_2$ is an orthorhombic compound, which is stable up to the congruent melting point at 860°C. The adjacent eutectic point results from the reactions of Gd_2Cu_9 with the liquid and of GdCu with the liquid at 820 and 770°C, respectively [13].

Therefore, the master alloys were prepared by RF levitation melting with a Hüttinger 30 kW generator of the pure elements in protective Ar-atmosphere after evacuating to HV either by melting in a water-cooled cold-boat (4–5 g) or in a water-cooled Hukin-crucible (about 30 g) to prevent any reaction of the melt with the crucible. Each sample was remolten three times to optimize homogeneity.

The single crystals were obtained by a Bridgeman technique in an A.D. Little System in inert Ar gas after HV in conically shaped BN crucibles by application of about 15 g for one run. The pulling speed was 4.5 mm/h, the heating was done by a RF Hüttinger 40 kW generator. The starting temperature was 860°C. The orientation of the single crystal was checked by metallographic techniques and Laue Photographs with Mo radiation. A computer program by Gunnar Christiansen (Lab of Appl. Physics of TU Lyngby, Denmark) was used for the orientation process [14]. The final shape of the crystal was a polyeder with an average diameter of 2.5 mm.

Polycrystalline sample material for the neutron scattering experiment was prepared in a water-cooled copper boat in a high-frequency furnace. A protective argon atmosphere has been used to avoid oxidation of the sample during melting. The grain size of the powder used in the double-wall cylindric sample container was 50 μm and the mass about 8 g.

Magnetization measurements have been performed using a SQUID magnetometer in fields up to 6 T and are in agreement with Ref. [11].

The single-crystal neutron scattering experiments have been performed at the D9 hot source four circle diffractometer (Institute Laue-Langevin, Grenoble) using a wavelength of 0.5 Å. Magnetic and nuclear intensities of the $GdCu_2$ single crystal have been determined by comparing scans at 45 K (just above the Néel temperature $T_N = 42$ K) with scans at 15 K.

Before doing the single-crystal experiments we performed measurements on a powdered sample at

the D4b diffractometer using a double-wall cylinder (10 mm long, 1 mm wall thickness, with 25 mm diameter) and an 'orange'-type cryostat with a vanadium tail (in order to eliminate parasitic Bragg peaks).

3. Results

Fig. 1 shows the reciprocal *ab* and *ac* planes of $GdCu_2$. Full circles correspond to the nuclear Bragg reflections, open circles indicate the positions of the magnetic satellites. The magnetic satellites which have been observed could be indexed by a modulation vector $\boldsymbol{Q}_0 = (\frac{2}{3}\,1\,0)$. This type of ordering can be viewed as an *antiferromagnetic* modulation of the moments in *b* direction and a *cycloidal* propagation in *a* direction with a pitch angle of 120°.

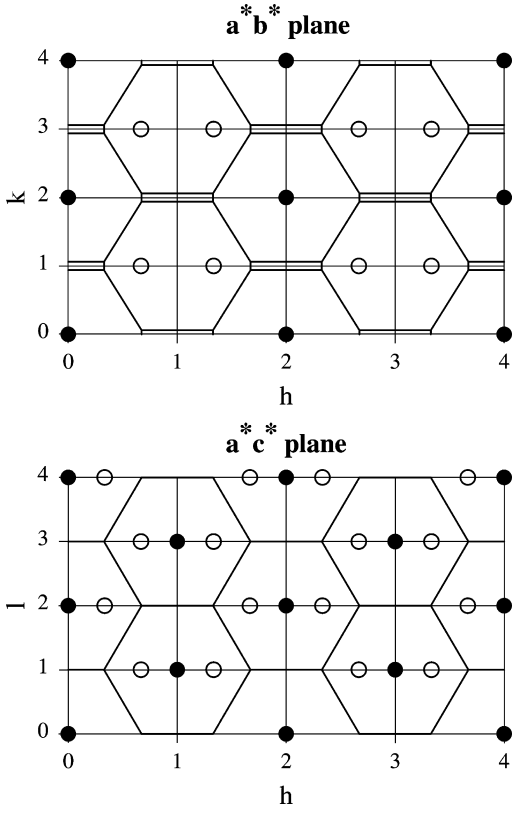

Fig. 1. Positions of magnetic (open circles) and nuclear (full circles) reflections in the reciprocal *ab* and *ac* planes of $GdCu_2$.

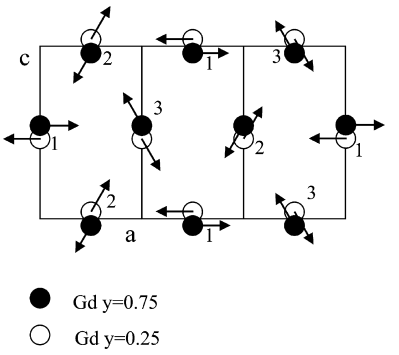

Fig. 2. Magnetic structure of $GdCu_2$, the different symbols denote atoms belonging to the same *ac* plane, for simplicity the copper atoms are not shown. The magnetic structure can be viewed as a superposition of three simple antiferromagnetic lattices as indicated by the numbers.

The proposed magnetic structure of $GdCu_2$ is shown in Fig. 2. There are two different domains possible, one with a left-handed and another with a right-handed cycloid. The magnetic unit cell consists of three structural unit cells aligned in *a* direction. From the projection into the *ac*-plane the cycloidal propagation in *a* direction can be seen. The filled and open symbols denote two different neighboring *ac* planes showing the antiferromagnetic propagation in *b* direction. This antiferromagntic arrangement along *b* is obvious from our notation of the propagation vector $\boldsymbol{Q}_0 = (\frac{2}{3}\,1\,0)$, which has not been reduced to the first Brillouin zone for this reason. An equivalent description of the magnetic structure using the reduced propagation vector $\boldsymbol{q}_0 = (\frac{1}{3}\,0\,0)$ is possible. However, $\boldsymbol{Q}_0 = (\frac{2}{3}\,1\,0)$ will be used through the rest of this paper, because indexing all magnetic reflections with nonzero intensity as satellites to nuclear reflections with nonzero intensity is possible thereby taking already account of some selection rules.[1]

[1] The projection of the crystallographic three-dimensional structure into the *ab* plane is a simple rectangular lattice with the new lattice parameters *a*/2 and *b*/2. This is the reason why reflections with *h* and *k* odd vanish for $l = 0$. The moments in the magnetic structure are aligned ferromagnetically along *c* direction. With respect to this projection of the 3D lattice to the *ab* plane, i.e. analyzing the 2D lattice, the propagation vector $(\frac{2}{3}\,1)$ (which means $(\frac{1}{3}\,\frac{1}{2})$ with respect to the 2D reciprocal lattice) is at the border of the corresponding 2D first Brillouin zone. The $\frac{1}{2}$ in $(\frac{1}{3}\,\frac{1}{2})$ reflects the antiferromagnetic ordering in *b* direction.

Table 1
Intensities as measured by the single-crystal neutron scattering experiments in comparison with the values calculated on the basis of the magnetic structure shown in Fig. 2. In addition, the calculated intensities for a slightly modified structure corresponding to $\sigma = -0.45$ (see text for details) are given. The common scale factor for all intensities was chosen to give the best agreement for the experimental and theoretical intensities of the nuclear peaks

$(h\,k\,l) \pm \boldsymbol{Q}_0$	Calc. int.		Exp. int.
Magnetic intensity	$\sigma = 0$	$\sigma = -0.45$	
$(2\,2\,0) - \boldsymbol{Q}_0$	5.30	5.94	3.14
$(0\,\bar{1}\,3) + \boldsymbol{Q}_0$	1.35	1.14	0.90
$(1\,2\,3) - \boldsymbol{Q}_0$	1.60	1.36	0.63
$(0\,2\,0) + \boldsymbol{Q}_0$	4.73	4.73	3.59
$(1\,4\,1) - \boldsymbol{Q}_0$	4.40	4.33	2.70
$(2\,1\,3) - \boldsymbol{Q}_0$	0.95	0.89	0.90
$(1\,1\,4) - \boldsymbol{Q}_0$	1.19	0.96	1.08
$(\bar{1}\,\bar{1}\,4) + \boldsymbol{Q}_0$	1.19	0.96	0.72
Magnetic intensity on $3\boldsymbol{Q}_0$			
(0 0 5)	0	0.04	0
(0 0 3)	0	0.07	0
(0 3 0)	0	0.13	0
Nuclear intensity			
(1 0 3)	29.97		29.65
(2 0 2)	0.22		0.72
(0 4 0)	10.00		10.78
(0 0 6)	8.09		9.88

In Table 1 the intensities calculated on the basis of this magnetic structure are compared with the experimental data. Note that within the experimental error there is no higher order satellite $3\boldsymbol{Q}_0$ (at the forbidden nuclear reflections) and no magnetic intensity on the nuclear peaks (no ferromagnetic component) in agreement with the postulated magnetic structure. However, changing the moment direction of those moments, which are not aligned parallel to the a direction by 10° into $\pm c$ direction (corresponding to $\sigma = -0.45$, see below) leads to very small intensities on $3\boldsymbol{Q}_0$. The expected change in intensity is shown in Table 1 and is below the experimental resolution.

Due to the use of a neutron wavelength of 0.5 Å (in order to decrease absorption) and due to the low symmetry of the sample the resolution was not good enough to determine the magnetic structure from the powder measurements only. However, the strong magnetic intensity can be indexed according to a propagation of $(\frac{2}{3}\,1\,0)$ as indicated in Fig. 3. In this figure we show the result of a Rietveld refinement at 60 K (i.e. above T_N, the R-value is $R_{nucl} = 4.95\%$) and at 2 K ($R_{nucl} = 3.84\%$, $R_{mag} = 6.21\%$) using FULLPROF [15]. The shown refinement at 2 K (nuclear + magnetic scattering) was done by assuming the cycloidal magnetic structure with a modulation vector $\boldsymbol{Q}_0 = (\frac{2}{3}\,1\,0)$ and only refining the size of the Gd-moments, giving a value of 6.9 μ_B (expected saturation moment: 7 μ_B). The refinement was done for the whole accessible 2-θ range up to 38°, but for clarity we show only the range up to 20° in the figure, together with the Miller indices of the strongest nuclear peaks ($h\,k\,l$) and magnetic

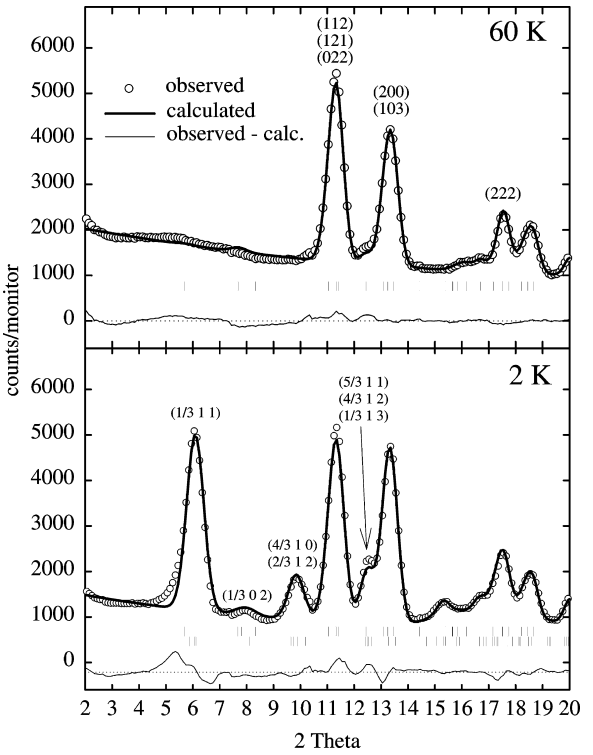

Fig. 3. Neutron powder diffraction pattern of $GdCu_2$ at 60 and 2 K, the line through the symbols corresponds to a fit using the FULLPROF Rietveld program. The vertical bars indicate the position of nuclear and magnetic peaks, the line below shows the difference between the experimental and calculated pattern. For clarity only the 2-θ range up to 20° is shown, together with the Miller indices of the strongest nuclear peaks ($h\,k\,l$) and the corresponding magnetic satellites ($h\,k\,l + Q_0$ or $h\,k\,l - Q_0$).

satellites ($h\,k\,l + Q_0$ or $h\,k\,l - Q_0$). As an example, the ($\frac{1}{3}$ 1 1) magnetic reflection is a satellite of (1 2 1). The refinements were done using a nuclear scattering length of 1.13×10^{-14} m for the natural Gd-isotope mixture and the used neutron wavelength of 0.5 Å. This scattering length was found to fit best the measured nuclear intensities and is in agreement with Ref. [16]. From the quality of the fits it can be deduced that the powder measurements are in agreement with the proposed magnetic structure and therefore support the results of the single-crystal experiments.

4. Model

A structure with moments in the *ac* plane is in accordance with the anisotropic exchange in $NdCu_2$ measured by magnetic excitations in the field-induced ferromagnetic phase (with magnetic field in *b* direction) [17]. In these magnetic excitation measurements of $NdCu_2$ only those exchange constants could be determined which couple the *a* and *c* components of the magnetic moments. The analysis of the excitations of $NdCu_2$ shows, that there exists a minimum in the dispersion at $\boldsymbol{Q}_0 = (\frac{2}{3}\ 1\ 0)$. Assuming that the exchange in isostructural RCu_2 compounds is comparable, it follows, that any isostructural compound having *a* or *c* as the easy axis should order at this wave vector [17]. This is true for instance for $DyCu_2$, and according to our new results also for $GdCu_2$ (here the anisotropy of the magnetic properties is only determined by the anisotropy of the magnetic exchange [18]). In Fig. 2, the nearly hexagonal symmetry of the crystal structure may be seen by turning it to 60°, the *ac* plane of the orthorhombic structure corresponds to the hexagonal plane and the *b*-axis to the hexagonal axis. Also the magnetic structure of this compound reflects this hexagonal symmetry, as may be seen by rotating and shifting Fig. 2.

These facts suggest that the magnetic properties can possibly be described by an exchange interaction of hexagonal symmetry, as it was possible for the case of $NdCu_2$ [17]. The following analysis will show, that this is true grosso modo, however, a small anisotropic coupling which only is nonzero

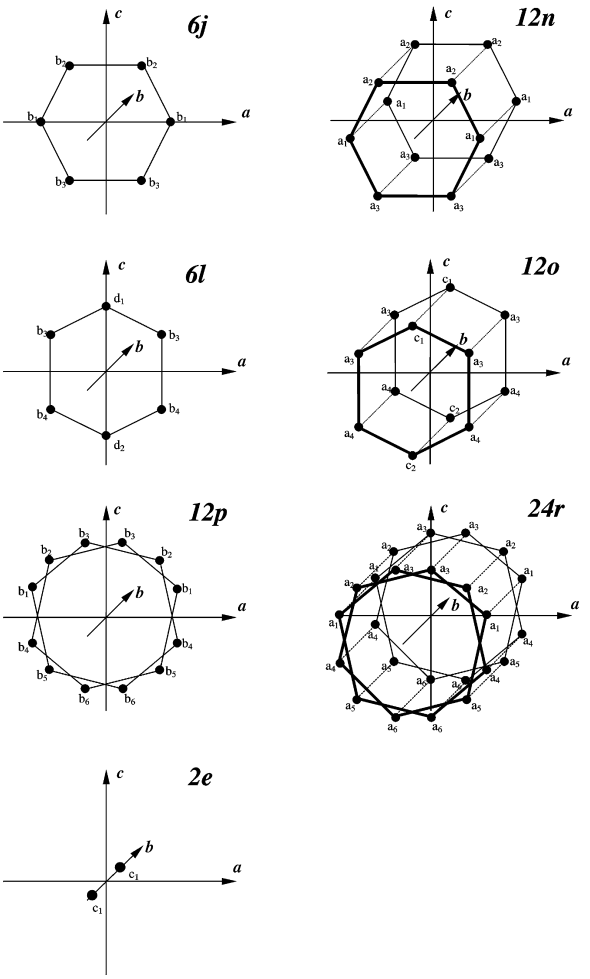

Fig. 4. Different types of bilinear exchange interactions in RCu_2 compounds assuming hexagonal symmetry of the exchange. The indexed letters indicate, which of the exchange constants are related for orthorhombic symmetry.

assuming an orthorhombic distortion of the hexagonal lattice is needed to stabilize the observed magnetic structure. It is remarkable that this orthorhombic distortion, reflected by the *c*/*a* ratio of the actual crystallographic structure (i.e. $c/a = \sqrt{3}$ in the hexagonal case), diminishes at the transition from the paramagnetic to the ordered state, i.e. *c*/*a* gets closer to $\sqrt{3}$ (compare Refs. [11,19]). Thus, the magnetoelastic energy favors an exchange interaction of hexagonal symmetry.

For the observed cycloidal structure to occur, the off diagonal components of the exchange

interaction have to be nonzero. By calculating the contribution of the most general interaction allowed by hexagonal symmetry (see Fig. 4, type 24*r*) it can be shown, that for hexagonal symmetry the Fourier transform of the interaction tensor $\bar{\bar{\mathcal{J}}}(\boldsymbol{Q} = \boldsymbol{Q}_0 = (\frac{2}{3}\ 1\ 0))$ is always diagonal.

Therefore, the non-collinear magnetic ordering process can only be explained by taking into account the orthorhombic symmetry of the compound. However, using a simple model it will be shown that the off diagonal components of the coupling may be very small compared to the diagonal elements. This fact may be demonstrated by noting that the magnetic structure can be thought of as a superposition of three simple collinear antiferromagnetic lattices (indicated by the numbers in Fig. 2). The size of the ordering temperature may be determined by the probably strong diagonal components of the interaction within and between these sublattices. The relative orientation of the moments on the different sublattices is then very sensitive to the fact whether there exists a nonzero off diagonal nteraction constant or not, leading to either a collinear or a cycloidal magnetic structure.

In the following model, anisotropy in the exchange is restricted to the nearest neighbors within the nearly hexagonal plane. The interaction tensors of the model are summarized in Table 2.

Although this is a very simple model exchange, it can account well for the observed magnetic properties of $GdCu_2$. It is not necessary to take into account exchange constants, which couple moments parallel to *b* with those in the *ac* plane, therefore the components $\mathcal{J}^{ab}$ and $\mathcal{J}^{cb}$ of the

Table 2
Model bilinear magnetic interaction tensors between neighboring Gd atoms in $GdCu_2$

Exchange tensor $\bar{\bar{\mathcal{J}}}(ij)$	Distance $\boldsymbol{R}_i - \boldsymbol{R}_j$	Hex. type	Orth. type
$\begin{pmatrix} B & 0 & 0 \\ 0 & B & 0 \\ 0 & 0 & B \end{pmatrix}$	$\begin{pmatrix} 0 \\ \pm b/2 \\ 0 \end{pmatrix}$	2*e*	$2c_1$
$\begin{pmatrix} C_a & 0 & \pm D \\ 0 & C_b & 0 \\ \mp D & 0 & C_c \end{pmatrix}$	$\begin{pmatrix} \pm a \\ 0 \\ 0 \end{pmatrix}$		$2b_1$
$\begin{pmatrix} F_a & 0 & \pm E \\ 0 & F_b & 0 \\ \pm G & 0 & F_c \end{pmatrix}$	$\begin{pmatrix} \pm a/2 \\ 0 \\ c/2 \end{pmatrix}$	6*j*	$2b_2$
$\begin{pmatrix} F_a & 0 & \mp G \\ 0 & F_b & 0 \\ \mp E & 0 & F_c \end{pmatrix}$	$\begin{pmatrix} \pm a/2 \\ 0 \\ -c/2 \end{pmatrix}$		$2b_3$
$\begin{pmatrix} T & 0 & 0 \\ 0 & T & 0 \\ 0 & 0 & T \end{pmatrix}$	$\begin{pmatrix} 0 \\ 0 \\ \pm c \end{pmatrix}, \begin{pmatrix} \pm 3a/2 \\ 0 \\ c/2 \end{pmatrix}, \begin{pmatrix} \pm 3a/2 \\ 0 \\ -c/2 \end{pmatrix}$	6*l*	$2d_{1,2}, 2b_3, 2b_4$

exchange interaction tensor $\bar{\bar{\mathcal{J}}}$ have been omitted. Anisotropy of the exchange and the orthorhombic symmetry of the crystal is taken into account only for the nearest neighbors in the *ac* plane. For hexagonal symmetry the off diagonal element D would become exactly zero and the other elements would be subject to the conditions

$$E = G = \sqrt{3}/4(C_a - C_c), \quad F_a = C_a/4 + 3C_c/4,$$
$$F_b = C_b \text{ and } F_c = C_c/4 + 3C_a/4.$$

Calculating the Fourier transform of the interactions in Table 2 gives

$$\bar{\bar{\mathcal{J}}}(\boldsymbol{Q}) = \begin{pmatrix} U_a(\boldsymbol{Q}) & 0 & X(\boldsymbol{Q}) \\ 0 & U_b(\boldsymbol{Q}) & 0 \\ X^*(\boldsymbol{Q}) & 0 & U_c(\boldsymbol{Q}) \end{pmatrix} \quad (1)$$

with the notation ($\gamma = a, b, c$)

$$\begin{aligned} U_\gamma(\boldsymbol{Q}) = {} & 2B\cos(Q_b\pi) + 2C_\gamma\cos(2Q_a\pi) \\ & + 2F_\gamma\cos(Q_a\pi + Q_c\pi) \\ & + 2F_\gamma\cos(Q_a\pi - Q_c\pi) \\ & + 2T\cos(2Q_c\pi) + 2T\cos(3Q_a\pi + Q_c\pi) \\ & + 2T\cos(3Q_a\pi - Q_c\pi), \end{aligned} \quad (2)$$

$$\begin{aligned} X(\boldsymbol{Q}) = {} & 2\mathrm{i}D\sin(2Q_a\pi) + 2\mathrm{i}E\sin(Q_a\pi)\mathrm{e}^{\mathrm{i}Q_c\pi} \\ & - 2\mathrm{i}G\sin(Q_a\pi)\mathrm{e}^{-\mathrm{i}Q_c\pi}. \end{aligned} \quad (3)$$

Here Q_a, Q_b, Q_c denote the components of $\boldsymbol{Q}$ along the crystallographic axes. Within a mean field theory, which will be presented in detail in Ref. [20] the upmost eigenvalue of this matrix (Eq. (1)) has to be maximized with respect to $\boldsymbol{Q}$ to determine the magnetic structure and the ordering temperature. Diagonalizing yields three eigenvalues ($3kT_n/J(J+1)$ with $n = 1, 2, 3$)

$$\frac{3kT_1}{J(J+1)} = U_b(\boldsymbol{Q}), \quad (4)$$

$$\begin{aligned} \frac{3kT_{2,3}}{J(J+1)} = {} & \frac{U_a(\boldsymbol{Q}) + U_c(\boldsymbol{Q})}{2} \\ & \pm\sqrt{\frac{[U_a(\boldsymbol{Q}) - U_c(\boldsymbol{Q})]^2}{4} + X^*(Q)X(\boldsymbol{Q})}. \end{aligned} \quad (5)$$

The first eigenvalue $3kT_1/J(J+1)$ corresponds to a collinear spin structure with the moments pointing into b direction (with an eigenvector $\boldsymbol{M}_1(\boldsymbol{Q}) \propto (0\,1\,0)$ representing the Fourier transform of the ordered magnetic moments) and therefore cannot be the upmost eigenvalue in $GdCu_2$. The eigenvectors corresponding to T_2 and T_3 are given by

$$\boldsymbol{M}_{2,3}(\boldsymbol{Q}) \propto \begin{pmatrix} X(\boldsymbol{Q}) \\ 0 \\ \dfrac{U_a(\boldsymbol{Q}) - U_c(\boldsymbol{Q})}{2} \pm \sqrt{\dfrac{[U_a(\boldsymbol{Q}) - U_c(\boldsymbol{Q})]^2}{4} + X^*(\boldsymbol{Q})X(\boldsymbol{Q})} \end{pmatrix}. \quad (6)$$

For $\boldsymbol{Q}$ in the *ab* plane, i.e. also for $\boldsymbol{Q}_0 = (\frac{2}{3}\,1\,0)$, $X(\boldsymbol{Q})$ is purely imaginary (compare Eq. (3)). According to Eq. (2), $U_i(\boldsymbol{Q})$ is real. Therefore, the phase difference between the a and c component of the eigenvectors $\boldsymbol{M}_{2,3}(\boldsymbol{Q})$ is 90°. This is in agreement with the main Fourier component $\boldsymbol{M}(\pm\boldsymbol{Q}_0)$ of the magnetic structure used in the interpretation of the neutron scattering experiments (i.e. $\boldsymbol{M}(\pm\boldsymbol{Q}_0) = M/2(1\,0 \mp \mathrm{i})$, compare Fig. 2). For hexagonal symmetry of the interaction the difference $U_a(\boldsymbol{Q}_0) - U_c(\boldsymbol{Q}_0)$ and $X(\boldsymbol{Q}_0)$ are exactly zero, as may be seen by inserting $\boldsymbol{Q}_0 = (\frac{2}{3}\,1\,0)$ into Eq. (2). The ratio $\sigma = [U_a(\boldsymbol{Q}_0) - U_c(\boldsymbol{Q}_0)]/|2X(\boldsymbol{Q}_0)|$ may be used to characterize the eigenvectors corresponding to T_2/C and T_3/C:

$$\boldsymbol{M}_{2,3}(\boldsymbol{Q}) \propto \begin{pmatrix} \mathrm{i} \\ 0 \\ \sigma \pm \sqrt{1 + \sigma^2} \end{pmatrix}. \quad (7)$$

For the magnetic structure corresponding to this eigenvector the magnitude of the magnetic moment varies with its angle according to an 'elliptic' propagation. Note that when comparing the magnetic structure at low temperatures with Eq. (7) it is assumed that it does not change with temperature.

Only for $|\sigma| \ll 1$ the eigenvector ($\mathrm{i}\,0 \pm 1$) (corresponding to the cycloidal propagation with vanishing higher harmonics $3\boldsymbol{Q}_0$, compare Table 1) can be achieved. Therefore, in accordance with the findings in $NdCu_2$, there is strong evidence that the

diagonal elements $U_a(\boldsymbol{Q})$ and $U_c(\boldsymbol{Q})$ of the exchange are equal and the orthorhombic symmetry of the compound mainly causes nonzero off diagonal *ac* exchange tensor components ($X(\boldsymbol{Q}_0)$). According to Eq. (5) the ordering temperature T_N is given by

$$T_N = \frac{J(J+1)}{3k}[U_a(\boldsymbol{Q}_0) + |X(\boldsymbol{Q}_0)|]. \quad (8)$$

From Eqs. (4) and (5) it follows, that only if $U_b(\boldsymbol{Q}_0) < U_a(\boldsymbol{Q}_0) + |X(\boldsymbol{Q}_0)|$ this temperature will be the highest of the 3 values (T_1, T_2, T_3).

The analysis of the magnetic excitations of $NdCu_2$ [17] gave evidence that the anisotropy of the exchange is caused by a big difference of U_a and U_b. However, by de Gennes scaling of the exchange determined by the magnetic excitations and the magnetic phase diagram of $NdCu_2$, $U_i(\boldsymbol{Q})$ can be estimated for $GdCu_2$. The maximum in $U_b(\boldsymbol{Q})$ would then predict a collinear structure for $GdCu_2$ with an ordering vector of $(\frac{2}{3}\,0\,0)$, magnetic moments parallel to the *b* direction and an ordering temperature of 76 K (corresponding to T_1 in Eq. (4)). Therefore, the parameters of $NdCu_2$ cannot be used to describe the magnetic structure of $GdCu_2$ directly. The fact that T_N would be as high as 76 K suggests that the scaling of the exchange $U_i(\boldsymbol{Q})$ in the nearly hexagonal *ac* plane (i.e. for U_a and U_c) and perpendicular to it (i.e. for U_b) is *not* the same.

5. Calculation of the susceptibility

To check the validity of the proposed model we performed low-field measurements of the magnetization. In Fig. 5, we show the magnetization along the three crystallographic axes at 2 K and compare it with the result of the following model calculation. Using the magnetic structure given in Fig. 2 it is possible to calculate the magnetic susceptibility at zero temperature. The direction of the magnetic moment $\boldsymbol{M}_i$ at the site *i* and the effective magnetic field $\boldsymbol{H}_i^{\text{eff}}$ is equal, because there is no single ion anisotropy in $GdCu_2$, i.e.

$$\boldsymbol{M}_i = M\hat{\boldsymbol{H}}_i^{\text{eff}} = M\frac{\boldsymbol{H}_i^{\text{eff}}}{\boldsymbol{H}_i^{\text{eff}}}. \quad (9)$$

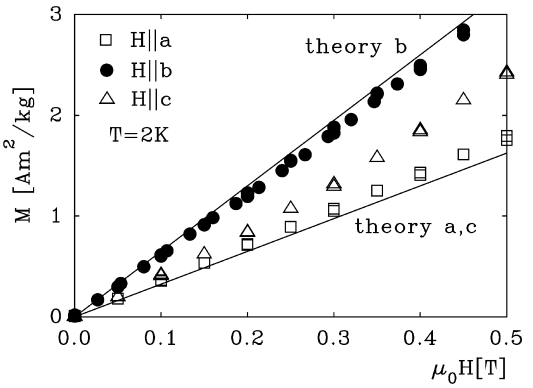

Fig. 5. Magnetization of $GdCu_2$ for fields parallel to the orthorhombic *a*-, *b*-, and *c*-axis at 2 K. The initial slope (corresponding to the susceptibility) can be calculated within a MF theory (see text) and is indicated.

The effective field $\boldsymbol{H}_i^{\text{eff}}$ is a sum of the internal exchange field $\boldsymbol{H}_i^{\text{mf}}$ and the external applied field $\boldsymbol{H}$.

$$\boldsymbol{H}_i^{\text{eff}} = \boldsymbol{H}_i^{\text{mf}} + \boldsymbol{H}. \quad (10)$$

By inserting Eq. (10) into Eq. (9) and denoting the angle between the external magnetic field $\boldsymbol{H}$ and the direction of the internal exchange field $\boldsymbol{H}_i^{\text{mf}}$ as α_i it is possible to calculate the component of the magnetic moment along the external field

$$\boldsymbol{M}_i \cdot \hat{\boldsymbol{H}} = M\frac{\boldsymbol{H}_i^{\text{mf}} + \boldsymbol{H}}{|\boldsymbol{H}_i^{\text{mf}} + \boldsymbol{H}|} \cdot \hat{\boldsymbol{H}}$$

$$= M\frac{\cos\alpha_i + H/H_i^{\text{mf}}}{\sqrt{1 + 2H/H_i^{\text{mf}}\cos\alpha_i + (H/H_i^{\text{mf}})^2}}. \quad (11)$$

Expanding Eq. (11) for small external fields $\boldsymbol{H}$ it is possible to calculate the change in the component of $\boldsymbol{M}_i$ along the direction of the external field $\boldsymbol{H}$

$$\Delta\boldsymbol{M}_i \cdot \hat{\boldsymbol{H}} = M\sin^2(\alpha_i)\frac{H}{H_i^{\text{mf}}}. \quad (12)$$

Summing up the contributions of the different neighbors according to our model exchange it is possible to show, that at zero external field the magnitude of the exchange field H_i^{mf} is equal for all different sites *i*, only the direction varies.

By averaging over the magnetic unit cell (Fig. 2) we can calculate the magnetic moment component

$\Delta \boldsymbol{M}_i \cdot \hat{\boldsymbol{H}}$ for small external fields along the *a*-, *b*- and *c*-axis — the result is

$$\Delta \boldsymbol{M} \cdot \hat{\boldsymbol{H}}_a = \frac{1}{2} M \frac{H_a}{H^{\mathrm{mf}}},$$

$$\Delta \boldsymbol{M} \cdot \hat{\boldsymbol{H}}_b = M \frac{H_b}{H^{\mathrm{mf}}},$$

$$\Delta \boldsymbol{M} \cdot \hat{\boldsymbol{H}}_c = \frac{1}{2} M \frac{H_c}{H^{\mathrm{mf}}}. \tag{13}$$

The absolute magnitude of the exchange field H^{mf} depends on the accurate values of the exchange constants (e.g. $B, F, \ldots$, see Table 2). Therefore, only the relative magnitude of the susceptibilities in *a*, *b* and *c* direction can be compared directly with the experiment. From Eq. (13) we get for the magnitude of the magnetic susceptibility $\chi_{a,b,c}$ along the three crystallographic axes

$$\chi_a = \chi_c = \tfrac{1}{2}\chi_b. \tag{14}$$

In Fig. 5, the magnetization at low fields is shown at 2.2 K. The magnetic behavior is nearly isotropic in high fields (compare Ref. [11]). However, below 1 T a small anisotropy can be found and the susceptibility for the three axes is different. The measurement and the theoretical result as given by Eq. (14) are in good qualitative agreement (see Fig. 5). To get a more accurate estimation, the small change of the mean fields $\boldsymbol{H}_i^{\mathrm{mf}}$ which is induced by a rotation of the moments in an external field and a possible small tilt of the moments (corresponding for example to nonzero σ) has to be considered, both leading to $\chi_a \neq \chi_c$.

6. Conclusion

The analysis of the magnetic bilinear R–R exchange in orthorhombic $GdCu_2$ (with a nearly hexagonal *ac* plane) by a mean-field theory suggests, that the magnetic exchange tensor is dominated by diagonal components. It shows hexagonal symmetry except for a small off diagonal contribution of neighboring Gd^{3+} ions within the same *ac* plane. This small off diagonal contribution may cause the observed cycloidal propagation of the moments within one *ac* plane. The anisotropy of the diagonal exchange constants, which has already been discussed extensively in Ref. [17], confines the moments to the nearly hexagonal *ac* plane of the crystal. The magnitude of the exchange energy and thus also the corresponding anisotropy energy is smaller than the crystal-field anisotropy which has been observed in other RCu_2 compounds. From the data presented here we conclude that the magnetic modulation vector in $GdCu_2$ is $\boldsymbol{Q}_0 = (\frac{2}{3}\,1\,0)$ as it was found for instance for $TbCu_2$ and $DyCu_2$. Referring to the model presented in Refs. [17,21], which states, that RCu_2 compounds may order either with a propagation of $(\frac{2}{3}\,0\,0)$ or $(\frac{2}{3}\,1\,0)$ we conclude, that $GdCu_2$ belongs to the second group. Consequently, the magnetic moments should be confined to the *ac* plane of the crystal and show an antiferromagnetic arrangement in *b* direction. We have proposed a magnetic structure which is in accordance with this prediction. The magnetic neutron intensities calculated from this structure agree with our measurements within the experimental error. A possible temperature dependence of the propagation vector $\boldsymbol{Q}_0$, a possible small deviation from its commensurate value and the magnitude of higher harmonics might be estimated more accurately from magnetic X-ray scattering experiments.

Acknowledgements

We appreciate the fruitful discussions with M. Ellerby, M. Loewenhaupt and G. Lander. We acknowledge support by the Austrian Science Foundation (FWF) project nos. P-11239-PHY, P-11581-PHY and S5605. Part of this work was performed within the program of the Sonderforschungsbereich 463 (funded by the Deutsche Forschungsgemeinschaft).

References

[1] A.R. Storm, K.E. Benson, Acta Crystallogr. 16 (1963) 701.
[2] P. Svoboda, M. Doerr, M. Loewenhaupt, M. Rotter, T. Reif, F. Bourdarot, P. Burlet, Europhys. Lett. 48 (1999) 410.
[3] R.C. Sherwood, H.J. Williams, J.H. Wernik, J. Appl. Phys. 35 (1964) 1049.

[4] T.O. Brun, G.P. Felcher, J.S. Kouvel, J. Magn. Magn. Mater. 5 (1971) 1376.
[5] N.H. Luong, J.J.M. Franse, T.D. Hien, J. Magn. Magn. Mater. 50 (1985) 153.
[6] B. Lebech, Z. Smetana, V. Sima, J. Magn. Magn. Mater. 70 (1987) 97.
[7] M. Loewenhaupt, T. Reif, P. Svoboda, S. Wagner, M. Waffenschmidt, H.v. Loehneysen, E. Gratz, M. Rotter, B. Lebech, T. Hauss, Z. Phys. B 101 (1996) 499.
[8] A. Koyanagi, Y. Yoshida, Y. Kimura, R. Settai, K. Sugiyama, Y. Onuki, J. Phys. Soc. Japan 67 (1998) 2510.
[9] N.H. Luong, J.J.M. Franse, Phys. Stat. Sol. 66 (81) 399.
[10] N.H. Luong, J.J.M. Franse, T.D. Hien, J. Phys. F 15 (1985) 1751.
[11] M.K. Borombaev, R.Z. Levitin, A.S. Markosyan, V.A. Reimer, A.V. Sinitsyn, Z. Smetana, Z. Sov. Phys. JETP 66 (1987) 866.
[12] K. Poldy, H. Kirchmayer, Phys. Stat. Sol. B 65 (1974) 553.
[13] Th. B. Massalski, H. Okamoto, P.R. Subramanian, L. Kacprzak (Eds.), Binary Phase Diagrams, Vol. 140–144, ASM International, 1990, p. 1131.
[14] G. Christiansen, L. Gerward, I. Alstrup, Acta Crystallogr. A 31 (1975) 142.
[15] J. Rodriguez-Carvajal, Physica B 192 (1993) 55.
[16] T. Chattopadhyay, G.J. McIntyre, U. Koebler, Solid State Commun. 100 (1996) 117.
[17] M. Rotter, M. Loewenhaupt, S. Kramp, T. Reif, N.M. Pyka, W. Schmidt, R. Kamp, Europ. Phys. J. B 14 (2000) 29.
[18] B. Haelg, A. Furrer, Phys. Rev. B 34 (1986) 6258.
[19] E. Gratz, A. Lindbaum, J. Magn. Magn. Mater. 137 (1994) 115.
[20] A. Lindbaum, M. Rotter (2000), review article in preparation.
[21] M. Loewenhaupt, M. Rotter, S. Kramp, Physica B 276–278 (2000) 602.

ELSEVIER

Journal of Magnetism and Magnetic Materials 236 (2001) 267–271

Journal of magnetism and magnetic materials

www.elsevier.com/locate/jmmm

Magnetic exchange driven magnetoelastic properties in $GdCu_2$

M. Rotter[a,*], M. Doerr[a], M. Loewenhaupt[a], A. Lindbaum[b], H. Müller[b], J. Enser[b], E. Gratz[b]

[a] *Institut für Angewandte Physik, Technische Universität Dresden, D- 01062 Dresden, Germany*
[b] *Institut für Experimentalphysik, Technische Universität Wien, Wiedner Hauptstraße 8-10, A-1040 Wien, Austria*

Received 29 March 2001; received in revised form 18 July 2001

Abstract

The magnetoelastic properties of $GdCu_2$ have been investigated by thermal expansion and magnetostriction measurements. $GdCu_2$ orders antiferromagnetically with a noncollinear magnetic structure. The anisotropic magnetostriction is of similar magnitude as in other RCu_2 compounds and can be explained by a contribution of the bilinear exchange interaction to the magnetoelastic energy. For several compounds this contribution is as important as the single ion magnetoelastic exchange. The pressure dependence of the Néel temperature of $GdCu_2$ is found to be in agreement with the data of thermal expansion.

PACS: 75.50.E; 75.30.E; 75.80

Keywords: Anisotropic magnetic exchange; Noncollinear antiferromagnetism; Magnetostriction; Thermal expansion; Gadolinium compounds

1. Introduction

Magnetoelastic properties have been investigated extensively in rare earth systems and are mainly attributed to the presence of strong single ion magnetoelastic coupling [1]. However, in some Gd compounds relatively large magnetoelastic effects are observed which cannot be explained by this mechanism, because Gd^{3+} is an S-state ion with $L = 0$. This fact is not widely known, because in many cases magnetoelastic effects are not analyzed and the number of compounds studied is very limited. Details about the second mechanism, the contribution of exchange interactions to the magnetoelastic energy, are still unknown and it is desirable to accumulate more detailed data of thermal expansion and magnetostriction in Gd-compounds. Therefore, we have performed a study of the orthorhombic intermetallic compound $GdCu_2$.

The thermal expansion of $GdCu_2$ has been measured already in 1985 on polycrystals by dilatometric experiments [2] and by X-ray diffraction on powder [3] and single crystals [4]. The measurements of the thermal expansion and magnetostriction reported here are performed by dilatometry on a single crystal in fields up to 15T.

*Tel.: +49-351-463-4460; fax: +49-351-463-3199.
E-mail address: rotter@physik.tu-dresden.de (M. Rotter).

0304-8853/01/$ - see front matter
PII: S0304-8853(01)00474-7

2. Results

The single crystal was produced by the Bridgeman method, details are given in Refs. [5,6]. Thermal expansion and magnetostriction measurements have been performed using a capacitance dilatometer, which has been designed to measure very small single crystals [7]. Measurements at low temperatures down to 500 mK have been performed in a bottom loading ^{3}He temperature insert of a 15 T superconducting magnet (Heliox, Oxford Instruments).

Fig. 1 shows the thermal expansion measured along the *a*-, *b*- and *c*-axis in zero field in comparison with results of powder X-ray diffraction [3,8]. Below the ordering temperature T_N = 40.5 K the thermal expansion coefficient is positive in the *a*-direction and negative in the *b*- and *c*-direction. These anisotropic contributions cancel each other leading to a nearly zero volume effect. Such a behavior is caused by a magnetoelastic energy of similar magnitude as in other RCu_2 compounds [8,9]. Above T_N the crystal expands in all crystallographic directions as expected. It can be mentioned that the results are in good agreement with those obtained by X-ray diffraction on single crystals [4].

Fig. 2 shows the field induced magnetostriction for external fields along the *a*-, *b*- and *c*-axis. All measurements were done with increasing and decreasing field and they show only a small hysteresis. Below $\mu_0 H = 5$ T the magnetostrictive effects are rather small. Above this value two remarkable kinks occur at 5.5 and 8.0 T, approximately, which are connected to the two magnetic phase transitions which were also found in magnetization measurements [4]. Above 8.0 T the system is in the induced ferromagnetic state and no further transitions could be seen when continuing some of the scans up to 15 T (not shown here). From all the data it is evident that the field induced magnetostriction is strongly different for the different crystallographic axes (leading again to a very small volume effect) but is nearly independent of the magnetic field direction. The only difference between the different field directions was found examining the low field

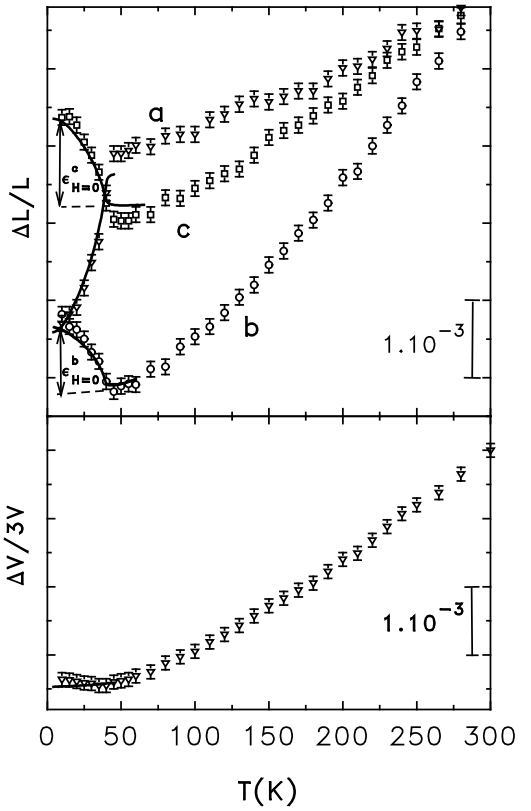

Fig. 1. Thermal expansion coefficient of $GdCu_2$ along the orthorhombic *a*-, *b*- and *c*-direction (upper figure) and the volume expansion calculated from these data (bottom figure, scale expanded by factor 3 to facilitate comparison with upper figure). The symbols denote the results of powder X-ray diffraction [3,8], the lines correspond to expansion measurements on a single crystal using the capacitance method (present investigation). The values $\varepsilon_{H=0}$ denote the relative length changes in the ordered state with respect to the nonmagnetic state (for details see text).

behavior more closely (compare inset in Fig. 2, there the derivatives of the $\Delta c/c$ curves are shown as an example). There some small differences between the curves may be deduced. A transition at 0.6 and 1.2 T is observed for fields parallel to *a*- and *c*-, respectively. No phase transition is observed for $\mathbf{H}_{\|}b$. This is in accordance with the findings from the magnetization experiments on a single crystal [4] and can be attributed to the fact, that in zero field the moments are confined to the *ac*-plane.

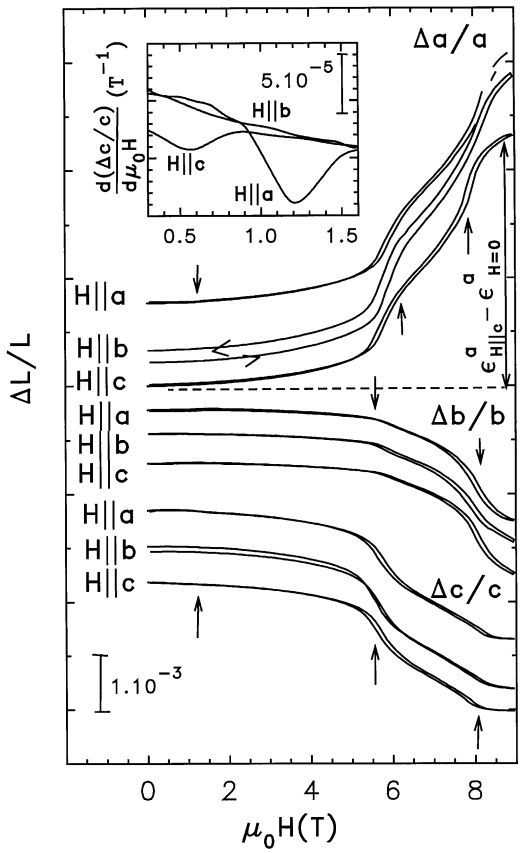

Fig. 2. Magnetostriction $\Delta a/a$, $\Delta b/b$ and $\Delta c/c$ of $GdCu_2$ for magnetic fields parallel to the orthorhombic a-, b- and c-axis at 4.2 K. The arrows indicate the position of phase transitions. For each curve the hysteresis is shown. The inset shows the low field data of the derivative of $\Delta c/c$ with respect to the magnetic field.

3. Discussion

It is possible to calculate the thermal expansion and magnetostriction ε (ε denotes any of the relative length changes $\Delta a/a$, $\Delta b/b$, $\Delta c/c$ with respect to the nonmagnetic state) in a simple model based on the magnetoelastic contribution due to the exchange interaction. The Helmholtz free energy F per ion may be written as a sum of exchange, magnetoelastic and elastic contributions

$$F = -\frac{1}{2}\sum_{\mathbf{q}\in BZ}\mathbf{M}^T(-\mathbf{q})\left[\overline{\overline{\mathscr{J}}}(\mathbf{q},\varepsilon=0) + \varepsilon\frac{\partial\overline{\overline{\mathscr{J}}}(\mathbf{q},\varepsilon)}{\partial\varepsilon}\bigg|_{\varepsilon=0}\right]\mathbf{M}(\mathbf{q}) + K\frac{\varepsilon^2}{2}, \quad K>0 \tag{1}$$

Here, $\overline{\overline{\mathscr{J}}}(\mathbf{q},\varepsilon)$, $\mathbf{M}(\mathbf{q})$ denote the Fourier transform of the anisotropic exchange interaction tensor and of the magnetic moment, respectively [10]. Note that expression (1) becomes more complicated if the anisotropy of the elastic constant K is also taken into account [1], however, without changing the final result. Minimizing F with respect to ε gives

$$\varepsilon = \frac{1}{2K}\sum_{\mathbf{q}\in BZ}\mathbf{M}^T(-\mathbf{q})\frac{\partial\overline{\overline{\mathscr{J}}}(\mathbf{q},\varepsilon)}{\partial\varepsilon}\bigg|_{\varepsilon=0}\mathbf{M}(\mathbf{q}). \tag{2}$$

This formula can be evaluated for the zero field and for the saturated phases along a, b and c. For the zero field phase (magnetic modulation vector $\mathbf{q}_0 = (2/3\,1\,0)$) we use Eq. [5]

$$\mathbf{M}(\pm\mathbf{q}_0) = \frac{M}{2}\begin{pmatrix}1\\0\\\mp i\end{pmatrix}. \tag{3}$$

Here, M denotes the saturation moment of Gd. Substituting Eq. (3) into Eq. (2) leads to the following expression for the magnetoelastic distortion in zero field:

$$\varepsilon_{H=0} = \frac{M^2}{4K}\frac{\partial\mathscr{J}_{aa}(\mathbf{q}_0,\varepsilon)+\mathscr{J}_{cc}(\mathbf{q}_0,\varepsilon)}{\partial\varepsilon}\bigg|_{\varepsilon=0}. \tag{4}$$

For the saturated ferromagnetic phases in high magnetic field we insert in Eq. (2) ($\hat{\mathbf{H}}$ denotes the unit vector in the direction of the applied magnetic field)

$$\mathbf{M}(\mathbf{q}) = \begin{cases} M\hat{\mathbf{H}} & q=0,\\ 0 & q\neq 0,\end{cases} \tag{5}$$

and get

$$\varepsilon_{\mathbf{H}\|a} = \frac{M^2}{2K}\frac{\partial\mathscr{J}_{aa}(q=0,\varepsilon)}{\partial\varepsilon}\bigg|_{\varepsilon=0}, \tag{6}$$

$$\varepsilon_{\mathbf{H}\|b} = \frac{M^2}{2K}\frac{\partial\mathscr{J}_{bb}(q=0,\varepsilon)}{\partial\varepsilon}\bigg|_{\varepsilon=0}, \tag{7}$$

$$\varepsilon_{\mathbf{H}\|c} = \frac{M^2}{2K}\frac{\partial\mathscr{J}_{cc}(q=0,\varepsilon)}{\partial\varepsilon}\bigg|_{\varepsilon=0}. \tag{8}$$

Analyzing the exchange interaction of orthorhombic (but nearly hexagonal) $GdCu_2$ it is now possible to find a relation between Eqs. (4) and (6)–(8) and compare this result with the

experimental data measured by thermal expansion and magnetostriction. With the assumption that the magnetoelastic interaction is dominated by the next neighbor contribution in b-direction it can be shown by symmetry that

$$\mathcal{J}_{\gamma\gamma}(q=0,\varepsilon) = -\mathcal{J}_{\gamma\gamma}(\mathbf{q}_0,\varepsilon) \quad (\gamma = a,b,c). \tag{9}$$

Combining now Eqs. (4)–(9) we obtain as a result of the model calculation

$$\varepsilon_{H=0} = -\frac{\varepsilon_{\mathbf{H}\|a} + \varepsilon_{\mathbf{H}\|c}}{2}. \tag{10}$$

The result of Eq. (10) should be valid for all crystallographic directions. It can be verified by a comparison of the zero field data of thermal expansion (shown in Fig. 1) with the data of magnetostriction (see Fig. 2): to find the values $\varepsilon^{\gamma}_{H=0}$ it is necessary to extrapolate the thermal expansion curves of the nonmagnetic state from higher temperatures to temperatures below T_N. The differences between these extrapolated curves and the measured ones (in Fig. 1 shown for the b- and c-axis for example) give the values $\varepsilon^{a}_{H=0} = -2.1\times10^{-3}$, $\varepsilon^{b}_{H=0} = 0.9\times10^{-3}$ and $\varepsilon^{c}_{H=0} = 1.1\times10^{-3}$ at $T = 4\,\mathrm{K}$. On the other hand, from the difference in the magnetostriction curves between $\mu_0 H = 0$ and 9 T we get the values of $\varepsilon^{\gamma}_{\mathbf{H}\|a}$, $\varepsilon^{\gamma}_{\mathbf{H}\|b}$ and $\varepsilon^{\gamma}_{\mathbf{H}\|c}$. It should be mentioned that in order to find the difference in length between the saturated magnetic and the nonmagnetic state, the zero field value from Fig. 1 has to be added to the total magnetostriction shown in Fig. 2. The result of the calculation is summarized in Table 1.

By comparing the data shown in Table 1 (last two columns) we find the relation (10) is valid within 20% for any of the three crystallographic axes. This agreement is very good for a model that only takes into account the next neighbor interaction. We take this as an evidence that the magnetoelastic interaction in $GdCu_2$ is indeed dominated by the next neighbor exchange interaction in b-direction. In contrast to this behavior, the nearest neighbor in the (nearly) hexagonal ac plane would give a contribution $\mathcal{J}_{\gamma\gamma}(q=0,\varepsilon) = -2\mathcal{J}_{\gamma\gamma}(\mathbf{q}_0,\varepsilon)$ leading to $\varepsilon_{H=0} = -(\varepsilon_{\mathbf{H}\|a} + \varepsilon_{\mathbf{H}\|c})/4$, which is in disagreement with the experimental data (for comparison, the magnetoelastic interaction in $NdCu_2$ [8,11] is dominated by the next neighbors in a-direction).

Now two other points should be discussed: Note at first the experimental result that the strains do not depend on the direction of the magnetic field (compare Fig. 2), i.e.

$$\varepsilon_{\mathbf{H}\|a} \sim \varepsilon_{\mathbf{H}\|b} \sim \varepsilon_{\mathbf{H}\|c} \equiv \varepsilon_{\mathrm{sat}}. \tag{11}$$

Comparing this experimental result to the model equations (6)–(8) and (9) it follows that

$$\left.\frac{\partial\left[\mathcal{J}_{aa}(\mathbf{q}_0,\varepsilon)\right]}{\partial\varepsilon}\right|_{\varepsilon=0} \sim \left.\frac{\partial\left[\mathcal{J}_{bb}(\mathbf{q}_0,\varepsilon)\right]}{\partial\varepsilon}\right|_{\varepsilon=0} \sim \left.\frac{\partial\left[\mathcal{J}_{cc}(\mathbf{q}_0,\varepsilon)\right]}{\partial\varepsilon}\right|_{\varepsilon=0}. \tag{12}$$

This means that the derivatives of the diagonal components of the exchange interaction are equal with respect to any strain ε and Eq. (10) becomes simply

$$\varepsilon_{\mathrm{sat}} \sim -\varepsilon_{H=0}. \tag{13}$$

The experimental result (11) is very peculiar since there is evidence that the magnetic exchange interaction is anisotropic (the experimental evidence that the ordered moment in zero field is confined to the ac-plane may be attributed to the exchange anisotropy $\mathcal{J}_{bb}(\mathbf{q}_0,\varepsilon) < \mathcal{J}_{aa}(\mathbf{q}_0,\varepsilon) \sim \mathcal{J}_{cc}(\mathbf{q}_0,\varepsilon)$ [12]). There is no reason, why its derivative with respect to the strain should be isotropic (12). Looking for any deviations from Eq. (11) in the experimental data (Fig. 2) we see

Table 1
Comparison of measured data and magnetostriction data calculated by Eq. (10) for a $GdCu_2$ single crystal

Cryst. direction γ	$\varepsilon^{\gamma}_{\mathbf{H}\|a} - \varepsilon^{\gamma}_{H=0}$ (From Fig. 2)	$\varepsilon^{\gamma}_{\mathbf{H}\|c} - \varepsilon^{\gamma}_{H=0}$ (From Fig. 2)	$\varepsilon^{\gamma}_{H=0}$ (From Fig. 1)	$\varepsilon^{\gamma}_{H=0} = -(\varepsilon^{\gamma}_{\mathbf{H}\|a} + \varepsilon^{\gamma}_{\mathbf{H}\|c})/2$ (From Eq. (10))
a	$+4.4\times10^{-3}$	$+4.4\times10^{-3}$	-2.1×10^{-3}	-2.3×10^{-3}
b	-2.0×10^{-3}	-2.0×10^{-3}	$+0.9\times10^{-3}$	$+1.1\times10^{-3}$
c	-2.2×10^{-3}	-2.2×10^{-3}	$+1.1\times10^{-3}$	$+1.1\times10^{-3}$

that the magnetostriction ($\Delta a/a$, $\Delta c/c$) for fields parallel to b is slightly higher in comparison with fields parallel to a or c. We take this as an evidence that the strain derivative of $\mathcal{J}_{bb}(\mathbf{q}_0,\varepsilon)$ is indeed slightly different from that of $\mathcal{J}_{aa}(\mathbf{q}_0,\varepsilon)\sim\mathcal{J}_{cc}(\mathbf{q}_0,\varepsilon)$ as expected from the anisotropy of the exchange interaction [12].

Another important issue raised by a former analysis of the magnetic contribution to the thermal expansion was the validity of Ehrenfest's theorem in this compound [2]. According to this theorem the pressure dependence of the Néel temperature T_N is related to the magnetic contribution of the volume expansion coefficient $\alpha = (1/V)(\partial V/\partial T)$ and the specific heat c

$$\frac{\partial \ln T_N}{\partial p} = \frac{V\alpha}{c}. \tag{14}$$

Here, V denotes the molar volume. The dilatometric measurements of the thermal expansion of polycrystals [2] indicated a large positive value of the magnetic contribution to the volume expansion coefficient (about $\alpha = 3\times10^{-5}\,\mathrm{K}^{-1}$), which is in contradiction to the negative pressure dependence of the Néel temperature of $-0.2\times10^{-8}\,\mathrm{Km}^2\,\mathrm{N}^{-1}$ as determined by magnetization measurements in a high pressure cell [2].

Taking from our X-ray data the volume expansion $\Delta V/V = \varepsilon^a_{H=0}+\varepsilon^b_{H=0}+\varepsilon^c_{H=0}$ (shown in Fig. 1, bottom) we find that the magnetic contribution to the volume expansion in $GdCu_2$ is very small, but positive. The corresponding negative magnetic thermal expansion coefficient $\alpha = -3\times10^{-5}\,\mathrm{K}^{-1}$ indicates a negative pressure dependence of the Néel temperature thus removing the difficulties in applying Ehrenfest's relation to $GdCu_2$ in Ref. [2].

The positive value of α for the polycrystalline data in Ref. [2] is probably caused by the fact, that it is extremely difficult to produce an isotropic polycrystal in RCu_2 compounds [4] (we also have performed several dilatometric measurements of thermal expansion on polycrystalline samples which indicate a strong preferred orientation).

A further test of Ehrenfest's relation with respect to the data of anisotropic thermal expansion requires the determination of the shift of the Néel temperature under uniaxial stress. From the experimental data of thermal expansion and the Eqs. (4) and (12) the signs of the strain derivatives of the exchange interaction can be derived: $(\partial\mathcal{J}_{\gamma\gamma}(\mathbf{q}_0,\varepsilon)/\partial\varepsilon^a)<0$, $(\partial\mathcal{J}_{\gamma\gamma}(\mathbf{q}_0,\varepsilon)/\partial\varepsilon^b)>0$ and $(\partial\mathcal{J}_{\gamma\gamma}(\mathbf{q}_0,\varepsilon)/\partial\varepsilon^c)>0$. Therefore, uniaxial pressure along a should increase the Néel temperature, whereas uniaxial pressure along b or c will decrease it. This is a possible outlook to further experiments.

Acknowledgements

We appreciate the fruitful discussions with M. Ellerby. This work was performed within the program of the Sonderforschungsbereich 463 (funded by the Deutsche Forschungsgemeinschaft). Part of this work was supported by the Austrian science foundation (FWF) projects No. P-11239-PHY, P-11581-PHY and S5605.

References

[1] P. Morin, D. Schmitt, in: K.H.J. Buschow, E.P. Wohlfarth (Eds.), Ferromagnetic Materials, Vol. 5, Elsevier, Amsterdam, 1990, 1.
[2] N.H. Luong, J.J.M. Franse, T.D. Hien, J. Phys. F.: Met. Phys. 15 (1985) 1751.
[3] E. Gratz, A. Lindbaum, J. Magn. Magn. Mater. 137 (1994) 115.
[4] M.K. Borombaev, R.Z. Levitin, A.S. Markosyan, V.A. Reimer, A.V. Sinitsyn, Z. Smetana, Z. Sov. Phys. JETP 66 (1987) 866.
[5] M. Rotter, A. Lindbaum, E. Gratz, H. Müller, G. Hilscher, H. Sassik, H.E. Fischer, M.T. Fernandes-Diaz, R. Arons, E. Seidl, J. Magn. Magn. Mater. 214 (2000) 281.
[6] M. Rotter, A. Schneidewind, M. Loewenhaupt, M. Doerr, A. Stunault, A. Hiess, A. Lindbaum, E. Gratz, G. Hilscher, H. Sassik, Physica B 284–288 (2000) 1329.
[7] M. Rotter, H. Müller, E. Gratz, M. Doerr, M. Loewenhaupt, Rev. Sci. Instrum. 69 (1998) 2742.
[8] M. Rotter, Ph.D. Thesis, Technische Universität Wien, 1994.
[9] M. Loewenhaupt, M. Doerr, L. Jahn, T. Reif, C. Sierks, M. Rotter, H. Müller, Physica B 246–247 (1998) 472.
[10] M. Rotter, M. Loewenhaupt, M. Doerr, A. Lindbaum, H. Michor, Phys. Rev. B 64 (2001) 14402, 1–8.
[11] S.W. Zochowski, M. Rotter, E. Gratz, K.A. McEwen, J. Magn. Magn. Mater. 140–144 (1995) 1129.
[12] M. Rotter, M. Loewenhaupt, S. Kramp, T. Reif, N.M. Pyka, W. Schmidt, R.V.D. Kamp, Eur. Phys. J. B 14 (2000) 29.

ELSEVIER

Physica B 284–288 (2000) 1329–1330

PHYSICA B

www.elsevier.com/locate/physb

Magnetic scattering on $GdCu_2$

M. Rotter[a,*], A. Schneidewind[a], M. Loewenhaupt[a], M. Doerr[a], A. Stunault[b], A. Hiess[c], A. Lindbaum[d], E. Gratz[e], G. Hilscher[e], H. Sassik[e]

[a]*Institut für Angewandte Physik, Technische Universität Dresden, D-01062 Dresden, Germany*
[b]*XMaS, the UK (CRG) European Synchrotron Radiation Facility, BP 220, F-38043 Grenoble Cedex, France*
[c]*Institut Laue Langevin, F-38042 Grenoble, France*
[d]*European Comission Institute for Transuranium Elements, Postfach 2340, D-76125 Karlsruhe, Germany*
[e]*Institut für Experimentalphysik, Technische Universität Wien, 1040 Vienna, Austria*

Abstract

Magnetic neutron and X-ray scattering experiments have been performed to analyze the magnetic structure of $GdCu_2$. At 10 K a noncollinear, spiral propagation with a propagation vector $\tau = (0.677\,1\,0)$ fits best to the experimental data. The symmetry of the exchange interaction needed for the formation of such a magnetic structure is discussed using a mean field model. The orthorhombic structure of $GdCu_2$ can be viewed as a distorted hexagonal structure. © 2000 Elsevier Science B.V. All rights reserved.

Keywords: $GdCu_2$; Magnetic structure; Magnetic X-ray scattering; Neutron scattering

The RCu_2 compounds (R = rare earth) with the exception of $LaCu_2$ exhibit the orthorhombic $CeCu_2$ type structure (space group Imma, D_{2h}^{28}), which can be viewed as a distorted AlB_2-type structure. $LaCu_2$ displays the related hexagonal AlB_2 structure (space group P_6/mmm, D_{6h}^{1}).

The spin structure in the various RCu_2 intermetallics is intimately related to the interplay of the exchange and the crystal field. Because of the pure S state of the Gd^{3+} ion the influence of the crystal field in $GdCu_2$ is negligible leading to a nearly isotropic magnetisation [1]. This Gd-based compound can be used to clarify which magnetic structure appears if the exchange interaction is solely responsible for the magnetic structure.

Neutron scattering experiments have been performed at 4 K, yielding cycloidal moments in the *ac* plane with a propagation vector of (2/3 1 0). No magnetic intensity has been observed on higher harmonics. Fig. 1 shows the proposed cycloidal magnetic structure in a projection onto the (nearly hexagonal) *ac*-plane. The anisotropy of the magnetisation at 2 K has been explained on the basis of this commensurate structure [2].

In this paper we discuss a model for the magnetic interactions as deduced from recent experiments on this compound. First we note in Fig. 2 that the magnetisation of $GdCu_2$ (measured in a SQUID magnetometer at 0.5 T) becomes isotropic in the *ac*-plane above 10 K. An incommensurate magnetic structure can explain this behavior.

To investigate the magnetic structure in more detail we performed resonant X-ray magnetic scattering experiments on the BM28 Xmas beamline, the UK CRG beamline at the ESRF. We used a $GdCu_2$ single crystal grown by a Bridgeman technique (with a pulling speed of 4.5 mm/h and RF heating). A closed cycle refrigerator allowed to reach temperatures down to 10 K. The energy was tuned to the Gd-L_{II}-edge (E = 7.932 keV). The incident polarisation was perpendicular to the (vertical) scattering plane. Polarisation analysis was used to select the scattered photons with a polarisation parallel to the scattering plane (rotated channel σ–π). This allowed to separate the magnetic scattering from the charge scattering, and to reduce the fluorescence background by several orders of magnitude.

Measurements on several magnetic satellites yield an incommensurate magnetic structure in the temperature

* Corresponding author. Fax: 49-351-463-3199.
E-mail address: rotter@physik.tu-dresden.de (M. Rotter)

0921-4526/00/$ - see front matter
PII: S0921-4526(99)02608-3

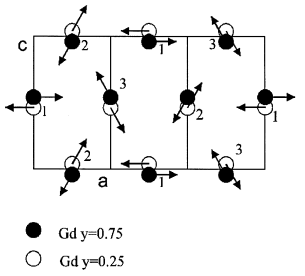

Fig. 1. The proposed magnetic structure of $GdCu_2$. The numbers indicate the three different super-imposed simple antiferromagnetic lattices. In the incommensurate structure (above 10 K) the turning angle after $3a$ is not exactly 360°.

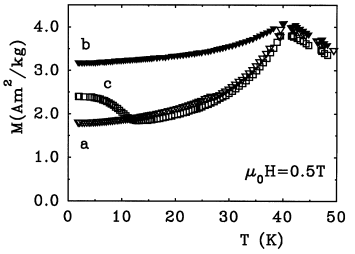

Fig. 2. Temperature dependence of the magnetization of $GdCu_2$.

range from 40 down to 10 K. The temperature variation of the propagation vector $(2/3 + \varepsilon\, 1\, 0)$ is due to thermal expansion (see Fig. 3). The observation of an incommensurate structure in the whole temperature range from 10 to 40 K is consistent with the isotropic susceptibility in the *ac*-plane above 10 K. The observed *ac*-anisotropy of the magnetization below 10 K suggests a transition into a commensurate phase.

The analysis of the magnetic bilinear R–R exchange in orthorhombic $GdCu_2$ (with a nearly hexagonal *ac*-plane)

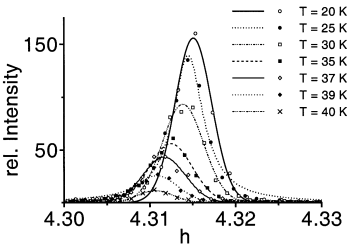

Fig. 3. Q-scans of the magnetic $(13/3 - \varepsilon\ -1\ 3)$ reflection.

by a mean field theory suggests, that the magnetic exchange tensor is dominated by diagonal components [2]. It shows hexagonal symmetry except for a small off diagonal contribution of neighboring Gd^{3+} ions within the same *ac*-plane. This small off diagonal contribution may cause the cycloidal propagation of the moments within one *ac*-plane. Further X-ray scattering experiments would be important to give evidence about the transition to the presumably commensurate phase below 10 K.

Acknowledgements

The work was supported by the Deutsche Forschungsgemeinschaft (Sonderforschungsbereich 463) and by the Austrian Science Foundation pro. No. S-5605.

References

[1] M.K. Borombaev et al., Z. Sov. Phys. JETP 66 (1987) 866.
[2] M. Rotter et. al., J. Mag. Mag. Mat., submitted for publication.

Interpreting magnetic X-ray scattering on Gd-compounds using the McPhase simulation program

M. Rotter [a,b] A. Schneidewind [b] M. Doerr [b] M. Loewenhaupt [b] A. M. el Massalami [c] C. Detlefs [d]

[a] *Institut für Physikalische Chemie, Universität Wien, A–1090 Wien, Austria*
[b] *Institut für Festkörperphysik, Technische Universität Dresden, D–01062 Dresden, Germany*
[c] *Instituto de Fisica - UFRJ, Caixa Postal 68528, 21945-970, Rio de Janeiro, Brazil*
[d] *European Synchrotron Radiation Facility, BP 220, F-38043 Grenoble, France*

Abstract

Magnetic x-ray scattering experiments on Gd-compounds provide valuable information about the magnetic structure, which is difficult to obtain by neutron scattering due to the large absorption cross section of Gd. The interpretation of the results is usually difficult and sometimes ambiguous and it would be desirable to have quantitative calculations in order to verify or disprove theoretical models by the data of scattering experiments. Such model calculations have been performed for the magnetic properties of the antiferromagnets $GdNi_2B_2C$ and $GdCu_2$. The results of this calculation are compared with experimental data from magnetic x-ray scattering experiments.

Key words: magnetic x-ray diffraction, Gd compounds, $GdNi_2B_2C$, $GdCu_2$
PACS: 75.25.+z, 75.30.Gw

The magnetic anisotropy of rare earth compounds usually is caused by the crystal field, unless the $4f$ angular momentum is zero ($L = 0$) such as in the case of Gd^{3+}. The small but finite magnetic anisotropy of $L = 0$ rare earth compounds is reflected in the orientation of the moments with respect to the crystal lattice, which can be determined by magnetic scattering experiments. Because neutron diffraction on Gd compounds is difficult due to the large absorption cross section of Gd, magnetic x-ray diffraction (MXD) using synchrotron light sources is a welcome alternative. The moment direction can be investigated using polarization analysis . The confrontation of these data with a quantitative model analysis may lead to new insights about the magnetic interactions. Here we assume a simple model based on the following Hamiltonian

$$\mathcal{H} = -\frac{1}{2}\sum_{ij}^{i\neq j}\left\{\mathcal{J}(ij)\mathbf{J}_i\mathbf{J}_j + \sum_{\alpha\beta} J_i^{\alpha}\mathcal{J}_{\alpha\beta}^{CD}(ij)J_j^{\beta}\right\} \quad (1)$$

where the anisotropy enters only via the second term which corresponds to the classical dipole interaction

$$\frac{\mathcal{J}_{\alpha\beta}^{CD}(ij)}{(g_J\mu_B)^2} = \frac{3(R_i^{\alpha}-R_j^{\alpha})(R_i^{\beta}-R_j^{\beta}) - \delta_{\alpha\beta}|\mathbf{R}_i-\mathbf{R}_j|^2}{|\mathbf{R}_i-\mathbf{R}_j|^5}$$

In these equations $\mathbf{R}_i$ denotes the lattice vector of the i^{th} Gd ion, J_i^α ($\alpha = 1, 2, 3$) the three components of the total angular momentum, g_J the Landé factor and μ_B the Bohr magneton. In the following we report the interpretation of MXD on two noncollinear antiferromagnets using a model analysis based on the Hamiltonian (1).

1. $GdCu_2$

$GdCu_2$ crystallizes in the orthorhombic $CeCu_2$ type of structure (space group *Imma*). At the Néel temperature of $T_N = 41$ K the specific heat indicates an equal moment magnetic structure [1]. A noncollinear magnetic structure [2] was found by neutron diffraction. MXD [3] and μSR [4] agree with these results. The magnetostriction was interpreted quantitatively using correlation functions derived from the magnetic structure [5].

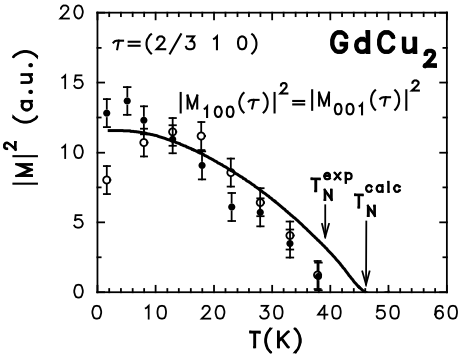

Fig. 1. $GdCu_2$ - temperature dependent measured MXD intensities on (3.6667 -1 1). Open (full) symbols correspond to $\pi\pi$ ($\pi\sigma$) MXD intensities, respectively. Lines correspond to the calculated temperature dependence of the squared FT of the magnetic moment configuration.

We have used MXD with polarization analysis to investigate the temperature dependence of the magnetic structure. In order to interpret our data a model calculation based on the Hamiltonian (1) was performed using the *McPhase* program [6, *www.mcphase.de*]. From the diagonal, but anisotropic exchange parameters found for $NdCu_2$ [7] only the isotropic part was taken and de Gennes scaled in order to obtain the exchange interaction for $GdCu_2$:

$$\frac{\mathcal{J}^{\mathrm{GdCu_2}}(ij)}{(g_J^{Gd}-1)^2} = \frac{\sum_{\alpha=a,b,c}\mathcal{J}_{\alpha\alpha}^{\mathrm{NdCu_2}}(ij)}{3(g_J^{Nd}-1)^2} \qquad (2)$$

In addition, the classical dipolar exchange for 1584 neighbors up to 3 nm was taken into account in the *McPhase* calculation.

At low temperatures the calculated magnetic structure differs by a small tilt of the magnetic moments (8 deg. in the *ac* plane) from the structure suggested by the neutron scattering experiments [2]. Such a tilt cannot be deduced with the neutron diffraction and was already suggested by μSR [4]. The temperature dependence of the Fourier transform (FT) of the magnetic moments $\mathbf{M}(\tau)$ has been computed and is compared in fig. 1 to the temperature dependence of the MXD intensity measured on the main propagation vector with *ab* in the scattering plane. The temperature dependence of the $\pi\sigma$ intensity (sensitive to both M_{100} and M_{010}) agrees well with the calculated moment component along a (M_{100}), because the component M_{010} is zero at all temperatures (both in the calculation and as determined from the MXD results in the *ac* scattering plane [8]). The calculation predicts $M_{100} = M_{001}$ at all temperatures. Therefore it is difficult to understand the $\pi\pi$ data, which indicate, that M_{001} decreases below 10 K. Additional sources of anisotropy, other than the dipolar interaction have to be considered so as to account for this observation, which is also supported by a sharp increase of the susceptibility in c-direction below 10 K [3].

2. $GdNi_2B_2C$

$GdNi_2B_2C$ crystallizes in a body centered tetragonal structure (space group *I4/mmm*). The Néel temperature is $T_N = 19.5$ K and a spin reorientation has been reported at $T_R = 13.5$ K. The magnetic structure has been investigated by MXD [9]. Above T_R the moments point along (010) with a propagation vector of $\tau = (0.55\ 0\ 0)$ while below T_R a (001) component of the moment appears. The propagation vector is only weakly temperature dependent (<0.5%).

For the *McPhase* calculation it is necessary to include 5 neighbors in order to get a global maximum

of the FT of the isotropic interaction constants $\mathcal{J}(ij)$ at $\tau = (0.55\ 0\ 0)$. We used for the neighbors at (010) -12 μeV, (110) -27 μeV, (0.5 0.5 0.5) -29 μeV, (220) +17 μeV and at (001) +29 μeV.

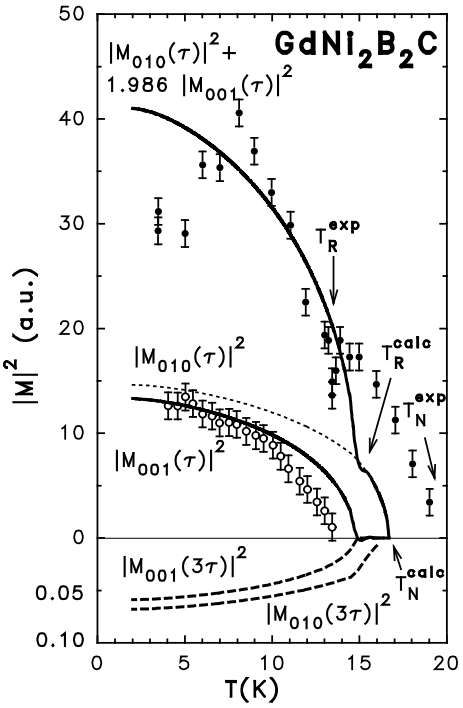

Fig. 2. Measured temperature dependence of the resonant (open symbols) and the non-resonant (full symbols) intensity of the first harmonic (1.447 0 0) magnetic reflection (data taken from [9] and scaled for comparison). Lines correspond to the calculated temperature dependence of the squared FT of the moment components M_{010} and M_{001} for the ordering wave vector τ and the harmonic 3τ.

The experimentally observed magnetic structures including the moment directions are well reproduced by the calculation. The low temperature modification of the magnetic structure deserves some comments. By MXD a spiral and a transverse wave were suggested as possible magnetic structures [9]. The *McPhase* calculation clearly stabilizes a spiral structure. Fig. 2 compares MXD data with the calculated temperature dependence of the FT of the magnetic moment **M**. Note that the measured resonant intensity corresponds to the component M_{001} (scaling with $|M_{001}|^2$), which appears below the spin reorientation temperature in accordance with the experiment [9]. The measured non-resonant intensity has to be compared to a linear combination of the M_{001} and M_{010} (see fig. 2). The calculated longitudinal component M_{100} is zero at all temperatures. The factor of 1.986 in the linear combination is derived from $\cos^2(\Theta)/\sin^2(2\Theta)$. The calculation underestimates the stability range of the high temperature collinear magnetic structure. This temperature range is determined by the magnitude of the dipolar anisotropy, which confines the moments to the (010) direction.

In conclusion, a numerical calculation based on isotropic exchange and the dipolar interaction is able to predict the magnetic moment orientation for both systems under investigation. The remaining quantitative inconsistencies with the MXD experiment are attributed to anisotropic interactions, which are not taken into account in the model (1).

Part of this work was performed within the program of the Sonderforschungsbereich 463 (funded by the Deutsche Forschungsgemeinschaft).

References

[1] M. Rotter, M. Loewenhaupt, M. Doerr, A. Lindbaum, H. Michor, Phys Rev. B 64 (2001) 014402–014409.

[2] M. Rotter, A. Lindbaum, E. Gratz, H. Müller, G. Hilscher, H. Sassik, H. E. Fischer, M. T. Fernandes-Diaz, R. Arons, E. Seidl, J. Mag. Magn. Mat. 214 (2000) 281–290.

[3] M. Rotter, A. Schneidewind, M. Loewenhaupt, M. Doerr, A. Stunault, A. Hiess, A. Lindbaum, E. Gratz, G. Hilscher, H. Sassik, Physica B 284-288 (2000) 1329–1330.

[4] F. N. Gygax, D. Andreica, A. Schanck, Y. Onuki, J. Magn. Mag. Mat. 246 (2002) 101–109.

[5] M. Rotter, M. Doerr, M. Loewenhaupt, A. Lindbaum, H. Müller, J. Enser, E. Gratz, J. Magn. Mag. Mat. 236 (2001) 267–271.

[6] M. Rotter, submitted to J. Magn. Mag. Mat. (2003).

[7] M. Rotter, M. Loewenhaupt, S. Kramp, T. Reif, N. M. Pyka, W. Schmidt, R. v. d. Kamp, Europ. Phys. J. B 14 (2000) 29–42.

[8] A. Schneidewind, Ph.D. thesis, Technische Universität Dresden (2002).

[9] C. Detlefs, A. I. Goldman, C. Stassis, P. C. Canfield, B. K. Cho, J. P. Hill, D. Gibbs, Phys. Rev. B 53 (10) (1996) 6355–6361.

Diffraction experiments on $GdCu_2In$ using hot neutrons

M. Rotter [a,b] M. Doerr [b] M. Loewenhaupt [b] A. Lindbaum [c]
K. Ziebeck [d] B. Beuneu [e]

[a] *Institut für Physikalische Chemie, Universität Wien, A–1090 Wien, Austria*

[b] *Institut für Festkörperphysik, Technische Universität Dresden, D–01062 Dresden, Germany*

[c] *Institut für Festkörperphysik, Technische Universität Wien, A–1040 Wien, Austria*

[d] *Department of Physics, Loughborough University, Loughborough, LE 11 3TK, U. K.*

[e] *Laboratoire Léon Brillouin, CEA-CNRS, Saclay, 91191 Gif sur Yvette Cedex, France*

Abstract

Gd compounds with nonmagnetic partner elements are attractive probes for evaluating magnetic exchange interactions. In the Gd^{3+} ion the f-electrons have zero angular momentum with a spherical charge density. Therefore the crystal field interaction is negligible. Special interest deserve the compounds with one Gd atom per primitive unit cell, because the magnetic anisotropy may be calculated from first principles under the assumption, that the classical dipole-dipole interaction dominates. We investigated the magnetic structure of the Heusler compound $GdCu_2In$ by neutron diffraction and find complex antiferromagnetism. Using numerical methods it is possible to interpret the data within the dipolar model. A spin reorientation just below the Néel temperature is predicted.

Key words: hot neutrons, neutron diffraction, dipolar anisotropy
PACS: 75.25.+z
PACS: 75.30.Gw

1 Introduction

The sources of magnetic anisotropy of rare earth compounds are single ion, dipolar and exchange anisotropy. The largest contribution usually comes from

single ion anisotropy, unless the angular momentum is zero ($L = 0$) such as in the case of Gd^{3+} ($S = J = 7/2$)). The small but finite magnetic anisotropy of $L = 0$ rare earth compounds is topic of various speculations about it's origin: An important contribution can come from the dipole interaction [1]. Also crystal field and exchange effects coming from higher multiplets have been discussed as the source [2,3]. It is well accepted, that the dipole interaction drives the anisotropy of Gd metal [1,4–7]. In Gd compounds few investigations of the anisotropy of magnetic interactions have been performed, especially on antiferromagnets. In compounds with one atom per primitive unit cell the magnetic anisotropy may be calculated from first principles under the assumption, that the classical dipole-dipole interaction dominates [8]. $GdCu_2In$ is such a system and has been the topic of a neutron diffraction study described in the following.

2 Experimental

The neutron data was collected on powdered samples of $GdCu_2In$ using the 7C2 - hot source diffractometer of the LLB, Saclay [8]. The Néel temperature of $GdCu_2In$ is $T_N = 12$ K. Diffraction patterns were taken at 20 K and 2 K using hot neutrons with a wavelength of 0.058 nm and are shown in fig. 1 (for each pattern the background signal has been subtracted). The absorption of the sample was reduced by using a double wall cylindric sample holder (outer diameter 12 mm, inner diameter 10 mm). The pattern at 20 K in the magnetically disordered state can be indexed according to the $L2_1$ Heusler crystal structure (see fig. 2) with the lattice constant $a = 0.662$ nm . The small intensities at 2.4 and 2.8 $Å^{-1}$ cannot be indexed and are attributed to traces of another phase, most probably $GdCu_2$. At 2 K magnetic Bragg peaks are found, from which we dedecued a propagation vector $\tau = (1/3 \quad 1 \quad 0)$ for $GdCu_2In$. The fit corresponds to the magnetic structure (shown in fig. 3, bottom) calculated with the program package *McPhase* as discussed below.

3 Model

For Gd-based systems the Hamiltonian consists of an isotropic exchange interaction and the classical dipole interaction:

$$\mathcal{H} = -\frac{1}{2}\left\{\sum_{ij}\mathcal{J}(ij)\mathbf{J}_i\mathbf{J}_j + \sum_{\alpha\beta}J_i^\alpha\mathcal{J}_{\alpha\beta}^{CD}(ij)J_j^\beta\right\} \tag{1}$$

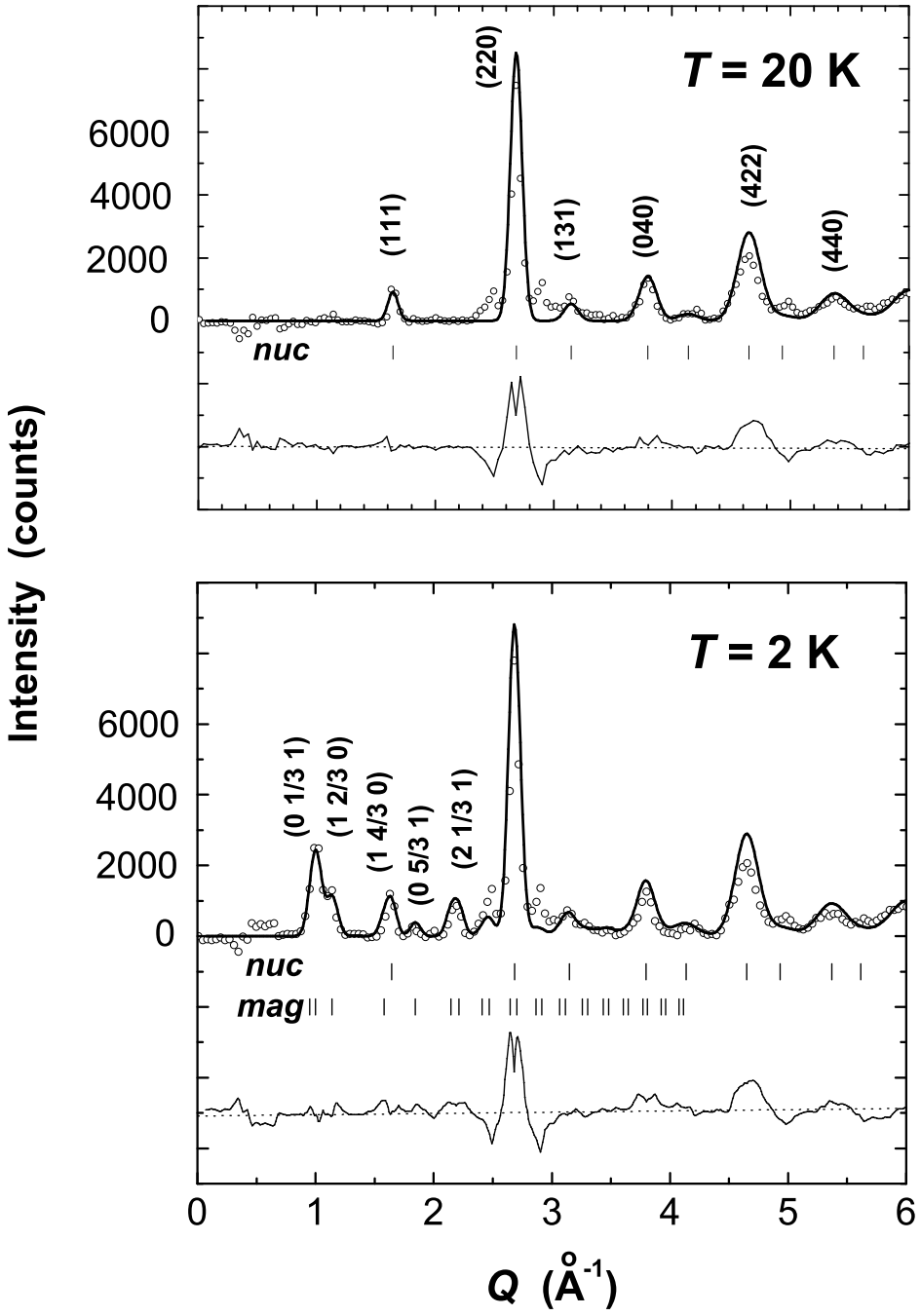

Fig. 1. Diffraction pattern of $GdCu_2In$ in the paramagnetic (top) and in the low temperature, antiferromagnetically ordered state (bottom).

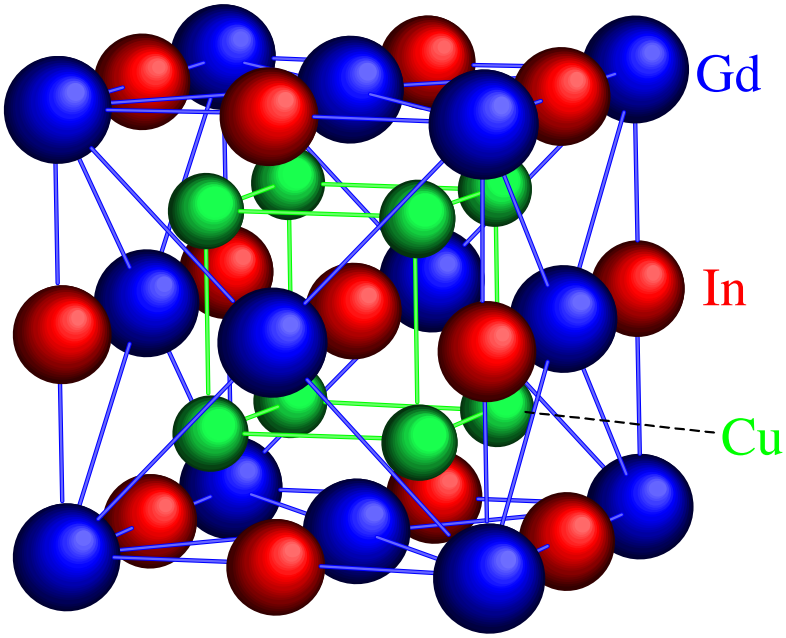

Fig. 2. Heusler structure of $GdCu_2In$.

In this expression (1) the $4f$ moment of the i^{th} Gd^{3+} ion is represented by the three components of the angular momentum operator J_i^α ($\alpha = 1, 2, 3$). The only anisotropy in (1) enters via the second term which corresponds to the classical dipole interaction given by

$$\mathcal{J}_{\alpha\beta}^{CD}(ij) = (g_J \mu_B)^2 \frac{3(R_i^\alpha - R_j^\alpha)(R_i^\beta - R_j^\beta) - \delta_{\alpha\beta}|\mathbf{R}_i - \mathbf{R}_j|^2}{|\mathbf{R}_i - \mathbf{R}_j|^5} \tag{2}$$

Here $\mathbf{R}_i$ denotes the lattice vector of the i^{th} Gd ion, g_J the Landé factor and μ_B the Bohr magneton.

Based on the above assumptions an isotropic exchange has been set up such as to give a maximum of the Fourier transform of the exchange constants at (1/3 1 0) and the correct ordering temperature. From these conditions equations for the isotropic exchange parameters follow (compare [9]), which can be fullfilled only if more than 3 neighbors are considered. This procedure leads to the following 4 nearest neighbor interaction constants $\mathcal{J}(ij)$, which are associated with the neighbors at (1/2 1/2 0) (-33.3 μeV), (1 0 0) (12 μeV), (1/2 1/2 1) (4 μeV) and (2 0 0) (-2 μeV).

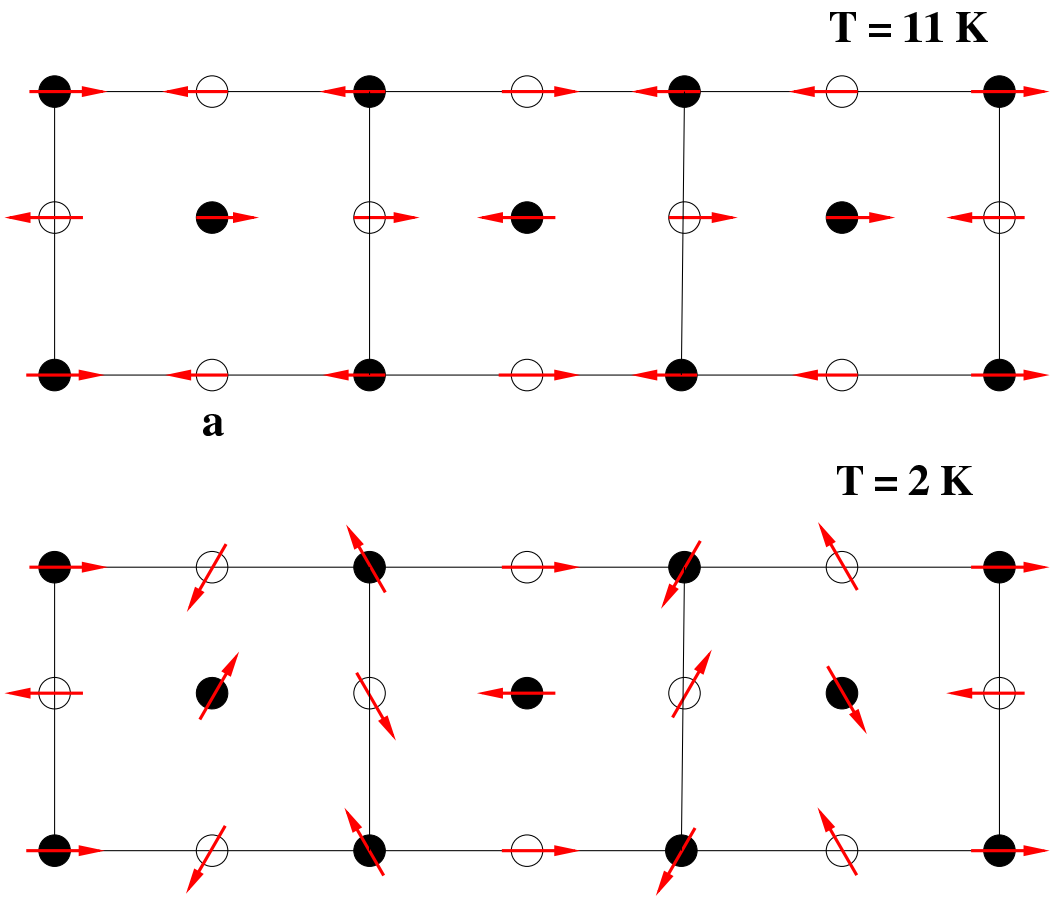

Fig. 3. Calculated magnetic structure $T = 11$ K (top) and at low temperature $T = 2$ K (bottom). Gd atoms situated in the same plane are shown by full (open) circles.

These parameters and the classical dipole interaction constants given by equ. (2) were used in the program **McPhase** (*www.mcphase.de*) [10] to calculate the temperature dependence of the magnetic structure on the basis of a mean field theory. A spin reorientation associated with a change of the magnetic structure from noncollinear to collinear has been computed. The corresponding magnetic structures are shown in fig. 3. The moment directions are restricted to the plane of the figure. The computed high temperature magnetic structure is in accordance with the expectations from the analytical high temperature expansion of the model (compare [8,11]). The magnetic neutron diffraction data shown in fig. 1 can be described by the computed noncollinear low temperature modification of the magnetic structure with magnetic moments of $6\mu_B$/Gd. Note that this value of the magnetic moment is smaller than the value of $7\mu_B$/Gd expected for the free Gd^{3+} ion.

In conclusion we want to emphasize, that the saturation process of the magnetic moments in Gd compounds may involve noncollinear modifications of the magnetic structure. Using the program package McPhase it is possible to compute the magetic structure and interpret the observed neutron diffraction

pattern within the framework of a mean field model.

Acknowledgement

We are grateful to J. P. Ambroise for helpful assistance at LLB, Saclay. Part of this work was performed within the program of the Sonderforschungsbereich 463 (funded by the Deutsche Forschungsgemeinschaft). We acknowledge financial support by the Austrian Science Fund (FWF) project No. P-14932-PHY, by the Austrian Academy of Sciences (APART 10739) and by the European Commission in the frame of the HPRI access program.

References

[1] J. Jensen, A. R. Mackintosh, Rare Earth Magnetism, Clarendon Press Oxford, 1991.

[2] F. Simon, A. Rockenbauer, T. Feher, A. Janossy, C. Chen, A. J. S. Chowdhury, J. W. Hodby, Phys. Rev. B 59 (18) (1999) 12072–12077.

[3] R. W. Cochrane, C. Y. Wu, W. P. Wolf, Phys. Rev. B 8 (9) (1973) 4348–4370.

[4] N. M. Fujiki, K. De'Bell, D. J. W. Geldart, Phys. Rev. B 36 (16) (1987) 8512–8516.

[5] D. J. W. Geldart, P. Hargraves, N. M. Fujiki, R. A. Dunlap, Phys. Rev. Lett. 62 (23) (1989) 2728–2831.

[6] J. M. Coey, V. Skumryev, K. Gallagher, Nature 401 (1999) 35–36.

[7] S. N. Kaul, S. Srinath, Phys. Rev. B 62 (2) (2000) 1114–1117.

[8] M. Rotter, M. Loewenhaupt, M. Doerr, A. Lindbaum, H. Sassik, K. Ziebeck, B. Beuneu, submitted to Phys. Rev. B (2003).

[9] M. Loewenhaupt, T. Reif, P. Svoboda, S. Wagner, M. Waffenschmidt, H. v. Löhneysen, E. Gratz, M. Rotter, B. Lebech, T. Hauss, Z. Phys. B 101 (1996) 499–510.

[10] M. Rotter, submitted to J. Magn. Mag. Mat. (2003).

[11] M. Rotter, M. Loewenhaupt, M. Doerr, A. Lindbaum, H. Michor, Phys Rev. B 64 (2001) 014402–014409.

J. Phys.: Condens. Matter 5 (1993) 7955–7958. Printed in the UK

The influence of the crystal field on the anisotropic thermal expansion in $TmCu_2$

E Gratz, A Lindbaum and M Rotter

Institute for Experimental Physics, TU Vienna, Wiedner Hauptstrasse 8–10, A-1040 Vienna, Austria

Received 21 May 1993, in final form 24 August 1993

Abstract. The lattice parameters a, b and c of $TmCu_2$ have been measured in the temperature range from 4.2 K up to 300 K using x-ray powder diffraction. The influence of the crystal field on the thermal expansion in $TmCu_2$ in the paramagnetic region has been determined by comparing the thermal expansion of the non-magnetic YCu_2 with that of $TmCu_2$ ($TmCu_2$ orders magnetically at $T_N = 6.3$ K). The data thus obtained are compared with a theoretical model given by Gratz *et al* in 1993 using a set of crystal field parameters published by Gubbens *et al* in 1992. From this analysis we get information about the unknown elastic and magnetoelastic properties of $TmCu_2$.

1. Introduction

The aim of this paper is to show the crystal-field (CF) influence on the temperature variation of the lattice parameters a, b and c of $TmCu_2$ (orthorhombic $CeCu_2$ structure) in the temperature range from 4.2 K to 300 K by comparison with the isostructural YCu_2. Recently Gubbens *et al* [2] published a set of CF parameters for this compound determined from neutron scattering data, measurements of the magnetization, specific heat and thermal expansion. The aim of this paper is to apply this set of parameters to analyse the anisotropic thermal expansion for $TmCu_2$ (Tm^{3+} : $J = 6$) as it has been done in our recent publication for $ErCu_2$ and $NdCu_2$ (see Gratz *et al* [1]).

2. Experimental details

Polycrystalline samples of $TmCu_2$ and YCu_2 have been prepared by induction melting under a protective argon atmosphere. After annealing at 700 °C for one week no trace of foreign phases could be observed by the x-ray analysis.

A conventional Siemens D-500 x-ray powder diffractometer with an Oxford helium-flow cryostat and Co Kα radiation has been used for the measurements of the lattice parameters a, b and c as a function of temperature. Germanium was used as an internal standard for calibration at each temperature.

3. Results and discussion

The temperature variation of the lattice parameters a, b and c of $TmCu_2$ and YCu_2 is shown in figure 1. In order to make the comparison easier we normalized the lattice

parameters to 300 K, that is, we divided them by the values at 300 K. The values of YCu_2 are given by the different broken lines in this figure. The lattice parameters at 300 K for $TmCu_2$ are $a = 4.267 \pm 0.001$ Å, $b = 6.713 \pm 0.003$ Å, $c = 7.248 \pm 0.001$ Å and for YCu_2 $a = 4.301 \pm 0.001$ Å, $b = 6.874 \pm 0.003$ Å, $c = 7.297 \pm 0.001$ Å.

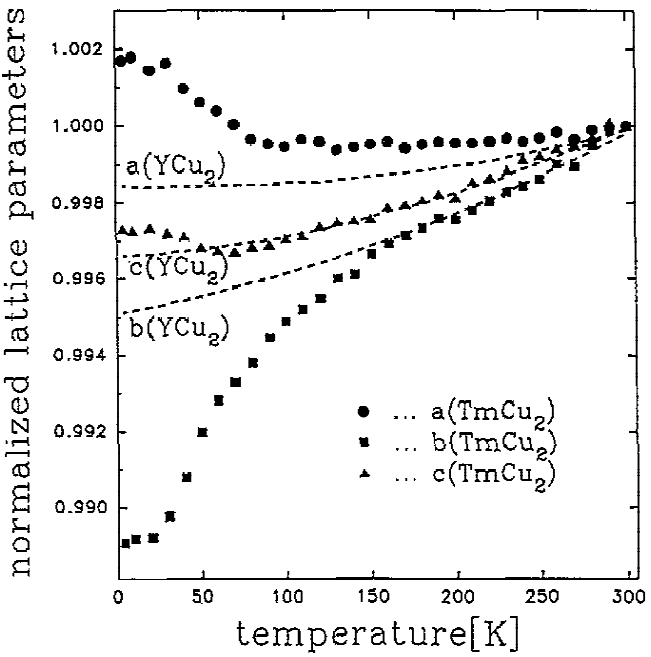

Figure 1. Temperature dependence of the normalized lattice parameters of $TmCu_2$ (symbols) and YCu_2 (broken lines).

The measured variations of $a(T)$, $b(T)$ and $c(T)$ for $TmCu_2$ deviate remarkably from those of the isostructural YCu_2 compound. The experimentally determined differences of the normalized lattice parameters of $TmCu_2$ and YCu_2 in the temperature range from 4.2 K to 300 K are shown in figure 2. As in our previous paper [1] we attribute the anomalous behaviour in the anisotropic thermal expansion of $TmCu_2$ to the CF influence.

If $a_i(T)$ $(i = 1, 2, 3)$ denotes the lattice parameters a, b and c of the magnetic compound $TmCu_2$ and $r_i(T)$ the lattice parameters of the non-magnetic isostructural compound YCu_2, the difference of the lattice parameters (normalized to $T_n = 300$ K) is given by (10) in [1]:

$$\frac{a_i(T)}{a_i(T_n)} - \frac{r_i(T)}{r_i(T_n)} = A_i(\langle O_2^0\rangle_T - \langle O_2^0\rangle_{T_n}) + B_i(\langle O_2^2\rangle_T - \langle O_2^2\rangle_{T_n}). \qquad (1)$$

Here the $\langle O_l^m\rangle_T$ and $\langle O_l^m\rangle_{T_n}$ denote the expectation values of the Stevens operators with $l = 2$ an $m = 0, 2$ at the variable temperature T and at the normalization temperature T_n (= 300 K), respectively. The CF parameters recently determined by Gubbens *et al* [2] (see also table 1) have been used for the calculation of the thermal expectation values of the Stevens operators. The coefficients A_i and B_i, which include elastic and magnetoelastic properties of the compounds are fitted to the experiment (for more details see our recent paper [1]). The obtained values for the six unknown coefficients are: $A_1 = 5.9\times10^{-5}$, $A_2 = -1.1\times10^{-4}$, $A_3 = 1.1\times10^{-5}$, $B_1 = 2.1\times10^{-4}$, $B_2 = -3.9\times10^{-5}$ and $B_3 = -6.6\times10^{-5}$.

The curves in figure 2 show the results of the calculation.

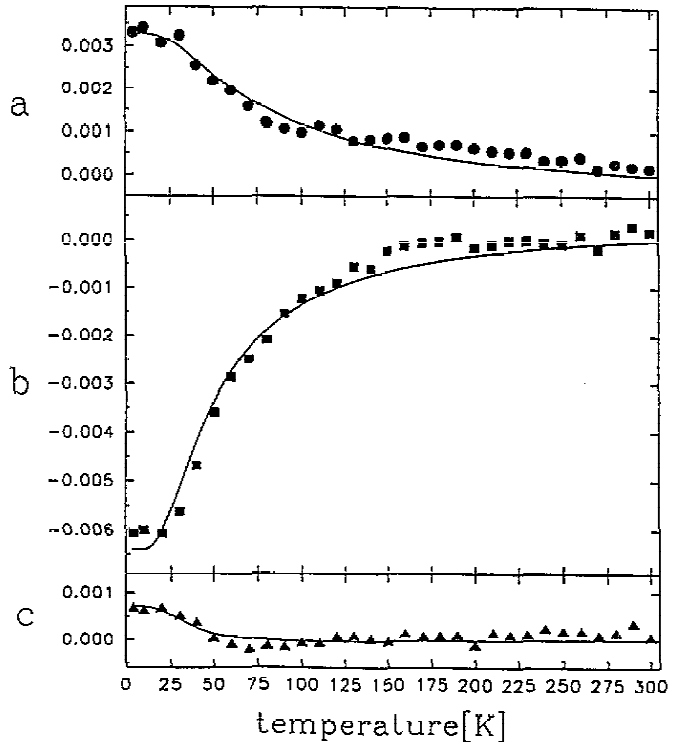

Figure 2. Experimentally determined differences of the normalized lattice parameters in the *a*, *b* and *c* directions of $TmCu_2$ and YCu_2 (symbols) together with the calculated results (curves).

Table 1. CF parameters for the orthorhombic $TmCu_2$ compound.

B_2^0	B_2^2	B_4^0	B_4^2	B_4^4
−0.94 K	−1.23 K	-0.9×10^{-2} K	-0.39×10^{-2} K	-0.36×10^{-2} K
B_6^0	B_6^2	B_6^4	B_6^6	
0.58×10^{-4} K	2.47×10^{-4} K	-0.48×10^{-4} K	6.31×10^{-4} K	

4. Summary

The anisotropic thermal expansion of $TmCu_2$ has been measured using x-ray powder diffraction. We were able to show that these anomalies in the anisotropic thermal expansion of $TmCu_2$ are due to the CF influence and can be described quantitatively, if we use the CF parameters published by Gubbens *et al* [2]. This analysis is based on the assumption that the elastic and magnetoelastic coupling parameters are temperature independent and can be determined by a fit to the experimental data. Recently we applied the same procedure for the analysis of the anisotropic thermal expansion of $ErCu_2$ and $NdCu_2$ [11] with the similar success.

Acknowledgments

This work was supported by the Austrian Science Foundation (FWF-Project P-8913).

References

[1] Gratz E, Rotter M, Lindbaum A, Mueller H, Bauer E and Kirchmayr H 1993 *J. Phys.: Condens. Matter* **5** 567
[2] Gubbens P C M, Buschow K H J, Divis M, Heidelmann M and Loewenhaupt M 1992 *J. Magn. Magn. Mater.* **104–107** 1283

A miniature capacitance dilatometer for thermal expansion and magnetostriction

M. Rotter,[a] H. Müller, and E. Gratz
Institut für Experimentalphysik, Technical University Vienna, Wiedner Hauptstr 8-10, 1040 Wien, Austria

M. Doerr and M. Loewenhaupt
Institut für Angewandte Physik und Didaktik, University of Technology Dresden, Mommsenstr 13, 01069 Dresden, Germany

(Received 15 December 1997; accepted for publication 9 April 1998)

A very small capacitive sensor for measuring thermal expansion and magnetostriction of small and irregular shaped samples has been developed. A capacitive method with tilted plates is used. The tilted plate capacitance formula is used for the calculation of the capacitor gap, the calibration is performed by measuring the signal of a standard material. The active length of the sample can be less than 1 mm. The absolute resolution is about 1 Å. All mechanical connections of the dilatometer are carried out by tiny Cu–Be springs, enabling the small force on the sample to be adjusted (50–500 mN) and no additional sample fixing is necessary. The cell has been tested in the temperature range 0.3–200 K and in static magnetic fields up to 15 T. The zero signal of the dilatometer has been determined by measuring a silver sample. The correct operation and reproducibility has been verified by measuring the thermal expansion of Cu. The thermal expansion and magnetostriction of a $DyCu_2$ single crystal has been determined. The advantage of this method compared to specific heat measurements is that a large temperature range can be covered with one equipment. This high static and dynamic range of sample length, temperature, and magnetic field suggests a number of possible applications, like the investigation of crystal field effects on the magnetoelastic properties of single crystals or structural phase transitions. © *1998 American Institute of Physics.* [S0034-6748(98)01007-7]

I. INTRODUCTION

The capacitance method is one of the most sensitive methods for measuring small length changes of solids. In practice the accuracy is limited frequently by mechanical sample quality and dilatometer effects. However, to reach the highest possible sensitivity and reproduceability, special effort is needed in the design of the capacity cell and the sample preparation. Therefore a dilatometer has been developed by combining our own experience with already published methods.

The roots of capacitance dilatometry date back to 1961, when White[1] combined experiences of a two-terminal capacitance method for measuring thermal expansion[2] with Thompson's[3] three-terminal method for capacity measurements using a ratio transformer bridge. He achieved a hitherto unreachable resolution of 10^{-7} mm. Afterwards the two-terminal method was scarcely used again.[4]

White's design principles of absolute and relative dilatometers were adopted and improved by a number of different authors. It led to absolute thermal expansion measurements on a number of reference metals[5] like Cu,[6–8] Ag,[7] Au,[7] and Al.[8] Green,[9] Chanddrasekhar, and Fawcett[10,11] were among the first to use the dilatometers for magnetostriction measurements. Tilford and Swenson used an inverted configuration of White's cell to measure the thermal expansion of solid Ar, Kr, and Xe.[12] Miller *et al.* extended the temperature range of White's cell (1–300 K) up to 550 K.[13] The reproducibility of the dilatometer was increased by replacing the oxygen-free copper reference rods with silicon[14] or sapphire.[15] However, using for the whole cells Si or quartz with metal-plated electrodes[16,17] is problematic and has not been widely adopted except in pulsed magnetic fields.[18] Subrachmanyam and Subramanyam[19] went back to a copper dilatometer for the use of samples differing in length, however, still samples should have parallel surfaces. Sparavigna *et al.* designed an apparatus for simultaneous measurement of thermal expansion and thermal diffusivity[20] still keeping the main features of White's dilatometer design.

Another method—differing from White's design—goes back to the pushrod dilatometers with capacitive displacement sensor kept at constant temperature.[21,22] However, the pushrod has been used mainly at temperatures above room temperature.[23,24] The idea of separating the sample from the displacement sensor was fascinating, because samples of different lengths and shapes can be used. Several authors applied this principle in dilatometers with a capacitor based on parallel spring movements[25] which is not dismantled on sample change.[26–30]

The drift of capacitance with time could be reduced by the use of sapphire isolation washers instead of epoxy–mylar isolation.[29,31] Studies of the absolute accuracy of capacitance displacement sensors[32–34] led to further developments, like the elastic diaphragm sensor.[35]

[a]Electronic mail: exphys@xphys.tuwien.ac.at

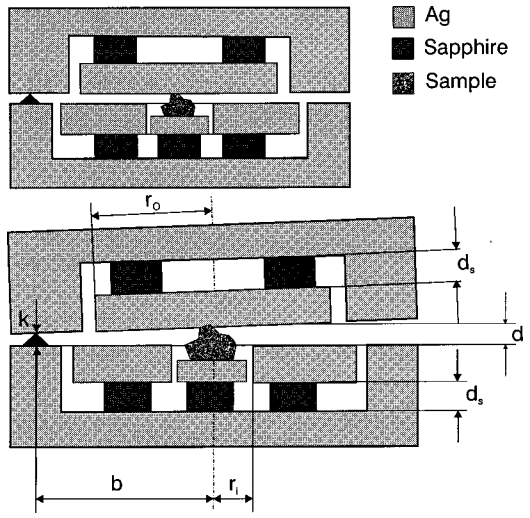

FIG. 1. Schematic drawing of the capacitance dilatometer.

An important basis for the design of our sensor was the invention of the tilted plate principle,[26,36] which has also been used in a dilatometer for amorphous ribbons.[37]

II. THE DILATOMETER

Our aim was to construct a sensor for studying phase transitions on intermetallic rare earth compounds. Since for these compounds only small single crystals (1 mm^3) are available and for such investigations a wide range of physical parameters is necessary, it was required to design a small and compact dilatometer for a wide temperature range and high magnetic fields combining most advantages of the existing capacitive dilatometers but avoiding their disadvantages.

Capacitive cells with parallel plates are easy to calibrate, but they have either big dimensions or difficulties with the sample handling. Even if the problem of thermal stability of such big cells is solved, limited space in most of the magnetic coil systems causes problems, particularly when magnetostriction parallel and perpendicular ($\lambda_\parallel$ and $\lambda_\perp$) to the field has to be measured. To minimize the cell size our capacitor design is based on the tilted plate principle[26,36] with the sample placed in a hole in the lower capacitance plate (see Fig. 2), determining the maximal sample size ($3\times3\times3$ mm^3). To obtain a reasonable accuracy the active length of the sample should be bigger than 0.5 mm. The sample can have nearly any irregular shape, only the base surface should be flat to give a stable sample position.

Our tilted plate construction has a high plate area and a low volume, which gives a good sensitivity in connection with very small sensor dimensions (diameter: 22 mm, height: 14 mm).

Figure 1 shows the schematic arrangement of the dilatometer. The lower part consists of a plate holder (Ag). It includes the ringlike lower capacitor plate (Ag) and the sample support (Ag). The upper part consists of the upper plate holder (Ag) and the disklike upper capacitor plate. It is separated from the lower one by two needle bearings (brass) and the sample to obtain a well defined support on three points. Both capacitor plates as well as the sample support

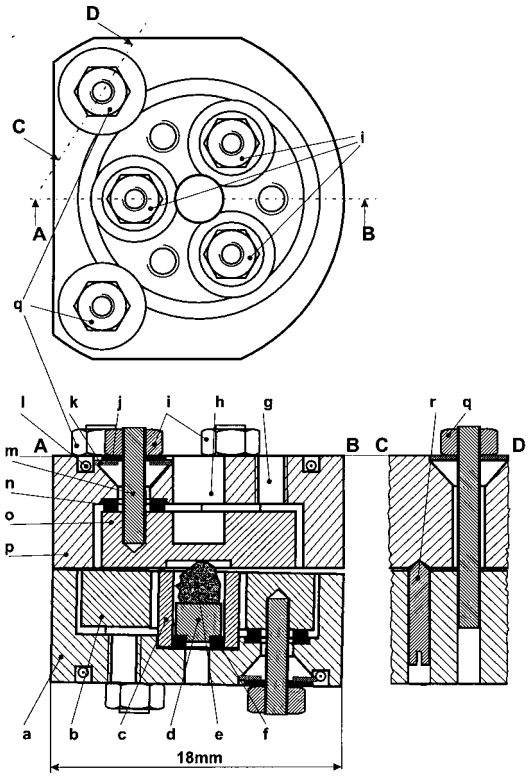

FIG. 2. Detailed drawing of the miniature tilted plate capacitance dilatometer: (a) lower capacitance-plate-holder (Ag), (b) lower capacitance-plate (Ag), (c) electrical shielding of sample space (brass), (d) sample support (Ag), (e) sample, (f) isolation washer for electrical sample isolation (sapphire), (g) mounting holes, (h) temperature sensor hole, (i) plate holder nuts (brass), (j) electrical isolation (kapton), (k) disk spring (Cu–Be), (l) groove for temperature stabilization of capacitance wires, (m) thread bolt (brass), (n) isolation washer for electrical isolation of capacitance plate (sapphire), (o) upper capacitance plate (Ag), (p) upper capacitance plate holder (Ag), (q) adjustment nuts, and (r) needle bearing.

are insulated from the holders by sapphire washers.[29] The needle bearings define an exact pivot point and avoid any transversal shift between the upper and lower plate holder.

Figure 2 shows the detailed drawing of the complete dilatometer. In addition to the schematic drawings the following parts are shown. The electrical shielding of the sample (c) is essential for screening the sample support (d) from the lower plate. The groove (l) holds the capacitance wires and ensures a good thermal contact to improve temperature stabilization. The thread bolt (m) together with the disk spring (k) fix the position of the capacity plate and performs the electrical connection to the plate. The disk spring fitting in the conical hole produces a well defined force to keep the position of the capacity plate with respect to the holder.[29,31] This improved design looks much simpler than that one of Pott and Schefzyk.[29] The stress on the sample can be adjusted with a torque driver at the nuts (q). To obtain a good electrical insulation between plate holders [(a) and (p)] and the capacitor plates [(b) and (o)] the kapton insulation ring (j) and the Cu–Be disk spring (k) must be aligned exactly and fit precisely in the hole.

Although this sensor is more difficult to calibrate than normal parallel plate dilatometers, several advantages outnumber this computational effort:

(1) A self-compensating construction gives a small temperature dependence of the zero signal. Sample support and lower capacitance plate are placed on sapphire washers of the same kind to perform equivalent motions during expansion (see Fig. 1).
(2) The inverting construction[12] causes that the expansion of the sample opens the capacitor. This provides a high dynamic measurement range and avoids crashing of the capacitor plates and sample damage.
(3) All mechanical connections are done by Cu–Be disk springs, which are pressed into a cone by an adjustment nut. In this way the following features are obtained:
—the stress on the sample can be adjusted,
—no other fixing of the sample is necessary in magnetic fields, (i.e., by glues which might get loose at low temperatures and high fields),
—all stresses are well defined on assembling the cell (using a special torque driver).
(4) The insulation of the capacitance plates is done by using sapphire washers.[29,31] This avoids the use of glue, which causes excessive (undefined) capacitance drift.
(5) The sample is placed in the center of the capacitor and the capacitance leads are thermally anchored to the cell in a special *V* slot. This gives excellent thermal equilibrium conditions of the sample and all other parts of the dilatometer.
(6) The essential parts of the dilatometer are made of silver,[38] this has the following advantages compared to OFHC copper;
—50% lower heat capacity per volume,
—no nuclear heat capacity at low temperatures and high magnetic fields.
(7) Simple construction (four parts and a set of sample supports) facilitates manufacturing and cleaning.
(8) To measure samples of different lengths and shapes a set of sample supports with several lengths is used. This avoids the adjustment by a sample screw, which introduces an additional source of uncertainty.
(9) The dilatometer range can easily be extended to temperatures above room temperature. Because of the used insulation materials (sapphire, kapton) an application of the cell up to 500 K seems to be possible without major changes, but has to be verified by further experiments. Choosing other materials the use of the design up to 1300 K and more is suggested. The extension of the temperature range of the dilatometer below 300 mK should also be possible.

Figure 3 shows the dilatometer in a temperature insert of the cryostat and in a superconducting magnet system. The two different positions in the coil parallel and perpendicular to the magnetic field are outlined as full and dashed lines, respectively.

III. CALIBRATION

This sensor measures the relative length change of the sample, therefore a calibration procedure is necessary.[1] It is performed using the tilted plate capacitance formula.[26,36]

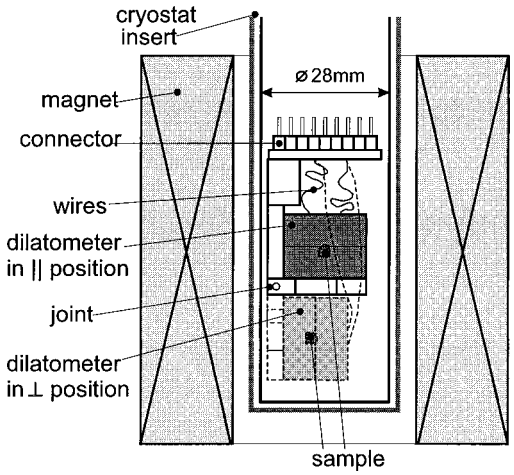

FIG. 3. Arrangement of the dilatometer, temperature insert, and magnet system.

This presents no major problem using computer controlled data acquisition.
The capacity change caused by thermal expansion has four contributions;

(1) change of the sample length,
(2) change of the radii of the capacitor plates,
(3) change of the length of the silver plate holders,
(4) partly compensated by the change of thickness of the capacitor plates and the sapphire washers.

The measured capacity $C(T)$ is used to calculate the gap $d(T)$ by the following formula:

$$C(T)=\frac{2\epsilon_0}{d(T)}\left[A_0(T)\,\frac{(1-\sqrt{1-\gamma_0^2})}{\gamma_0^2}-A_i(T)\,\frac{(1-\sqrt{1-\gamma_i^2})}{\gamma_i^2}\right], \tag{1}$$

with

$$\gamma_0=\frac{r_0}{b}\left[\frac{k(T)}{d(T)}-1\right], \tag{2a}$$

$$\gamma_i=\frac{r_i}{b}\left[\frac{k(T)}{d(T)}-1\right], \tag{2b}$$

where r_0 is the outer plate radius, r_i the inner plate radius, b the distance between center of capacitor and pivot (see Fig. 1).

$$k(T)=k(T_0)+2d_s\left[\frac{\Delta l_{\mathrm{Ag-Lit}}}{l}(T)-\frac{\Delta l_{\mathrm{Sapphire}}}{l}(T)\right], \tag{3}$$

where $k(T_0)$ is the pivot distance at $T_0=300$ K, d_s the thickness of sapphire washers (0.8 mm), $(\Delta l_{\mathrm{Ag-Lit}}/l)(T)$ is the thermal expansion of Ag from literature,[7] and $\Delta l_{\mathrm{Sapphire}}/l\,(T)$ the thermal expansion of sapphire from literature.[5]

To determine the pivot distance $k(T_0)$ the plates can initially be adjusted parallel (by minimizing the reading of the capacitance bridge and/or by the procedure described by Villar *et al.*[14]).

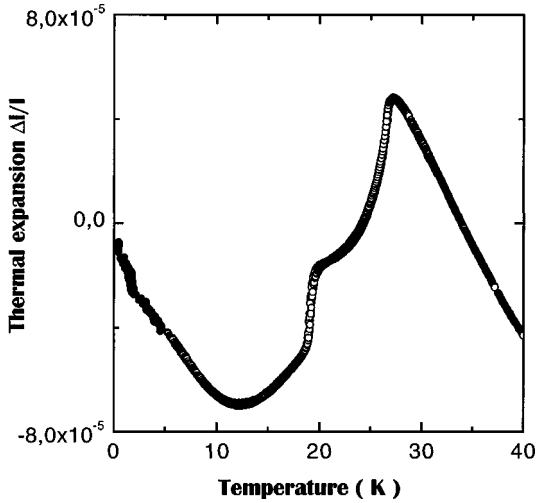

FIG. 4. Thermal expansion along the a direction of a $DyCu_2$ single crystal measured by the capacitive dilatometer.

$$A_i(T)=A_i(T_0)\left[1+\frac{\Delta l_{\text{Ag-Lit}}}{l}(T)\right]^2 \tag{4a}$$

is the inner capacitance area ($r_i^2\pi$).

$$A_0(T)=A_0(T_0)\left[1+\frac{\Delta l_{\text{Ag-Lit}}}{l}(T)\right]^2 \tag{4b}$$

is the outer capacitance area ($r_0^2\pi$).

Because $d(T)$ appears in the term of $C(T)$ [Eq. (1)] and in γ [Eqs. (2a) and (2b)], Eq. (1) has to be solved numerically with respect to $d(T)$.

Fringe corrections have to be considered only if big capacitance changes occur. For signals in the magnitude of a "normal" metal (like Ag or Cu) fringing corrections can be neglected. In this case an estimation according to W. C. Heerens[34] leads to corrections which are in the order of magnitude of the reproduceability of the cell. For big capacitance changes the corrections can be applied, therefore it is necessary to measure the capacity two times with inverted high and low connections.

Once the gap $d(T)$ has been calculated for each temperature, the thermal expansion of the sample $\Delta l_{\text{Sample}}(T)/l$ is obtained by the following relations:

$$\frac{\Delta l_{\text{Sample}}}{l}(T)=\frac{\Delta d_{\text{Sample}}}{l_{\text{Sample}}}(T)-\frac{\Delta d_{\text{Ag-Sample}}}{l_{\text{Ag-Sample}}}(T)+\frac{\Delta l_{\text{Ag-Lit}}}{l}(T), \tag{5}$$

where $\Delta d=d(T)-d(T_0)$, $\Delta d_{\text{Sample}}(T)$ is the measurement of the sample, and $\Delta d_{\text{Ag-Sample}}(T)$ is the measurement of an Ag–Sample (calibration sample).

The capacity has been measured by an "Andeen Hagerling 2500 A 1 kHz Ultraprecision Capacity Bridge." A gap of 0.18 mm results in a capacity of approximately 4 pF.

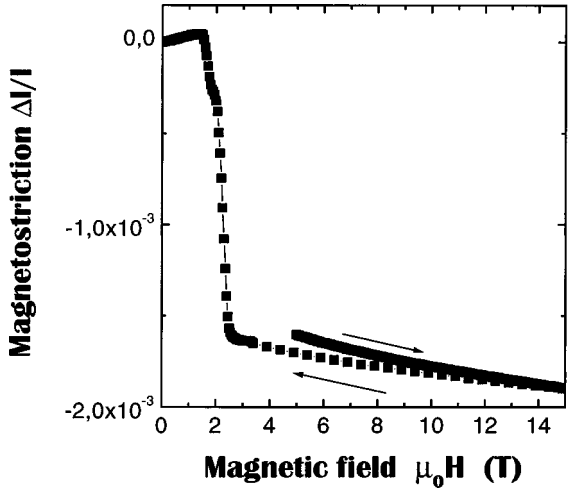

FIG. 5. Longitudinal magnetostriction of a $DyCu_2$ single crystal with the magnetic field aligned parallel to the a direction measured by the capacitive dilatometer at $T=4.3$ K.

IV. RESULTS

The correct operation has been verified by measuring the thermal expansion of pure copper (5 N). The maximum deviation from literature data[5] is in the order of 1% in $\Delta l/l$.

After calibration experiments the dilatometer performance was checked by extensive and systematic measurements on intermetallic compounds. Both temperature dependent runs at a constant magnetic field (up to 15 T) and field dependent runs at a constant temperature (from 300 mK to 200 K) have been performed. Above 2.2 K a variable temperature insert prepared for a high field magnet with 50 mm bore was used. Alternatively, the dilatometer was mounted in a ^{3}He insert with a sample space diameter of 40 mm for the low temperature experiments from 300 mK to 4 K. Results for a $DyCu_2$ single crystal with sample size 1.13 (a)×2.12 (b)×1.79 (c) mm^3 can be seen in Fig. 4. The compound shows two magnetic phase transitions (18 and 27 K)[39,40] connected with significant jumps in sample length. Several temperature cycles with different slopes (1–5 mK/s) have been performed above 2.2 K. The deviation of the different curves is within the symbol size, showing that the reproduceability of the dilatometer is in the order of 10^{-7} mm.

Figure 5 shows the magnetostriction of $DyCu_2$ for $T=4.3$ K. The resolution does not depend on the field value. The jumps at 1.5 and 2.0 T are connected with transitions between different magnetic states of the sample.

Eddy currents cause a additional heating of the cell, depending on the field sweep rate. The power supply of the magnet allows us to work with constant sweep rate of 0.2 T/min. At 0.8 K a constant warm up of 0. K which stays stable within 1 mK is observed. Above 2 K this effect can be neglected.

ACKNOWLEDGMENTS

Appreciation is given to the mechanicians of our workshop, A. Lahner and J. Sicherl, who have manufactured all the precise parts of the dilatometer. This work has been sup-

ported by the Austrian Science Foundation (FWF) Project No. P11239 and the Deutsche Forschungsgemeinschaft SFB 463 ''Seltenerd-Übergangsmetall-Verbindungen: Struktur-Magnetismus-Transport.''

[1] G. K. White, Cryogenics **1**, 151 (1961).
[2] D. Bijl and H. Pullan, Physica (Amsterdam) **21**, 285 (1955).
[3] A. M. Thompson, IRE Trans. Instrum. **1–7**, 245 (1958).
[4] R. R. Birss, G. J. Keeler, P. Pearson, and R. J. Potton, J. Phys. E **11**, 928 (1978).
[5] G. K. White, Thermochim. Acta **218**, 83 (1993).
[6] R. H. Carr, R. D. McCammon, and G. K. White, Proc. R. Soc. London, Ser. A **280**, 72 (1963).
[7] G. K. White and J. G. Collins, J. Low Temp. Phys. **7**, 43 (1972).
[8] F. R. Kroeger and C. A. Swenson, J. Appl. Phys. **48**, 853 (1977).
[9] B. A. Green and B. S. Chandrasekhar, Phys. Rev. Lett. **11**, 331 (1963).
[10] E. Fawcett, Phys. Rev. B **2**, 1604 (1970).
[11] E. Fawcett, Phys. Rev. B **2**, 3887 (1970).
[12] C. R. Tilford and C. A. Swenson, Phys. Rev. B **5**, 719 (1972).
[13] D. A. Miller, J. W. Kauffman, and C. R. Kannewurf, Rev. Sci. Instrum. **42**, 155 (1971).
[14] R. Villar, M. Hortal, and S. Vieira, Rev. Sci. Instrum. **51**, 27 (1980).
[15] I. J. Brown and M. A. Brown, J. Phys. C **16**, 1031 (1983).
[16] H. Ibach, Phys. Status Solidi **31**, 625 (1969).
[17] T. H. Johansen, J. Feder, and T. J. Jossang, Rev. Sci. Instrum. **57**, 1168 (1986).
[18] G. Kido, Physica B **155**, 199 (1989).
[19] H. N. Subrachmanyan and S. V. Subramanyam, Pramana, J. Phys. **27**, 647 (1986).
[20] A. Sparavigna, G. Giachello, M. Omini, and A. Strigazzi, Int. J. Thermophys. **11**, 1111 (1990).
[21] E. T. Lacheisserie, Rev. Phys. Appl. **10**, 169 (1975).
[22] T. Auweiler, dissertation, Universität Köln, 1995 (unpublished).
[23] K. V. Rao and J. Maiti, Indian J. Pure Appl. Phys. **15**, 437 (1977).
[24] V. Horvatic, J. Gladic, Z. Vucic, and O. Milat, Meas. Sci. Technol. **2**, 381 (1991).
[25] R. V. Jones, J. Sci. Instrum. **28**, 38 (1951).
[26] G. Brändli and R. Griessen, Cryogenics **13**, 299 (1973).
[27] H. R. Ott and B. Lüthi, Z. Phys. B **28**, 141 (1977).
[28] M. O. Steinitz, J. Genossar, W. Schnepf, and D. Tindall, Rev. Sci. Instrum. **57**, 297 (1986).
[29] R. Pott and R. Schefzyk, J. Phys. E **16**, 444 (1983).
[30] W. Stamm, dissertation, Universität GH Duisburg, 1988 (unpublished).
[31] C. A. Swenson, Rev. Sci. Instrum. **68**, 1312 (1997).
[32] M. A. Brown and C. E. Bulleid, J. Phys. E **11**, 429 (1978).
[33] A. R. Khan, I. J. Brown, and M. A. Brown, J. Phys. E **13**, 1280 (1980).
[34] W. C. Heerens, J. Phys. E **19**, 897 (1986).
[35] P. Roth and E. Gmelin, Rev. Sci. Instrum. **63**, 2051 (1992).
[36] J. Genossar and M. Steinitz, Rev. Sci. Instrum. **61**, 2469 (1990).
[37] S. Ishio, J. Magn. Magn. Mater. **79**, 358 (1989).
[38] M. Lang, dissertation, Universität Darmstadt, 1991 (unpublished).
[39] N. Iwata, Y. Hashimoto, T. Kimura, and T. Shigeoka, J. Magn. Magn. Mater. **81**, 354 (1989).
[40] M. Loewenhaupt, M. Doerr, L. Jahn, T. Reif, C. Sierks, M. Rotter, and H. Müller, Physica B (to be published).

Modeling magnetostriction in RCu_2 compounds using *McPhase*

M. Rotter, M. Doerr, and M. Loewenhaupt
Institut für Angewandte Physik, TU Dresden, D-01062 Dresden, Germany

P. Svoboda
Department of Electron Systems, Charles University, 12116 Prague, The Czech Republic

In RCu_2 compounds (R = rare earth) magnetostriction results from two different sources, the single ion crystal field contribution and the two ion exchange interaction. The crystal field contribution can also be observed above the magnetic ordering temperature and leads to giant magnetostriction in high magnetic fields at some members of the series. The exchange contribution has to be considered additionally when describing the magnetostriction in the magnetically ordered state. A new feature of the mean field–Monte Carlo simulation program *McPhase* (http://www.mcphase.de) allows to calculate the magnetic phase diagram and model the exchange contribution. We present new data of thermal expansion and the longitudinal and transversal magnetostriction of $NdCu_2$ with magnetic field applied along the a, b, and c direction of the orthorhombic single crystal. These data are compared to the results of a *McPhase* simulation, which is based on exchange parameters derived from measurements of the magnetic excitations. The magnetoelastic interaction is compared to the case of $GdCu_2$. The analysis can be extended to other RCu_2 compounds. © *2002 American Institute of Physics.* [DOI: 10.1063/1.1449363]

I. MAGNETOELASTIC INTERACTIONS IN RCu_2 COMPOUNDS

According to Ref. 1 the static and dynamic magnetic properties of RCu_2 compounds in the magnetically ordered state can be described by a Hamiltonian, which is the sum of crystal field (CF), exchange (EX), and Zeeman contributions and the elastic energy

$$\mathcal{H}=\mathcal{H}_{\mathrm{CF}}+\mathcal{H}_{\mathrm{EX}}-\sum_{\mathbf{i}} g_J\mu_B\mathbf{H}\cdot\mathbf{J_i}+E_{\mathrm{el}}. \tag{1.1}$$

In order to describe magnetoelastic properties the strain dependence of the CF and EX part has to be considered (for the notation see Ref. 3):

$$\mathcal{H}_{\mathrm{CF}}=\sum_{lm,\mathbf{i}} B_l^m(\epsilon)O_l^m(\mathbf{J_i}), \tag{1.2}$$

$$\mathcal{H}_{\mathrm{EX}}=-\frac{1}{2}\sum_{\mathbf{ij},\alpha\beta}\mathbf{J_i^\alpha}\mathcal{J}_{\alpha\beta}(\epsilon,\mathbf{i}-\mathbf{j})\mathbf{J_j^\beta}, \tag{1.3}$$

$$E_{\mathrm{el}}=\frac{1}{2}\sum_{\alpha\beta\alpha'\beta'}\epsilon_{\alpha\beta}\epsilon_{\alpha'\beta'}c^{\alpha\beta\alpha'\beta'}. \tag{1.4}$$

From this model the diagonal components of the strain tensor ϵ can be derived. This is done for the special case of orthorhombic RCu_2 compounds with ferromagnetic bc planes (such as $NdCu_2$) and considering the strain dependence of the CF for $l=2$ and of the EX up to the next nearest bc plane. The following expressions are calculated using a mean field model, expanding the CF and EX parameters linear in the strain tensor ϵ and minimizing the free energy with respect to ϵ similar to[4,5]

$$\epsilon_{\alpha\alpha}=\epsilon_{\alpha\alpha}^{\mathrm{CF}}+\epsilon_{\alpha\alpha}^{\mathrm{EX}},$$

$$\epsilon_{\alpha\alpha}^{\mathrm{CF}}=\frac{1}{N}\sum_{\mathbf{i}}\left[A_\alpha\langle O_2^0(\mathbf{J_i})\rangle_{T,\mathbf{H}}+B_\alpha\langle O_2^2(\mathbf{J_i})\rangle_{T,\mathbf{H}}\right], \tag{1.5}$$

$$\epsilon_{\alpha\alpha}^{\mathrm{EX}}=\frac{1}{N}\sum_{\beta\mathbf{i}}\left[K_{\alpha\beta}\langle\mathbf{J_i^\beta J_i^\beta}\rangle_{T,\mathbf{H}}+L_{\alpha\beta}\langle\mathbf{J_i^\beta J_{i+a/2+b/2+c/2}^\beta}\rangle_{T,\mathbf{H}}+M_{\alpha\beta}\langle\mathbf{J_i^\beta J_{i+a}^\beta}\rangle_{T,\mathbf{H}}\right]. \tag{1.6}$$

$\langle\ \rangle_{T,\mathbf{H}}$ denote thermal expectation values, $\mathbf{i}$ the position vectors of the rare earth, $\mathbf{a}$, $\mathbf{b}$, and $\mathbf{c}$ the orthorhombic lattice vectors.

Using a new version of the *McPhase* simulation program it is possible to calculate the static correlation functions $\langle\mathbf{J_i^\beta J_{i'}^\beta}\rangle_{T,\mathbf{H}}$ in Eq. (1.6). The complete $\mathbf{H}$ and T dependence of the strain is determined by the expectation values $\langle\ \rangle_{T,\mathbf{H}}$. The model used for the simulation of the magnetically ordered phases has been described in Ref. 6 for external fields parallel to b. Here we extend it to fields in a and c using the magnetic exchange determined from the dispersion of the

TABLE I. Magnetoelastic parameters used in the evaluation of the strains by Eq. (1.5).

$\alpha=$	a	b	c
A_α[a]	-5×10^{-5}	$+7\times10^{-5}$	-8×10^{-6}
B_α[a]	-5×10^{-5}	$+3\times10^{-4}$	$+2\times10^{-4}$
$K_{\alpha a}$	$+4\times10^{-4}$	-1×10^{-4}	$+2\times10^{-5}$
$K_{\alpha b}$	$+5\times10^{-6}$	-6×10^{-5}	-4×10^{-5}
$K_{\alpha c}$	-1×10^{-4}	-4×10^{-4}	-1.8×10^{-4}
$L_{\alpha a}$			
$L_{\alpha b}$	$+1.5\times10^{-5}$		-1.3×10^{-5}
$L_{\alpha c}$			
$M_{\alpha a}$			
$M_{\alpha b}$	$+6\times10^{-6}$	-1.9×10^{-5}	
$M_{\alpha c}$			

[a]Values taken from Ref. 5.

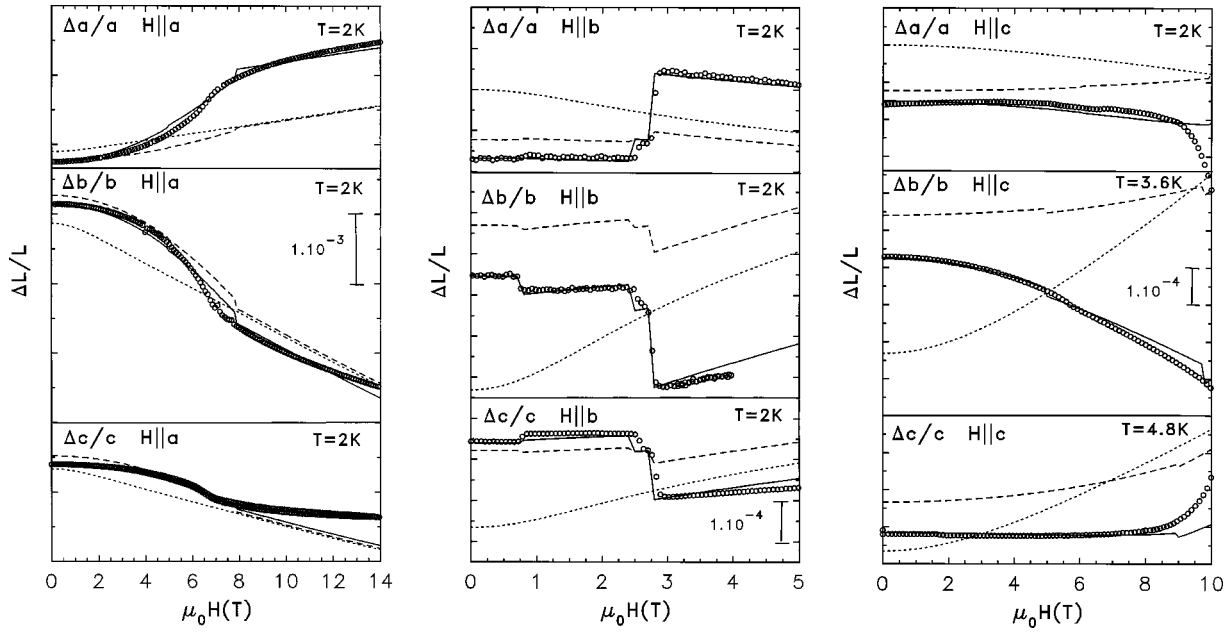

FIG. 1. Longitudinal and transversal magnetostriction of a $NdCu_2$ single crystal. The symbols indicate the measured data. The solid lines (—) correspond to results of the *McPhase* calculation taking into account both the exchange contribution $\epsilon_{\alpha\alpha}^{EX}$ and the CF contribution $\epsilon_{\alpha\alpha}^{CF}$ to the strain. For comparison the CF contribution $\epsilon_{\alpha\alpha}^{CF}$ is shown separately (long dashes – – –). Short dashes (- - -) indicate $\epsilon_{\alpha\alpha}^{CF}$ calculated without *McPhase*, i.e., considering only the paramagnetic CF eigenstates (see text).

magnetic excitations.[1] The CF contribution $\epsilon_{\alpha\alpha}^{CF}$ in Eq. (1.5) was calculated using the mean fields calculated with *McPhase* and the CF parameters given in Refs. 1 and 5.

II. RESULTS AND DISCUSSION

At low temperatures the contribution of phonons and electrons to the strain is negligible and the magnetostriction of $NdCu_2$ can be calculated using the model (1.5). Table I shows the magnetoelastic parameters used in our evaluation of Eq. (1.5). The values for A and B have been taken from Ref. 5. The magnetoelastic constants K,L, and M have been determined to give a reasonable quantitative adaptation of the calculated expressions (1.5) to the experimental data. Interactions beyond the nearest neighbor (i.e., $L,M\neq 0$) have only been taken into account when necessary in order to describe the experimental data. Magnetostriction data on $GdCu_2$ (see Ref. 2) yield $K_{a\alpha}^{GdCu_2}=+17\times10^{-5}$, $K_{b\alpha}^{GdCu_2}=-1\times10^{-5}$, and $K_{c\alpha}^{GdCu_2}=-1\times10^{-5}$ ($\alpha=a,b,c$). Comparing these values to $NdCu_2$ we infer that in the heavy RCu_2 compounds the exchange contribution to the magnetostriction is of comparable magnitude. Note that in the case of $GdCu_2$ $K_{\alpha a}=K_{\alpha b}=K_{\alpha c}$ ($\alpha=a,b,c$) in contrast to $NdCu_2$. Probably the orbital momentum ($L\neq 0$) of the Nd^{3+} ion leads to the strong anisotropy in the derivatives of the exchange tensor $\mathcal{J}_{\alpha\beta}$ with respect to the strain ϵ.

The results of the calculation are compared in Figs. 1 and 2 to new experimental data measured by capacitance dilatometry on a single crystal. The magnetostriction data are in good agreement with a previous study of $\Delta b/b$ for magnetic field in the b direction.[7] The solid lines correspond to results of the *McPhase* calculation taking into account both, the exchange ($\epsilon_{\alpha\alpha}^{EX}$) and CF ($\epsilon_{\alpha\alpha}^{CF}$) contribution to the strain. For comparison the CF contribution $\epsilon_{\alpha\alpha}^{CF}$ is shown separately (long dashes). Although magnetic order has been taken into account, this contribution alone cannot describe our experimental data adequately. In order to show the influence of magnetic order, $\epsilon_{\alpha\alpha}^{CF}$ has also been calculated assuming that the system stays paramagnetic down to zero temperature [i.e., by putting all $\mathcal{J}_{\alpha\beta}(\epsilon,\mathbf{i}-\mathbf{j})=0$ in Eq. (1.3) and calculating the $\langle O_l^m(\mathbf{J_i})\rangle_{T,\mathbf{H}}$ in Eq. (1.5) using the CF eigenstates].

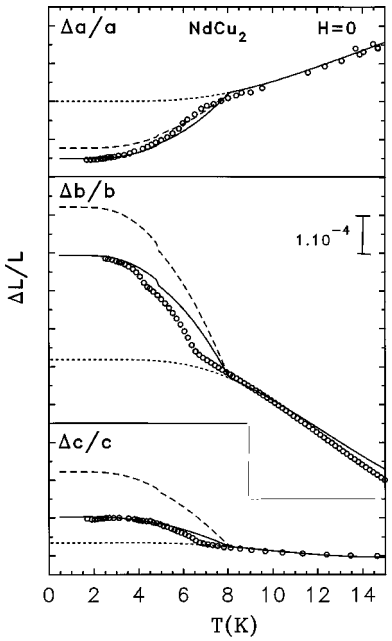

FIG. 2. Thermal expansion of a $NdCu_2$ single crystal in zero field in the crystallographic a, b, and c direction. For explanations of symbols see Fig. 1 and text.

The results of this calculation are shown by short dashes in Figs. 1 and 2.

The onset of the axis conversion[8] at around 8 T makes the interpretation of magnetostriction for fields in the c direction difficult (Fig. 1) and therefore values given for $K_{\alpha c}$ are less reliable than the other magnetoelastic constants given in Table I.

In conclusion, the present analysis shows that it is possible to model magnetostriction in compounds with very complex magnetic phase diagrams using *McPhase*. Good agreement between experiment and theory can be achieved, if the parameters in the Hamiltonian are well determined. Further improvements of *ab initio* calculations[9] may eventually lead to estimates of the magnetoelastic parameters.

In the case of $NdCu_2$ the CF contribution calculated according to Ref. 5 can only describe part of the experimental data. In the magnetically ordered phase it is important to consider the exchange contribution to the strain, which can be calculated by *McPhase*. The remaining discrepancies (e.g., the slope of $\Delta b/b$ and $\Delta c/c$ in high fields parallel a) suggest that possibly magnetoelastic CF contributions for $l>2$ are important. Furthermore, the CF model for small strains[4] is not sufficient to describe the giant magnetostriction for high fields parallel c. This is probably due to the importance of large quadrupolar interactions which leads to a magnetic axis conversion.[8]

In contrast to the rare earth elements[9] in the RCu_2 series the exchange contribution to the magnetostriction is of the same order as the single ion contribution. In order to establish more details of the exchange contribution it is necessary to extend the analysis of $NdCu_2$ and $GdCu_2$ to other RCu_2 compounds.

ACKNOWLEDGMENTS

Part of this work was performed within the program of the Sonderforschungsbereich 463 (funded by the Deutsche Forschungsgemeinschaft). One of the authors, P.S. would like to acknowledge the support of the Grant Agency of Charles University (Grant No. 165/01).

[1] M. Rotter *et al.*, Eur. Phys. J. B **14**, 29 (2000).
[2] M. Rotter *et al.*, J. Magn. Magn. Mater. **236**, 267 (2001).
[3] P. Morin and D. Schmitt, in *Ferromagnetic Materials*, edited by K. H. J. Buschow and E. P. Wohlfarth (Elsevier, Amsterdam, The Netherlands, 1990), Vol. 5, pp. 1–132.
[4] M. Divis, P. Lukac, and P. Svoboda, J. Phys.: Condens. Matter **2**, 7569 (1990).
[5] E. Gratz *et al.*, J. Phys.: Condens. Matter **5**, 567 (1993).
[6] M. Loewenhaupt *et al.*, Z. Phys. B: Condens. Matter **101**, 499 (1996).
[7] S. W. Zochowski, M. Rotter, E. Gratz, and K. A. McEwen, J. Magn. Magn. Mater. **140–144**, 1129 (1995).
[8] S. Kramp *et al.*, Eur. Phys. J. B **18**, 559 (2000).
[9] S. Buck and M. Fähnle, Phys. Rev. B **57**, 14044 (1998).

EUROPHYSICS LETTERS 15 November 1999

Europhys. Lett., **48** (4), pp. 410-414 (1999)

Structural change in $DyCu_2$ single crystal induced by magnetic field

P. Svoboda[1], M. Doerr [2], M. Loewenhaupt[2], M. Rotter [2], T. Reif[3]
F. Bourdarot[4] and P. Burlet[4]

[1] *Department of Electronic Structures, Charles University*
Ke Karlovu 5, 12116 Praha 2, Czech Republic
[2] *Institut für Angewandte Physik (IAPD) - TU Dresden, 01062 Dresden, Germany*
[3] *Institut für Festkörperforschung, Forschungszentrum Jülich - 52425 Jülich, Germany*
[4] *CEA, Département de Recherche Fondamentale sur la Matiére Condensée*
SPSMS/MDN, 38054 Grenoble, France

(received 19 July 1999; accepted 15 September 1999)

PACS. 64.60−i – General studies of phase transitions.

Abstract. – The metamagnetic transition in the orthorhombic antiferromagnets RCu_2 (R=Ce, Pr, Dy, Tb) in high magnetic fields parallel to the c-direction is connected with a conversion of the magnetic Ising axis from the orthorhombic a- to the c-direction. The new state remains stable even after switching off the field. A giant magnetostriction (GMS) $\Delta L/L \geq 1$ % is observed at the conversion. Neutron scattering experiments on a $DyCu_2$ single crystal reveal that this axis conversion is also connected with a structural transition from the orthorhombic $CeCu_2$-type structure to the hexagonal AlB_2-type structure due to strong magnetoelastic coupling. To our knowledge this is the first observation of a change from low to high crystal lattice symmetry by application of an external magnetic field.

Already some years ago the conversion of the Ising axis in high magnetic fields was discovered [1] in the orthorhombic compound $DyCu_2$ by magnetisation measurements, which showed unusual large hysteresis effects. Figure 1 shows an example: if a strong magnetic field is applied along the c-axis of a $DyCu_2$ single crystal, the magnetisation increases from 2.4 to $6.4\mu_B/f.u.$ (at $T = 30$ K). The saturation magnetisation (measured at 2 K) is $8.5\mu_B/f.u.$, approximately. After the conversion the magnetisation curve along the c-axis resembles closely the magnetisation curve of the (original easy) a-axis and vice versa. The axis conversion can be reversed either by applying a high field along the a-axis or by increasing the temperature above 150 K [2].

Studies on other RCu_2 compounds revealed a similar effect for R = Ce, Pr and Tb, too [3]. The temperature dependence of the conversion field of $DyCu_2$ was investigated by magnetisation measurements [2], showing that the conversion is also observed in the paramagnetic state, *i.e.* above $T_N = 27$ K (compare fig. 1). From specific-heat measurements in external magnetic field it was inferred that the conversion can also be induced by the variation of temperature at

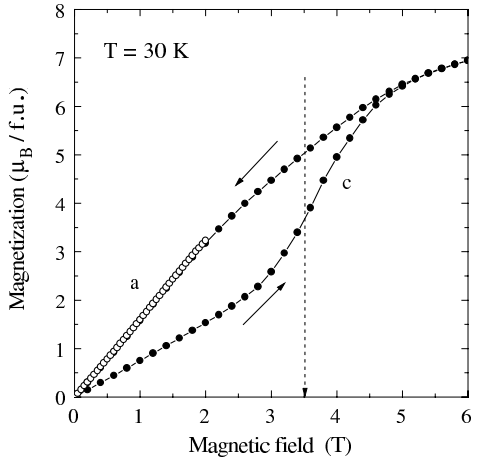

Fig. 1

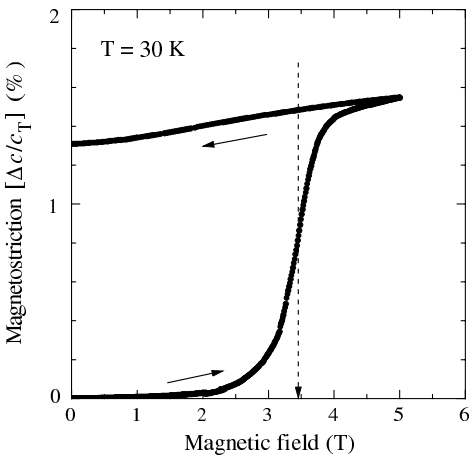

Fig. 2

Fig. 1. – Magnetisation of $DyCu_2$ along the c-direction at $T = 30$ K, showing the huge hysteresis typical for the axis conversion. The open symbols show the magnetisation along the a-axis, for comparison.

Fig. 2. – Giant magnetostriction of $DyCu_2$ at the axis conversion at $T = 30$ K.

constant field [4]. Magnetostriction measurements showed that the axis conversion is connected with a giant magnetostriction (GMS). Figure 2 shows that the crystal expands 1.5 % in the c-direction at $T = 30$ K, at 4 K the magnetostriction is nearly 4 % [2]. In the a-direction the crystal contracts simultaneously, whereas the lattice parameter b stays nearly unchanged in the conversion cycle. We will demonstrate in this letter by neutron diffraction on a $DyCu_2$ single crystal, that the drastic change of the lattice parameters a and c is connected with a structural change.

Figures 3 and 4 show the two types of structures that have to be considered. The orthorhombic $CeCu_2$-type structure (space group $Imma$, D_{2h}^{28}) can be viewed as a distorted hexagonal AlB_2 type (space group P_6/mmm, D_{6h}^{1}). Note that in the orthorhombic description a and c form the hexagonal plane.

It is remarkable that the magnetic (H,T)-phase diagrams of the virgin sample of $DyCu_2$ with field in a-direction and of the converted sample with field in c-direction are nearly identical [2]. This indicates that the magnetic exchange interactions are not significantly influenced by the huge change of the lattice constants associated with the conversion. Yoshida *et al.* proposed a model based on quadrupolar interactions [5] to explain the Ising axis conversion in $DyCu_2$.

The single crystal of $DyCu_2$ was grown by the Czochralsky method in a vacuum of 1.4×10^{-6} mbar and a pulling rate of 20 mm/h. Neutron diffraction measurements indicated that the crystal is of high quality and contains no other grains. The original crystal had a 10 mm diameter and 50 mm length. It was then cut into several small pieces. We used pieces of $3 \times 3 \times 4$ mm^3, approximately, for the experiments with neutrons.

Neutron scattering experiments have been performed at the D15 diffractometer of the Institute Laue Langevin (Grenoble) with a wavelength of 0.085 nm and 0.117 nm, and at the E4 diffractometer of the Hahn Meitner Institut (Berlin) with a wavelength of 0.246 nm.

The neutron scattering experiment consisted of three parts. At first a complete determination of the crystallographic structure was performed at $T = 1.5$ K yielding the

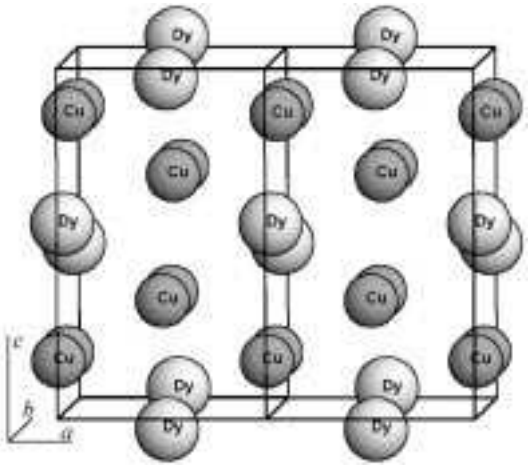

Fig. 3

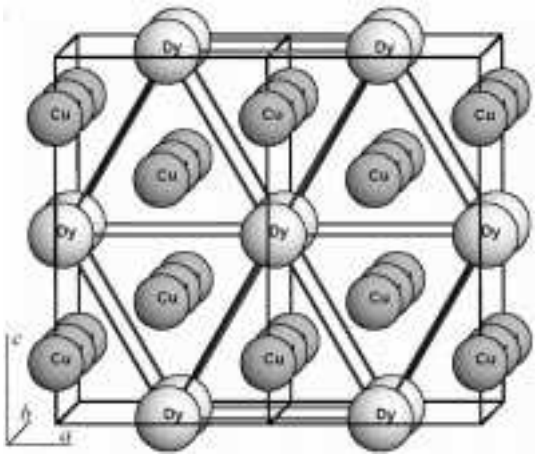

Fig. 4

Fig. 3. – Projection of the orthorhombic $CeCu_2$-type crystal structure onto the ac-plane. The shown cell is two times the unit cell along the a-axis.

Fig. 4. – Projection of the AlB_2-type structure onto the hexagonal plane (the ac-plane in the orthorhombic notation).

well-known $CeCu_2$-type structure with $a = 0.4294 \pm 0.0002$ nm, $b = 0.6742 \pm 0.0008$ nm, $c = 0.724 \pm 0.004$ nm, a cell volume of $V = 0.2097 \pm 0.0015$ nm^3 and the atomic positions $z_{\mathrm{Dy}} = 0.5426$, $y_{\mathrm{Cu}} = 0.0537$ and $z_{\mathrm{Cu}} = 0.1638$. Then the temperature was increased to 30 K (*i.e.* above the Néel temperature $T_{\mathrm{N}} = 27$ K) and a magnetic field of 5 T was applied along the c-direction with a ramp rate 0.05 T/min. To see the influence of the magnetic field on the lattice properties we measured the intensity of the (2 0 0), (0 4 0) and (−6 −8 −2) reflections simultaneously while ramping the field. The result is shown in fig. 5. Then, after the axis conversion, the field was removed and the temperature set back to 1.5 K. Again a complete structure determination was performed resulting in $a^{\mathrm{conv}} = 0.4227 \pm 0.0003$ nm (this corresponds to a GMS of $\Delta a/a = -1.55\%$ with respect to the unconverted state), $b^{\mathrm{conv}} = 0.6747 \pm 0.0003$ nm (+0.07%), $c^{\mathrm{conv}} = 0.7340 \pm 0.0037$ nm (+1.3%), $V^{\mathrm{conv}} = 0.2093 \pm 0.0013$ nm^3 (−0.17%). In the converted state the c/a ratio is $c^{\mathrm{conv}}/a^{\mathrm{conv}} = 1.7318 \pm 0.0095 \sim 1.7321 = \sqrt{3}$ ($z_{\mathrm{Dy}}^{\mathrm{conv}} = 0$, $y_{\mathrm{Cu}}^{\mathrm{conv}} = 0$, $z_{\mathrm{Cu}}^{\mathrm{conv}} = 0.16667 \sim 1/6$). The special value of $c^{\mathrm{conv}}/a^{\mathrm{conv}}$ indicates a change from orthorhombic to hexagonal symmetry.

In fig. 5 it can be seen that the intensity of the (0 4 0) reflection does not change during the conversion process within the experimental error, indicating that the atoms are moved mainly within the ac plane. The (−6 −8 −2) reflection disappears at 3.5 T, because it is forbidden in the hexagonal structure. The field value with the strongest intensity changes ($\mu_0 H = 3.5$ T) is in accordance with the conversion field 3.5 T at $T = 30$ K measured by macroscopic methods [2].

The observed change in intensity and position of the reflections before and after the axis conversion is a strong proof that *the axis conversion is associated with a change from the orthorhombic* $CeCu_2$ *to the hexagonal* AlB_2 *structure*. The intensity of (2 0 0) decreases for fields $\mu_0 H \geq 3$ T by about 20 %. The (2 0 0) reflection of the orthorhombic $CeCu_2$ structure corresponds to the (2 −1 0) (mind the hexagonal notation) of the hexagonal AlB_2 structure and has the same structure factor. The small decrease in intensity can be connected with the

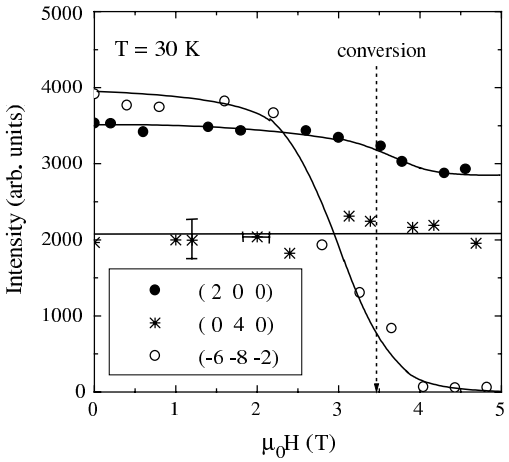

Fig. 5. – Field dependence of the intensity of the (0 4 0), (2 0 0) and (−6 −8 −2) reflections at the axis conversion at $T = 30$ K. The lines are a guide to the eye.

formation of microcracks in the sample at the conversion process.

A complete confirmation of the change from orthorhombic to hexagonal symmetry can be deduced by comparing the reflections measured at $T = 1.5$ K before and after the con-

TABLE I. – *Position and intensity of some selected reflections at* $T = 1.5$ K *before* (virg) *and after* (conv) *the axis conversion. The values of* h, k *and* l *refer to the orthorhombic reciprocal lattice of the* $CeCu_2$ *structure. The reflections (marked by *) obey the hexagonal extinction rules in the converted state. They could not be detected in the converted crystal within the experimental error.*

$(h\ k\ l)$	$I^{\mathrm{virg}}_{\mathrm{meas}}$	$I^{\mathrm{conv}}_{\mathrm{meas}}$
(2 0 0)	3538 ± 26	3091 ± 43
(4 0 0)	6426 ± 38	605 ± 18
(6 0 0)*	9800 ± 56	**0**
(0 2 0)	118 ± 3	123 ± 4
(0 4 0)	2010 ± 16	2108 ± 23
(0 6 0)	3007 ± 22	3212 ± 28
(1 0 1)	180 ± 3	130 ± 4
(3 0 1)	178 ± 6	73 ± 7
(2 3 1)*	1362 ± 13	**0**
(6 3 1)*	2467 ± 22	**0**
(0 4 2)	1058 ± 16	1371 ± 17
(2 4 2)	1116 ± 12	775 ± 13
(4 4 2)	1075 ± 12	147 ± 15
(6 4 2)	1637 ± 18	1825 ± 22
(1 5 2)	2643 ± 19	108 ± 9
(3 5 2)*	2833 ± 22	**0**
(5 5 2)*	3344 ± 25	**0**
(6 8 2)	3915 ± 26	265 ± 11
(1 9 2)*	989 ± 12	**0**

version. In table I the intensities of some characteristic reflections are shown. Due to the strong absorption of Dy the intensities depend strongly on the shape and orientation of the sample. Therefore any intensity values given have to be interpreted with great care. In most cases several equivalent reflections have been measured and the average intensity is given in table I. Note that the reflections with zero intensity in the converted state obey the hexagonal extinction rules.

As discussed above, the magnetic (H,T)-phase diagrams of the virgin sample with field in a-direction and of the converted sample with field in c-direction are identical [2]. The magnetic structure after the axis conversion was identified by measuring the magnetic satellites at $T = 1.5$ K. The results confirm the commensurate structure with $\boldsymbol{\tau}$=(2/3 1 0) [4,6]. Moreover, we found three equivalent magnetic domains characterized by a propagation turned by 60° in accordance with the hexagonal symmetry of the converted system. For that reason the magnetic two-ion exchange interaction cannot depend much on the lattice symmetry. The magnetoelastic coupling may arise from a strong strain dependence of either the magnetic two-ion exchange or the single-ion (crystal field) exchange interactions. Because we find that the exchange interaction does not depend on the lattice strain we conclude that a strong single-ion magnetoelastic coupling must be the reason for the observed symmetry change of the lattice.

The conversion of the easy axis in $DyCu_2$ increases the symmetry of the lattice by changing it from orthorhombic to hexagonal. To our knowledge *this is the first time that a change from low to high symmetry in external magnetic field has been observed* (for a review see [7] and references therein). This change in symmetry is accompanied by a GMS of several percents, which has been observed both macroscopically by dilatometric measurements of the sample length, and microscopically by neutron diffraction experiments as the change of lattice parameters.

***

The work was supported by the Deutsche Forschungsgemeinschaft (Sonderforschungsbereich 463). One of the authors, PS, wants to acknowledge the support of the Grant Agency of Charles University, grant No. 52/1998.

REFERENCES

[1] Hashimoto Y., Kindo K., Takeuchi T., Senda K., Date M. and Yamagishi A., *Phys. Rev. Lett.*, **72** (1994) 1922.

[2] Loewenhaupt M., Doerr M., Jahn L., Reif T., Sierks C., Rotter M. and Mueller H., *Physica B*, **246-247** (1998) 472.

[3] Sugiyama K., Nakashima M., Yoshida Y., Settai R., Takeuchi T., Kindo K. and Onuki Y., *Physica B*, **259-261** (1999) 896.

[4] Doerr M., Loewenhaupt M., Hahn W., Brueck E., Hagmusa I., Klaase J. and Rotter M., *Physica B*, **262** (1999) 340.

[5] Yoshida Y., Sugiyama K., Takeuchi T., Kimura Y., Aoki D., Kouzaki M., Settai R., Kindo K. and Onuki Y., *J. Phys. Soc. Jpn.*, **67** (1998) 1421.

[6] Koike Y., Metoki N., Morii Y., Yoshida Y., Settai R. and Onuki Y., *J. Phys. Soc. Jpn.*, **66** (1997) 4053.

[7] Andreev S., in *Magnetic Materials*, edited by K. H. J. Buschow, Vol. **8** (North-Holland, Amsterdam) 1995, p. 59.

Anomalous magnetic exchange interactions in $SmCu_2$

M. Rotter,* M. Doerr, M. Loewenhaupt, and U. Witte
Institut für Angewandte Physik, Technische Universität Dresden, D-01062 Dresden, Germany

P. Svoboda and J. Vejpravová
Department of Electronic Structures, Charles University, 12116 Prague 2, Czech Republic

H. Sassik
Institut für Experimentalphysik, Technische Universität Wien, Wiedner Hauptstraße 8-10, A-1040 Wien, Austria

C. Ritter
Institut Laue Langevin, F-38042 Grenoble, France

D. Eckert, A. Handstein, and D. Hinz
Institut für Festkörper- und Werkstofforschung, P.O.B. 270116, D-01171 Dresden, Germany
(Received 7 February 2001; revised manuscript received 21 June 2001; published 31 August 2001)

RCu_2 compounds (R=rare earth) show magnetic structures with very different propagation vectors. This behavior can be explained by the anisotropy of the magnetic exchange interaction in combination with the crystal field. In order to support this model the magnetic phase diagram of a $SmCu_2$ single crystal has been investigated by magnetization, thermal expansion, magnetostriction, electrical transport, and specific heat measurements. The magnetic structure in zero field has been determined by neutron diffraction on a powder sample using ^{154}Sm. The magnetic moments were found to be oriented parallel to the b direction in contrast to other RCu_2 compounds (R=Tb, Dy, Ho) with the same propagation. In order to explain the observed magnetic structure of $SmCu_2$ we infer that the anisotropic part of the exchange interaction tensor is reversed in comparison with the other RCu_2 compounds.

DOI: 10.1103/PhysRevB.64.134405 PACS number(s): 75.30.Et, 75.30.Gw, 75.50.−y

I. INTRODUCTION

There are two kinds of magnetic anisotropy in rare-earth compounds: the single-ion anisotropy caused by the crystal field (CF) and the anisotropy of the two ion interactions. Both types of anisotropy have to be considered to arrive at a consistent description of the magnetic properties of the orthorhombic intermetallic compound $NdCu_2$ (Refs. 1–3) (space group *Imma*).

The exchange parameters determined from inelastic neutron-scattering experiments on $NdCu_2$ (Ref. 1) can be used to make a prediction for the ordering temperature and the magnetic structure of some other isostructural RCu_2 compounds on the basis of a mean-field theory. These agree well with the available experimental results for the $TbCu_2$, $DyCu_2$, and $TmCu_2$ compounds[1]: the magnetic ordering vector τ is determined by the magnetic exchange interaction and depends on the moment direction, because the exchange interaction is anisotropic. If the magnetic moments point into the crystallographic b direction due to the CF, an ordering wave vector of $\tau\sim(2/3\ 0\ 0)$ is expected (as observed for $NdCu_2$ and $TmCu_2$). If the moments are oriented perpendicular to b then the ordering wave vector is $\tau=(2/3\ 1\ 0)$ (e.g., for $TbCu_2$ and $DyCu_2$).

$SmCu_2$ is a compound of this series that has not been investigated by neutron scattering due to the high absorption cross section of Sm. The measurement of the susceptibility indicates that in this compound an antiferromagnetic ordering occurs below 23 K with a magnetic moment in b direction similar to the case of $NdCu_2$ and $TmCu_2$.[4,5] As in $NdCu_2$ the measurements of the specific heat gave evidence for a second transition at 17 K, which probably is connected with a change of the ordering vector from a commensurate to an incommensurate value. If the model mentioned above is correct we would expect to find an antiferromagnetic ordering with a wave vector of about $\tau=(2/3\ 0\ 0)$.

II. EXPERIMENT

To clarify the magnetic ordering process in $SmCu_2$ we performed a neutron-diffraction experiment on a polycrystalline sample prepared with the isotope ^{154}Sm in order to reduce the absorption cross section. The polycrystalline sample for this neutron-scattering experiment was prepared at the Technical University (Vienna) by arc melting stoichiometric amounts of ^{154}Sm and Cu in protective argon atmosphere. Phase purity was checked by x-ray powder diffraction. The D1B diffractometer of the Institut Laue Langevin (Grenoble) was used because of its high resolution at low angles and its high flux of $6.5\times10^6\ n\,cm^{-2}\,s^{-1}$ at the sample position (which was essential for the small sample of 3 g with a small magnetic moment). To determine the temperature dependence of the magnetic structure a profile analysis at temperatures T=2, 20, and 30 K was performed using a wavelength of 0.25 nm. The data were fitted using the FULLPROF profile matching program. The diffraction pattern at 2 K was used to refine the structural parameters and the size of the magnetic moment at the same time. The refined unit-cell parameters at 2 K are $a=0.436\pm0.003$ nm, $b=0.685\pm0.006$ nm, $c=0.735\pm0.006$ nm; the atomic position parameters are

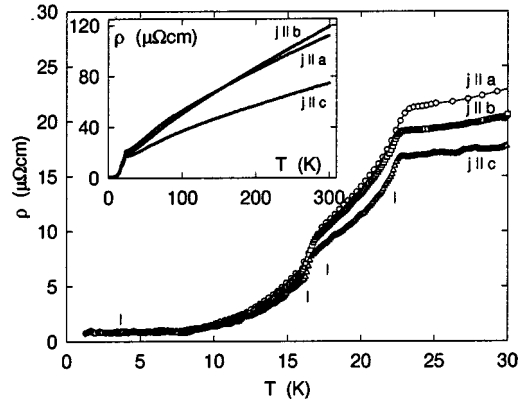

FIG. 1. Low-temperature part of the temperature dependence of the electrical resistivity parallel to the main crystallographic axes. The inset shows the resistivity up to the room temperature.

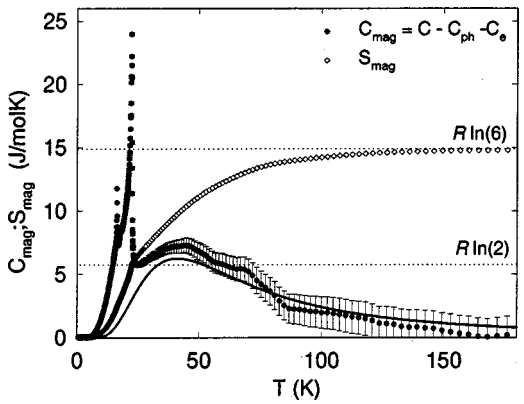

FIG. 2. Analysis of the magnetic part of specific heat together with the magnetic entropy. The full line shows the best fit of a Schottky contribution and the dashed lines correspond to the entropy of doublet and sextet, respectively.

$z_{Sm}=0.544\pm0.004$, $y_{Cu}=0.055\pm0.001$, and $z_{Cu}=0.170\pm0.001$.

The magnetic and dilatometric measurements were performed on a single crystal with dimensions $2.2\times2.9\times2.1$ mm^3. The single crystal of $SmCu_2$ was grown by the Czochralski pulling method using the tri-arc furnace at Charles University (Prague). We have used about 10 g of melt, consisting of pure constituents of Sm (3N5) and Cu (5N). The melt was kept in water-cooled copper crucible under pure argon (6N) protective atmosphere (pressure 1.3 bar). Due to the high volatility of Sm, 5 at.% of Sm was added to the stoichiometric composition. The growing conditions were as follows. Pulling speed: 10 mm/hour, rotation of the seed: 20 min^{-1}, rotation of the crucible: 10 min^{-1}. We have succeeded in growing a single-crystalline ingot about 40 mm long with 4 mm maximum diameter. X- ray diffraction (using Cu-Kα_1-Kα_2 radiation) was done afterwards to check the phase purity and to measure the lattice parameters of the single crystal at room temperature. The lattice parameters were found to be $a=0.43577\pm0.00003$ nm, $b=0.69343\pm0.00005$ nm, $c=0.73720\pm0.00006$ nm and the atomic positions are $z_{Sm}=0.545\pm0.001$, $y_{Cu}=0.065\pm0.001$, and $z_{Cu}=0.165\pm0.001$. All these parameters agree very well with those reported in the literature.[5] No other phase (even oxides) was observed within the precision of the x rays. Measurements of the temperature dependence of the electrical resistivity parallel to the main crystallographic axes (see Fig. 1) have also confirmed the high quality of the single crystal, yielding the residual resistivity ratios RRR=155, 175, and 78.5 for the current along *a*, *b*, and *c* axis, respectively (see the inset of Fig. 1).

Thermal expansion and magnetostriction was measured using a capacitance dilatometer in a 15 T Oxford Instruments superconducting magnet,[6] magnetization measurements were performed in a vibrating sample magnetometer (Oxford Instruments) in steady fields up to 14 T and in the 50 T pulsed field magnet of the Dresden high field facility.[7] Electrical resistivity and isobaric specific heat of $SmCu_2$ in the zero magnetic field were measured in the temperature range 0.5–300 K using a PPMS facility (Quantum Design).

III. RESULTS AND DISCUSSION

A. Specific heat

The results of specific heat measurements are shown in Figs. 2 and 3. For the analysis of the isobaric specific heat c_p we have considered three main contributions:

$$c_p=c_e+c_{ph}+c_{mag}, \tag{1}$$

where c_e is the electronic part, expressed as $c_e=\gamma T$ (γ denotes the Sommerfeld constant), c_{ph} is the phonon part, including the anharmonic effect,[8] written in the form

$$c_{ph}=\frac{9R_g}{1-\alpha_D T}\left(\frac{1}{x_D}\right)^3\int_0^{x_D}\frac{x^4\exp(x)}{[\exp(x)-1]^2}dx, \tag{2}$$

where $x_D=\Theta_D/T$, Θ_D is the Debye temperature, α_D is the anharmonic correction term, and R_g is the gas constant.

The magnetic part of the specific heat is caused by the magnetic exchange field (below T_N, for a discussion of the magnetic phases we refer to the Sec. III B) in addition to the crystal field. The orthorhombic crystal field splits the $4f^5$ ground state of the Sm^{3+} ion ($J=5/2$, $L=5$, $S=5/2$) into 3

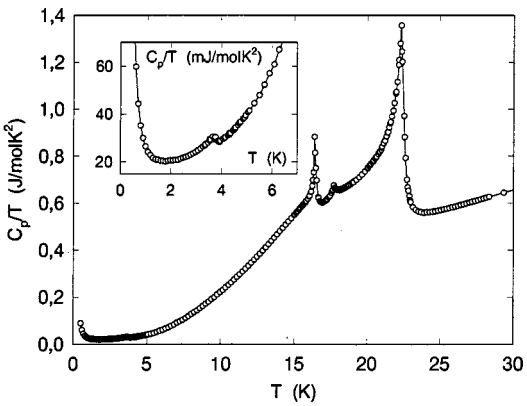

FIG. 3. Low-temperature part of the specific heat of $SmCu_2$ in the C/T vs T representation indicating the magnetic phase transitions at $T=16.4$, 17.7, and 22.3 K, respectively. The inset shows the anomaly corresponding to the lowest phase transition at 3.7 K.

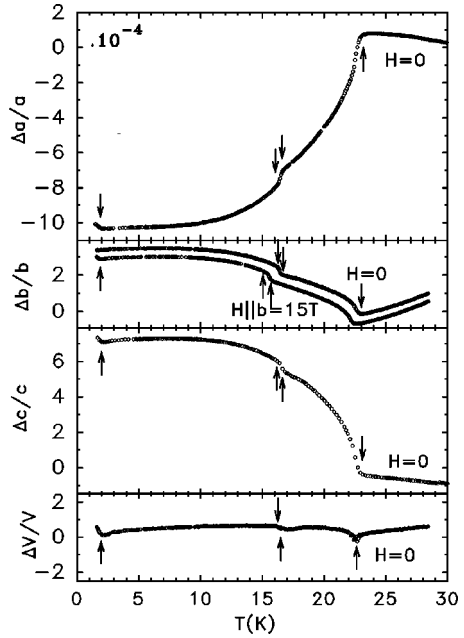

FIG. 4. Thermal expansion of $SmCu_2$ along the crystallographic a,b, and c directions at zero magnetic field. The relative volume change as deduced from $\Delta V/V=\Delta a/a+\Delta b/b+\Delta c/c$ is shown at the bottom. For the b direction also the 15 T curve is shown.

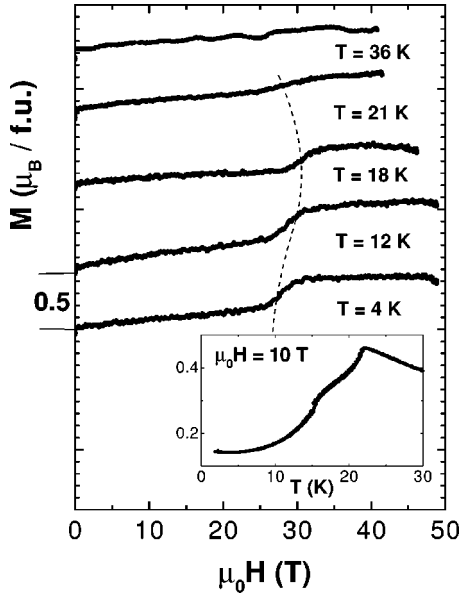

FIG. 5. Magnetization of $SmCu_2$ along the crystallographic b direction measured at different temperatures in a pulsed magnetic field. The inset shows the temperature dependence of the magnetization measured along b in a steady field of 10 T (vibrating sample magnetometer).

Kramer doublets. Thus for temperatures $T>T_N$ the magnetic specific heat c_{mag} can be expressed as a Schottky contribution of the $n=3$ Sm^{3+} crystal-field levels (the Δ_i denote the crystal-field level energies in Kelvins, $\Delta_1=0$):

$$c_{mag}=\frac{R_g}{T^2}\left\{\frac{\sum_{i=1}^{n}\Delta_i^2\exp\frac{-\Delta_i}{T}}{\sum_{i=1}^{n}\exp\frac{-\Delta_i}{T}}-\left(\frac{\sum_{i=1}^{n}\Delta_i\exp\frac{-\Delta_i}{T}}{\sum_{i=1}^{n}\exp\frac{-\Delta_i}{T}}\right)^2\right\}. \tag{3}$$

From the analysis we obtain $\gamma=17.0\pm0.3$ mJ/mol K^2, $\Theta_D=220\pm2$ K and $\alpha_D=(1.2\pm0.2)\times10^{-4}$ K^{-1}. The best fit of the Schottky contribution gives the positions of the two excited doublets as $\Delta_2=100\pm5$ K and $\Delta_3=120\pm5$ K, respectively, yielding the high-temperature magnetic entropy $S_{mag}=R_g\ln(6)$, as expected for the Sm^{3+} ion (see Fig. 2).

B. Expansion and magnetization measurements

The magnetic phase diagram of the $SmCu_2$ single crystal has also been investigated by thermal expansion and magnetostriction measurements. Figure 4 shows the field dependence of the thermal expansion along the crystallographic a,b, and c directions. Four phase transitions are observed at 2.0 K, 16.2 K, 16.8 K, and at $T_N=22.7$ K in zero magnetic field and agree well with the results of specific heat (see Fig. 3). Comparing these measurements to available literature data[4,5] we find, that the lowest transition and the intermediate phase above 16 K has not been reported yet. In Ref. 4, however, a transition at 10 K has been reported, which cannot be found in our data.

The thermal expansion determined by capacitance dilatometry agrees well with the results of x-ray powder diffraction above T_N.[5,9] Below T_N strong magnetoelastic effects along the b and c axis appear, which have not been seen in x-ray diffraction. Summing up $\Delta a/a$, $\Delta b/b$, and $\Delta c/c$ leads to a very small volume effect. The thermal expansion measured in a magnetic field shows that there are only very small changes of the transition temperatures in fields along the b direction. The transition temperatures change to 1.8 K, 14.7 K, 15.2 K, and 22.3 K at the maximum-available static field of 15 T. The forced magnetostriction in fields up to 15 T is negligible ($\Delta l/l<3\times10^{-5}$).

Besides the dilatometric experiments, magnetization measurements have been performed in magnetic fields parallel to the crystallographic b direction (see Fig. 5). The magnetization measured at constant fields in the temperature range between 2 K and 30 K yields anomalies at temperatures that are consistent with the values derived from the thermal expansion measurements (e.g., 2.7 K, 15.2 K, 15.6 K, and 21.9 K at 10 T). Below 2.7 K a small increase of the magnetization was detected. However, the two transitions around 15 K cannot be separated because of only small magnetization differences between the phases. The magnetization curves at constant temperatures measured in steady fields up to 14 T show no phase transitions indicating that the transition lines in the magnetic (H,T) phase diagram are nearly vertical in this field range and it is only possible to induce ferromagnetism in higher fields. Therefore, we performed magnetization measurements in pulsed fields at several temperatures. Because of the small value of the magnetic moment in $SmCu_2$ it was necessary to correct the magnetization curve by subtracting the signal without sample from the measured signals for each run. Please note, that both signals are of the same

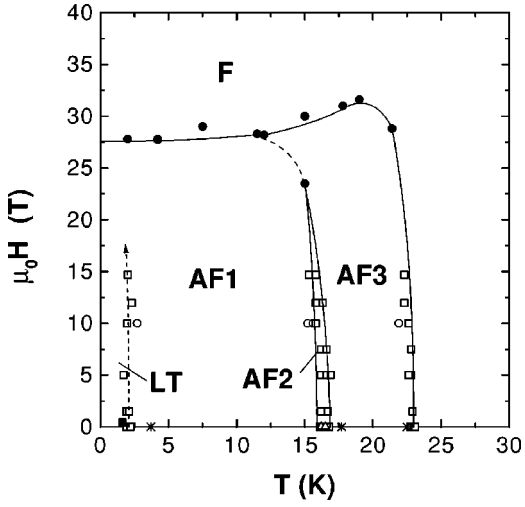

FIG. 6. Magnetic phase diagram of $SmCu_2$ for magnetic field parallel to the crystallographic *b*-direction as deduced from VSM magnetization (open circles), pulsed field magnetization (full circles), magnetostriction (open squares), thermal expansion (full squares), specific heat (stars), and resistivity (triangles) measurements. For the description of the different phases see text.

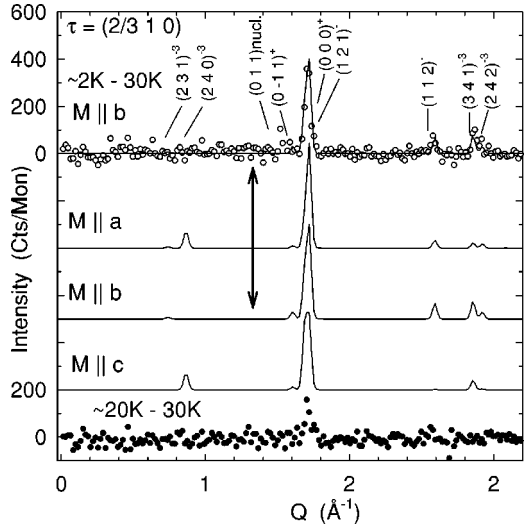

FIG. 7. Difference diffraction pattern at $T=2$ K (top) and $T=20$ K (bottom)—the pattern at 30 K has been subtracted. The line in the top pattern indicates a fit of a squared up structure with a propagation vector of (2/3 1 0). The Sm magnetic moment of $m_b=0.45\ \mu_B$/f.u. is assumed to be aligned parallel to *b* axis. Calculated patterns with the same propagation vector and Sm moment, however, aligned parallel to the *a* and *c* axis are shown for comparison (D1B, $\lambda=0.25$ nm).

order of magnitude. Therefore, the curves shown in Fig. 5 are not as smooth as for measurements in steady fields and the absolute values are correct only within ±20%. Nevertheless, the transition fields between 27 T and 29 T can clearly be identified (compare Ref. 10). The transition field value increases with increasing temperature and decreases again near the ordering temperature.

The magnetic saturation moment of $SmCu_2$ along the *b* direction is approximately $0.5\pm0.1\ \mu_B$/f.u. (see Fig. 5). In addition to crystal-field effects an almost complete compensation of the spin and orbital moment may be the reason for this small value.

The magnetic phase diagram as shown in Fig. 6 is constructed from the available data. At zero field it is characterized by antiferromagnetic order with a low-temperature phase AF1 and, between approximately 16.6 K and the Néel temperature $T_N=23.0$ K, a high temperature phase AF3. Between these two phases an intermediate phase AF2 exists in a narrow temperature region $16.0\ \text{K}<T<16.6$ K (which can be seen most clearly by the two first-order peaks of the specific heat measurement, Fig. 3). Such an intermediate phase was also found in $NdCu_2$ (Ref. 11) and described there as a commensurate phase with an extremely long period and squared up moments. Furthermore, a zero-field phase transition at 2.2 K was found by dilatometric measurements but its origin remains unclear. We propose a low-temperature phase that should be a modification of AF1. In specific heat measurements an anomaly can be seen at a slightly higher temperature of $T=3.7$ K (see inset of Fig. 3). The vibrating-sample magnetometer (VSM) magnetization data also show a low-temperature anomaly characterized by a small increase of the magnetic moment. Measurements using a ^{3}He insert are planned to characterize this low-temperature phase in detail. In magnetic fields the phases are stable up to 28 T, approximately. Above this field value all magnetic moments are oriented parallel to the external field forming the induced ferromagnetic phase F.

The proposed phase diagram resembles the situation of $TbCu_2$ and $DyCu_2$,[10] for which a propagation vector $\tau=(2/3\ 1\ 0)$ was found for AF1. But, in contrast to $SmCu_2$, in $TbCu_2$ and $DyCu_2$ the easy axis of magnetization is the *a* axis. Note also the unusual increase of the transition field AF3—F with temperature, which may be due to a temperature-dependent compensation of the Sm^{3+} spin and orbital moments.[12]

C. Neutron diffraction

Powder neutron diffraction was used in order to determine the magnetic structure of $SmCu_2$. In contradiction to the model expectation[1,3] [predicting $\tau=(2/3\ 0\ 0)$ as outlined in the Introduction] we find a propagation vector of $\tau=(2/3\ 1\ 0)$ at $T=2$ K for the phase AF1. In Fig. 7 the calculated magnetic-intensity pattern is shown in comparison with the experimental data. From these data we infer a magnetic structure that is shown in Fig. 8 in a projection onto the orthorhombic *ab* plane. In the phase AF3 at $T=20$ K the magnetic propagation vector changes to an incommensurate value. Any intensity on the higher-order satellites of the propagation vector $\tau=(2/3\ 1\ 0)$ is within the scatter of the data. In Fig. 9 the magnetic satellites (2/3 1 0), (1/3 1 1), (4/3 1 0), and (2/3 1 2) at 2 K are compared to the corresponding reflections at 20 K. By a careful refinement of the lattice parameters and the magnetic propagation vector at 20 K we find a propagation of $\tau^\star=(0.677\pm0.006, 0.989\pm0.011, -0.008\pm0.013)$. Considering the error involved in these values only a significant shift of *h* can be inferred.

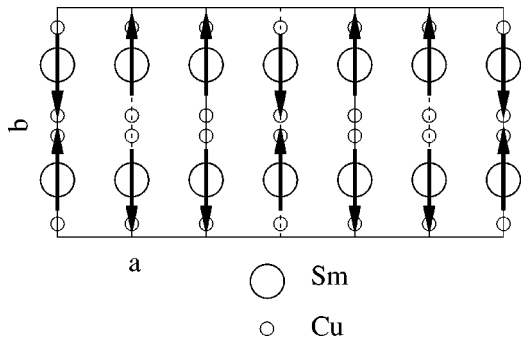

FIG. 8. Magnetic structure of $SmCu_2$ shown in a projection to the ab plane. The magnetic moments are oriented parallel to b. The magnetic unit cell consists of three crystallographic unit cells aligned in a direction.

The antiferromagnetically ordered moment of $m_b = 0.45 \pm 0.07\ \mu_B$/f.u. determined from neutron diffraction in zero magnetic field at $T = 2$ K is in accordance with the saturation moment measured by magnetization.

These results show that the anisotropy of the magnetic exchange interactions in $SmCu_2$ is different in comparison with other RCu_2 compounds. According to the model proposed in Ref. 1 the Fourier transform of the exchange-interaction tensor in RCu_2 compounds can be written as

$$\overline{\overline{\mathcal{J}}}(\mathbf{q}) = \begin{pmatrix} \mathcal{J}^{aa}(\mathbf{q}) & 0 & 0 \\ 0 & \mathcal{J}^{bb}(\mathbf{q}) & 0 \\ 0 & 0 & \mathcal{J}^{cc}(\mathbf{q}) \end{pmatrix} \tag{4}$$

with

$$\mathcal{J}^{aa}(\mathbf{q}) = \mathcal{J}^{cc}(\mathbf{q}). \tag{5}$$

Splitting this interaction tensor into an isotropic and an anisotropic part according to

$$\overline{\overline{\mathcal{J}}}(\mathbf{q}) = \mathcal{J}_{\mathrm{iso}}(\mathbf{q})\,\overline{\overline{1}} + \mathcal{J}_{\mathrm{an}}(\mathbf{q}) \begin{pmatrix} 1 & 0 & 0 \\ 0 & -1 & 0 \\ 0 & 0 & 1 \end{pmatrix}, \tag{6}$$

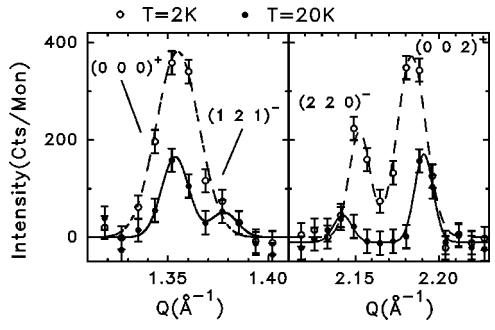

FIG. 9. Magnetic satellites $(0\ 0\ 0)^+$, $(1\ 2\ 1)^-$, $(2\ 2\ 0)^-$, and $(0\ 0\ 2)^+$ at 2 K (open symbols) in comparison with the corresponding reflections at 20 K (full symbols). The lines indicate fits of a Gaussian peaks to the data [with a line width of 0.016 Å^{-1} (left) and 0.013 Å^{-1} (right)].

it seems that the sign of anisotropic part $\mathcal{J}_{\mathrm{an}}(\mathbf{q})$ is opposite for $SmCu_2$ in comparison with the other RCu_2 compounds. We believe that such a behavior should have a simple physical reason. However, the microscopic origin of such an anisotropic exchange is still unclear. To show the consistency of our exchange model for $SmCu_2$ [Eq. (6) with $\mathcal{J}_{\mathrm{an}}^{\mathrm{SmCu_2}}(\mathbf{q}) = -\mathcal{J}_{\mathrm{an}}^{\mathrm{other}R\mathrm{Cu_2}}(\mathbf{q})$] we calculate several physical quantities and compare them to experimental results in the following.

Assuming that the sign of the anisotropy in the exchange tensor is changed for $SmCu_2$ it is possible to estimate some magnetic properties by exchanging the $\mathcal{J}^{aa} = \mathcal{J}^{cc}$ with the $\mathcal{J}^{bb}$ components of the diagonal-exchange tensor, which has been determined for $NdCu_2$.

Following Ref. 1 the Néel temperature can be estimated from

$$k_B T_N = \left(\frac{m_b}{g_J^{\mathrm{Sm}} \mu_B} \right)^2 \mathcal{J}_{\mathrm{Sm}}^{bb}[\boldsymbol{\tau} = (2/3\ 1\ 0)]. \tag{7}$$

Here $g_J^{\mathrm{Sm}} = 2/7$ denotes the Landé factor of the Sm^{3+} ion and $m_b = 0.5\ \mu_B$ the magnetic moment per Sm^{3+} ion as determined from magnetization. Taking for the $\mathcal{J}^{bb}$ component of the exchange in Sm the de Génnes scaled value of the $\mathcal{J}^{aa}$ component in Nd ($\mathcal{J}_{\mathrm{Nd}}^{aa}[\tau = (2/3\ 1\ 0)] = 79\ \mu\mathrm{eV}, g_J^{Nd} = 8/11$) according to

$$\mathcal{J}_{\mathrm{Sm}}^{bb}[\boldsymbol{\tau} = (2/3\ 1\ 0)] = \left(\frac{g_J^{Sm} - 1}{g_J^{Nd} - 1} \right)^2 \mathcal{J}_{\mathrm{Nd}}^{aa}[\boldsymbol{\tau} = (2/3\ 1\ 0)] \tag{8}$$

the expression (7) may be evaluated resulting in a value of 20.0 K for T_N. This is only 13% lower than the experimental value.

By applying the mean-field model developed for $TbCu_2$ and $DyCu_2$ (Ref. 13) to $SmCu_2$ (all these compounds order with the same wave vector) the critical field $H_c^{\mathrm{AF1}\to\mathrm{F}} \| b$ for the transition to the ferromagnetic phase may be calculated using again the $\mathcal{J}^{aa}$ component of the exchange determined in $NdCu_2$.[1]

Using the notation of Ref. 13 in order to number the exchange-interaction constants between the different sublattices the magnetic energies for the antiferromagnetic (AF1) and the ferromagnetic (F) aligned structures (per f.u. and at zero temperature) are given by

$$F_{\mathrm{AF1}} = \frac{m_b^2}{6} \left(\frac{g_J^{\mathrm{Sm}} - 1}{g_J^{\mathrm{Sm}} \mu_B} \right)^2 (2J_2^{bb} - 2J_1^{bb} - 3J_3^{bb} + 3J_4^{bb})$$

$$F_{\mathrm{F}} = -\frac{m_b^2}{2} \left(\frac{g_J^{\mathrm{Sm}} - 1}{g_J^{\mathrm{Sm}} \mu_B} \right)^2 (2J_1^{bb} + 2J_2^{bb} + J_3^{bb} + J_4^{bb}) - \frac{m_b}{k_B} H. \tag{9}$$

The Boltzmann constant k_B in the Zeeman term appears because the exchange parameters J_i and the magnetic energy is calculated in units of K. The critical field $H = H_c^{\mathrm{AF1}\to\mathrm{F}}$ denotes the point at which these two energies are equal ($F_{\mathrm{AF1}} = F_{\mathrm{F}}$) and an expression for $H_c^{\mathrm{AF1}\to\mathrm{F}}$ in terms of the exchange parameters J_i^{bb} may be derived:

$$H_c^{\mathrm{AF1}\rightarrow\mathrm{F}} = -\frac{1}{3} k_B m_b \left(\frac{g_J^{\mathrm{Sm}} - 1}{g_J^{\mathrm{Sm}} \mu_B} \right)^2 (2J_1^{bb} + 4J_2^{bb} + 3J_4^{bb}). \tag{10}$$

Using for J_i^{bb} again the values of J_i^{aa} given for $NdCu_2$ in Ref. 1 (i.e., $J_1^{bb} = 2.47$ K, $J_2^{bb} = -2.79$ K, $J_4^{bb} = -3.61$ K) a value of 27.0 T is calculated for $H_c^{\mathrm{AF1}\rightarrow\mathrm{F}}$ that agrees well with the observed transition field of 28 T.

IV. CONCLUSION

The change of the propagation vector in the magnetic phases of $SmCu_2$ resembles closely the behavior of $DyCu_2$ (Ref. 14) (i.e., commensurate at lower temperatures, incommensurate at higher temperatures). However, in contrast to this compound the moment of Sm is aligned parallel to *b*, as found in $NdCu_2$. It should be noted that the Sm^{3+} magnetic moment is rather small due to a compensation of the spin and orbital contributions.

We have shown that the magnetic propagation vector τ, the Néel temperature T_N and the critical field $H_c^{\mathrm{AF1}\rightarrow\mathrm{F}}$ agree with the model calculation, if a sign reversal of the exchange anisotropy in $SmCu_2$ is assumed in comparison to the other RCu_2 compounds. This anisotropy can be described by a symmetric exchange-interaction tensor with vanishing trace. However, the microscopic origin of such an exchange is not clear and we propose further theoretical studies on this subject.

ACKNOWLEDGMENTS

Part of this work was performed within the program of the Sonderforschungsbereich 463 (funded by the Deutsche Forschungsgemeinschaft). Another part of this work was made within the framework of the Research Center for Quantum Materials Physics in the Joint Laboratory for Magnetic Studies, Prague. The authors (P.S. and J.V.) would like to acknowledge the support of the Grant Agency of the Charles University (Grant No. 52/98) and the Grant Agency of the ASCR (Grant No. GAAV D 101 0023).

*Electronic address: rotter@physik.tu-dresden.de

[1] M. Rotter, M. Loewenhaupt, S. Kramp, T. Reif, N.M. Pyka, W. Schmidt, and R.v.d. Kamp, Eur. Phys. J. B **14**, 29 (2000).
[2] M. Loewenhaupt, M. Rotter, and S. Kramp, Physica B **276-278**, 602 (2000).
[3] M. Rotter, M. Loewenhaupt, and S. Kramp, Physica B **276-278**, 598 (2000).
[4] Y. Isikawa, K. Mori, H. Takeda, I. Umehara, K. Sato, Y. Onuki, and T. Komatsubara, J. Magn. Magn. Mater. **76-77**, 161 (1988).
[5] E. Gratz, N. Pillmayr, E. Bauer, H. Müller, B. Barbara, and M. Loewenhaupt, J. Phys.: Condens. Matter **2**, 1485 (1990).
[6] M. Rotter, H. Müller, E. Gratz, M. Doerr, and M. Loewenhaupt, Rev. Sci. Instrum. **69**, 2742 (1998).
[7] H. Krug, M. Doerr, D. Eckert, and H. Eschrig, Physica B **294-295**, 605 (2001).
[8] C.A. Martin, J. Phys.: Condens. Matter **3**, 5967 (1991).
[9] M. Rotter, Ph.D. thesis, Technische Universität Wien, 1994.
[10] M. Loewenhaupt, M. Doerr, L. Jahn, T. Reif, C. Sierks, M. Rotter, and H. Müller, Physica B **246-247**, 472 (1998).
[11] M. Loewenhaupt, T. Reif, P. Svoboda, S. Wagner, M. Waffenschmidt, H.v. Löhneysen, E. Gratz, M. Rotter, B. Lebech, and T. Hauss, Z. Phys. B: Condens. Matter **101**, 499 (1996).
[12] H. Adachi and H. Ino, Nature (London) **401**, 148 (1999).
[13] N. Iwata, Y. Hashimoto, T. Kimura, and T. Shigeoka, J. Magn. Magn. Mater. **81**, 354 (1989).
[14] T. Reif, M. Doerr, M. Loewenhaupt, M. Rotter, P. Svoboda, and S. Welzel, Physica B **276-278**, 600 (2000).

J. Phys.: Condens. Matter 5 (1993) 567–572. Printed in the UK

The influence of the crystal field on the anisotropic thermal expansion in $ErCu_2$ and $NdCu_2$

E Gratz, M Rotter, A Lindbaum, H Müller, E Bauer and H Kirchmayr

Institut für Experimentalphysik, Technische Universität Wien, A-1040, Wien, Austria

Received 18 May 1992, in final form 22 October 1992

Abstract. The anisotropic thermal expansion parameters $a(T)$, $b(T)$ and $c(T)$ of some $RECu_2$ intermetallics (RE = Y, Er, Nd) has been measured in the temperature range from 400 K down to 4.2 K using x-ray powder diffraction. The influence of the crystal field on the thermal expansion in $ErCu_2$ and $NdCu_2$ has been determined by comparing the thermal expansion of the non-magnetic isostructural YCu_2 with the Er and Nd compounds. The data thus obtained are described theoretically using a set of crystal-field parameters deduced from the analysis of inelastic neutron diffraction data.

1. Introduction

The intermetallic $RECu_2$ compounds crystallize in the orthorhombic $CeCu_2$ type of structure (space group D_{2h}^{28} (*Imma*)). More than ten years ago Hashimoto (1979) showed that the crystal field (CF) is of considerable importance for the magnetic properties of the $RECu_2$ compounds. In a number of recent publications the influence of the CF has been investigated in these low-symmetry compounds. The intermetallic compounds $CeCu_2$ (Gratz *et al* 1985), $SmCu_2$ (Gratz *et al* 1990), $NdCu_2$ (Gratz *et al* 1991), $ErCu_2$ (Gubbens *et al* 1991) and $TmCu_2$ (Zajac *et al* 1988) have been studied by various physical methods (neutron scattering, field dependent magnetization, specific heat, thermal expansion and transport properties). Due to the low symmetry of these compounds it is difficult to determine the whole set of nine crystal-field parameters from the experiments. These difficulties have partly been overcome by the theoretical investigations of Newman (1983) and Divis (1991). They showed that within some approximations the number of parameters can be reduced. For the compounds $ErCu_2$ and $NdCu_2$, sets of crystal-field parameters have been given by Gubbens *et al* (1991) and Gratz *et al* (1991).

The aim of this paper is to show the temperature variation of the lattice parameters a, b and c in $ErCu_2$, $NdCu_2$, and YCu_2 determined by x-ray powder diffraction in the temperature range from 4.2 K to 400 K. The observed anomalies in $a(T)$, $b(T)$ and $c(T)$ at lower temperatures in $ErCu_2$ and $NdCu_2$ are due to the crystal-field influence and can well be described with the above-mentioned sets of parameters.

The temperature variation of a, b and c of YCu_2 (which is non-magnetic and isostructural with $ErCu_2$ and $NdCu_2$) is used as a reference for the experimental determination of the crystal-field influence in the Er and Nd compounds.

0953-8984/93/050567+06$07.50

2. Sample preparation and experimental techniques

Polycrystalline samples of $ErCu_2$, $NdCu_2$ and YCu_2 have been prepared by induction melting under a protective argon atmosphere. After annealing at 700 °C for one week no trace of foreign phases has been found.

A conventional Siemens D500 diffractometer with Co Kα radiation has been used for the measurements of the lattice parameters (a, b, c) as a function of temperature. The room temperature sample holder of the diffractometer has been replaced by an Oxford He-flow cryostat which operates in the temperature range from about 4 K up to 500 K.

3. Results and discussion

The temperature dependence of the lattice parameters a, b and c of the three isostructural $RECu_2$ compounds (RE = Er, Nd, Y), measured from 4.2 K up to 400 K (300 K), is shown in figure 1. (To avoid oxidation during the measuring procedure we limited the upper temperature to 300 K in the case of $NdCu_2$.) These parameters are normalized to the values at 400 K (300 K). The lattice parameters at room temperature (300 K) are listed in table 1.

Table 1. Lattice parameters of $ErCu_2$, $NdCu_2$ and YCu_2 at 300 K.

$RECu_2$	a (Å)	b (Å)	c(Å)
$ErCu_2$	4.275 ± 0.001	6.748 ± 0.003	7.267 ± 0.003
$NdCu_2$	4.385 ± 0.001	7.036 ± 0.006	7.421 ± 0.002
YCu_2	4.301 ± 0.001	6.874 ± 0.003	7.297 ± 0.001

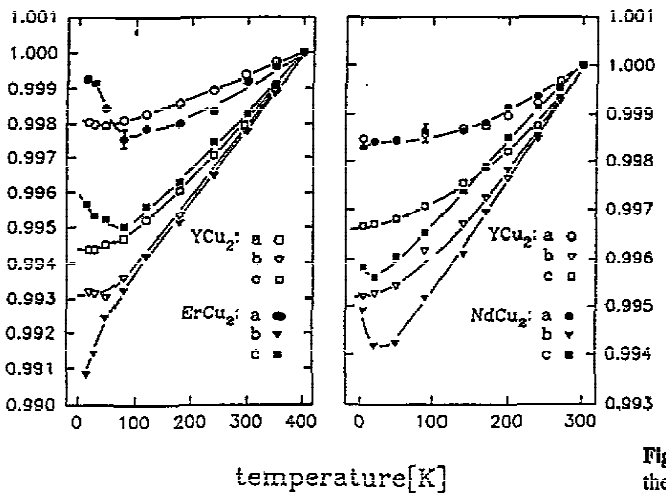

Figure 1. Temperature dependence of the normalized lattice parameters of YCu_2, $ErCu_2$ and $NdCu_2$.

For the calculation of the crystal-field contribution to the thermal expansion we assumed that the free energy $F(T, \epsilon)$ consists of a lattice and an electron part

denoted by $F_0(T,\epsilon)$ and (for $ErCu_2$ and $NdCu_2$) a magnetic part $F_{mag}(T,\epsilon)$. Here T is the absolute temperature and ϵ denotes the strain tensor.

$$F(T,\epsilon) \equiv F_0(T,\epsilon) + F_{mag}(T,\epsilon). \tag{1}$$

The model used for the calculation of $F_{mag}(T,\epsilon)$ is based on the single-ion crystal-field Hamiltonian

$$H_{cf}(\epsilon=0) = V_2^0 O_2^0(J) + V_2^2 O_2^2(J) + V_4^0 O_4^0(J) + V_4^2 O_4^2(J) + V_4^4 O_4^4(J) + V_6^0 O_6^0(J) + V_6^2 O_6^2(J) + V_6^4 O_6^4(J) + V_6^6 O_6^6(J) \tag{2a}$$

where V_i^j are the crystal-field parameters, O_i^m the Stevens operators and J the total angular momentum quantum number, and the magnetoelastic Hamiltonian for orthorhombic symmetry (Zvezdin *et al* 1985)

$$H_{me}(\epsilon) = \sum_{i=1}^{3} \epsilon_i (B_{i0}^1 O_2^0 + B_{i1}^1 O_2^2) + B^2 \epsilon_4 (J_1 J_2 + J_2 J_1) + B^3 \epsilon_5 (J_1 J_3 + J_3 J_1) + B^4 \epsilon_6 (J_2 J_3 + J_3 J_2) \tag{2b}$$

where $B_{i0}^1, B_{i1}^1, B^2, B^3, B^4$ are the magnetoelastic coupling parameters, $\epsilon_1, \ldots, \epsilon_6$ the components of the strain tensor and J_i the components of the total angular momentum operator.

H_{me} describes the coupling of the crystal field to the lattice and therefore the resulting strains. It is obtained by a series expansion of H_{cf} with respect to ϵ, where H_{me} is the linear term.

The magnetic contribution F_{mag} to the free energy is now given by

$$F_{mag}(T,\epsilon) = N \sum_{\nu} (\exp(-E_\nu/kT)/Z)(\Gamma_\nu | H_{cf}(\epsilon=0) + H_{me}(\epsilon) | \Gamma_\nu) = \langle H_{cf}(\epsilon=0) + H_{me}(\epsilon) \rangle_T \tag{3}$$

where E_ν and $|\Gamma_\nu\rangle$ are the eigenvalues and eigenstates of $H_{cf}(\epsilon=0)$, respectively. N denotes the number of rare earth atoms per unit volume.

Using equation (1) and the well known formula to calculate stresses σ_i and elastic constants c_{ij} (see e.g. Barron *et al* 1980)

$$\sigma_i(T,\epsilon) = (1/V)\partial F/\partial \epsilon_i \qquad c_{ij}(T,\epsilon) = (1/V)\partial^2 F/\partial \epsilon_i \partial \epsilon_j \qquad i,j = 1,\ldots,6 \tag{4}$$

and neglecting terms of order ϵ^2 it is possible to write $\sigma(T,\epsilon)$ as

$$\sigma_i(T,\epsilon) = \sigma_i^0(T,\epsilon=0) + \sigma_i^{mag}(T,\epsilon=0) + \sum_{j=1}^{6} c_{ij}\epsilon_j. \tag{5}$$

Because of the orthorhombic symmetry the c_{ij} with $i \leqslant 3$ and $j \geqslant 4$ vanish. The three equations (5) for $i = 1,2,3$ can be inverted to obtain the $\epsilon_i(T,\sigma)$ $(i = 1,2,3)$. The temperature dependence of ϵ at zero stress σ now reads

$$\epsilon_i(T) = \sum_{j=1}^{3} s_{ij}[\sigma_j^0(T,\epsilon=0) + \sigma_j^{mag}(T,\epsilon=0)] = \epsilon_i^0(T) + \epsilon_i^{mag}(T). \tag{6}$$

Here the s_{ij} are the elastic compliances (Barron *et al* 1980) and

$$\epsilon_i^0(T) = -(1/V)\sum_{j=1}^{3} s_{ij}\frac{\partial F}{\partial \epsilon_j^0}.$$

Using equations (1)–(3) the strain components ϵ_i^{mag} are given by

$$\epsilon_i^{mag} = (1/V)\sum_{j=1}^{3} s_{ij}\frac{\partial F}{\partial \epsilon_j^{mag}} = \mathbb{A}_i\langle O_2^0\rangle_T + \mathbb{B}_i\langle O_2^2\rangle_T \qquad i = 1,2,3 \tag{7}$$

with

$$\mathbb{A}_i = -(N/V)\sum_{j=1}^{3} s_{ij}B_{j1}^1 \qquad \mathbb{B}_i = -(N/V)\sum_{j=1}^{3} s_{ij}B_{j0}^1.$$

Because neither the non-magnetic contribution $F_0(T)$ to the free energy nor the strain components $\epsilon_i^0(T)$ of the magnetic compound are known, it is necessary to determine them from the measurement of an isostructural non-magnetic 'reference' compound (YCu_2).

In the following $a_i(T)$ $(i = 1,2,3)$ denote the temperature dependent lattice parameters of the magnetic compound ($ErCu_2$ or $NdCu_2$) and the $r_i(T)$ are the lattice parameters of YCu_2. For the following calculation we subdivide $a_i(T)$ (and $r_i(T)$) into a temperature independent part a_i^0, (r_i^0) and a temperature dependent part $\Delta a_i(T)$, ($\Delta r_i(T)$):

$$a_i(T) = a_i^0 + \Delta a_i(T) \qquad r_i(T) = r_i^0 + \Delta r_i(T). \tag{8}$$

Now the difference of the lattice parameters, normalized to any temperature T_N, can be written as:

$$a_i(T)/a_i(T_N) - r_i(T)/r_i(T_N) \simeq [\Delta a_i(T) - \Delta a_i(T_N)]/a_i^0 - [\Delta r_i(T) - \Delta r_i(T_N)]/r_i^0 = [\epsilon_i^a(T) - \epsilon_i^r(T)] - [\epsilon_i^a(T_N) - \epsilon_i^r(T_N)]. \tag{9}$$

If we assume that the strain of the reference compound ϵ_i^r represents the non-magnetic contribution ϵ_i^0 to the total strain of the magnetic compound in equation (6), then equation (8) can be written in the following form:

$$a_i(T)/a_i(T_N) - r_i(T)/r_i(T_N) = \epsilon_i^{mag}(T) - \epsilon_i^{mag}(T_N) = \mathbb{A}_i(\langle O_2^0\rangle_T - \langle O_2^0\rangle_{T_N}) + \mathbb{B}_i(\langle O_2^2\rangle_T - \langle O_2^2\rangle_{T_N}). \tag{10}$$

For the calculation of the expectation values at the variable temperature T ($\langle O_l^m\rangle_T$) and at the normalization temperature T_N ($\langle O_l^m\rangle_{T_N}$) in equation (10) we used the crystal-field parameters obtained from inelastic neutron scattering experiments ($NdCu_2$: Gratz *et al* 1991; $ErCu_2$: Gubbens *et al* 1991). The values are listed in table 2. Since for the $RECu_2$ compounds the elastic and magnetoelastic constants which determine the coefficients $\mathbb{A}_i$ and $\mathbb{B}_i$ are not known, it was necessary to determine these coefficients by fitting the model (equation (10)) to the experimental

Table 2. Crystal-field parameters for $ErCu_2$ and $NdCu_2$ (K).

$NdCu_2$:			
$V_2^0 = 1.35$	$V_2^2 = 1.56$		
$V_4^0 = 2.23 \times 10^{-2}$	$V_4^2 = 1.01 \times 10^{-2}$	$V_4^4 = 1.96 \times 10^{-2}$	
$V_6^0 = 5.52 \times 10^{-4}$	$V_6^2 = 1.35 \times 10^{-4}$	$V_6^4 = 4.89 \times 10^{-4}$	$V_6^6 = 4.25 \times 10^{-3}$
$ErCu_2$:			
$V_2^0 = -0.28$	$V_2^2 = -0.22$		
$V_4^0 = -0.30 \times 10^{-2}$	$V_4^2 = -0.14 \times 10^{-2}$	$V_4^4 = 0.30 \times 10^{-2}$	
$V_6^0 = -0.20 \times 10^{-4}$	$V_6^2 = -0.47 \times 10^{-4}$	$V_6^4 = -0.97 \times 10^{-4}$	$V_6^6 = -2.96 \times 10^{-4}$

Table 3. Fitted values A_i and B_i for $ErCu_2$ and $NdCu_2$.

$RECu_2$	A_1	A_2	A_3	B_1	B_2	B_3
$ErCu_2$	3×10^{-5}	3×10^{-5}	5×10^{-6}	-7×10^{-4}	2×10^{-4}	3×10^{-4}
$NdCu_2$	-5×10^{-5}	7×10^{-5}	-8×10^{-6}	-5×10^{-5}	3×10^{-4}	2×10^{-4}

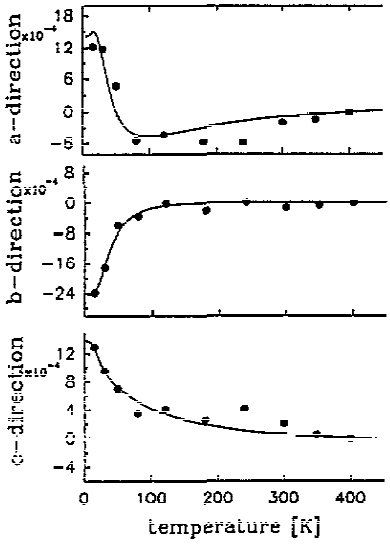

Figure 2. Experimentally determined differences of the normalized lattice parameters of $ErCu_2$ and YCu_2 (symbols). The lines represent the calculated results.

data. In table 3 we have listed the A_i and B_i values for which a least squares fit gave the best results.

In figures 2 and 3 the experimentally deduced influence of the crystal field on the thermal expansion in the three directions is given by the symbols. The lines in these figures show the theoretical results according to equation (10). It is obvious that the crystal-field influence is larger in $ErCu_2$ in comparison to $NdCu_2$. This may be attributed to the fact that the ground state in $ErCu_2$ is nearly a pure $|\pm 15/2\rangle$ Kramers doublet (as was suggested by Gubbens *et al* 1991), which strongly enhances $\langle O_{2T}^0 \rangle_T$ at low temperatures.

4. Summary

The anisotropic thermal expansion of three $RECu_2$ compounds (RE — Y, Er, Nd)

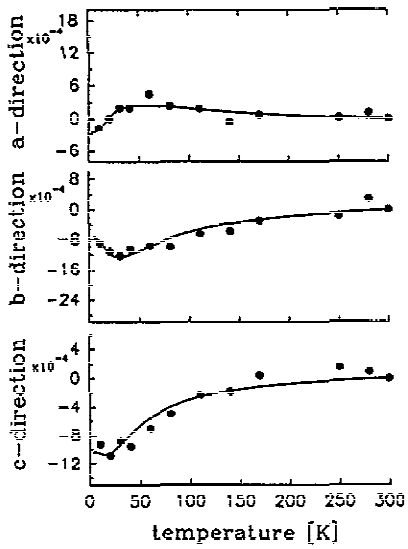

Figure 3. Experimentally determined differences of the normalized lattice parameters of $NdCu_2$ and YCu_2 (symbols). The lines represent the calculated results.

has been measured using x-ray powder diffraction. Within the paramagnetic region the anomalies in the anisotropic thermal expansion of $ErCu_2$ and $NdCu_2$ at low temperatures could be explained within the scope of the crystal-field theory. For the experimental determination of the values of $\mathbb{A}_i$ and $\mathbb{B}_i$ in equation (10) further investigations on single crystals are still necessary.

Acknowledgments

This work was partly supported by the Austrian Science Foundation project numbers P8913, P7327 and by the Austrian Ministry of Science and Research project 'Microcrystalline–amorphous Magnetic Materials'.

References

Barron T H K, Collins J G and White G K 1980 *Adv. Phys.* **29** 609

Debray D 1973 *J. Less-Common Met.* **30** 237

Divis M 1991 *Phys. Status Solidi* b **164** 227

Gratz E, Bauer E, Barbara B, Zemirli S, Steglich F, Bredl C D and Lieke W 1985 *J. Phys. F: Met. Phys.* **15** 1975

Gratz E, Loewenhaupt M, Divis M, Steiner W, Bauer E, Pillmayr N, Müller H, Nowotny H and Frick B 1991 *J. Phys.: Condens. Matter* **3** 9297

Gratz E, Pillmayr N, Bauer E, Müller H, Barbara B and Loewenhaupt M 1990 *J. Phys.: Condens. Matter* **2** 1485–98

Gubbens P C M, Buschow K H J, Divis M, Lange J and Loewenhaupt M 1991 *J. Magn. Magn. Mater.* **98** 141

Hashimoto Y 1979 *J. Sci. Hiroshima Univ.* A **43** 157–84

Newman D J 1983 *J. Phys. F: Met. Phys.* **13** 1511

Zajac S, Divis M, Sima V and Smetana Z 1988 *J. Magn. Magn. Mater.* **76 & 77** 197

Zvezdin A K, Matveev V M, Muchin A A and Popov A I 1985 *Rare Earth Ions in Magnetically Ordered Crystals* (Moscow: Nauka) p 98